This is not a painting

Scanning and printing a painting's appearance

Elkhuizen, Willemijn

DOI
10.4233/uuid:e9476c36-066e-4c9c-a570-90eef0d319cb

Publication date
2019

Document Version
Final published version

Citation (APA)
Elkhuizen, W. (2019). *This is not a painting: Scanning and printing a painting's appearance*. [Dissertation (TU Delft), Delft University of Technology]. https://doi.org/10.4233/uuid:e9476c36-066e-4c9c-a570-90eef0d319cb

This is not a painting

Scanning and printing a painting's appearance

Willemijn Elkhuizen

This is not a painting

Scanning and printing a painting's appearance

Dissertation

for the purpose of obtaining the degree of doctor
at Delft University of Technology
by the authority of the Rector Magnificus prof. dr. ir. T.H.J.J. van der Hagen
chair of the Board for Doctorates
to be defended publicly on
Friday 4 October 2019 at 10:00 o'clock

by

Willemijn Sietske ELKHUIZEN

Master of Science in Strategic Product Design,
Delft University of Technology, The Netherlands
born in Den Helder, The Netherlands

This dissertation has been approved by the promotors.

Composition of the doctoral committee:

Rector Magnificus,	chairperson
Prof. dr. ir. J.M.P. Geraedts,	Delft University of Technology, promotor
Prof. dr. J. Dik,	Delft University of Technology, promotor
Prof. dr. S.C. Pont,	Delft University of Technology, promotor
Independent members:	
Prof. dr. ing. C.M. Hein,	Delft University of Technology
Prof. dr. C.J.M. Zijlmans,	Leiden University
Prof. dr. R.G. Erdmann,	University of Amsterdam
Dr. E.H.C. Ullersma,	Océ Technologies B.V., a Canon Company
Prof. dr. P.J. Stappers,	Delft University of Technology, reserve member

A CANON COMPANY

This research was funded by Océ Technologies B.V., a Canon Company.

Keywords: 3D Scanning, 3D Printing, Appearance Reproduction, Paintings, Cultural Heritage

Printed by: Gildeprint

Front & Back: Depiction of *Fruit Still Life*, by Cornelis de Heem (c.1670), oil paint on canvas, 50 x 65 cm, Mauritshuis, Den Haag, inventory no. 50

ISBN 978-94-6323-821-2

An electronic version of this dissertation is available at
http://repository.tudelft.nl/.

Dedicated to Mark and Siem,
because you make me smile every day.

Contents

Summary

Introduction

The appearance of a painting cannot solely be described by the depiction that it presents to the viewer. When viewing the artifact in real life, we find that the painted surface is in effect a three-dimensional landscape of paint. Paintings, "moveable, largely two-dimensional images created for the primary purpose of providing a visual experience",[1] can be created using a vast variety of materials on a range of supports. They are commonly built up as a complex stratigraphy of layers, generally consisting of a support, ground layer(s), one or multiple layers of (semi-) transparent paints, and in many cases a protective varnish layer. The current appearance of a painting is determined by the way a painter used and applied the materials, but also effects of aging, conservation and restoration treatments, which all continue to influence the physical state of a painting.

Historically, cultural heritage (CH) reproductions were hand-crafted, and created for instance to disseminate or replace artworks, or to train in the skill of their creation. Also modern reproductions — or facsimiles — are still large hand-crafted, and for instance serve to provide access to (fragile) artworks or even complete (CH) sites, or to recreate their original appearance. Alternatively, reconstructions might reside only in the virtual domain. The continued development of digital imaging and digital fabrication technology (i.e. 3D printing) provides new opportunities for appearance reproduction, also suitable for application in the CH domain.

If we want to replicate material appearance, we need to understand how (the appearance of) material is perceived. A material is, however, not observed directly, but has to be lighted, and via the light that is scattered by the material humans can perceive it. Appearance is therefore the light-material-confounded proximal stimulus for the human visual system (HVS). Even though we see, recognize and interact with a vast number of materials every day, and can effortlessly distinguish between them, it turns out that the perceptual mechanisms that underlie this, are still quite poorly understood, including linking individual appearance attributes to measurable and fabrication parameters. One of the consequences of this is that an *integrated* approach to (total) appearance reproduction, including color, topography/texture/shape, gloss and transparency/translucency, is still lacking.

[1] International Council of Museums - Committee for Conservation, *ICOM CC - working group - paintings*, Workgroup web page, (Accessed: 28-May-2018).

Research aim, method and scope

The aim of this PhD thesis is to:

Develop an integrated 3D scanning and 3D printing system for the reproduction of the material appearance attributes of color, topography and gloss of paintings

More specifically, the aim is to create a perceptually matching appearance, by using a digital capturing and digital fabrication process, where the digital fabrication process makes use of only a limited set of inks, namely Cyan, Magenta, Yellow, Black, White and Transparent (CMYKWT). The reproduction of transparency/translucency was out-of-scope for this research project, for reasons of lacking opportunities to measure the stratigraphy of (semi-)transparent paint layers, at scale on a painting (at the start of this project).

With the capability to capture the fine surface details of a painting for purposes of creating a reproduction, another application for this scan data is envisioned, namely the documentation and monitoring of paintings, for the purpose of conservation. For this reason, a secondary aim of this PhD project is to:

Evaluate the suitability of 3D scanning — based on fringe-encoded stereo imaging — for documentation and monitoring of paintings

The research was carried out and validated in five different case studies, using in total eight different painting reproductions. All paintings that were reproduced and evaluated are oil paintings on canvas.

Results

Three reproductions, incorporating color and topography (scanned and fabricated prior to the start of this PhD project), were evaluated and compared to their respective original, by museum experts, to gain a better understanding of their appearance similarities and differences, to determine the further research focus (see **Chapter 2**). Reproductions were made of the *Self-portrait* by Rembrandt van Rijn,[2] *Flowers in a Blue Vase* by Vincent van Gogh,[3] and *The Jewish Bride* by Rembrandt van Rijn,[4] using 3D scanning based on fringe-encoded stereo imaging, and printed using Océ Technologies *Elevated Printing* technology at a resolution of 450 dots per inch (dpi), using CMYKW inks (no transparent ink). Although, differences on all appearance attributes (color, gloss, topography and translucency/transparency) were mentioned by experts, one key difference they mentioned, was the lack of spatially-varying gloss on the reproductions. Based on this initial exploration and literature research the choice was made to focus on capturing and fabrication of

[2] *Self-portrait* by Rembrandt van Rijn (c.1669), 60.2 cm × 65.4 cm, oil paint on canvas, Mauritshuis, The Hague, inventory no. 840

[3] *Flowers in a blue vase*, by Vincent van Gogh (c. June 1887), oil paint on canvas, 39 cm × 62 cm, Kröller Müller Museum, Otterlo, inventory no. KM107.055

[4] *Isaac and Rebecca, Known as 'The Jewish Bride'*, by Rembrandt van Rijn (c.1665 - c.1669), oil paint on canvas, 166.5 cm × 121.5 cm, Rijksmuseum, Amsterdam, inventory no. SK-C-216

spatially-varying gloss, as well as determining the applicability of the 3D scanning technique for the documentation and monitoring of paintings.

Consequentially, two iterations to (integrated) gloss capturing and fabrication are presented. In **Chapter 3** an initial approach to spatially-varying gloss capturing is presented, based on the quantifying luminance variations, in a stack of High-Dynamic Range (HDR) images, captured of a painted surface illuminated from different directions. This was linked to spatially-varying gloss fabrication, using an adapted version of Océ Technologies *Elevated Printing* Technology, adding a transparent ink to the default CMYKW ink channels. Spatially-varying gloss was fabricated by first printing the colored topography with a multi-level half-toning approach, creating a matte base layer, and subsequently half-toning and printing a single layer of transparent ink (digital varnish). Although the approach was capable of visualizing local gloss variations, the measurement was not independent of the color, nor fast enough to apply at high resolution on a complete paintings (given a substantial size in the range of 1 m^2). The case study, using a self-painted sample, showed that the fabrication approach was capable of printing distinct gloss levels as well as smooth gloss gradients, although the gloss range was limited. We also concluded that resolution of the scan was too low, and suggest that gloss should be measured at a similar spatial resolution as the color and topography.

An alternative imaging and optimized fabrication approach is proposed in **Chapter 4**. We propose an integrated system capable of capturing and fabricating color, topography and gloss, whereby the gloss scanning equipment was added to (an optimized version of) the 3D scanning system. The gloss was measured based on specular reflection polarization, whereby the specular reflection of the painting's surface is sampled around Brewster's angle, where these reflections are effectively polarized. Resulting, stitched color, height and gloss maps (sampled at 25 µm × 25 µm resolution) were inputs for an adapted version of Océ Technologies *Elevated Printing* technology. The spatially-varying gloss was fabricated using transparent ink, by printing six, consecutive layers of transparent ink, effectively increasing the surface roughness. Two paintings, painted in the style of Vincent van Gogh, called *Sunflowers*[5] and *Two Wrestling Figures*[6] served as case studies to verify the effectiveness and efficiency of the proposed system. The *Sunflowers* painting was scanned four times, consecutively rotated by 90°, to evaluate the influence of the scanning system geometric configuration on the gloss measurement. The case studies results show that the method is sufficiently fast for application in a realistic use case. The results can well be used for the purpose of physical reproduction and other applications needing first-order estimates of the appearance (e.g. conservation diagnostics and condition reports). The results also show that there is a consistency between the scan results from the four rotation angles, meaning the influence of the scanning geometry on the measurement is limited.

[5] *Sunflowers*, signed as W. Adam (c.2015), oil paint on canvas, 30 cm × 40 cm, a painting in the style of Vincent van Gogh, purchased by the author

[6] *Two Wrestling Figures*, by Charlotte Caspers (2017), oil paint on canvas, 100 cm × 80 cm, painted for the Dutch Television program *Het Geheim van de Meester*. It is a *painted* reconstruction of a work by Vincent van Gogh, found underneath: *Still Life with Meadow Flowers and Roses*, by Vincent Van Gogh (c.1886-1887), 80 cm × 100 cm, Kröller Müller Museum, Otterlo, inventory no. KM100.067

Chapter 5, elaborates on the above mentioned approach, and proposes a method for the gloss calibration and gloss gamut mapping, using a set of gloss calibration targets, printed in the primary printing colors (CMYKW), with uniform gloss in equal distant gloss steps. Scans of these targets were used to create a 1-dimensional gloss gamut mapping, by fitting a monotonic curve to the mean gloss scan values of the different targets. Analysis of fitted curves indicated that the gloss mapping is independent of the diffuse colors. The painting *Fruit Still Life* by Cornelis de Heem[7] was scanned, and the measured gloss was mapped to printable gloss levels using the relation described by the fitted curve. The mapped and printed result shows that the approach is able to reproduce the gloss details in the in-gamut range and does not show obvious banding effects, due to clipping. The printed result also shows better correspondence to the painting's appearance than a linear mapping, able to visualize subtle gloss variations for the in-gamut gloss values. Limitations of the gloss calibration approach are also identified in terms of gloss measurement uniformity, gloss mapping strategy and gloss printing.

In **chapter 6** three 3D scanning techniques are compared, evaluating their suitability for capturing the intricate details of the surface topography of a canvas painting. The following imaging methods were used: Multi-Scale Optical Coherence Tomography (MS-OCT), 3D scanning based on fringe-encoded stereo imaging (at two resolutions, with two different scanning systems), and 3D digital microscopy. A metal reference target with four grooves (with approximate depths of 1000, 500, 200 and 30 µm) was captured by all instruments and compared to measurements made with White Light Confocal Profilometry. The four scanners were used to capture segments (3D digital microscopy) or the complete surface topography (all others) of *Girl with a Pearl Earring* by Johannes Vermeer.[8] Three regions-of-interest were aligned using a scale-invariant template matching algorithm, and compared on their ability to visualize topographical details of interest. We find that the 3D digital microscopy and the MS-OCT offer the highest measurement accuracy and precision which is maximally three times more accurate than the 3D scanning, based on fringe-encoded stereo imaging. However, the small field-of-view of these techniques, makes these techniques relatively slow, and thereby less viable solutions for capturing larger (areas of) paintings. Based on the case study results, 3D data of *Girl with a Pearl Earring*, we found that it provides an unparalleled insight into the surface features of this painting, specifically related to 'moating' around impasto, the effects of paint consolidation in earlier restoration campaigns and aging, through visualisation of the crack pattern. Whether 3D scanning, (including the technique based on fringe-encoded stereo imaging), are also suitable for monitoring topographical changes in a painting's surface, remains to be investigated, as currently no (historic) 3D data exists, with this level of detail, for comparison.

[7] *Fruit Still Life*, by Cornelis de Heem (c. 1670), oil paint on canvas, 50 cm × 65 cm, Mauritshuis, The Hague, inventory no. 50

[8] *Girl with a Pearl Earring*, by Johannes Vermeer (c.1665), oil paint on canvas, 39 cm × 45 cm, Mauritshuis, The Hague, inventory no. 670

Discussion

With the rapid developments in 3D scanning and digital fabrication technology, the (potential) applications of these technologies in relation to CH domain is fast expanding. We argue that our contributions, in 3D scanning of paintings, are currently mainly targeted at their *'perceptual enhancement'*, although we envision that 3D data of paintings can also contribute to other applications like restoration and preservation, and monitoring.[9] We show that the 3D data can be used to visualize the crack patterns of a painting, and can thereby support the interpretation of its condition and conservation history (as discussed in Chapter 6). Going forward, multi-modal appearance scanning (including color, topography, gloss and translucency) might also be used as a more extensive documentation and monitoring of the artwork's appearance than the current photographs that are taken.

Digital fabrication can have a wide range of applications in the CH domain, having an impact in various CH sub-disciplines like restoration, education, creativity and dissemination.[10] We find that the work conducted in this thesis, and a variety of related and similar projects, show the potential of painting reproductions for a large number of these applications. We show that our painting reproductions can be used to create interactive exposition setups (also for specific target groups like children or visually impaired), provide a temporary replacement for the original, and enable the creation of 3D printed reconstructions of a painting's original appearance. Moreover, these projects also show the potential of the digital fabrication technique — full-color material jetting — for wider application in the CH domain.

As (3D printed) reproductions are created with increased visual similarity to the original painting, it inevitably raises questions on the immaterial aspects of making such reproductions. Based on the case studies carried out for this thesis (and other related cases), we would argue that 3D printed reproductions of paintings have their own merit and purpose, potentially complementing the function and aesthetic of the original paintings, much like other facsimiles or replicas serve such purpose. We believe reproductions can be a part of the solution to CH conservation and dissemination. Moreover, we believe that these modern, digital reproductions can take on a similar role as their historic (hand-made) counterparts, e.g. in disseminating art, recreating (lost) art and training — in this case scientists — about the intricate skills of creating certain appearances. In the end, whether and how reproductions are appreciated, also depends a great deal on the context, application, and implementation. In any case, it is important, — even enforced by the International Council of Museums[11] — that it is communicated to the viewer, when reproductions are shown in a museum context. Furthermore, a solely technological perspective on these immaterial aspects of creating and using reproductions will not be sufficient. We believe these questions ask for a wider reflection from multiple perspectives i.e. from museology, art history, restoration and conservation, and art education.

[9] R. Pintus, K. Pal, Y. Yang, T. Weyrich, E. Gobbetti, and H. Rushmeier, *A Survey of Geometric Analysis in Cultural Heritage,* Computer Graphics Forum, **35**, 1, (2016), 4–31

[10] R. Scopigno, P. Cignoni, N. Pietroni, M. Callieri, and M. Dellepiane, *Digital Fabrication Techniques for Cultural Heritage: A Survey*, Computer Graphics Forum **36**, 1 (2017), 6–21

[11] International Council of Museums, ICOM code of ethics for museums, (2017), Retrieved June 13, 2019

Whether a reproduction is directly recognized as a such, depends on a great deal on factors, like the context, level of expertise of the viewer, but also the viewing distance, illumination and viewing conditions. At a regular viewing distance, a painting and a reproduction might look remarkably similar. However, when examined them at *close range* digital reproductions are clearly distinguishable from paintings due to the specific nature of fabrication — using a limited set of six inks and a different fabrication technique —.

We also envision that knowledge on appearance capturing and fabrication (featuring spatially-varying appearance properties) can be used to create research probes, for the purpose of studying appearance perception. As appearance design is an crucial part of any product's design, we envision that digital appearance reproduction can also be usefully applied in that domain. Products for which this is particularly obvious, are prostheses. For this, of course, the capabilities should be extended to 3D appearance capturing and fabrication. Here, we also envision using digitally fabricated appearances, possibly in combination with a technique called 'optical mixing', as a material visualisation, communication and selection tool. Furthermore, the knowledge and skill gained in the reproduction of appearance is also one of the necessary ingredients to a more deliberate and informed approach to material appearance synthesis.

The case studies carried out in the context of this PhD thesis, were limited to the appearance reproduction of (varnished) oil paintings. This makes it difficult to generalize the results to other (painting) materials and appearances. Various limitations of the current reproduction workflow are recognized, i.e. gloss capturing is limited to (roughly) planar surfaces, and appearance attributes interact in capturing *and* fabrication. Furthermore, we recognize that our current approach to gloss calibration is not device independent, and color reproduction is limited to a colormetric reproduction workflow. For the appearance capturing the ability to further increase the scanning resolution is limited by depth-of-field of the optical system, which can pose difficulties for paintings with extensive warping, or high *impasto*. Also the reproduction workflow does *not* offer the possibility to capture or fabricate the appearance of metallic surfaces, or special optical effects like fluorescence, pearlescence or sparkle. Furthermore, printing technology used is limited in its building height (5 mm), albeit at a large planar scale (1.2 m $\times$ 2.4 m) as compared to other 3D printing systems. And finally, a systematic investigation into color, gloss and topography perception and their interactions remains to be further investigated, in the context of complex, real-world material appearance reproduction cases.

Conclusion

We conclude that we can successfully reproduce color, topography and spatially-varying gloss of paintings, in an integrated way. This can be achieved by combining 3D scanning — based fringe-encoded stereo imaging — with gloss scanning — based on reflection polarization. Experimental results show that the method is sufficiently fast for practical application. Results show that our proposed method to extend appearance scanning with gloss measurements is a valuable addition in the quest for more realistic reproductions, in terms of its practical applicability — number of images needed for reconstruction and speed — and its perceptual added value, when added to color and topography reproduction. For fabrication we propose a minimal set of just six printing materials, consisting of Cyan, Magenta, Yellow, Black, White and Transparent ink.

Furthermore, we conclude that 3D scanning data of paintings — captured using fringe-encoded stereo imaging — has good correspondence to other more accurate and precise 3D imaging techniques like 3D digital microscopy — based on focus variation — and Multi-Scale Optical Coherence Tomography (MS-OCT). Moreover, our 3D scanning technique was found to be more suitable for scanning larger areas — i.e. complete paintings — in terms of tile size, capturing speed and flexibility in resolution. We show that topographical data of a painting (of all of the above techniques) can be used to visualize height variations of a painting's surface, much more accurately, than existing photography or manual tracing techniques. These visualizations can support conservators in evaluating the state of the painting, and determining the need for any interventions.

The reproductions and 3D data sets created within the context of this PhD project, but also the custom-built scanning systems, serve as demonstrators, and are in effect accumulations of the knowledge generated in the project.

We propose future research might be conducted in various directions. The capabilities of digital appearance reproduction can be used to increase our understanding of for instance topography and gloss perception, studying appearance perception in complex, real-world cases, potentially helping to determine the most appropriate approach to their reproduction. Furthermore, we suggest to explore existing limitations in fabrication of spatially-varying gloss, as well as gloss gamut mapping. Furthermore, incorporating translucency capturing and fabrication would greatly expand the capabilities of appearance reproduction. To be able to generalize the findings of this thesis, other paintings and/or artifacts (made from different materials) will need to be replicated and evaluated. The application of appearance data, as well as physical reproductions can be explored further, specifically in the context of CH documentation, monitoring and restoration. Also possibilities for creating reconstructions - of original color, total appearance, or reconstructing missing (pieces of) paintings - should be further explored, also employing new methods from the domains of for instance artificial intelligence, and data science. We would urge that the application of appearance data, and physical reproductions be explored and evaluated in a broad multi-disciplinary context, also involving CH sub-disciplines, like museology, art history, restoration and conservation and art education. Only then, can we come to meaningful innovations, and consensus on

their usefulness and suitability within the CH domain. The expansion to appearance reproduction to truly three-dimensional artifacts remains a challenging direction for future research. This is also deemed relevant outside the CH domain, for instance in prostheses design. And finally, we also envision that various appearance reproduction efforts could be accumulated into a practical framework for appearance reproduction, providing guidance to choosing a suitable capturing and fabrication technique, capable to (best) match a range of appearance-related and other requirements (e.g. structural, size, or functional related). This framework should be developed in conjunction with a theoretical underpinning on appearance perception, applicable to appearance capturing and fabrication, supporting the efforts of appearance reproduction and perceptual enhancement.

Samenvatting

Introductie

The verschijningsvorm[12] van een schilderij kan niet alleen worden omschreven door de afbeelding die deze presenteert aan de kijker. Wanneer het artefact in het echt wordt bekeken, ontdekken we dat het in werkelijkheid een drie-dimensionaal landschap van verf is. Schilderijen, "verplaatsbare, grote twee-dimensionale afbeeldingen, primair gemaakt voor het verschaffen van een visuele indruk",[13] kunnen gemaakt zijn met een grote variatie aan materialen, op diverse ondergronden. Gewoonlijk zijn ze opgebouwd in een complexe stratigrafie van lagen, in het algemeen bestaand uit een ondergrond, één of meerdere lagen (semi-)transparante verf, en in veel gevallen een beschermende vernis. Het huidige verschijningsvorm van een schilderij is bepaald door de manier waarop een schilder materiaal heeft gebruikt en opgebracht, maar ook de effecten van veroudering, conservering en restauratie behandelingen, welke allemaal continu het de fysieke staat van het schilderij blijven beïnvloeden.

Historisch gezien, werden cultureel erfgoed reproducties met de hand gemaakt, en gecreëerd bijvoorbeeld om kunst te verspreiden, te vervangen, of om de vaardigheid van hun maken te trainen. Ook moderne reproducties — of facsimiles — worden vaak nog met de hand gemaakt, en dienen bijvoorbeeld om toegang te verschaffen tot (fragiele) kunstwerken of zelfs complete cultureel erfgoed locaties, of om hun originele uiterlijk te reconstrueren. Daarnaast, zijn er ook reconstructies die alleen in het virtuele domein bevinden. De voortdurende ontwikkeling van digitaal beeldvormende en digitale fabricage technieken (zoals 3D printen) bieden nieuwe mogelijkheden voor de reproductie van uiterlijk, welke ook geschikt zijn voor toepassing in het domein van cultureel erfgoed.

Als we materiële verschijningsvorm willen reproduceren, moeten we begrijpen hoe (de verschijningsvorm van) een materiaal wordt waargenomen. Een materiaal kan echter direct worden waargenomen, maar moet belicht worden, en via de verstrooiing van het licht door het materiaal, kan de mens het waarnemen. Verschijningsvorm is daarom een licht-materiaal-gecombineerde nabije stimulus voor het menselijk visuele systeem. Ondanks dat we een grote hoeveelheid materialen elke dag zien, herkennen en ermee omgaan, en moeiteloos onderling kunnen onderscheiden, blijkt het dat we de onderliggende perceptuele mechanismen, nog maar slecht begrijpen, inclusief het verbinden van de individuele uiterlijke eigenschappen met meetbare en fabricage parameters. Één van de gevolgen hiervan is dat een *geïntegreerde* aanpak voor de reproductie van (totale) materiële verschijningsvorm,

[12] Hiermee wordt de vertaling van *appearance* bedoelt, welke ons inziens geen betere Nederlandse vertaling heeft

[13] Vertaling van: International Council of Museums - Committee for Conservation, *ICOM CC - working group - paintings*, Workgroup web page, (Accessed: 28-May-2018).

inclusief kleur, topografie/textuur/vorm, glans en transparantie/translucentie, nog steeds ontbreekt.

Onderzoeksdoel, methode en afbakening

Het doel van dit proefschrift is als volgt:

Ontwikkel een geïntegreerde 3D scan- en 3D print-systeem voor het reproduceren van de materiële verschijningsvorm attributen: kleur, topografie en glans van schilderijen

Verder gespecificeerd, is het doel: het maken van een perceptueel overeenkomstige verschijningsvorm, door gebruik te maken van digitale beeldvorm- en fabricagetechnieken, waarbij het digitale fabricage proces gebruik maakt van een beperkte hoeveelheid aan materialen, namelijk cyaan, magenta, deel, zwart, witte en transparante inkt (CMYKWT). De reproductie van transparantie/ translucentie ligt buiten de afbakening van dit onderzoeksproject, omdat mogelijkheden ontbreken om op grotere schaal, de laag opbouw van de (semi-)transparante lagen in schilderijen te meten (bij de start van dit project).

Met de mogelijkheden om de fijne oppervlakte details van een schilderij te meten, met als doel het maken van reproducties, werd ook een andere applicatie voorzien voor deze scan data, namelijk het documenteren en monitoren van schilderijen, met als doel conservering. Met deze reden, in het secundaire doel van dit proefschrift als volgt:

Evalueer de geschiktheid van 3D scannen — gebaseerd op 'fringe-encoded stereo imaging' — voor het documenteren en monitoren van schilderijen.

Het onderzoek wat is uitgevoerd is gebaseerd en gevalideerd op basis van vijf case studies, gebruik makend van acht verschillende schilderij reproducties. Alle schilderijen die zijn gereproduceerd en geëvalueerd zijn olieverf op doek.

Resultaten

Drie reproducties, die kleur en topografie reproductie bevatten (gescand en gefabriceerd voorafgaand aan de start van dit project), zijn geëvalueerd en vergeleken door experts met hun respectievelijke origineel, om een beter begrip te krijgen van hun overeenkomsten en verschillen, om de verdere focus van het onderzoek te bepalen (zie hoofdstuk 2). Reproducties zijn gemaakt van het *Zelfportret* door Rembrandt van Rijn,[14] *Bloemen in blauwe vaas* door Vincent van Gogh,[15] en *Het Joods Bruidje* door Rembrandt van Rijn,[16] door middel van 3D scannen, gebaseerd

[14] *Zelfportret* door Rembrandt van Rijn (c.1669), 60.2 cm × 65.4 cm, olieverf op doek, Mauritshuis, Den Haag, inventaris nr. 840

[15] *Bloemen in blauwe vaas*, door Vincent van Gogh (c. juni 1887), olieverf op doek, 39 cm × 62 cm, Kröller Müller Museum, Otterlo, inventaris nr. KM107.055

[16] *Isaac en Rebecca, bekend als 'Het Joods bruidje'*, door Rembrandt van Rijn (c.1665 - c.1669), olieverf op doek, 166.5 cm × 121.5 cm, Rijksmuseum, Amsterdam, inventaris nr. SK-C-216

op *fringe-encoded stereo imaging*, en geprint door middel van Océ Technologies *Elevated Printing* technologie, op een resolutie van 450 dpi (*dots per inch*), gebruik makend van CMYKW inkten (geen transparante inkt). Alhoewel experts verschillen benoemden voor alle materiaal verschijningsvorm attributen (kleur, glans, topografie en transparantie/translucentie), werd één belangrijk aspect benoemd, namelijk het ontbreken van spatiaal variërende glans op de reproducties. Gebaseerd om deze initiële exploratie en literatuuronderzoek, is de keuze gemaakt om te focussen om het meten en fabriceren van spatiaal variërende glans, als mede het beoordelen van de toepasbaarheid van de 3D scan techniek voor het documenteren en monitoren van schilderijen.

Als gevolg hiervan worden twee iteraties voor (geïntegreerde) glans meting en fabricage gepresenteerd. In **Hoofdstuk 3** wordt een initiële aanpak voorgesteld, voor het meten van spatiale glans variatie, gebaseerd om het kwantificeren van luminantie, in een stapel *High Dynamic Range (HDR)* afbeeldingen, genomen van een geschilderd oppervlak, wat uit verschillende richtingen belicht wordt. Dit werd verbonden aan spatiaal-variërende glans fabricage, gebruik makend van een aangepaste versie van Océ Technologies *Elevated Printing* technologie, met toevoeging van een transparante inkt aan de standaard CMYKW inkt kanalen. Spatiaal varierende glans werd gefabriceerd door eerst de gekleurde topografie te printen, met een *multi-level half-toning* aanpak, welke een mat oppervlakte vormt, om vervolgens een enkele laag ge-half-tonende transparante inkt te printen (digitale vernis). Ondanks dat de aanpak in staat was de lokale glans variaties te visualiseren, was de meetmethode niet onafhankelijk van kleur, en bovendien niet snel genoeg om op hoge resolutie toe te passen om hele schilderijen (gegeven een substantiële afmeting in het bereik van 1 m^2). De case studie, gebruik makend van een zelf-geschilderd proefstuk, liet zien dat het mogelijk was om verschillende, te onderscheiden, glans niveaus te printen evenals geleidelijke glans overgangen. We concludeerden daarnaast dat de scan resolutie te laag was, en stellen voor om de glans te meten op een vergelijkbare resolutie als de kleur en topografie.

Een alternatieve meet- en geoptimaliseerde fabricage-aanpak wordt voorgesteld in **Hoofdstuk 3**. We stellen een geïntegreerd systeem voor dat in staat is om kleur, topografie en glans vast te leggen en te fabriceren, waarbij de glans scan apparatuur is toegevoegd aan (een geoptimaliseerde versie van) het 3D scan systeem. De glans werd gemeten gebaseerd op het principe van polarisering van de spiegelende reflecties, waarbij de spiegelende reflecties van het schilderij gemeten werden onder *Brewster's* hoek, waar deze reflecties effectief gepolariseerd zijn. De resulterende kleur, topografie en glans afbeeldingen (bemonsterd op 25 µm × 25 µm), vormden de input voor een aangepaste versie van Océ Technologies *Elevated Prining* technologie. De spatiaal variërende glans werd gefabriceerd met een transparante inkt, door het printen van zes opeenvolgende lagen van transparante inkt, welke effectief het oppervlakte verruwen. Twee schilderijen, geschilderd in de stijl van Vincent van Gogh, genaamd *Zonnebloemen*[17] en *Twee Worstelaars*[18] diende als case stud-

[17] *Zonnebloemen*, ondertekend als W. Adam (c.2015), olieverf op doek, 30 cm × 40 cm, een schilderij in de stijl van Vincent van Gogh, gekocht door de auteur

[18] *Twee Worstelaars*, door Charlotte Caspers (2017), olieverf op doek, 100 cm × 80 cm, geschilderd voor

ies om de effectiviteit en efficiëntie van het voorgestelde systeem te verifiëren. Het *Zonnebloemen* schilderij werd vier keer gescand, achtereenvolgend geroteerd met 90°, om de invloed van de geometrische configuratie van het scan systeem de evalueren. De case studies laten zien dat de methode voldoende snel is voor applicatie in een realistisch gebruik-scenario. De resultaten kunnen goed gebruikt worden voor het maken van fysieke reproducties en andere applicaties die een eerste-orde benadering nodig hebben van de verschijningsvorm (e.g. conservering-diagnostiek en conditie rapporten). De resultaten laten ook consistentie zien tussen de verschillende rotaties, wat betekent dat invloed van de scan geometrie beperkt is. **Hoofdstuk 5** gaat dieper in op het bovengenoemde aanpak, en stelt een methode voor, voor glans kalibratie en glans *gamut mapping*, gebruikmakend van een set glans kalibratie kaarten, geprint in de primaire print kleuren (CMYKW), met uniforme glans met gelijkmatig verdeelde glans stappen. Scan van deze targets zijn gebruikt om een 1-dimensionale glans *gamut mapping* te maken, door het monotone curve te passen op de gemiddelde glans waardes van de verschillende kaarten. Analyse van de curves gaf aan dat de glans *mapping* onafhankelijk van kleur is. Het schilderij *Fruitstilleven* door Cornelis de Heem[19] werd gescand en de gemeten glans toegewezen aan de printbare glans niveaus, gebruik makend van de relatie beschreven door de kalibratie curve. De toegewezen en geprinte resultaten laten zien dat de aanpak in staat is om glans details te reproduceren van de *in-gamut* glans waardes en vertoont geen overduidelijke glans *banding* effecten, veroorzaakt door *clipping*. De geprinte resultaten laten ook een betere correspondentie zien met het uiterlijk van het schilderij dan een lineaire *mapping*, en maakt het mogelijk om subtiele glans variaties zichtbaar te maken voor de *in-gamut* glans waardes. Beperkingen van deze glans kalibratie aanpak werden ook geïdentificeerd op het gebied van het meten van glans uniformiteit, glans *mapping* strategie en glans printen.

In **Hoofdstuk 6** worden drie 3D scan technieken met elkaar vergeleken, waarbij hun toepasbaarheid wordt geëvalueerd voor het scannen van zeer kleine details van het oppervlak van een schilderij op doek. De volgende beeldvormende methodes zijn gebruikt: Multi-Schaal Optische Coherentie Tomografie (MS-OCT), 3D scannen op basis van *fringe-encoded stereo imaging* (op twee verschillende resoluties, met twee systemen), en 3D digitale microscopie. Een metalen referentie object met vier groeven (met een geschatte diepte van 1000, 500, 200 en 30 µm) werd gemeten door alle instrumenten en vergeleken met metingen gemaakt met een Wit-Licht Confocale Profilometrie. De vier scanners werden gebruikt om segmenten (in het geval van de 3D digitale microscopie) of het complete oppervlak (alle andere) te scannen van *Meisje met de Parel* door Johannes Vermeer.[20] Drie *regions-of-interest*

het Nederlandse televisieprogramma *Het Geheim van de Meester*. Het is een *geschilderde* reconstructie van een werk van Vincent van Gogh, gevonden onder: *Stilleven met akkerbloemen en rozen*, door Vincent Van Gogh (c.1886-1887), 80 cm × 100 cm, Kröller Müller Museum, Otterlo, inventaris nr. KM100.067

[19] *Fruitstilleven*, door Cornelis de Heem (c. 1670), olieverf op doek, 50 cm × 65 cm, Mauritshuis, Den Haag, inventaris nr. 50

[20] *Meisje met de Parel*, door Johannes Vermeer (c.1665), olieverf op doek, 39 cm × 45 cm, Mauritshuis, Den Haag, inventaris nr. 670

werden onderling uitgelijnd door middel van een *scale-invariant template matching* algoritme, en vergeleken op hun vermogen om topografische interessante details te visualiseren. We vonden dat de 3D digitale microscopie en de MS-OCT de hoogste nauwkeurigheid en precisie hebben, welke maximaal drie keer nauwkeuriger zijn dan de 3D scan techniek, gebaseerd op *fringe-encoded stereo imaging*. Echter, de kleine *field-of-view* van deze technieken, maakt deze technieken relatief langzaam zijn, en daarmee minder geschikte oplossingen voor het scannen van grotere (gebieden van) schilderijen. Gebaseerd op de case studie, 3D data van *Meisje met de Parel*, vonden we dat dit ongeëvenaarde inzichten verschafte op het gebied van topografische details van dit schilderij, specifiek gerelateerd aan *'moating'* rond impasto, de effecten van verf consolidatie in eerdere restauratie campagnes en veroudering, door de visualisatie van het craquelure patroon. Of 3D scanning, (inclusief de techniek gebaseerd op *fringe-encoded stereo imaging*) ook geschikt zijn voor het monitoren van topografische veranderingen in het oppervlak van een schilderij, moet nog worden onderzocht, omdat momenteel er geen (historische) 3D data bestaat, met dit niveau van detail, ter vergelijking.

Discussie

Met de razendsnelle ontwikkeling van 3D scan en digitale fabricage technieken, nemen de (potentiële) toepassingen voor deze technologieën voor het cultureel erfgoed domein ook snel toe. We beargumenteren dat onze bijdrage, in 3D scannen van schilderijen, momenteel vooral gericht zijn op de toepassing *'perceptual enhancement'*, alhoewel we ook voorzien dat 3D data van schilderijen zou kunnen bijdragen aan andere toepassingen zoals restauratie en behoud, en monitoring.[21] We laten zien dat de 3D data gebruikt kan worden om de craquelure patronen in schilderijen zichtbaar te maken, en daarmee de interpretatie van de conditie en conservering-historie kan ondersteunen (zoals besproken in Hoofstuk 6). Vooruit kijkend, zou multi-modaal scannen van de verschijningsvorm (inclusief kleur, topografie, glans en transparantie), mogelijk ook gebruikt kunnen worden voor uitgebreidere documentatie en monitoring van het uiterlijk van een kunstwerk, vergeleken met de huidige fotografie.

Digitale fabricage kan een breed scala aan toepassingen hebben in het domein van cultureel erfgoed, wat een impact kan hebben op diverse sub-disciplines van cultureel erfgoed zoals restauratie, educatie, creatief gebruik en dissiminatie.[22] We beargumenteren dat het werk verricht in de context van dit proefschrift, alsmede een scala aan verwante en vergelijkbare projecten, het potentieel laten zien van schilderijen reproducties voor een groot aantal van deze toepassingen. We laten zien dat onze schilderij reproducties gebruikt kunnen worden voor het maken van interactieve expositie toepassingen (ook voor specifieke doelgroepen zoals kinderen of mensen met een visuele beperking), gebruikt kunnen worden als een tijdelijke vervanging voor het origineel, en het mogelijk maken om 3D geprinte reconstructies

[21] R. Pintus, K. Pal, Y. Yang, T. Weyrich, E. Gobbetti, and H. Rushmeier, *A Survey of Geometric Analysis in Cultural Heritage,* Computer Graphics Forum, **35**, 1, (2016), 4–31

[22] R. Scopigno, P. Cignoni, N. Pietroni, M. Callieri, and M. Dellepiane, *Digital Fabrication Techniques for Cultural Heritage: A Survey*, Computer Graphics Forum **36**, 1 (2017), 6–21

te maken van het oorspronkelijke verschijningsvorm van een schilderij. Bovendien, laten deze projecten ook de mogelijkheden zien van de digitale fabricage techniek — *full-color material jetting* — voor een bredere applicatie in het domein van cultureel erfgoed.

Wanneer (3D geprinte) reproducties worden gemaakt met zo'n grote visuele gelijkenis met het originele schilderij, roept dit onherroepelijk vragen op ten aanzien van de immateriële kant van maken van dergelijk reproducties. Gebaseerd op de case studies die zijn uitgevoerd in de context van dit proefschrift (en andere gerelateerde cases) beargumenteren wij dat 3D geprinte reproducties van schilderijen hun eigen verdienste hebben en doel kunnen dienen, potentieel in aanvulling op de functie en esthetiek van het originele schilderij, net als ander facsimiles of kopieën zo'n doel dienen. We geloven dat reproducties onderdeel kunnen zijn van de oplossing tot het behoud en de verspreiding van cultureel erfgoed. Bovendien, geloven wij dat deze moderne, digitale reproducties eenzelfde rol kunnen spelen als hun historische (hand-gemaakte) tegenhangers, bijvoorbeeld in het verspreiden van kunst, herscheppen van (verloren gegane) kunst en het trainen van — in dit geval wetenschappers — in de ingewikkelde vaardigheden die nodig zijn voor het maken van bepaalde verschijningsvorm. Of en hoe reproducties uiteindelijk beoordeelt worden, is ook in sterke mate afhankelijk van de context, toepassing en de manier waarop het wordt geïmplementeerd. In ieder geval is het belangrijk — zelfs verplicht door de International Council of Museums[23] — dat het communiceert wordt aan de kijker, wanneer een reproductie wordt getoond in een museum context. Bovendien is een uitsluitend technische blik op de immateriële aspecten van het maken en toepassen van reproducties niet voldoende. We geloven dat deze vragen roepen om een bredere reflectie vanuit verschillende disciplines, zoals de museologie, kunsthistorie, restauratie en behoud, en kunst educatie.

Of een reproductie direct herkend wordt als zodanig, hangt af van een groot aantal factoren, zoals de context, het niveau van expertise van de kijker, maar ook de kijkafstand, verlichting en kijk condities. Op een reguliere kijkafstand kunnen een schilderij en reproductie verrassend veel op elkaar lijken. Echter, wanneer deze van *dichtbij* bekeken worden, zijn digitale reproducties duidelijk te onderscheiden van schilderijen door de specifieke manier van fabriceren — gebruik makend van een beperkte set van zes inkten en een andere fabricage techniek —.

Wij voorzien ook dat de kennis over het meten en fabriceren van de verschijningsvorm (die spatiaal variërende eigenschappen hebben) gebruikt kan worden als onderzoeks*probe*, voor onderzoek naar visuele perceptie. Omdat het ontwerpen van de verschijningsvorm cruciaal is voor het ontwerp van een product, voorzien we dat digitale reproductie van de verschijningsvorm ook hier nuttig toegepast kan worden. Producten waarvoor dit in het bijzonder van belang is, zijn protheses. Hiervoor moeten natuurlijk de mogelijkheden worden uitgebreid naar 3D scannen en fabricage. Hier voorzien we ook dat digitaal gefabriceerde verschijningsvormen, mogelijk gebruikt kunnen worden in combinatie met een techniek genaamd *optical mixing*, voor materiaal visualisatie-, communicatie- en selectie*tool*. Bovendien, zijn de kennis en vaardigheden, opgedaan over de reproductie van verschijningsvorm

[23] International Council of Museums, ICOM code of ethics for museums, (2017), Retrieved June 13, 2019

ook een noodzakelijk ingrediënt voor een meer doelbewuste en geïnformeerde aanpak in materiële verschijningsvorm synthese.

The case studies uitgevoerd in de context van dit proefschrift, waren beperkt tot het reproduceren van materiële verschijningsvorm van (geverniste) olieverfschilderijen. Dit maakt het lastig om de resultaten te generaliseren naar ander (verf) materialen en verschijningsvormen. Verschillende beperkingen van de huidige reproductie werkwijze worden ook onderkent, welke zijn dat de glans meting beperkt is tot (grofweg) platte oppervlakken, en dat er interacties zijn tussen de verschillende uiterlijke eigenschappen in termen van meting en fabricage. Bovendien, onderkennen we dat onze huidige aanpak voor glans calibratie niet onafhankelijk is van de gebruikte systemen, en dat kleur reproductie beperkt is tot een colorimeterische reproductie werkwijze. Het mogelijkheid om de resolutie van de verschijningsvorm metingen verder te verhogen worden beperkt door de scherptediepte van het optische systeem, het gene potentieel problemen kan geven bij schilderijen die vergaande krom-trekking vertonen of hoge impasto hebben. Ook biedt de reproductie werkwijze *geen* mogelijkheden voor de meten en fabriceren van metalen oppervlaktes, danwel speciale optische effecten zoals fluorescentie, parelmoereffect of glinstering. Bovendien is het bouwvolume van de print technologie beperkt in bouwhoogte (5 mm), ofschoon het wel een groot bouw oppervlak (1.2 m $\times$ 2.4 m) heeft, vergeleken met andere print systemen. En tenslotte, moet een systematisch onderzoek naar kleur, glans en topografie perceptie nog verder onderzocht worden, in de context van complexe, 'echte-wereld' materiële verschijningsvorm reproducties.

Conclusie

We concluderen dat we succesvol kleur, topografie en spatiaal-variërende glans van schilderijen kunnen reproduceren, op een geïntegreerde manier. Dit is bereikt door het combineren van 3D scannen — gebaseerd op *fringe-encoded stereo imaging* — met glans scannen — gebaseerd op reflectie polarisatie. Experimentele resultaten laten zien dat de methode voldoende snel is voor praktische toepassing. De resultaten tonen dat de door ons voorgestelde methode voor het uitbreiden van verschijningsvorm scannen met glans metingen, een waardevolle toevoeging is in het streven naar meer realistische reproducties, in termen van praktische toepasbaarheid — aantal beelden nodig voor het reconstrueren en snelheid — en zijn perceptuele toegevoegde waarde, wanneer deze wordt toegevoegd aan kleur en topografie reproductie. Voor het fabriceren stellen we een minimale set voor van slechts zes materialen, die bestaat uit cyaan, magenta, geel, zwarte, witte en transparante inkt.

Bovendien concluderen we dat 3D scan data van schilderijen — gemeten door middel van finge-encoded stereo imaging — een goede overeenkomst vertonen met andere, meer nauwkeurige 3D meetmethodes zoals 3D digitale microscopie en Multi-Schaal Optische Coherentie Tomografie (MS-OCT). Bovendien bleek onze 3D scan techniek meer geschikt voor het scannen van grotere oppervlakken — zoals een volledig schilderij — in termen van de individuele scan afmeting, de scan snelheid en flexibiliteit in resolutie. We laten zien dat de topografische data van een

schilderij (van alle technieken) gebruikt kan worden om de hoogte variaties van het oppervlak te visualiseren. Deze visualisaties kunnen een conservator ondersteunen in de beoordeling van de staat van het schilderij, en de noodzaak voor interventies bepalen.

De reproducties en 3D data sets die gemaakt zijn in de context van dit proefschrift, maar ook de custom-built scanning systemen, dienen als *demonstrators*, en vertegenwoordigen de kennis die gegenereerd is in dit project.

We stellen toekomstig onderzoek voor in diverse richtingen. De capaciteiten van digitale reproductie van verschijningsvorm kunnen bijvoorbeeld worden gebruikt om ons begrip van topografie en glans perceptie te vergroten, in het bestuderen van de verschijningsvorm perceptie, in complexe, 'echte-wereld' situaties, welke mogelijk kunnen helpen bij het bepalen van meer geschikte aanpakken voor hun reproductie. Bovendien stellen we voor om bestaande beperkingen op het gebied van het fabriceren van spatiaal-variërende glans en glans *gamut mapping* verder te onderzoeken. Daarnaast zou het incorporeren van translucentie meting en fabricage de mogelijkheden van verschijningsvorm reproductie sterk uitbreiden. On the bevindingen van dit proefschrift te kunnen generaliseren, moeten andere schilderijen of artefacten (gemaakt van andere materialen) worden gescand en geëvalueerd. The toepassing van verschijningsvorm data, alsmede fysieke reproducties kan verder worden onderzocht, specifiek in de context van cultureel erfgoed documentatie, monitoring en restauratie. Ook mogelijkheden voor het maken van reconstructie — van originele kleur, totale verschijningsvorm of het reconstrueren van missende (delen van een) schilderij(en) — dient verder te worden onderzocht, ook gebruik makend van domeinkennis van bijvoorbeeld kunstmatige intelligentie en *data science*. Wij zouden willen aandringen dat de toepassing van verschijningsvorm data, en fysieke reproducties wordt onderzocht en geëvalueerd in een brede multi-disciplinaire context, waarbij verschillende cultureel erfgoed subdisciplines betrokken zijn, zoals museologie, kunst geschiedenis, restauratie en conservering, en kunst educatie. Alleen dan kunnen we komen tot zinnige innovaties, en een consensus bereiken over hun nut en de toepasbaarheid binnen het domain van cultureel erfgoed. De uitbreding van verschijningsvorm reproductie naar werkelijk drie-dimensionale objecten is een uitdagende richting voor toekomstig onderzoek. Dit wordt ook relevant geacht buiten het cultureel erfgoed domein, bijvoorbeeld in het ontwerpen van prothesen.

En tot slot stellen we ons ook voor dat de verschillende inspanningen voor het reproduceren van verschijningsvorm kunnen worden verzameld in een praktisch *framework* voor verschijningsvorm reproductie, welke hulp kan bieden bij het kiezen van een geschikte meet- en fabricage techniek, in staat om een reeks aan verschijningsvorm-relateerde en andere eisen (bijvoorbeeld structureel, afmeting of functioneel gerelateerd), (het beste) te matchen. Dit *framework* moet worden ontwikkeld in combinatie met een theoretische onderbouwing van perceptie van verschijningsvorm, toepasbaar op verschijningsvorm meting en fabricage, welke de inspanningen ondersteunt voor verschijningsvorm reproductie en *perceptual enhancement*.

Glossary

2D (Digital) Printing The ability to fabricate two-dimensional variations on a substrate, using a set of instructions, which are digitally controlled.

2.5D Printing The ability to fabricate topographical variations in surface height, using a set of instructions, which are digitally controlled, though not capable of creating three-dimensional artifacts which have overhangs or undercuts — parts of the object which require the support of the 3D structure or a supporting material to be fixated in the intended location.

3D printing The ability used to additively fabricate three-dimensional objects, using a set of instructions, which are digitally controlled.

Appearance see *Material appearance*

Bitmap A binary material representation, denoting for every position (*Pixel*) the presence or absence of material. Bitmaps are generally the outcome of a *Halftoning* process. For *3D Printing* commonly a stack of bitmaps is used.

BRDF Bi-directional Reflection Distribution Function, are used to describe angular relations between incoming and outgoing radiation for a surface/material.

CH Cultural Heritage, in the context of this thesis, denotes (the domain dealing with) tangible cultural artifacts (but could also be natural objects), which have been passed on by past generations.

CIELAB A standardized three-dimensional, device-independent color space (also see *ICC-profile*).

CIEXYZ A standardized three-dimensional, device-independent color space (also see *ICC-profile*).

CMYK Cyan, Magenta, Yellow and Key(=Black), denoting the primary colors most commonly used in (digital) printing systems.

CMYKW Cyan, Magenta, Yellow, Key(=Black), and White, denotes the extension of the primary printing colors with White, used in printing to substitute the role of a white substrate in its contribution to color appearance, indispensable in 2.5D and 3D full-color printing (also see *CMYK*, *2.5D printing*, *3D printing*, and *Full-color printing*).

CMYKWT Cyan, Magenta, Yellow, Key(=Black), White and Transparent, denoting the six printing materials used in the context of this project (also see *CMYK*).

Color Appearance attribute related to the perception of material-light interactions caused by a material's capability to selectively absorb light.

Craquelure Crack patterns, as typically found in paintings, caused by to for instance aging and/or drying/curing of paint.

DPI Dots per inch, a commonly used unit to denote the printing resolution.

Digital Fabrication The ability to fabricate something based on a set of instructions, which are digitally controlled. Such a process can be additive (like *3D Printing*), subtractive (like CNC milling) or a combination of both.

Digital Printing The ability to fabricate an image (2D) of object (3D), based on a set of instructions, which are digitally controlled.

Facsimile A reproduction or copy of an cultural heritage artifact (or site/space), which resembles the original's (current) appearance.

Fabrication see *Digital Fabrication*

Full-color printing The ability to create a range of color appearances and smooth color transitions (in 2D and 3D) with a limited set of printing materials (also see *CMYK* and *Half-toning*).

Gamut The volume within a multi-dimensional space which defines the boundaries of appearance that can be reproduced. The gamut of color printing is typically defined in a three-dimensional color space (also see *CIELAB* and *CIEXYZ*).

Gloss Appearance attribute related to the perception of material-light interactions caused by a material's capability to reflect light in a specular fashion.

Half-toning The process of transforming a continuous gradient property definition (defined in 2D or 3D) into a discrete assignment of material for every *Pixel* or *Voxel*. This process in needed for printing as every position can only have one material assigned to it. In the case of color half-toning, this discrete, juxtaposition of different colors can create the illusion of a wide range of color appearances, and smooth gradients, through optical mixing — as the human visual system is not capable of discerning the individual dots.

ICC-profile An approach standardized by the International Color Consortium (ICC)[24] for transforming data, taken from calibration procedure(s), to characterize input and output devices, connecting them via a device-independent Profile Connection Space (PCS) (also see *CIELAB* and *CIEXYZ*).

Impasto (Deliberately) created three-dimensional variations on a painting's surface, for instance used by painters to create additional reflections for highlights, or emphasizing the textural appearance of the material they depict. Alternatively, three-dimensional brushstrokes can be the consequence of a fast-paced, expressive painting style.

Light The part of the electro-magnetic spectrum (roughly between 380 nm and 780 nm), which can be perceived by the human visual system.

Material appearance The physical, objective optical structure that a material leads to under a certain lighting. Appearance is thereby a the light-material-confounded proximal stimulus for the human visual system.

Material perception The interpretation of the human visual system of the physi-

[24] International Color Consortium, Standards that refer to ICC-profiles, (Accessed: May 25, 2019)

cal, objective optical structure that a material leads to under a certain lighting.

Metamer (Two) different material/illumination combinations, which have the ability to create a similar appearance.

Metamerism The perceptual effect where (two) different material/illumination combinations create a similar perceptual effect. The term is often used to denote the situation where, in changing a (illumination) condition, the difference or mismatch in appearance becomes apparent.

Painting A "moveable, largely two-dimensional images created for the primary purpose of providing a visual experience; ... Paintings may be executed on any type of support, including but not limited to: wood, textile, metal, stone, glass, and plastic".[25]

Pixel The smallest addressable element in a (two-dimensional) array, defining the data resolution. It can refer to a camera sensor *pixel*, digital image *pixel*, or printing *pixel* (also see *Voxel*).

Printing In the context of this thesis, printing refers to *Digital Printing*.

Relief Appearance attribute related to the perception of three-dimensional variations of a surface. Synonyms used in this thesis are *Texture* and *Topography*.

Reproduction The (virtual) or physical recreation of (the appearance of) an artifact (or site/space), which can be executed using a variety of techniques and materials.

Reproduction Workflow A collection of actions and procedures which needs to be followed to reproduce (a sub-set of) attributes, in this thesis related to appearance.

Reconstruction A visualization of a prior state of (the appearance of) an artifact (or site/space), which can be recreated virtually or physically, using a variety of techniques and materials.

RGB Red, Green, Blue, relating to the primary sensitivities of the human visual system to visible range of the electro-magnetic spectrum, also most commonly used as the primary imaging channels in (digital) photography.

Surface texture see *Texture*

Surface reflectance The interactions between material and light, at the outer boundaries of an object/material (i.e. its surface), which can exhibit spatial as well as angular variations (also see *BRDF* and *SVBRDF*).

SVBRDF Spatially-Varying Bi-direction Reflective Distribution Function, are used to describe spatial-angular relations between incoming and outgoing radiation for a surface/material.

Topography Appearance attribute related to the perception of material-light interactions caused by three-dimensional variations of a surface. Synonyms used in this thesis are *Relief* and *Texture*.

[25] International Council of Museums - Committee for Conservation, *ICOM CC - working group - paintings*, Workgroup web page, (Accessed: 28-May-2018).

Translucency Appearance attribute related to the perception of material-light interactions caused by a material's capability to transmit light, where light is scattered in the material (also see *Transparency*).

Transparency Appearance attribute related to the perception of material-light interactions caused by a material's capability to transmit light, where light is *not* scattered in the material (also see *Translucency*).

Texture In the context of this thesis, texture refers to: the appearance attribute related to the perception of material-light interactions caused by three-dimensional variations of a surface. Synonyms used in this thesis are *Topography* and *Relief*.

Voxel A three-dimensional pixel (see *Pixel*)

Visual appearance see *Appearance*

Workflow see *Reproduction Workflow*

1

Introduction

"Have you already taken a good look at all my intricately painted details, applied by mijnheer De Heem when he created me? Did you notice the cute little butterfly and quirky snail? And the small droplets dripping from the cut orange and peach? Can you imagine the prickly sensation on your skin, when picking up one of those thorny chestnut husks? It all looks so real, doesn't it? And how would those grapes have tasted? I wonder how mijnheer De Heem managed to paint all my details so well.

They say I look like a typical descendant of the 'Cornelis De Heem'-family. Apparently we have the same, recognizable look. I think, without exception, we are of the blood type 'Still Life'. I heard most of us have fruits or flowers depicted, many have both. My most opulent relatives even have depictions of oysters or lobster. But I must say, I have only met a few of them in real life. Then again, I must have met some of my relatives, closest to me in age, when I was created. I fear they did not make much of an impression on me at the time.

I also like to think that I remember something of my creation itself. Like the smell of the sweet grapes and citrus fruits, combined with a musty undertone of autumn leaves. But I can't say I do. Although, to be honest, that might be an overly romanticized version of my creation. Those fruits would probably not have smelled so nice by the time I was finished. And even likely, my own scent, a pungent mix of paint, oil and diluents, would have overpowered everything anyway. They say fresh paintings stink quite a bit."

— The painting

1

1.1. *Ceci n'est pas une peinture* (This is not a painting)

"Do you now believe me, and I am sincere, that I would give 10 years of my life if I could sit here for fourteen days with a dry crust of bread for food."

— Vincent van Gogh (anecdote translated from [1])

This is what Vincent van Gogh remarked to his friend Arnold Kerssemakers, when sitting in front of *The Jewish Bride* by Rembrandt van Rijn,[1] when he visited the recently opened Rijksmuseum in Amsterdam in 1885. From a letter he wrote to his brother, we know that he was not only mesmerized by the depiction of the painting, but also took inspiration from the Rembrandt's painting style:

"The best paintings - precisely the most perfect from a technical point of view - seen from close to are touches of color next to one another, and create their effect at a certain distance"

— Vincent van Gogh [2]

Now take a look at the printed image of this painting (Figure 1.1). Although we can appreciate the depiction of the figures, we do not perceive the full richness of a painted surface as we would, as if we were standing in front of the painting. We miss the richness of the color, and the three-dimensional texture created by the brush strokes. We cannot fully appreciate the way Rembrandt applied paint in thick strokes with a palet knife, to resemble the fabric of the man's sleeve. We also do not see the crack patterns — craquelure — in the paint layers running across the surface, showing us the effects of aging on the artwork. The typical shine of the painting's surface and translucency of the paint layers, giving the red dress a glowing effect, are also lost in this depiction. In short, the visual effect of a painting cannot be reproduced with a flat representation on paper or screen.

How fascinating would it be if everybody could experience what Van Gogh did over 100 years ago. What if this rich viewing experience could be provided to people around the world, without the need to visit the Rijksmuseum in Amsterdam. What if viewing paintings did not require visiting a museum that requires strict security and climate control? What if you could experience this in your own living room? Alternatively, imagine that all paintings of one artist could be brought together in an overview exhibition, to provide a full overview of a painter's oeuvre. This can be very challenging to achieve, due to issues like security and fragility of artworks for transportation. This fragility, was recently demonstrated in an announcement

[1] *Isaac and Rebecca, known as 'The Jewish Bride'*, by Rembrandt van Rijn (c.1665 - c.1669), oil paint on canvas, 166.5 cm × 121.5 cm, Rijksmuseum, Amsterdam, inventory no. SK-C-216

Figure 1.1: Depiction of *Isaac and Rebecca, known as 'The Jewish Bride'*, by Rembrandt van Rijn (c.1665 - c.1669), oil on canvas, 166.5x121.5cm, Rijksmuseum, Amsterdam (fair use permitted by Rijksmuseum)

by the Van Gogh Museum, that the famous *Sunflowers*, by Vincent van Gogh[2] will never leave the museum again [3].

Now also consider the aspect of time – the fact that a painting, like everything around us, degrades. *The Jewish Bride*, like all paintings, is subject to irreversible degradation over time. This is caused by (photo)chemical degradation (e.g.[4, 5]), treatments and restorations in the past, and not to mention acts of vandalism. This causes changes like discolorations, cracks in the surface, but also more profound changes, like elaborate over-painting of the original, or tears in the canvas. Currently, we only see the artwork in its current state, including all these changes, making it hard to imagine its original appearance. But what if the original appearance of an artwork could be recreated, as if it was painted yesterday? This is rarely, if ever, done or even possible with the original painting, as such interventions would damage the original, making them irreversible, and thereby considered unethical [6]. For example, varnish layers and old retouches, which were added to the *Sunflowers* in previous restorations, cannot be removed, as they have become mixed with the original paint [7]. What if there was a way to create this view into the past (or future), in a perceptually convincing way?

[2] *Sunflowers*, by Vincent van Gogh, Arles (1889), oil on canvas, 95 cm × 73 cm, Van Gogh Museum, Amsterdam (Vincent van Gogh Foundation), inventory no. s0031V1962

1

1.2. A painting

"We do not know how art began
any more than we know how language started."

— E.H. Gombrich [8]

Some of the oldest forms of art known to us, were arguably created as early as 30.000 BC [9, 10]. Cave paintings show us mankind's early skills to use a colored substance to create depictions (on a wall). Following a wide range of innovations, the means and skill to create depictions in the form of paintings — using a wide of materials to paint and as substrate — has greatly evolved. Going forward we define paintings to be: "moveable, largely two-dimensional images created for the primary purpose of providing a visual experience; ... Paintings may be executed on any type of support, including but not limited to: wood, textile, metal, stone, glass, and plastic." (from ICOM-CC [11]). Ancient Greek, Roman, Egyptian and medieval paintings were painted with encaustic or tempera on panels. In the 15th century oil paint became a popular painting material, applied on wooden panels and canvases. With the invention of the paint tube, and the development of synthetic pigments and colorants, from the 19th century onward, the variety and ways to use paint grew tremendously. Nowadays an even wider variety of painting materials is available to artists, including acrylic paints, all types of paint in seemingly endless color shades. There are even paints showing optical effects like fluorescence, sparkle, and pearlescence.

Nevertheless, painters - even of early tempera paintings - already had a range of colorants and pigments to their disposal, and had extensive knowledge on material processing and application, which was passed on for generations [12–14]. Painters were skilled craftsmen in the use and application of these materials. For instance painters might intentionally apply paint thickly, creating a 3D effect, in order to achieve a specific optical effect. Besides the initial application by the artist also effects of aging, conservation and restoration treatments, influence the physical state of a painting, and thereby influences its appearance. The result is that the appearance of a painting is not static, that it has changed over time and will continue to do so.

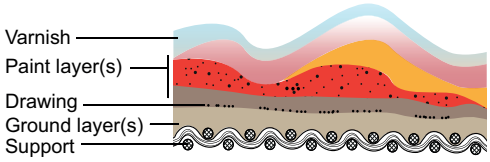

Figure 1.2: Schematic depiction of the layer build-up of a painting, showing the support (canvas in this case), ground layer(s), upon which a underdrawing or sketch might be drawn, followed by one or multiple paint layers, and finally a layer of protective varnish.

The surface of a painting is therefore rarely completely flat, and is generally built up as a complex stratigraphy of layers. A schematic depiction of such a layered structure is shown in Figure 1.2. Generally speaking, a painting consists of a support e.g. a canvas or panel, ground layer(s) and one or multiple layers of paint, ranging from completely opaque to semi-transparent glazes. In many cases a painting also has a protective varnish layer. Paint itself is comprised of a binding medium (i.e. a transparent fluid like egg yolk, oil, or more modern acrylic polymers) combined with a colorant (soluble) or pigment (non-soluble). As the name suggests, the binder functions to bind the pigments together and provides adhesion to the substrate.

1.3. Facsimiles and cultural heritage copies

Many examples exist of reproductions - or facsimiles - of artworks. In the past reproductions were made for instance to disseminate the artwork — simply creating copies — or replace a disintegrating work of art, or in order for (apprentice) painters to learn the skill of painting. In more recent times, the reasons for making reproductions generally boils down to two main goals: creating wider access to art and/or an attempt to preserve or restore the original work of art. Facsimiles of ancient scrolls, manuscripts and books are often made to limit handling the fragile originals. There are even companies specializing in the craft of creating such facsimiles (e.g. [15]). Also complete cultural heritage sites have been recreated - like the Caves of Lascaux [16] or the Tomb of Tutankhamun [17] - to safeguard the original location against the harmful influences of the large amounts of visitors to these sites, whilst at the same time providing access to its heritage, through the reproduction. Individual paintings have been recreated too, for instance show them to the public, as the original is located in a private collection or restore them to their original location (e.g. [18, 19]). Figure 1.3 depicts such a recreation, showing (a) the original painting *The Wedding Feast at Cana* by Paolo Véronèse in the Louvre Museum (Paris, France) (in the background), and (b) the facsimile in the painting's original location in the monastery's refectory of the Basilica of San Giorgio Maggiore (Venice, Italy), created by Factum Arte [18].

In Japan there is even a complete museum dedicated to reproductions of the world's most famous artworks [20]. It is important to note here, that historical and (non-western) cultural attitudes to copying and copies can be quite different to contemporary, western ideas on these topics [21]. Furthermore, there are research initiatives (e.g. [22]) as well as commercial ventures (e.g. [23]) that aim to visualize the original appearance of artworks, for instance attempting to revert the effects of aging, by rejuvenating the color appearance.

Currently, a large proportion of reconstructions only resides in the digital realm, displayed on screens, thereby missing the essential materiality of the artworks: lacking the detail, appearance and often the scale of the original. Many other facsimiles are made using a combination of digital technology and many hours of highly-skilled craftsmanship. Either due to the lack of materiality, or the vast amount of labour (and therefore money) needed to create these facsimiles, the application of them is limited. However with the continued technological development this might change in the near future.

Figure 1.3: (a) The original painting *Wedding Feast at Cana*, by Paolo Véronèse[a] (in the background) in the Louvre Museum, Paris, and (b) the facsimile at the painting's original location in the monastery's refectory of the Basilica of San Giorgio Maggiore, Venice, created by Factum Arte [18] (courtesy of Factum Arte).

[a] *The Wedding Feast at Cana*, Paolo Véronèse (1563), oil on canvas, 6.77 m × 9.94 m, Louvre, Paris, inventory no. 142

1.4. Advancements in imaging and digital fabrication

Developments in imaging systems and printing technologies provide new opportunities to create physical (as opposed to virtual) reproductions of objects with complex material appearances, like paintings.

With the newest high-end imaging sensors, high-resolution measurements of an object's appearance can be made. Ongoing developments in digital photography (e.g. with even increasing pixel counts), combined with new image processing algorithms, keep increasing the possibilities to extract information about for instance an object's shape and appearance.

2D printing technology has developed from a technique able to create black-and-white prints based on digital input (in the early 1980s) to full-color printing for applications like graphic arts (e.g. posters, banners, car stickers). This has now evolved further into what is phrased as *2.5D printing* or *elevated printing* [24]; the capability to create full-color prints with height variations (up to several centimeters). Innovations in print materials and printing strategies, offer the potential to create an even wider range of appearances (e.g. spatially-varying gloss [25]), visualized in Figure 1.4.

Parallel to that, 3D printing has evolved from prototyping oriented applications (e.g. making visual/tangible prototypes of products to be manufactured using other techniques), to technologies which themselves are used to fabricate functional components/products. Affordances of 3D printing techniques are for instance their capability to fabricate complex shapes and unique, ultra-customized products. Also systems have been developed capable of multi-material 3D printing (e.g. [26, 27]). Being able to combine materials, defining the material properties per voxel —a

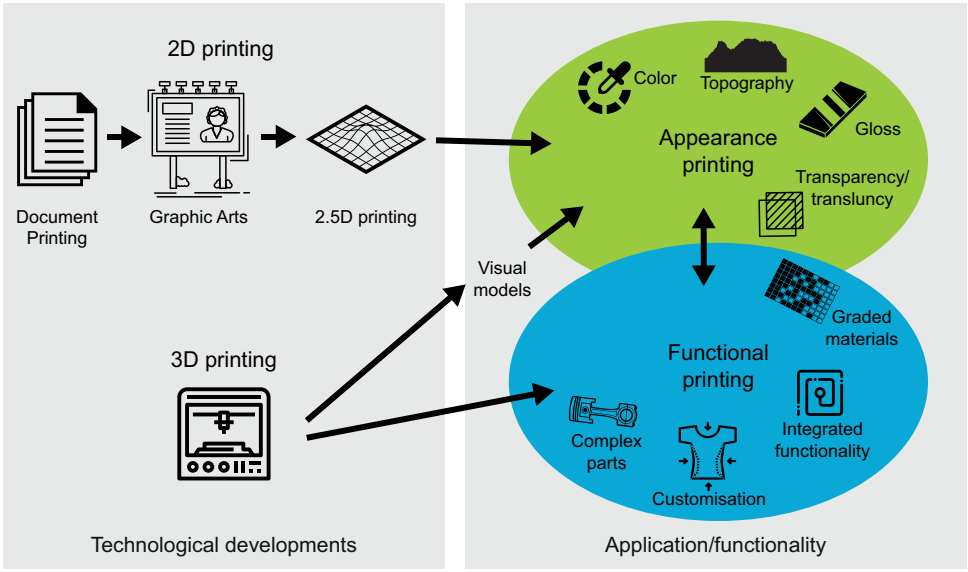

Figure 1.4: Developments in 2D and 3D printing technologies.

three-dimensional pixel —allows for a great expansion of potential applications. This allows for function integration: for example by grading materials, where one property slowly transitions into another (e.g. going from flexible to rigid), new mechanical designs might be created (e.g. [28]). Another example of function integration is 3D printed electronics(e.g. [29]). In terms of appearance printing, multi-material 3D printing essentially merges with the advancements of 2.5D printing, where multiple materials can be combined to create variations in appearance (e.g. [30, 31]). The developments and merging of 2D and 3D printing capabilities are visualized in figure 1.4. Of course, applications might also be envisioned where both appearance and functional requirements, are achieved through 3D printing (e.g. in prosthetics [32]), consumer products [29]), interactive 3D reproductions of paintings [33, 34]).

Although these new systems are technically capable of accurately capturing or fabricating one or several aspects of an object's appearance, currently there is no approach integrating the reproduction of the various appearance modalities like color, gloss, shape (or topography) and transparency/translucency. This presents an opportunity for developing an integrated workflow, which can reproduce the various attributes of an object's appearance.

1.5. Material perception and appearance reproduction

A wide range of research domains deal with aspects of material appearance among which are: psycho-physics — studying the relationship between physical stimuli and the perceptional effects they produce —, (3D) imaging, computer graphics, appearance metrology, optics, and 2D/3D printing. Advancements in these fields, related to material appearance perception, capturing, modeling and fabrication should be studied and combined to develop an integrated reproduction workflow. In the following paragraphs we aim to exemplify how knowledge from these domains is relevant for appearance reproduction and the evaluation of these reproductions. In addition, more details can be found in the following chapters: an overview of gloss perception and reproduction can be found in Chapter 3; Chapter 4 incorporates related work on color, topography and gloss capturing and fabrication; and more details on 3D scanning techniques, suitable for capturing paintings, can be found in Chapter 6.

1.5.1. Material perception

If we want to replicate material appearance, we need to understand how (the appearance of) material is perceived. Here we define appearance as the physical, objective optical structure that a material leads to under a certain lighting. The material itself is what is called the distal stimulus. It cannot be observed directly, but has to be lighted, and via the light that is scattered by the material humans can perceive it. Appearance is the light-material-confounded proximal stimulus for the human visual system (HVS). The HVS then needs to interpret the appearance to infer the material (and lighting) from it. These inferences are in general not 1-to-1 related to the actual physical properties, because it has no unique solution. Consequently, perception of material is subject to all sorts of interactions between its physical parameters, to perceptual biases, and dependent on task, context, etcetera. Even though we see, recognize and interact with a vast number of materials every day, and can effortlessly distinguish between them, it turns out that the perceptual mechanisms that underlie this, are still quite poorly understood. As stated by Adelson [35], and more recently Fleming [36], contrary to the vast amount of literature on object perception, there is much less research on understanding material perception. Nonetheless, the knowledge that was up to date generated about this topic should be taken into account, and will hereafter be discussed.

Material recognition and categorization

A part of material perception research deals with the understanding of material recognition and/or categorization (summarized by Fleming [37]). If we recognize a material (class) as such (for example as metal), this usually goes together with a set of associated attributes (in the case of metal for instance smooth, hard, cold, glossy). Fleming *et al.* [38] showed that ratings on nine subjective attributes (e.g. glossiness, colorfulness, hardness, roughness) of real-world material photographs

were systematically related to class membership (e.g. metal, paper, stone) with a 90% accuracy. In other words, those sets of attributes or *material signatures* as Fleming called them, are key ingredients of our perception of a certain material. Zhang *et al.* [39] confirmed the structure of this material space using a limited set of canonical material modes and showed how it interacts with lighting in a predictable material-specific manner. Recently, Van Zuijlen *et al.* [40] found a similar space for materials *depicted* in paintings. From these studies it is impossible to conclude which optical or image features are the main determinants for the recognition of the materials as such. But importantly, we can conclude that for recognition of a material as such and thus for rejection or acceptance of a reproduction's appearance as part of the class of material(s) it is trying to replicate — in our case paint —, its *material signature* is key. The material signature of paint was not tested in the studies above, but it can safely be assumed that the set of attributes listed above will together determine that. Insights into the specific ratings (or attribute weights) and variety within the category (oil) paint could potentially help to create better reproductions. However, as such mechanisms are still poorly understood, currently the approach of closely matching the optical properties related to those attributes (e.g. the gloss, colors, hardness, surface structure), is the most viable approach to create the best possible matching appearance.

Estimating material properties and parameters

Another approach to material perception research is the estimation of material properties and parameters, taking a more in-depth focus into the perception of individual attributes. Fleming [36] stated that these studies broadly fall into two classes; estimation of optical properties (e.g. glossiness, translucency) and the estimation of mechanical properties (e.g. viscosity, elasticity). We found that the perception of appearance is generally clustered into the perceptual attributes; color, topography/texture/shape, gloss and transparency/translucency (e.g. [41, 42]). Although we might intuitively link these perceptual attributes to specific (physical) material properties: for instance linking selective spectral absorbance to color perception, or linking surface reflectance of light to gloss perception, research has shown that there is certainly not a simple one-to-one correspondence between a single physical phenomenon and perceptual attribute. For instance, multiple studies have found that the perception of gloss and 3D texture/shape influence each other [43–46]; whereas only a one way influence, texture height influencing gloss perception, was found using 2.5D-printed samples [47]. It has also been found that illumination characteristics (i.e. light fields) influence the judgements of glossiness [48–54]. The implication of this is that it is very hard to study the reproduction of appearance, whilst focusing only on one or part of the appearance attributes. As all these attributes perceptually interact, a failure to capture and/or fabricate one attribute accurately could influence the evaluation of another. For instance, if the reproduction of a painting's topography were inaccurate or somehow different to the painting, this could potentially influence the judgment of the gloss reproduction. Additionally, we should be aware of the illumination conditions in which painting and reproduction are evaluated, as this might also influence the judgement of for instance gloss.

With the existence of these perceptual interactions (appearance attributes and illumination/viewing conditions), we might ultimately be able to 'boost' one attribute, to effectively enhance another. Also Fleming [36] speculates on the existence of such (quasi-)metamers for material appearance, for a range of practical viewing and illumination conditions. He does however point out, that it is then probably also possible to come up with a condition in which this apparent similarity will not hold. Considering the current (lack of) understanding of such metamers it is thus reasonable to strive for physically exact reproduction instead of trying to implement attribute interactions.

Color perception Of all, color perception has been the studied longest, with some theories, on for instance color discrimination, already dating back to the 1930's. This has led to, for instance the establishment of standard illuminants [55] and standard observers [56]. For a large part the functioning of cameras and printers is based on this knowledge – this is why cameras have an Red-Green-Blue (RGB) 2D sensor-array and why printers print in small dots, using Cyan-Magenta-Yellow-Black (CMYK) inks, creating the desired color, through additive and subtractive color mixing, respectively. Nonetheless, we should realise that color is a perceptual construct, and therefore subjective. There is no one-to-one relation to the physical (objective) spectral properties of a material, exemplified by the fact that for instance pink, brown and purple are not part of the spectrum. This as also led to the transition of approaching color as a linear spectrum, to the adoption of three-dimensional color spaces (like *CIELAB* and *CIEXYZ*) [57]. In more recent times the topic of color perception has been revisited, in an effort to better understand color perception for instance in complex environments and light fields — as we encounter them in everyday life. The influence of (complex) illumination on color perception is studied at length (overview in Maloney and Brainard [58]), as well as the interaction between color and other surface properties (e.g. [50, 59–62]). Research seems to suggest that the perception of color is relatively constant under varying glossiness and in natural illumination conditions, although small effects of material properties on perceived color have been found (e.g. [61]). This color constancy effect however, should not be confused with color differences that can be experienced (for instance in printed reproductions), as a consequence of problems with, or even technical impossibilities of matching the colors of original and printed materials. In this case, two perceptually (seemingly) identically colored materials can appear different when viewed under illumination with different spectral properties (also see Section 1.5.2).

Gloss perception Gloss perception has also been long studied, in an effort to understand its dimensionality; many focusing on linking gloss perception to measurable parameters (see Section 3.2 for more details). In early work by Hunter [63] (1937), he suggests that there might be up to six kinds of gloss. Later research by O'Donnell and Billmeyer Jr. [64], Billmeyer and O'Donnell [65] (1986 & 1987), using a limited set of painted samples, and other studies, using computer renderings to research gloss perception [66, 67], found two dimensions to describe gloss

perception related to distinctness-of-image gloss and contrast gloss.

Furthermore Leloup *et al.* [68] provide an overview of aspects that play a role in gloss perception: illumination, object properties, and viewing conditions, including for instance binocular vision and motion. Studies find a non-linear relationships between gloss measurements and gloss perception on achromatic and chromatic painted samples [52, 69]. However, Leloup *et al.* [68] point out, as was already known, that these types of existing gloss measurements relate poorly with gloss perception. Therefore, they conclude, new ways of measuring and describing gloss should be developed taking into account these influencing parameters. We might therefore conclude, that with the lack of understanding the underlying gloss perception principles, there is at least one parameter that has to be measured without any doubt, namely the peak reflection for any given point — commonly found at the incident illumination mirror angle — as this relates to the distinctness-of-image gloss as well as the contrast gloss (relative to the diffuse color).

Recent work has also focused on relating image statistics to the perception of gloss. Although Motoyoshi *et al.* [70] propose that the luminance histogram skewness can explain variation in gloss perception, it was later found that this statistic alone cannot explain all variance, specifically not for non-rendered images (e.g. [71, 72]). Wiebel *et al.* [72] found a combined effect of skewness and contrast (standard deviation) of the histogram, where the latter was actually found to be a better predictor of perceived gloss. Marlow *et al.* [73] proposed a model focusing on particular image cues, namely characteristics of specular highlights. Based on this model, Marlow and Anderson [74] found specular highlight contrast, coverage and sharpness to predict gloss perception. Similarly, Di Cicco *et al.* [75] found gloss contrast and blurriness, but not coverage, to predict a large part of the variance in perceived gloss on painted grapes in 17th paintings, suggesting that painters at the time also had implicit knowledge of such relations and effects. These studies have in common that highlight contrast is always found to be a factor for gloss perception. This is also directly related to the peak reflection, typically found at the mirror reflection angle.

Topography/texture perception Following Anderson [41], (the perception of) three-dimensional shape variations might be categorized in three (rough) categories: microscopic scale, which plays a significant role in surface reflections but cannot be distinguished with the naked eye; mesoscale, describing the coarseness of the surface (what would be called 3D texture or topography); and finally the macroscopic scale, which we would generally describe to be the shape of an object.

Various studies found that the mesoscale as well as the microscale roughness influence the perception of roughness or gloss [76, 77] of a surface, where it was found that the microscale roughness had a linear relationship and the mesoscale roughness a non-linear resolationship to the perceived glossiness. In these studies the perceived gloss scale is based on (a large number of) relative judgements of rendered stimuli with varying roughness. Also here, we should therefore be aware that the measurement and fabrication of one attribute (i.e. topography) can influence

the perception of another (i.e. gloss). In the case of this non-linear relationship, it is important to be aware of (potential) errors at different scales, which can create specific scale-dependent effects.

Pont and Koenderink [78, 79] show that a combination of global image statistics and spatial structure of 3D textured surface images, can be used on infer illumination (i.e. light field), which in turn can help to estimate other surface parameters. Ho *et al.* [80] find that changes in viewpoint lead to systematic errors in the estimation of topographical height variations. The underlying mechanism, where illumination and texture interact, as also described by Belhumeur *et al.* [81], was implemented by Schuller *et al.* [82] to create convincing bas-reliefs from 3D shapes. Similarly, these type of interactions, might allow, for instance, to emphasise topographical features in reproductions.

Other studies, where the characteristics of this mesoscopic scale are used, is in their role in the estimation of mechanical properties of materials, like viscosity or elasticity (discussed in [35, 36, 41], and their relationship studied in e.g. [83, 84]). This is of course also relevant, as we might see the resulting shape of (thickly) applied paint, as a consequence of its original viscosity and elasticity (and later its rigid form, which has aged, underwent treatments etc.). Therefore, the resulting shape(s) (now solidified) might be indicative of the (initial) material properties, and therefore an important discriminator for the recognition and categorization of (oil)paint.

Transparency/translucency perception The perception of transparency and translucency relate to the transmission of light in materials, where in the case of translucency light is scattered in the volume of the material (i.e. like wax or human skin), where transparent material lack this scattering (i.e. like clear water or glass). Perception literature on transparency and translucency, focuses on various mechanisms which might explain their perception. Early work, based on ideal thin films found that we can perceive (the illusion of) transparency in situations when a background (with at least two colors) is partially visible through a transparent filter and partially directly, creating so-called X-junctions at the intersection of layers [85–89]. Koenderink *et al.* [90] found that Kubelka-Munk two-flux theory [91] — commonly used to model reflection and transmission of light in colored layers, like paint(ed) layers — can be used to model the transparency effects of these type of experiments. However, they also state that using this theory "is difficult because the number of possible interpretations is very large and possibly involves additional scene parameters" (e.g. like illumination direction).

Others focused on the effect of light refraction, rendering glass-like blobs in an environment [92], suggesting we likely use the degree of distortion of the background for estimating the refractive index of a material. Also perception of translucent materials was explored rendering 3D shapes under varying lighting conditions, showing that the illumination but also the phase function (i.e. backward of forward scattering of light in the material), relates to our translucency perception [93, 94]. They show that especially in back lit illumination conditions, translucency is very visible. Furthermore, Vu *et al.* [95] actually used 3D printed samples, with varying

translucency, to study the relationship between light transmittance and perceptual translucency.

Although Sayim and Cavanagh [96] show that an understanding of many of these principles has long been used by artists to *depict* transparency or translucency, we postulate that these mechanisms do not necessarily play a role in (the perception of) (semi-)transparent paint layers (i.e. varnishes and glazes) themselves. We do not typically find these X-junctions in paintings (created using transparent overlays), rather painters probably create this type of transparency illusion by mixing lighter or darker paint (to create X-junctions). Also these (semi-)transparent paint layers are very thin, therefore we assume the effects of refraction are negligible. Furthermore, the translucent effects created by light scattering in a volume (as in [93, 94]), do not seem to apply for paintings (and also not the back lit illumination condition).

As is already investigated for different types of varnishes, their predominant effect on a painting's appearance is the reduction of surface roughness [97–101], thereby influencing the gloss and apparent color saturation. In the case of varnishes, it was found that the spectral absorbance was actually minimal [100]. Based on preliminary work, we postulate that glazes probably create their visual effect, partially by influencing the surface roughness (similar to varnishes), as well as creating additional selective spectral absorbance, thereby changing the color appearance (for instance creating more intense black) [102]. However, more research is needed, to confirm this hypothesis.

1.5.2. Appearance reproduction

There are already various approaches to capturing and reproducing one or multiple attributes of appearance. The following paragraphs give a short overview of advancements in appearance capturing, modeling and fabrication. More details can be found in Section 4.2. We predominantly discuss methods targeted at capturing and/or fabricating the appearance of planar (but non-flat) surfaces (like paintings, bas-reliefs, parchments, and fabrics).

2D Color reproduction

The vast majority of 2D color reproduction employs principles of colormetric color matching, capturing appearance using RGB sensors and printing using CMYK inks. Guidelines (for cultural heritage imaging) and well established standards exist for these workflows [103–105].

A theory that has been foundational to the (paint and) printing industry is the Kubelka-Munk theory [91], also referred to as the two-flux theory. This theory can be used to model absorption and scattering of light, in translucent, colored layers, applied on opaque, scattering substrates — this often being the case for ink layers. Consequently the theory can be used to estimate the needed concentration and/or amount of (mixtures of) ink(s), to create a certain color appearance. Although the theory relies on many assumptions (e.g. assuming diffuse illumination, uniform distribution of colorant in the layer, uniform scattering and absorption throughout the layer, and ignores surface reflection) — which are generally not met in reality — it it is still forms the basis of much of the color science to this day. Extensions

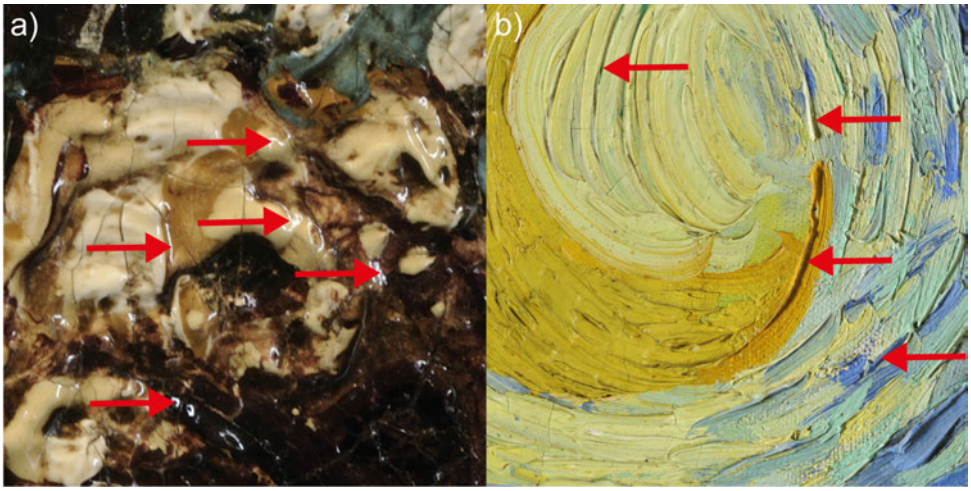

Figure 1.5: Two photographic details of paintings showing interactions between color appearance and surface reflections, shadowing and shading where a) show an example of highlights that are visible on the *Night Watch* by Rembrandt van Rijn,[a] and b) shows shading and shadowing on *The Starry Night* by Vincent van Gogh.[b] Some examples areas are indicated with arrows (Images from Google Arts & Culture, fair use permitted by Rijksmuseum and Moma)

[a] *Militia Company of District II under the Command of Captain Frans Banninck Cocq, known as the 'Night Watch'*, Rembrandt van Rijn (1642), oil on canvas, 379.5 cm × 453.5 cm, Rijkmuseum, Amsterdam, inventory no. SK-C-5

[b] *The Starry Night*, Vincent van Gogh, Saint Rémy (June 1889), oil on canvas, 73.7 cm × 92.1 cm, MoMa, New York, inventory no. 472.1941

of this theory (i.e. the four-flux model) and work to improve the implementation of these more complex models — also for relief and 3D printing (e.g. [106–108]) — is still an active field of research.

Photography, combined with (2D) full-color printing, can be used to reproduce color appearance (of paintings). However, in many cases the effects created by other appearance attributes, like the glossiness or topographical variation of the surface, on the color appearance are not completely eliminated. This leads to for instance highlights as light spots, and shadowed and shaded areas as darker areas in an image. If this is then printed, illuminated and viewed, these artifacts can 'break' the illusion of its original appearance. These effects are depicted in Figure 1.5. An approach to minimizing such highlights, shadows and shading effects in painting imaging has been proposed by Berns *et al.* [109] (also for the purpose of archiving and computer rendering). This does however, make the photography more complicated, with additional captures and computation to come to the resulting image, possibly limiting its uptake as a standard practice. Furthermore, in this work they assume that the specular reflectance is uniform across the surface, and can therefore be approximated with a reference sample measurement, represented in a bi-directional reflection distribution function (BRDF). In line with their concluding remarks, we argue (and found) that this uniformity is indeed not the case for

many real-world cases, and therefore the spatial variation should also be captured (and reproduced).

As colormetric color matching and the use of only four inks has limitations in terms of color reproduction (metamerism and limited gamut), several approaches have been proposed for multi-spectral color reproduction [31, 110–113], using between five and ten inks. However, as also mentioned by Berns [110], the improvements in color accuracy for creating printed reproductions, might only be relevant for relatively few high demanding applications, like painting reproduction and high-end photography printing.

3D Color reproduction

Although 3D color printing technologies have been around for quite some time, for instance binder jetting [114] and sheet lamination [115], since several years various new full-color 3D printing systems have become available, based on 2D inkjet printing combined with material extrusion [116], (multi-material) binder jetting combined with powder bed fusion [117] and multi-material jetting technology [24, 27, 118, 119]. Specifically the latter technologies are deemed interesting for material appearance reproduction due to their higher resolution, smooth surface finish, voxel-by-voxel control of material placement, which (potentially) allows for the creation of complex spatially-varying appearances, including translucency. Following the introduction of these new fabrication capabilities, various workflows for full-color 3D printing have been proposed, either, using or mitigating the effects of the printing materials' translucency [30, 31, 120–122].

Topography reproduction

There are various techniques capable of capturing fine topographical surface variations, which have been demonstrated for capturing paintings details (like cracks and brushstrokes): three-color laser scanning [123–126], structured light [127–130], and focus variation microscopy [131, 132], although the latter had up to recently not been used to capture larger areas or a complete painting (more details in Section 6.2). In terms of appearance capturing (and fabrication), it makes most sense to use an approach which has inherent alignment of topography to color (and other attributes), eliminating the need for (computational) alignment and avoiding potential visual artifacts due to misalignment.

Other passive imaging methods (not using illumination patterns or structure for 3D scanning) have also been used to capture topographical variations (and color) of planar artifacts. The use of photogrammetry to capture a stone bas-relief is shown in Figure 1.6. However, as can be seen from Figure 1.6(b) and (d), — showing the scan without color information — the level of detailing in the topographical data is limited (even with high resolution and a structured image capturing approach). This is not necessarily a problem for computer renderings, as this lack of three-dimensionality can be 'masked' by the color overlay (which also includes shading in and shading effects). However, such data is less suited for creating 3D printed reproductions, as the fine topographical details are needed to create the actual 3D shape (i.e. the perceptual ambiguity is more easily violated with physical reproductions, due to variations in lighting and viewing angles).

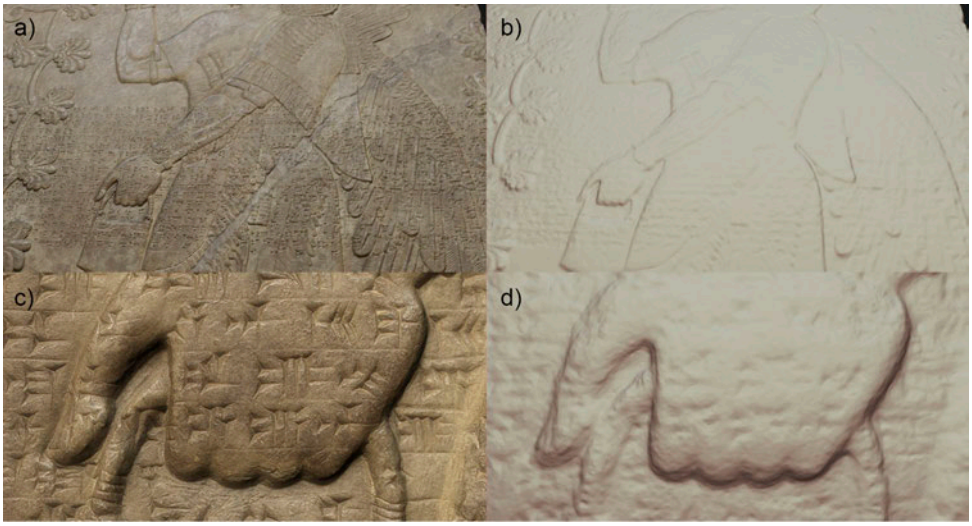

Figure 1.6: Snapshots of two interactive 3D models of *Assyrian Genie Bas Relief*,[a] (a-b) overall 3D model, (c-d) high resolution 3D model. (b, d) the topography rendered as a white, matte surface, excluding the color information (Courtesy of Cultural Heritage Imaging)

[a] Eagle-Headed Deity, Neo-Assyrian Period (9th century B.C.), gypseous alabaster, 223 cm × 211 cm × 8 cm, Los Angeles County Museum of Art, Gift of Anna Bing Arnold, inventory no. 66.4.4

Several 3D scanning systems [125, 126, 130] have been combined with 3D printing systems to create printed reproductions [24, 118] (limited to examples combining topography with full-color printing, also see Section 6.2). Other approaches to topography (and color) fabrication have also been used for painting reproductions, for instance combining milling, 2D printing, and hand painting (e.g. [133]). For other (painting) reproductions few details were made public about the exact reproduction process [134].

Although there are many studies dealing with the dimensional and geometrical accuracy of 3D printing (e.g. [135, 136]), its effect on perception does not appear to have been systematically investigated (yet), despite various mentions of its importance for a range of 3D printing applications (e.g. in [137–142]). Aspects influencing the appearance of 3D prints that have been researched are for instance: the effect of slicing and support material positioning (e.g. [143, 144], and effect of printing parameters on appearance (e.g. [145]). Furthermore, we should realise that in the full appearance reproduction workflow, the scanning as well as the printing can be cause of topographical differences. The confounding effect of both should therefore be investigated and disentangled.

(2D) Gloss reproduction

A range of approaches have been suggested to capture and represent appearance of (roughly) flat surfaces exhibiting (spatial) gloss variations, mainly for the purpose of creating computer renderings (more details in Section 3.2 and 4.2). Specifically approaches which capture spatial variation, and with high angular sampling density (e.g. [146–150]) are deemed suitable for capturing glossy surfaces of (varnished) paintings. However, these techniques do all require a large number of images of every area to be able to extract the (gloss) appearance parameters. Combined with demanding requirements for the spatial resolution needed for printing (>300dpi [151]), relative to rendering, these approaches become very data and time consuming. This can turn out to be problematic when, for instance a museum restricts scanning of (famous) artworks to their closing hours.

For the fabrication of spatially-varying gloss various approaches have been suggested using adapted 2D printing systems: combining inks with various reflectance properties [152], combining a mono-color 3D printed micro texture with a reflective layer and a (2D) color print [153]; changing the printer parameters to influence the micro-structure of printed surfaces and thereby the gloss [25]; or half-toning a transparent ink on top of a color print [154]. The latter approach is deemed the most viable in terms of practical applicability (limited number of inks needed), flexibility (can be manipulated independent of sub-layers) and accuracy (in terms of registration).

Translucency reproduction

Up to this day the measurement of sub-surface scattering remains challenging. Various approaches have been suggested based on: point-by-point measurement using laser illumination (e.g. [155]); line/area measurement in a frontal and through-lit setup (e.g. [156, 157]), or specifically for human skin, whereby knowledge of the layer stratigraphy is taken into account (e.g. [158, 159]). The first two approaches are not deemed viable due to extensive acquisition time, and our expectation that paintings are too opaque for through-lighting, respectively. Imaging of the layer stratigraphy has also been applied on paintings, using Optical Coherence Tomography (OCT) (e.g. [160]), whereby recently the step was made to scan larger areas of a painting (see Chapter 6). It remains to be investigated whether such approaches could be combined to estimate sub-surface scattering properties of paint layers. Furthermore, it remains to be investigated if the sub-surface scattering actually significantly influences visual perception, for it to be useful to measure and replicate (see above paragraph of transparency/translucency perception).

The results of some of these capturing approaches were used to fabricate objects exhibiting sub-surface scattering using a mix of fabrication methods [161], as well as two-color 3D printing [162]. Recently approaches have been suggested for full-color 3D printing, including sub-surface scattering [122, 163], whilst other specifically present approaches to mitigate the effects of sub-surface scattering, which for instance cause blurring of fine details [120, 121].

1

1.6. Research aim, questions, and methodology

To explore these new possibilities of appearance reproduction, reproducing a painting's appearance will be used as case studies in this thesis. Their surfaces are complex in nature: within and between paintings a wide variation in color, topography, gloss and translucency can be found. On the other hand, by focusing on the appearance of paintings, the research scope is also confined. In other words, this limits the research scope from attempting to reproduce a virtually unlimited number of material appearances that can be found in the physical world around us, to the reproduction of one type of material appearance, namely (oil-)painted surfaces. Furthermore, as exemplified in the above, we also envision a range of applications for such life-like reproductions.

1.6.1. Creating life-like reproduction of paintings

The main aim of this PhD thesis is to:

Develop an integrated 3D scanning and 3D printing system for the reproduction of the material appearance attributes of color, topography and gloss of paintings

More specifically, the aim is to create a perceptually matching appearance, by using a digital capturing and digital fabrication process. This also means using different materials and a different stratigraphy of layers than the painting. This is illustrated in Figure 1.7. The left part shows a schematic cross-section of a painting, comprised of a support (a canvas is depicted here), ground layer(s), possibly an underdrawing, paint layer(s) and a varnish. The digitally fabricated reproduction on the right is also built up on a support, in multiple layers of ink-voxels, using only a limited number of inks, with varying optical properties (here represented by Cyan, Magenta, Yellow, Black, White and Transparent (CMYKWT) voxels.

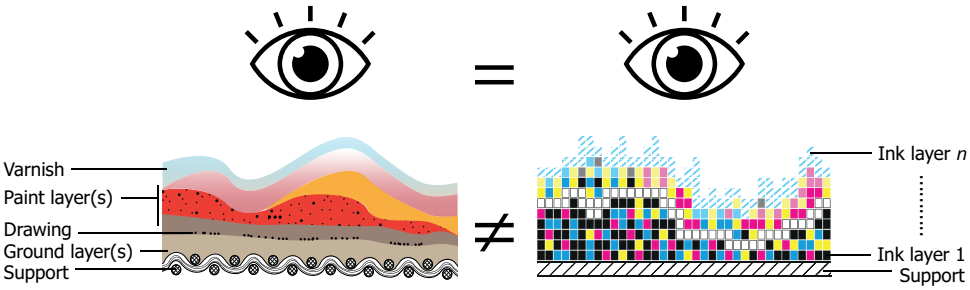

Figure 1.7: The aim is to create reproductions that match the visual appearance of the painting, but creating that effect using different materials and buildup than the painting, and by a digital reproduction process.

With the capability to capture the fine surface details of a painting for purposes of creating a reproduction, another application for this scan data is envisioned, namely the documentation and monitoring of paintings, for the purpose of conservation. For this reason, a secondary aim of this PhD project is to:

Evaluate the suitability of 3D scanning — based on fringe-encoded stereo imaging — for documentation and monitoring of paintings

1.6.2. Research questions

The research aim(s) can be further specified with the following research questions:

RQ 1 *Which factors govern the material appearance of a painting and of a 3D printed Fine Art reproduction?*

RQ 2 *Which factor(s) should be studied to minimize the material appearance difference between a 3D Fine Art reproduction and a painting?*

RQ 3 *Which parameters of a 3D reproduction system are important, can be measured and/or manipulated to reproduce spatially-varying gloss of paintings?*

RQ 4 *What are the interactions between color, gloss, topography, (and translucency) reproduction parameters?*

RQ 5 *Which technique, resolution and precision are suitable for documentation and monitoring of the topographical details of a painting?*

1.6.3. Research methodology

The methodological frame that is used for this PhD project is *design inclusive research* [164]. Specific to this methodological approach is the integration of design related actions, as an integral part of the research cycle. An overview of the research cycles in this thesis is presented in Figure 1.8, with a short description of every research phase. The subsequent chapters (Chapter 2 to 6) each correspond with a research cycle. The design of the scanner prototype(s) and subsequently the fabrication of reproductions are manifestations of integrated knowledge of multiple domains. Moreover, the outcomes of every research cycle lends itself to multi-disciplinary insights, explanations and predictions, in this thesis for instance informing the domains of psycho-physics, imaging, 3D printing, and conservation. Details of the employed methods (and outcomes) of each research cycle can be found in the corresponding chapters (Chapter 2 to 6).

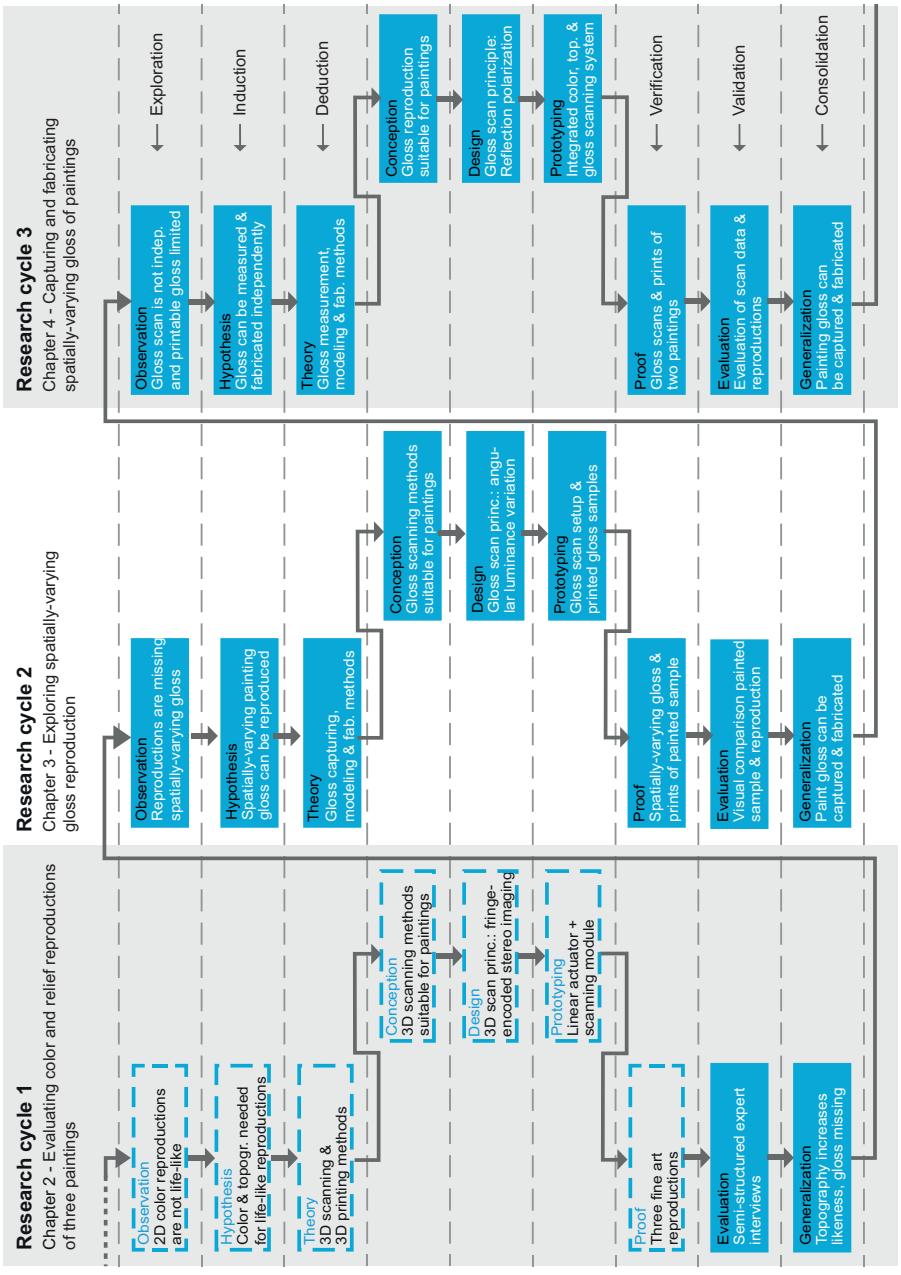

Figure 1.8: Overview of research cycles in this PhD project, following the *design inclusive research* methodology

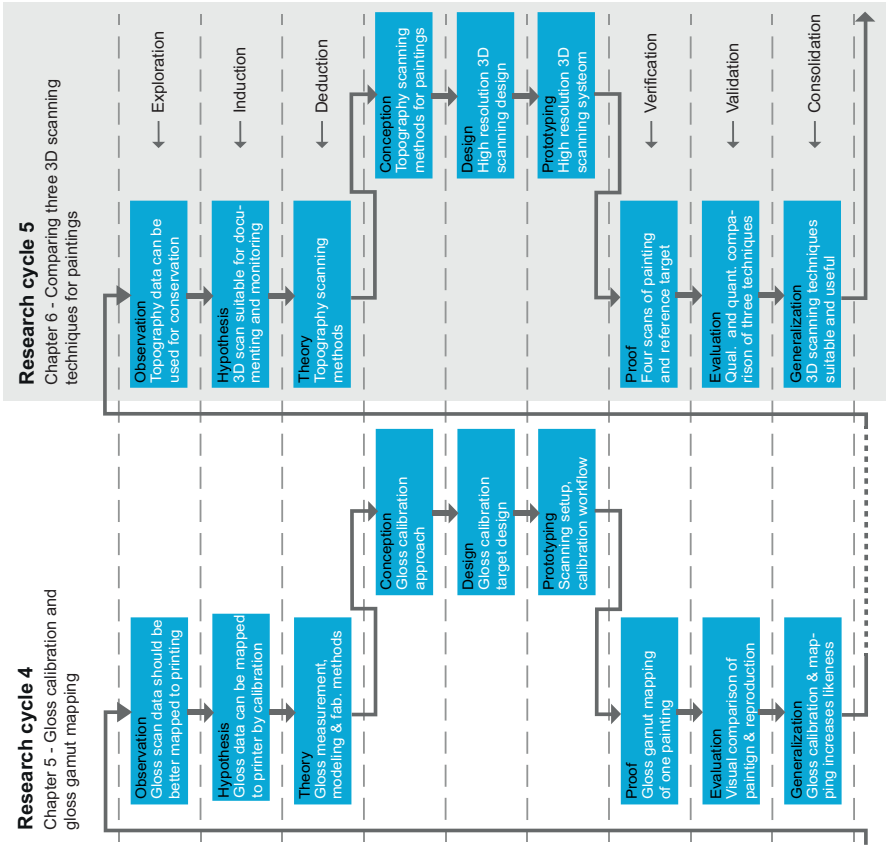
Research cycle 4
Chapter 5 - Gloss calibration and gloss gamut mapping
Observation
Gloss scan data should be better mapped to printing
Hypothesis
Gloss data can be mapped to printer by calibration
Theory
Gloss measurement, modeling & lab. methods
Conception
Gloss calibration approach
Design
Gloss calibration target design
Prototyping
Scanning setup, calibration workflow
Proof
Gloss gamut mapping of one painting
Evaluation
Visual comparison of paintign & reproduction
Generalization
Gloss calibration & mapping increases likeness
Research cycle 5
Chapter 6 - Comparing three 3D scanning techniques for paintings
Observation
Topography data can be used for conservation
Hypothesis
3D scan suitable for documenting and monitoring
Theory
Topography scanning methods
Conception
Topography scanning methods for paintings
Design
High resolution 3D scanning design
Prototyping
High resolution 3D scanning systeom
Proof
Four scans of painting and reference target
Evaluation
Qual. and quant. comparison of three techniques
Generalization
3D scanning techniques suitable and useful
Exploration
Induction
Deduction
Verification
Validation
Consolidation

1.7. Research framework and scope

1.7.1. Research framework

Figure 1.9 depicts the research framework, visualizing the relevant parameters relevant for this PhD thesis and their relations, with the primary research parameters (blue), the related research parameters (green), and the parameters which are out of scope (gray). The link to the research questions is also visualised. The review of the state-of-the-art (see Section 1.5), and the evaluation of three reproduction featuring color and topography (see Chapter 2) informed the framework structure (RQ 1). The framework is subdivided into parameters relating to the visual perception domain (left) and parameters relating to the technical domain (right). Besides the primary parameters, relating to the appearance modalities — color, topography, gloss and translucency —, also the interaction between them, and other parameters, like viewing conditions, illumination characteristics and human visual system, are important to consider in the research and design phases. Following the initial evaluation of three reproductions (see Chapter 2), a division is made into parameters constituting the primary focus of this research, related parameters, and out-of-scope parameters (RQ 2). In the technical domain, RQ 3 primarily deals with gloss reproduction parameters, RQ 4 with the interactions within the technical reproduction parameters, and RQ 5 relates to the topography capturing and modeling parameters, although not in their relation to visual appearance.

1.7.2. Research scope

The research was carried out and validated in five separate case studies, using in total eight paintings, which are listed in Table 1.1 (hereafter references to these paintings will be denoted by title and painter). The focus of the case studies was limited to oil paintings on canvas. The styles of painting that were reproduced ranged from Dutch Golden Age paintings, to (current-day replicas of) Dutch impressionists.

Some materials and techniques used in painting, creating specific appearances, are out of scope for this thesis, due to technical limitations. One such appearance that cannot be captured or fabricated with the technologies employed in this thesis is the effect created by the use of gold (leaf). As the 3D scanning setup employs a cross-polarized setup (for details see Chapter 2 and 4), a golden (or otherwise metallic) surface cannot be imaged, as there is no diffuse reflection from metallic surfaces. Furthermore, the reproduction of optical effects like fluorescence, phosphorescence (i.e. glow-in-the-dark), iridescence, sparkle, found for instance in post-modern art, is also out of scope for this thesis. These effects cannot be captured with the current 3D scanning setup, nor recreated with the limited set of inks that is currently available for the 3D printing system used. And finally, it should be noted that effects like undercuts — where paint has a true 3D shape, occluding areas underneath the paint, when observed in a frontal view — cannot be captured using the current 3D scanning setup, nor reproduced by a 3D printing system, which does not have a support material — a material which supports the printing material during printing and is removed afterwards.

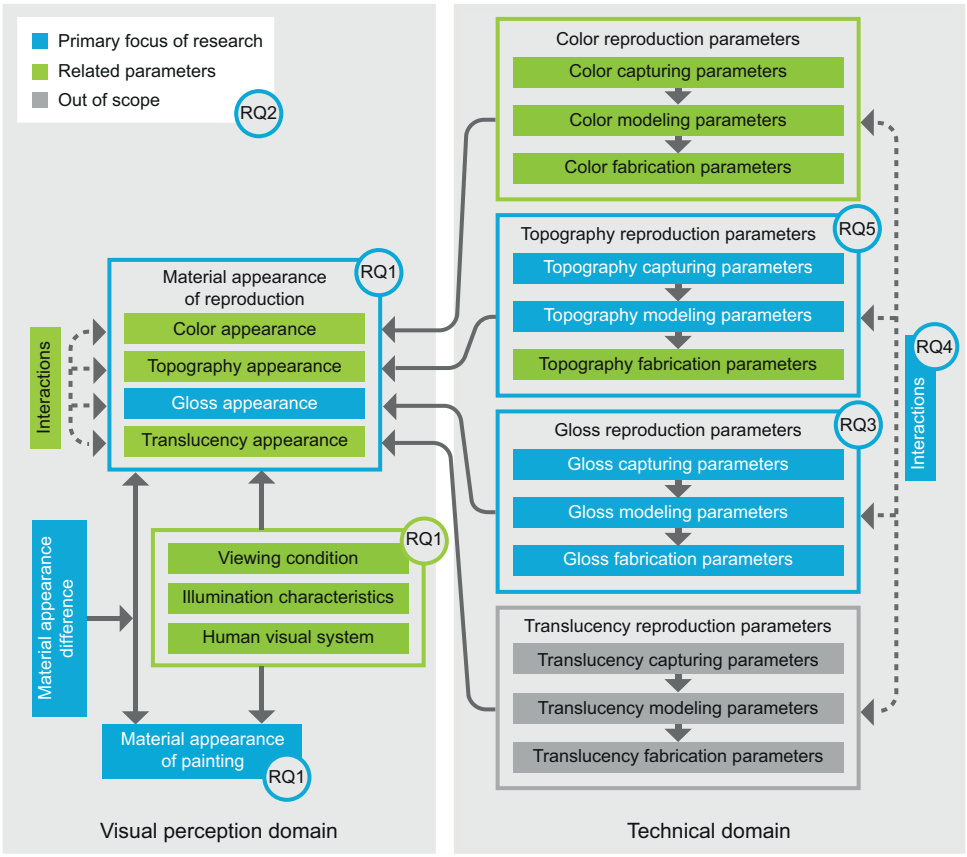

Figure 1.9: Research framework, with primary research parameters (blue), related research parameters (green), and out of scope parameters (gray)

Besides spatial variation in color, topography and gloss, many paintings are built up with multiple (semi-transparent) layers (see schematic depiction in Figure 1.2). A painter might stack multiple translucent layers on top of each other or on top of opaque paints, for instance to create soft transitions (sfumato) or vibrant color appearances. The stratigraphy of these translucent layers, could not (at the start of this thesis) be captured on a large scale across a paintings surface. Still now, although the stratigraphy can now be captured (using Multi-Scale-OCT, see Chapter 6), the optical properties of the individual layers cannot be derived from this information directly. Additionally, the transformation of this layered composition, whereby the stacking of layers is converted into a stacking of layers using printing materials — possibly with additional inks — requires a new (full-color) reproduction workflow, for which only recently approaches have been proposed (e.g. [122, 163]). For this reason, the reproduction of these layered structures, and thereby effect of transparency/translucency lies outside the scope of this thesis.

Table 1.1: Scanned (and reproduced) paintings

Title	Painter	Dating	Material	Size (w x h, cm)	Collection & Inventory no.
Self-portrait	Rembrandt van Rijn	c.1669	Oil on canvas	60 x 65	Mauritshuis, The Hague, no. 840
Flowers in a Blue Vase	Vincent van Gogh	c.June 1887	Oil on canvas	39 x 62	Kröller Müller Museum, Otterlo no. KM107.055
Isaac and Rebecca, known as 'The Jewish Bride'	Rembrandt van Rijn	c.1665-1669	Oil on canvas	167 x 122	Rijksmuseum, Amsterdam, no. SK-C-216
Saul and David	Rembrandt van Rijn	c.1651-1654 and c.1655-1658	Oil on canvas	165 x 130	Mauritshuis, The Hague, no. 621
Sunflowers [a]	signed as W. Adam	c.2015	Oil on canvas	30 x 40	N/A
Two Wrestling Figures [b]	Charlotte Caspers	2017	Oil on canvas	100 x 80	N/A
Fruit Still Life	Cornelis de Heem	c.1670	Oil on canvas	50 x 65	Mauritshuis, The Hague, no. 50
Girl with a Pearl Earring	Johannes Vermeer	c.1665	Oil on canvas	39 x 45	Mauritshuis, The Hague, no. 670

[a] A painting in the style of Vincent van Gogh, purchased by the author

[b] Painted for the Dutch Television program *Het Geheim van de Meester*. It is a *painted* reconstruction of a work by Vincent van Gogh, found underneath the painting *Still Life with Meadow Flowers and Roses* by Vincent Van Gogh, c.1886-1887, Oil on canvas, 80 x 100cm, Kröller Müller Museum, Otterlo, inventory no. KM100.067

1.8. Thesis outline

This thesis comprises of a collection of conference and journal articles (one in preparation). The corresponding publication information can be found at the beginning of each chapter. A full list of publications by the author can be found at the end of this thesis. The outline of this thesis is as follows:

Chapter 2 presents an evaluation of three reproductions, featuring color and topography, by semi-structured interviews with experts. Paintings reproduced for this case study are: *Self-portrait*, by Rembrandt van Rijn (c.1669), *Flower in a Blue Vase*, by Vincent van Gogh (c. June 1887), and *The Jewish Bride*, by Rembrandt van Rijn (c.1665-1669) (details in Table 1.1).

In **Chapter 3** an exploration into gloss capturing and fabrication is presented. The gloss scanning principle used in this case study is based on measuring the angular variance in luminance, and the spatially-varying gloss is printed using multi-level halftoning algorithm to print multiple layers of a digital varnish. A painted sample with various colors and gloss levels (created with two varnishes) is used as a case study.

The research into gloss reproduction is extended in **Chapter 4** presenting an alternative approach to gloss scanning, making use of reflectance polarisation at Brewster's angle, which has a better independence of color. This is combined with an optimized gloss printing strategy, offering a wider range of printable gloss levels. The (integrated) approach to color, topography and gloss reproduction, is used to create reproductions of two paintings *in the style of* Vincent van Gogh, namely the *Sunflowers*, signed by W. Adam (c.2015), and *Two Wrestling Figures*, by Charlotte Caspers (2017) (details in Table 1.1).

A further optimization of the gloss reproduction workflow is presented in **Chapter 5**, discussing an approach to gloss calibration and gloss gamut mapping. Flat, printed targets, in the primary printing colors (CMYKW), with a range of gloss levels — covering the complete range of printable gloss levels — were used to calibrate the gloss scanning system. The corresponding gloss values were used to create a mapping from the measured gloss values, to printable gloss levels. The reproduction workflow, including calibration and mapping, was applied to one painting in this case study, namely *Fruit Still Life*, by Cornelis de Heem (1670) (details in Table 1.1).

Next, **Chapter 6** presents the comparison of three 3D scanning technologies, suitable to scan the surface topography of paintings. Three techniques were used to scan *Girl with a Pearl Earring*, by Johannes Vermeer (c.1665) (details in Table 1.1). Multi-Scale Optical Coherence Tomography, 3D scanning based on fringe-encoded stereo imaging (at two resolutions) and 3D focus variation microscopy are compared qualitatively and quantitatively. Furthermore, the (potential) application of 3D scanning data, that can be obtained with these techniques, for the purposes of conservation is discussed.

In **Chapter 7** the ethical issues related to creating (life-like) reproductions of paintings are discussed. Applications of reproductions and potential benefits of using reproductions are presented. We conclude with the potential for dissemination of knowledge on material appearance reproduction in a more general sense -

outside the application domain of creating painting reproductions.

The final chapter, **Chapter 8**, presents the conclusions that can be drawn from the research that was conducted as part of this thesis. Answers to the research questions, as formulated in paragraph 1.6, are also presented. Furthermore, we present an outlook for future work, related to material appearance reproduction, as well as offering a broader perspective on new opportunities for research, using this work as a starting point.

To conclude, Figure 1.10 gives overview of chapters and their connection to the research questions.

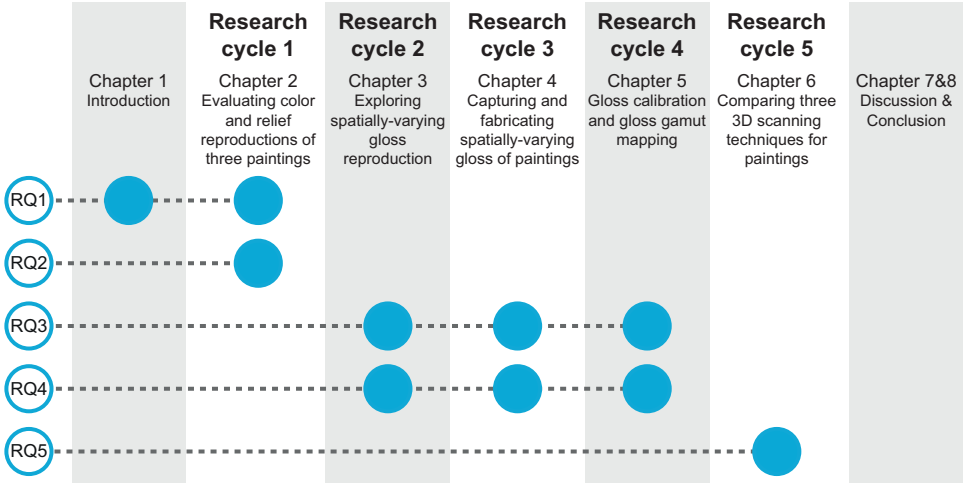

Figure 1.10: Thesis outline and link to research questions

1.9. Note on the use of terminology

There is a substantial body of work that uses the term *texture* to describe the (perception of) three-dimensional variations in surface shape (e.g.[42, 43, 165]). In Chapter 2 and 3 the term *texture* is used in this meaning.[3] However, the term *texture* is also used to describe (color) variations/patterns in a two-dimensional image. This is practiced in the domains of visual perception, computer graphics, and 3D printing (e.g. [121, 166]). For instance, Pont et al. define texture as "the local variation of pixel intensity for projections of the characteristic surface corrugations onto several image pixels" [78]. More broadly, Haindl and Filip regard "a textured image or the *visual texture* to be a realization of a random field, and our effort is simply to find its parameterizations in such a way that the real texture representing certain material appearance measurements will be visually indiscernible from the corresponding random field's realization, whatever the observation conditions might be" [167]. For this reason we deemed the term *texture* to be too ambiguous in relation

[3] A choice was made to refrain from editing the text regarding this terminology, including the original text of the publications as an integral whole

to this research topic, and have therefore switched to using the term *topography* instead, when referring to the (perception of) the three-dimensional variation of a (painting's) surface. The term *topography* is therefore used in all other parts of this thesis. For the sake of completeness, we should mention here that the term *relief* is also used to describe three-dimensional variations of a surface, for example in visual perception and 3D scanning literature (e.g. [41, 123, 168]). This term is also (sporadically) practiced by the author ([169, 170]), although not in the publications featured in this thesis.

References

[1] N. Denekamp, *Vincent van Gogh 400 dagen in Amsterdam* (Thoth, 2015) p. 80.

[2] L. Jansen, H. Luijten, and N. Bakker, eds., *Vincent van Gogh - The Letters* (Van Gogh Museum and Huygens Institute, Amsterdam and The Hague, 2009).

[3] Van Gogh Museum, *Zonnebloemen blijven voortaan thuis,* (2019), (Accessed: 2019-02-17).

[4] A. Van Loon, *Color changes and chemical reactivity in seventeenth-century oil paintings*, Phd thesis, University of Amsterdam (2008).

[5] G. Van der Snickt, J. Dik, M. Cotte, K. Janssens, J. Jaroszewicz, W. De Nolf, J. Groenewegen, and L. Van der Loeff, *Characterization of a Degraded Cadmium Yellow (CdS) Pigment in an Oil Painting by Means of Synchrotron Radiation Based X-ray Techniques,* Analytical Chemistry **81**, 2600 (2009).

[6] International Council of Museums, *ICOM code of ethics for museums*, Tech. Rep. (2017).

[7] S. Smallenburg, *Van Goghs Zonnebloemen is te zwak om nog te reizen,* (2019).

[8] E. Gombrich, *The Story of Art*, pocket edi ed. (Phaidon Press Limited, 2012).

[9] P. Pettitt and A. Pike, *Dating European palaeolithic cave art: Progress, prospects, problems,* Journal of Archaeological Method and Theory **14**, 27 (2007).

[10] H. Valladas, J. Clottes, J.-M. Geneste, M. Garcia, M. Arnold, H. Cachier, and N. Tisnérat-Laborde, *Palaeolithic paintings: Evolution of prehistoric cave art,* Nature **413**, 479 (2001).

[11] International Council of Museums - Committee for Conservation, *ICOM CC - working group - paintings,* (Accessed: 2018-05-28).

[12] R. L. Feller, *Artists Pigments - a handbook of their history and characteristics (volume 1)* (Publishing Office, National Gallery of Art, Washington, Washington, D.C., 1986) pp. 1–302.

[13] A. Roy, *Artists Pigments - a handbook of their history and characteristics (volume 2)* (Publishing Office, National Gallery of Art, Washington, Washington, D.C., 1993) pp. 1–234.

[14] E. West FitzHugh, *Artists Pigments - a handbook of their history and characteristics (volume 3)* (Publishing Office, National Gallery of Art, Washington, Washington, D.C., 1997) pp. 1–370.

[15] Facsimile Editions, *Company website,* (Accessed: 2019-05-25).

[16] Lascaux Centre International de l'Art Pariétal (Lascaux IV), *Museum website,* (Accessed: 2019-05-25).

[17] Factum Arte, *Facsimile of the tomb of Tutankhamun,* (2012), (Accessed: 2019-05-25).

[18] Factum Arte, *A facsimile of 'The Wedding at Cana' by Paolo Veronese,* (2007), (Accessed: 2019-05-25).

[19] Factum Arte, *Mapping a Map: Factum Arte at the Sala Bologna,* (2011), (Accessed: 2019-05-25).

[20] Otsuka Museum of Art, *Museum website,* (Accessed: 2019-05-25).

[21] N. Ex, *Zo goed als oud: de achterkant van restaureren* (De Boekerij BV, Amsterdam, The Netherlands, 1993).

[22] NWO Wetenschap, *Kleur rood verdwijnt langzaam uit schilderijen Van Gogh - NWO-onderzoeksprogramma Science4Arts,* (2015), (Accessed: 2019-05-25).

[23] NOS, *"My Dream Exhibition": Van Gogh re-invented in the Amsterdam Beurs van Berlage,* (2012).

[24] Océ Technologies BV - a Canon Company, *Project Eiger Elevated printing,* (Accessed: 2019-05-25).

[25] T. Baar, S. Samadzadegan, H. Brettel, P. Urban, and M. V. Ortiz Segovia, *Printing gloss effects in a 2.5D system,* in *Electronic Imaging: Measuring, Modeling, and Reproducing Material Appearance*, edited by M. V. Ortiz Segovia, P. Urban, and J. P. Allebach (2014).

[26] Stratesys, *Objet260 Connex3 for Color 3D Printing,* (Accessed: 2019-05-25).

[27] P. Sitthi-Amorn, J. E. Ramos, Y. Wangy, J. Kwan, J. Lan, W. Wang, and W. Matusik, *MultiFab: A Machine Vision Assisted Platform for Multi-material 3D Printing,* ACM Transactions on Graphics **34** (2015), 10.1145/2766962.

[28] M. J. Mirzaali, M. E. Edens, A. H. de la Nava, S. Janbaz, P. Vena, E. L. Doubrovski, and A. A. Zadpoor, *Length-scale dependency of biomimetic hard-soft composites,* Scientific Reports **8**, 1 (2018).

[29] T. Hou, Y. Song, W. S. Elkhuizen, J. Jiang, and J. M. Geraedts, *3D Wireless Power Transfer Based on 3D Printed Electronics,* in *IEEE 14th International Conference on Automation Science and Engineering (CASE)* (IEEE, Munich, Germany, 2018) pp. 499–505.

[30] A. Brunton, C. Ates Arikan, and P. Urban, *Pushing the Limits of 3D Color Printing,* ACM Transactions on Graphics **35**, 1 (2015).

[31] L. Shi, V. Babaei, C. Kim, M. Foshey, Y. Hu, P. Sitthi-Amorn, S. Rusinkiewicz, and W. Matusik, *Deep Multispectral Painting Reproduction via Multi-Layer ,*

Custom-Ink Printing, ACM Transactions on Graphics **37**, 1 (2018).

[32] K. Xiao, S. Wuerger, F. Mostafa, A. Sohaib, and J. M. Yates, *Colour Image Reproduction for 3D Printing Facial Prostheses,* in *New Trends in 3D Printing* (InTech, 2016) pp. 89–109.

[33] M. Baay, *SmartFrame: Design of an exposition setup for 3D-printed fine-art replicas*, MSc thesis (Delft University of Technology, Delft, The Netherlands, 2016).

[34] H. De Bliek, *Making art accessible to visually impaired museum visitors*, MSc thesis (Delft University of Technology, Delft, The Netherlands, 2019).

[35] E. H. Adelson, *On Seeing Stuff: The perception of materials by humans and machines,* in *Human Vision and Electronic Imaging*, Vol. 4299 (2001) pp. 1–12.

[36] R. W. Fleming, *Material Perception,* Annual Review of Vision Science **3**, 365 (2017).

[37] R. W. Fleming, *Visual perception of materials and their properties,* Vision research **94**, 62 (2014).

[38] R. W. Fleming, C. Wiebel, and K. Gegenfurtner, *Perceptual qualities and material classes,* Journal of vision **13**, 1 (2013).

[39] F. Zhang, H. de Ridder, P. Barla, and S. Pont, *A systematic approach to testing and predicting light-material interactions,* Journal of Vision **19**, 1 (2019).

[40] M. Van Zuijlen, P. Upchurch, S. Pont, and M. Wijntjes, *Material property space analysis for depicted materials,* in *Vision Science Society* (2019) p. 251.

[41] B. L. Anderson, *Visual perception of materials and surfaces,* Current Biology **21** (2011), 10.1016/j.cub.2011.11.022.

[42] Commission Internationale de l'Eclairage, *A framework for the measurement of visual appearance*, Tech. Rep. (International Commission on Illumination, Vienna, Austria, 2006).

[43] Y.-X. Ho, M. S. Landy, and L. T. Maloney, *Conjoint Measurement of Gloss and Surface Texture,* Psychological Science **19**, 196 (2008).

[44] P. Vangorp, J. Laurijssen, and P. Dutré, *The influence of shape on the perception of material reflectance,* ACM Transactions on Graphics **26**, 77 (2007).

[45] M. Olkkonen and D. H. Brainard, *Joint effects of illumination geometry and object shape in the perception of surface reflectance,* i-Perception **2**, 1014 (2011).

[46] M. W. A. Wijntjes and S. C. Pont, *Illusory gloss on Lambertian surfaces,* Journal of Vision **10** (2010), 10.1167/10.9.13.

[47] T. Baar, S. Samadzadegan, P. Urban, and M. V. Ortiz Segovia, *Interrelation between gloss and texture perception of 2.5D-printed surfaces,* in *Electronic Imaging: Measuring, Modeling, and Reproducing Material Appearance* (Society for Imaging Science and Technology, 2016) pp. 1–6.

[48] K. Doerschner, *Estimating the glossiness transfer function induced by illumi-*

nation change and testing its transitivity, Journal of Vision **10**, 1 (2010).

[49] R. W. Fleming, R. O. Dror, and E. H. Adelson, *Real-world illumination and the perception of surface reflectance properties.* Journal of vision **3**, 347 (2003).

[50] M. Olkkonen and D. H. Brainard, *Perceived glossiness and lightness under real-world illumination,* Journal of Vision **10** (2010), 10.1167/10.9.5.

[51] I. Motoyoshi and H. Matoba, *Variability in constancy of the perceived surface reflectance across different illumination statistics,* Vision Research **53**, 30 (2012).

[52] G. Obein, K. Knoblauch, and F. Viénot, *Difference scaling of gloss: Nonlinearity, binocularity, and constancy,* Journal of Vision **4**, 711 (2004).

[53] S. C. Pont and S. F. Te Pas, *Material - Illumination ambiguities and the perception of solid objects,* Perception **35**, 1331 (2006).

[54] S. F. te Pas and S. C. Pont, *A comparison of material and illumination discrimination performance for real rough, real smooth and computer generated smooth spheres,* in *Proceedings of the 2nd symposium on Appied perception in graphics and visualization - APGV '05* (ACM Press, New York, New York, USA, 2005) p. 75.

[55] ISO, *ISO 11664-2 Colorimetry - Part 2: CIE standard illuminants,* (2007).

[56] ISO, *ISO 11664-1 Colorimetry - Part 1:CIE standard colorimetric observers,* (2007).

[57] R. S. Berns, *Principles of Color Technology*, 3rd ed. (John Wiley & Sons, New York, New York, USA, 2000).

[58] L. T. Maloney and D. H. Brainard, *Color and material perception: Achievements and challenges,* Journal of Vision **10**, 1 (2010).

[59] B. Xiao and D. H. Brainard, *Surface gloss and color perception of 3D objects,* Vision Neuroscience **25**, 371 (2008).

[60] M. Olkkonen, T. Hansen, and K. R. Gegenfurtner, *Color appearance of familiar objects: effects of object shape, texture, and illumination changes.* Journal of vision **8**, 1 (2008).

[61] M. Giesel and K. R. Gegenfurtner, *Color appearance of real objects varying in material, hue, and shape,* Journal of vision **10**, 10 (2010).

[62] M. Ludwig and G. Meyer, *Brightness Perception of Surfaces with Mesoscale Structures,* Journal of Imaging Science and Technology **61**, 1 (2017).

[63] R. S. Hunter, *Methods of determining gloss,* Journal of Research of the National Bureau of Standards **18** (1937).

[64] F. X. O'Donnell and F. W. Billmeyer Jr., *Psychometric scaling of gloss,* in *Review and Evaluation of Appearance: Methods and Techniques, ASTM STP 914*, edited by J. Rennilson and W. Hale (American Society for Testing and Materials, Philadelphia, USA, 1986) pp. 14–32.

[65] F. W. Billmeyer and F. X. D. O'Donnell, *Visual gloss scaling and multidimensional scaling analysis of painted specimens,* Color Research and Application

12 (1987).

[66] J. A. Ferwerda, F. Pellacini, and D. P. Greenberg, *A psychophysically-based model of surface gloss perception,* in *Human Vision and Electronic Imaging*, Vol. 4299 (2001) pp. 291–301.

[67] J. Wills, S. Agarwal, D. Kriegman, and S. Belongie, *Toward a Perceptual Space for Gloss,* ACM Transactions on Graphics **28**, 1 (2009).

[68] F. B. Leloup, G. Obein, M. R. Pointer, and P. Hanselaer, *Toward the soft metrology of surface gloss: A review,* Color Research & Application **39**, 559 (2014).

[69] W. Ji, M. R. Pointer, R. M. Luo, and J. Dakin, *Gloss as an aspect of the measurement of appearance,* Journal of the Optical Society of America **23**, 22 (2006).

[70] I. Motoyoshi, S. Nishida, L. Sharan, and E. H. Adelson, *Image statistics and the perception of surface qualities,* Nature **447**, 206 (2007).

[71] B. L. Anderson and J. Kim, *Image statistics do not explain the perception of gloss and lightness,* Journal of Vision **9**, 1 (2009).

[72] C. B. Wiebel, M. Toscani, and K. R. Gegenfurtner, *Statistical correlates of perceived gloss in natural images,* Vision Research **115**, 175 (2015).

[73] P. J. Marlow, J. Kim, and B. L. Anderson, *The Perception and Misperception of Specular Surface Reflectance,* Current Biology **22**, 1909 (2012).

[74] P. J. Marlow and B. L. Anderson, *Generative constraints on image cues for perceived gloss,* Journal of Vision **13**, 1 (2013).

[75] F. Di Cicco, M. W. A. Wijntjes, and S. C. Pont, *Understanding gloss perception through the lens of art: Combining perception, image analysis, and painting recipes of 17th century painted grapes,* Journal of Vision **19**, 1 (2019).

[76] L. Qi, M. J. Chantler, J. P. Siebert, and J. Dong, *How Mesoscale and Microscale Roughness Affect Perceived Gloss,* in *3rd International Conference on Appearance* (Edinburgh, UK, 2012) pp. 48–51.

[77] S. Padilla, O. Drbohlav, P. Green, and M. Chantler, *Measurement of Perceptual Roughness in Fractal Surfaces,* in *CIE - Lighting Quality and Energy Efficiency* (Kuala Lumpur, Malaysia, 2014) pp. 61–66.

[78] S. C. Pont and J. J. Koenderink, *Bidirectional Texture Contrast Function,* International Journal of Computer Vision **62**, 17 (2005).

[79] S. Pont and J. J. Koenderink, *Shape, surface roughness and human perception,* in *Handbook van texture analysis*, edited by M. Mirmehdi, X. Xie, and J. Suri (Imperial Colllege Press, London, UK, 2008) Chap. 7, pp. 197–222.

[80] Y.-x. Ho, L. T. Maloney, and M. S. Landy, *The effect of viewpoint on perceived surface roughness in binocularly viewed scenes,* Journal of Vision **7**, 1 (2006).

[81] P. N. Belhumeur, D. J. Kriegman, and A. L. Yuille, *The Bas-Relief Ambiguity,* International Journal of Computer Vision **35**, 33 (1999).

[82] C. Schuller, D. Panozzo, and O. Sorkine-Hornung, *Appearance-Mimicking*

Surfaces, Acm Transactions on Graphics **33**, 10 (2014).

[83] J. J. van Assen and R. Fleming, *The influence of optical material appearance on the perception of liquids and their properties,* Journal of Vision **15**, 1 (2015).

[84] F. Schmidt, V. C. Paulun, J. J. R. van Assen, and R. W. Fleming, *Inferring the stiffness of unfamiliar objects from optical, shape, and motion cues,* Journal of Vision **17**, 1 (2017).

[85] F. Metelli, *Stimulation and perception of transpareny,* Psychological Research **47**, 185 (1985).

[86] M. Singh and B. L. Anderson, *Toward a perceptual theory of transparency,* Psychological Review **109**, 492 (2002).

[87] R. Robilotto and Q. Zaidi, *Perceived transparency of neutral density filters across dissimilar backgrounds,* Journal of Vision **4**, 5 (2004).

[88] F. Faul and V. Ekroll, *On the filter approach to perceptual transparency,* Journal of Vision **11**, 1 (2011).

[89] W. Gerbino, *Achromatic transparency,* in *Oxford Handbook of Perceptual Organisation*, edited by J. Wagemans (2014) pp. 1–21.

[90] J. Koenderink, A. van Doorn, S. Pont, and W. Richards, *Gestalt and phenomenal transparency,* Journal of the Optical Society of America A **25**, 190 (2008).

[91] P. Kubelka and F. Munk, *Ein Beitrag zur Optik der Farbanstriche,* Zeitschrift für technische Physik **12**, 593 (1931).

[92] R. W. Fleming, F. Jäkel, and L. T. Maloney, *Visual Perception of Thick Transparent Materials,* Psychological Science **22**, 812 (2011).

[93] R. W. Fleming and H. H. Bülthoff, *Low-level image cues in the perception of translucent materials,* ACM Transactions on Applied Perception **2**, 346 (2005).

[94] B. Xiao, B. Walter, I. Gkioulekas, T. Zickler, E. Adelson, and K. Bala, *Looking against the light: How perception of translucency depends on lighting direction,* Journal of Vision **14**, 1 (2014).

[95] B. M. Vu, P. Urban, T. M. Tanksale, and S. Nakauchi, *Visual perception of 3D printed translucent objects,* in *24th Color and Imaging Conference* (Society for Imaging Science and Technology, 2016) pp. 94–99.

[96] B. Sayim and P. Cavanagh, *The art of transparency,* i-Perception **2**, 679 (2011).

[97] E. R. de la Rie, *The influence of varnishes on the appearance of paintings,* Studies in conservation **32**, 1 (1987).

[98] L. Simonot and M. Elias, *Color change due to a varnish layer,* Color Research and Application **29**, 196 (2004).

[99] M. Elias and L. Simonot, *Bi-directional reflectance of a varnished painting Part 1: Influence of the refractive indices without using the approximations of Saunderson correction – exact computation,* Optics Communications **231**,

17 (2004).

[100] M. Elias, L. Simonot, M. Thoury, and J. M. Frigerio, *Bi-directional reflectance of a varnished painting Part 2: Comparison between the effects of the refractive indices, of the surface states and of the absorption of the varnish – experiments and simulations,* Optics Communications **231**, 25 (2004).

[101] E. R. de la Rie, J. K. Delaney, K. M. Morales, C. a. Maines, and L.-P. Sung, *Modification of Surface Roughness by Various Varnishes and Effect on Light Reflection,* Studies in Conservation **55**, 134 (2010).

[102] G. Harteveld, *Investigation of the Effect of the Green Glaze Layer in the Background of 'Girl with a Pearl Earring' by Johannes Vermeer*, MSc thesis (Delft University of Technology, Delft, The Netherlands, 2019).

[103] Federal Agencies Digitization Initiative (FADGI) - Still Image Working Group, *Technical Guidelines for Digitizing Cultural Heritage Materials : Creation of Raster Image Master Files*, Tech. Rep. (Federal Agencies Digitization Initiative Still Image Working Group, 2010).

[104] H. V. Dormolen, *Metamorfoze Preservation Imaging Guidelines*, Tech. Rep. (National Library of the Netherlands (Koninklijke Bibliotheek), The Hague, The Netherlands, 2012).

[105] International Color Consortium, *Standards that refer to ICC profiles,* (Accessed: 2019-05-25).

[106] T. Phan Van Song, C. Andraud, and M. V. Ortiz Segovia, *Implementation of the four-flux model for spectral and color prediction of 2.5D prints,* in *Printing for Fabrication (NIP32)* (IS&T, Manchester, UK, 2016) pp. 26–30.

[107] T. Phan Van Song, C. Andraud, and M. V. Ortiz-Segovia, *Towards spectral prediction of 2.5D prints for soft-proofing applications,* in *6th International Conference on Image Processing Theory, Tools and Applications, IPTA 2016* (IEEE, 2016) pp. 1–6.

[108] T. Phan Van Song, C. Andraud, L. R. Sapaico, and M. V. Ortiz Segovia, *Color prediction based on individual characterizations of ink layers and print support,* in *Electronic Imaging* (IS&T, Burlingame, CA, 2018) pp. 1–6.

[109] R. S. Berns, T. Chen, D. R. Wyble, and L. Chen, *Update: Practical Total Appearance Imaging of Paintings,* in *Archiving* (Copenhagen, Denmark, 2012) pp. 1–6.

[110] R. S. Berns, F. H. Imai, P. D. Burns, and D.-Y. Tzeng, *Multi-spectral-based color reproduction research at the Munsell Color Science Laboratory,* in *Electronic Imaging: Processing, Printing, and Publishing in Color*, Vol. 3409 (Zurich, Switzerland, 1998) pp. 1–12.

[111] R. S. Berns, L. A. Taplin, P. Urban, and Y. Zhao, *Spectral color reproduction of paintings,* in *Colour in Graphics, Imaging, and Vision* (Society for Imaging Science and Technology, 2008) pp. 484–488.

[112] S. Le Moan and P. Urban, *A new connection space for low-dimensional spectral color management,* Electronic Imaging: Measuring, Modeling, and Re-

producing Material Appearance **9018**, 1 (2014).

[113] S. Samadzadegan and P. Urban, *Spatio-Spectral Gamut Mapping and Separation,* Journal of Imaging Science and Technology **59**, 1 (2015).

[114] 3D Systems, *Company website,* (Accessed: 2019-05-25).

[115] MCor Technologies, *Company website,* (Accessed: 2019-05-25).

[116] XYZprinting, *Company website,* (Accessed: 2019-05-25).

[117] HP, *Company website,* (Accessed: 2019-05-25).

[118] Stratasys, *Company website,* (Accessed: 2019-05-25).

[119] Mimaki, *Company website,* (Accessed: 2019-05-25).

[120] V. Babaei, K. Vidimče, M. Foshey, A. Kaspar, P. Didyk, and W. Matusik, *Color contoning for 3D printing,* ACM Transactions on Graphics **36**, 1 (2017).

[121] O. Elek, D. Sumin, R. Zhang, T. Weyrich, K. Myszkowski, B. Bickel, A. Wilkie, and J. Křivánek, *Scattering-aware Texture Reproduction for 3D Printing,* ACM Transactions on Graphics **36** (2017), 10.1145/3130800.3130890.

[122] A. Brunton, C. A. Arikan, T. M. Tanksale, and P. Urban, *3D printing spatially varying color and translucency,* ACM Transactions on Graphics **37**, 1 (2018).

[123] F. Blais, J. Taylor, L. Cournoyer, M. Picard, L. Borgeat, L.-G. Dicaire, M. Rioux, J.-A. Beraldin, G. Godin, C. Lahnanier, and G. Aitken, *Ultra-High Resolution Imaging at 50 micron using a Portable XYZ-RGB Color Laser Scanner,* in *International Workshop on Recording, Modeling and Visualization of Cultural Heritage*, edited by M. Baltsavias, A. Gruen, L. van Gool, and M. Pateraki (National Research Council Canada, Ascona, Switzerland, 2005) pp. 1–16.

[124] F. Blais, J. Taylor, L. Cournoyer, M. Picard, L. Borgeat, G. Godin, J.-A. Beraldin, M. Rioux, and C. Lahanier, *Ultra high-resolution 3D laser color imaging of paintings: the 'Mona Lisa' by Leonardo da Vinci,* in *7th International Conference on Lasers in the Conservation of Artworks*, edited by M. Castillejo, P. Moreno, M. Oujja, R. Radvan, and J. Ruiz (National Research Council Canada, Madrid, Spain, 2007) pp. 1–8.

[125] Verus Art, *Verus Art textured reproductions,* (2017), (Accessed: 2019-05-25).

[126] Factum Arte, *Lucida: Discovering an artwork through its surface*, Tech. Rep. (Factum Foundation, Madrid, Spain, 2016).

[127] D. Akça, A. Grün, B. Breuckmann, and C. Lahanier, *High Definition 3D-Scanning of Arts Objects and Paintings,* in *Optical 3-D Measurement Techniques VIII*, Vol. II, edited by A. Gruen and H. Kahmen (Zurich, Switzerland, 2007) pp. 50–58.

[128] M. Karaszewski, M. Adamczyk, R. Sitnik, J. Michoński, W. Załuski, E. Bunsch, and P. P. Bolewicki, *Automated full-3D digitization system for documentation of paintings,* in *Optics for Arts, Architecture, and Archaeology IV*, Vol. 8790, edited by L. Pezzati and P. Targowski (Munich, Germany, 2013) pp. 1–11.

[129] B. Breuckmann, *3-Dimensional Digital Fingerprint of Paintings,* in *19th Euro-*

pean Signal Processing Conference (IEEE, Barcelona, Spain, 2011) pp. 1249–1253.

[130] T. Zaman, P. Jonker, B. Lenseigne, and J. Dik, *Simultaneous capture of the color and topography of paintings using fringe encoded stereo vision,* Heritage Science **2**, 1 (2014).

[131] I. Cacciari, P. Nieri, and S. Siano, *3D Digital Microscopy for Characterizing Punchworks on Medieval Panel Paintings,* Journal on Computing and Cultural Heritage **7**, 1 (2014).

[132] K. J. Van den Berg, M. Daudin, I. Joosten, B. Wei, R. Morrison, and A. Burnstock, *A comparison of light microscopy techniques with scanning electron microscopy for imaging the surface of cleaning of paintings,* in *9th International Conference on NDT of Art* (Jerusalem, Israel, 2008) pp. 25–30.

[133] D. Zalewski, *The factory of fakes - how a workshop uses digital technology to craft perfect copies of threatened art,* The New Yorker , 66 (2016).

[134] Van Gogh Museum, *Van Gogh Museum Edition Collection,* (Accessed: 2017-10-13).

[135] C. Polzin, S. Spath, and H. Seitz, *Characterization and evaluation of a PMMA-based 3D printing process,* Rapid Prototyping Journal **19**, 37 (2013).

[136] D. Dimitrov, W. van Wijck, K. Schreve, and N. de Beer, *Investigating the achievable accuracy of three dimensional printing,* Rapid Prototyping Journal **12**, 42 (2006).

[137] T. Baar, H. Brettel, and M. V. O. Segovia, *A survey of 3D image quality metrics for relief print evaluation,* in *Colour and visual computing symposium* (2013) pp. 1–6.

[138] A. Armillotta and M. Cavallaro, *Edge quality in Fused Deposition Modeling: I. Definition and analysis,* Rapid Prototyping Journal **23**, 1079 (2017).

[139] A. Armillotta, S. Bianchi, M. Cavallaro, and S. Minnella, *Edge quality in fused deposition modeling: II. experimental verification,* Rapid Prototyping Journal **23**, 686 (2017).

[140] D. Dimitrov, K. Schreve, and N. De Beer, *Advances in three dimensional printing - State of the art and future perspectives,* Rapid Prototyping Journal **12**, 136 (2006).

[141] T. D. Ngo, A. Kashani, G. Imbalzano, K. T. Nguyen, and D. Hui, *Additive manufacturing (3D printing): A review of materials, methods, applications and challenges,* Composites Part B **143**, 172 (2018).

[142] X. Liu, L. Chen, M. V. Ortiz Segovia, J. A. Ferwerda, and J. P. Allebach, *Characterization of relief printing,* in *Electronic Imaging: Measuring, Modeling, and Reproducing Material Appearance* (2014).

[143] W. Wang, H. Chao, J. Tong, Z. Yang, X. Tong, H. Li, X. Liu, and L. Liu, *Saliency-Preserving Slicing Optimization for Effective 3D Printing,* Computer Graphics Forum **34**, 148 (2015).

[144] X. Zhang, X. Le, A. Panotopoulou, E. Whiting, and C. C. L. Wang, *Perceptual models of preference in 3D printing direction,* ACM Transactions on Graphics **34**, 1 (2015).

[145] G. Galimberti, E. Doubrovski, M. Guagliano, B. Previtali, and J. C. Verlinden, *Investigating the Links between Process Parameters and Their Influence on the Aesthetic Evaluation of Selective Laser Melted Parts,* 27th Annual International Solid Freeform Fabrication Symposium - An Additive Manufacturing Conference , 2367 (2016).

[146] A. Gardner, C. Tchou, T. Hawkins, and P. Debevec, *Linear light source reflectometry,* ACM Transactions on Graphics **22**, 749 (2003).

[147] P. Ren, J. Wang, J. Snyder, X. Tong, and B. Guo, *Pocket reflectometry,* ACM Transactions on Graphics **30** (2011), 10.1145/2010324.1964940.

[148] G. Chen, Y. Dong, P. Peers, J. Zhang, and X. Tong, *Reflectance scanning: Estimating Shading Frame and BRDF with Generalized Linear Light Sources,* ACM Transactions on Graphics **33** (2014), 10.1145/2601097.2601180.

[149] A. Ghosh, T. Chen, P. Peers, C. a. Wilson, and P. Debevec, *Estimating Specular Roughness and Anisotropy from Second Order Spherical Gradient Illumination,* Computer Graphics Forum **28**, 1161 (2009).

[150] M. Aittala, T. Weyrich, and J. Lehtinen, *Practical SVBRDF capture in the frequency domain,* ACM Transactions on Graphics **32** (2013), 10.1145/2461912.2461978.

[151] Fogra Research Insitute for Media Technologies, *ProcessStandard Digital Handbook*, Tech. Rep. (Aschheim (Munich), Germany, 2018).

[152] W. Matusik, B. Ajdin, J. Gu, J. Lawrence, H. P. A. Lensch, F. Pellacini, and S. Rusinkiewicz, *Printing spatially-varying reflectance,* ACM Transactions on Graphics **28**, 1 (2009).

[153] Y. Lan, Y. Dong, F. Pellacini, and X. Tong, *Bi-scale appearance fabrication,* ACM Transactions on Graphics **32** (2013), 10.1145/2461912.2461989.

[154] S. Samadzadegan, T. Baar, P. Urban, M. V. Ortiz Segovia, and J. Blahová, *Controlling colour-printed gloss by varnish-halftones,* in *Electronic Imaging*, Vol. 9398, edited by M. V. Ortiz Segovia, P. Urban, and F. H. Imai (2015).

[155] M. Goesele, H. Lensch, J. Lang, C. Fuchs, and H.-P. Seidel, *DISCO: Acquisition of Translucent Objects,* ACM Transactions on Graphics **23**, 835 (2004).

[156] P. Peers, K. vom Berge, W. Matusik, R. Ramamoorthi, J. Lawrence, S. Rusinkiewicz, and P. Dutré, *A compact factored representation of heterogeneous subsurface scattering,* ACM Transactions on Graphics **25**, 746 (2006).

[157] J. Wang, S. Zhao, X. Tong, S. Lin, Z. Lin, Y. Dong, B. Guo, and H.-Y. Shum, *Modeling and rendering of heterogeneous translucent materials using the diffusion equation,* ACM Transactions on Graphics **27**, 1 (2008).

[158] C. Donner and H. W. Jensen, *Light diffusion in multi-layered translucent materials,* ACM Transactions on Graphics **24**, 1032 (2005).

[159] A. Ghosh, T. Hawkins, P. Peers, S. Frederiksen, and P. Debevec, *Practical modeling and acquisition of layered facial reflectance,* ACM Transactions on Graphics **27**, 1 (2008).

[160] T. Callewaert, J. Dik, and J. Kalkman, *Segmentation of thin corrugated layers in high-resolution OCT images,* Optics Express **25**, 1 (2017).

[161] Y. Dong, J. Wang, F. Pellacini, X. Tong, and B. Guo, *Fabricating spatially-varying subsurface scattering,* ACM Transactions on Graphics **29**, 1 (2010).

[162] M. Hašan, M. Fuchs, W. Matusik, H. Pfister, and S. Rusinkiewicz, *Physical reproduction of materials with specified subsurface scattering,* ACM Transactions on Graphics **29**, 1 (2010).

[163] A. Hosny, S. J. Keating, J. D. Dilley, B. Ripley, T. Kelil, S. Pieper, D. Kolb, C. Bader, A.-M. Pobloth, M. Griffin, R. Nezafat, G. Duda, E. A. Chiocca, J. R. Stone, J. S. Michaelson, M. N. Dean, N. Oxman, and J. C. Weaver, *From Improved Diagnostics to Presurgical Planning: High-Resolution Functionally Graded Multimaterial 3D Printing of Biomedical Tomographic Data Sets,* 3D Printing and Additive Manufacturing **5**, 103 (2018).

[164] I. Horváth, *Comparison of three methodological approaches of design research,* in *International conference on engineering design* (2007) pp. 1–11.

[165] R. S. Hunter, *The Modes of Appearance and Their Attributes,* in *Review and Evaluation of Appearance: Methods and Techniques, ASTM STP 914*, edited by J. Rennilson and W. Hale (American Society for Testing and Materials, Philadelphia, USA, 1986) pp. 5–13.

[166] K. J. Dana, B. van Ginneken, S. K. Nayar, and J. J. Koenderink, *Reflectance and Texture of Real-World Surfaces,* ACM Transactions on Graphics **18**, 1 (1999).

[167] M. Haindl and J. Filip, *Visual Texture* (Springer-Verlag London, London, 2013).

[168] H. T. Nefs, J. J. Koenderink, and A. M. Kappers, *Shape-from-shading for matte and glossy objects,* Acta Psychologica **121**, 297 (2006).

[169] W. S. Elkhuizen, B. A. Lenseigne, C. Weijkamp, S. C. Pont, J. M. Geraedts, and J. Dik, *A 3D printed reconstructing of a painting's original size - Showing the original size of Saul and David by Rembrandt,* in *Visual Science of Art Conference* (Barcelona, Spain, 2016) p. 1.

[170] W. S. Elkhuizen, T. T. W. Essers, B. Lenseigne, C. Weijkamp, Y. Song, S. C. Pont, J. M. P. Geraedts, and J. Dik, *Reproduction of Gloss, Color and Relief of Paintings using 3D Scanning and 3D Printing,* Eurographics workshop on Graphics and Cultural Heritage , 1 (2017).

2

Evaluating color and topography reproductions of three paintings

"You might not tell from my sophisticated appearance, but I am actually of quite humble origin beneath the surface. At the core I am a plain-weave canvas of medium weight, not very exotic. My ground layer is also pretty plain: an unflattering gray tint, rather common for paintings of my generation. There is nothing unique about me up to that layer.

They say the creation of a painting is a painful process. First, they stretch your skin, tight as a drum, onto a strainer. Then they apply the ground layer with a large knife, scraping it across your skin. But I must say, although it is apparently a painful process, it does result in the perfect blank canvas. Crisp and pristine, ready for the first brushstrokes, which brought me into existence.

For the most part, I have been painted with common pigments like vermilion, red and yellow lakes, lead white, iron oxides, and bone black. What is peculiar, is that I have orpiment painted all over me. It used to give me this mesmerizing, gold-like sheen in my youthful years, especially on my lemon. This has almost completely gone now. The weird thing is that orpiment does not mix easily with oil and should not be combined with some other pigments. It also gives a grainy texture on my surface, besides it being poisonous for humans. This makes it a mystery why Mijnheer De Heem liked to use it so much. He must have known about these issues. Anyway, I must have looked stunning at the time he sold me."

— The painting

Abstract

Paintings are near-planar objects with material characteristics that vary widely. The fact that paint has a material presence is often overlooked, mostly because we often encounter these artworks in the form of two-dimensional reproductions. Capturing paintings in the third dimension is not only important for study, restoration and conservation, but it also inspires 3D printing methods [1], particularly through the high demands it makes on reproducing color, gloss and texture. "A hybrid solution between fringe projection and stereo imaging is proposed as 3D imaging method, with a setup involving two cameras and a projector. Fringe projection is aided by sparse stereo matching to serve as image encoder. These encoded images processed by the stereo cameras solve the correspondence problem in stereo matching, leading to a dense and accurate topographical map, while simultaneously capturing the composition of the painting in full color" [1]. The topographical map and color data are used to make hardcopy 3D reproductions, using a specially developed printing system. Several paintings by Dutch masters Rembrandt and Van Gogh have been scanned and reproduced using this technique. These 3D printed reproductions have been evaluated by experts, both individually and in a side-by-side comparison with the original.

This chapter has been published as: **W.S. Elkhuizen**, T. Zaman, W. Verhofstad, P.P. Jonker, J. Dik, J.M.P. Geraedts, *Topographical scanning and reproduction of near-planar surfaces of paintings*, In proceedings of Electronic Imaging: Measuring, Modeling and Reproducing Material Appearance, **9018**, (2014) Note: a few small corrections and/or clarifications have been made to the original published text.

2.1. Introduction

2.1.1. Digitization of cultural heritage

As stated by Zaman *et al.* [2]: "Making Cultural Heritage artifacts accessible to the public is an important mission of museums, libraries and archives". They state that to facilitate this, they often digitize the artifacts to remediate them and make them available on the Internet. Doing this has several advantages. Besides making the artifacts accessible for everyone, digitizing will build a database that can be easily accessed. These digital files of the artifacts can be used for purposes of preservation, relevant for items that are slowly degrading. Moreover, digitization facilitates conservation, art history studies, and restoration. Finally they can be used for exploitation for publicity or profit [2].

2.1.2. A painting is a 3D landscape of paint

Paintings are generally 2D projections of a 3D world, carefully considered and realized by the artist. Zaman *et al.* [2] state: "Painters like Rembrandt and later Van Gogh - apart from using cues such as depth from luminance and shape from shading - more and more used paint in 3D as a medium to give form to the local 3D shape of objects in their paintings", proof of which can be found in the analysis of Rembrandt's work [3]. Also Vincent van Gogh states in one of his letters: "Sometimes the subject calls for less paint, sometimes the material, the nature of the subjects themselves, demands impasto" [4]. Although his writings of a few years later also seem to contradict this: "Don't let it trouble you when in my studies I just leave the brush strokes as I put them on, with smaller or larger clots of paint. That doesn't matter at all; if one leaves them for a year (or half a year is enough), and then scrapes them off quickly with a razor, one gets a much more solid color than would be the case after painting thinly" [4].

Until recently these 3D effects created by painters (also called 'impasto'), as well as 3D texture due to aging (crackle) were overlooked in most digitization efforts of paintings. Retrieving this extra dimension had limited use, only for applications such as topographic analysis; the detection of local surface defects for restoration purposes. However, thanks to current developments in Augmented Reality, consumer 3D screens and 3D printers, the relevance of 3D scanning and publishing is increasing [2].

This paper elaborates on the design of a 3D scanner, suitable for simultaneous capture of color and topography of a painting. Three paintings have been scanned using this 3D scanner: *Self-portrait* by Rembrandt (owned by the Mauritshuis), *Flowers in a Blue Vase* by Vincent van Gogh (owned by Kröller Müller Museum), and *The Jewish Bride* also by Rembrandt (owned by the Rijksmuseum). The data is printed using Océ High Resolution 3D printing technology, creating full color 3D prints. Finally museum experts, who were knowledgeable on the selected paintings, evaluated the reproductions on quality and relevance. This paper presents the results of this evaluation, and will suggest further areas for research.

2.1.3. Existing 3D imaging methods

Zaman [1] states:"Few case studies have been published that focus on the topographical scanning and digitization of paintings, but there have been many case studies on the digitization of statues" [5, 6]. In these case studies the topographical and color data are captured separately, which have to be matched afterwards, making this method prone to misalignments of topography and color. A method to capture topographical and color data simultaneously is by the use of a white light laser scanner [7, 8]. Although this is a very accurate method, with a laser beam diameter of (less than) 100 µm, the capture speed is low. In the described configuration, (50 µm resolution, 10 kHz capture speed) the capture time, excluding processing and overhead time, of *The Jewish Bride* (1.22 m × 1.67 m) would take 22 hours: too long for paintings that require overnight scanning (between opening hours of the museum) [9].

Also several case studies have been published that make use of a fringe projection [7, 10, 11]. The scanning setup consists of a projector and only one camera for the triangulation of the depth data. The drawback of this method is that the resolution is limited to that of the projector, which is often no more than 1 or 2 Megapixel (The newest consumer cameras have a resolution of 40Mp). One study was found using a setup of one projector and two cameras [12]. This implementation is inefficient for capturing larger paintings, as the scanner is not automated in x or y-direction. Besides that the researchers note that the scanner has difficulty capturing highly reflecting surfaces, which will pose a problem for scanning varnished paintings. We can therefore conclude that paintings require a novel 3D scanning method, which is further described below.

2.2. Method

2.2.1. Development of 3D scanner

In order to scan the topography and color of paintings with sufficient accuracy and efficiency, Zaman [1] set to develop a high-resolution 3D scanner with the following requirements:

- Non invasive, portable and low cost
- Size (XY): 2 m × 2 m, Depth (Z): 2 cm; we assumed most paintings fall within these boundaries
- Resolution: 50 µm/pixel; the resolving power of the human eye at a distance of 75 cm [13]
- Color Accuracy: ΔE conform the Technical Guidelines for Digitizing Cultural Heritage Materials, FADGI [14]

After careful analysis we devised a principle solution based on a combination of stereo vision and fringe projection. Stereo vision is a passive method with excellent color reproduction and a good absolute triangulation; however it requires images with much saliency i.e. it fails on surfaces without texture. To overcome this, we used a projector to project fringe patterns on the painting. Triangulation using fringe-projected patterns is a relative triangulation method that requires no saliency

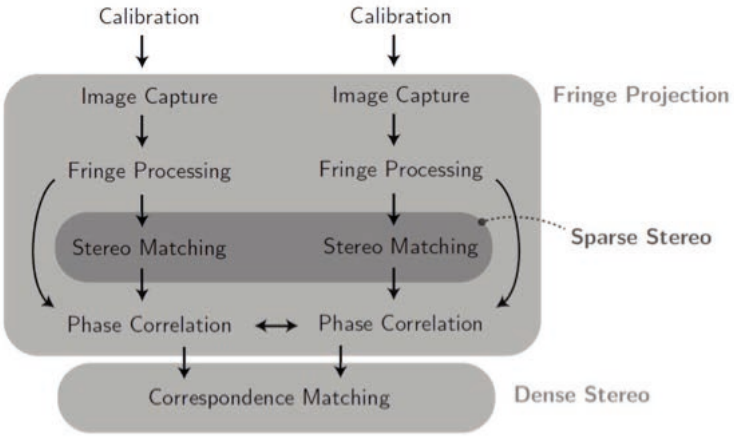

Figure 2.1: Procedure for using fringe projection to aid dense stereo matching

in the image as texture is actively projected. Our method has phase unwrapping problems, but these can be solved. In combining the methods of stereo vision and fringe projection we obtain all advantages and no disadvantages by using the following procedure. The stereo matching is first performed on salient points in the image only. Then these points are used to anchor the relative matches of the fringes triangulation, making all matched pixels in the image absolute 3D points. Finally all points are fused with points obtained from dense stereo matching, providing for each pixel in the image both depth and color [1] (see Figure 2.1).

A set of 2x3 fringes is used to triangulate the depth information, with two sets of phase-shifted fringes (0°, 120°, 270°), one vertically oriented and one horizontally oriented. The color data is obtained by taking the average of the RGB values from different shifted fringe captures. This results in an image that yields the intensity of the scene as would have been measured by a normal RGB camera without fringes and normal illumination. The output of our procedure is a 3-D point cloud where each point is labeled with a color RGB. For easy data validation, we estimate the plane orientation and mesh all the values into two 2-D (X, Y) maps; a depth map (Z) and RGB map [1].

Figure 2.2 shows the set-up of the 3D scanner with the (Optoma PK301) pico-projector and (Scheimpflug) lenses on the 40-megapixel DSLR (Nikon D800E) cameras. A linear translation axis was used to scan with a 17 cm × 10 cm 40 Megapixel window over the painting. For the properties of each window see Table 2.1. The vertical translation was done manually (see Figure 2.3). One capture took two minutes and processing took ten minutes per capture. All captures were 3D stitched to form the final dataset of the image [1].

The lenses on the DSLR cameras had a convenient fitting to accommodate polarization filters. These were oriented in such a way that surface reflections from the plane in front of them were optimally suppressed. We achieved cross-polarization

by putting another polarization filter in front of the illuminant (projector), oriented so that it is polarized perpendicular to those of the camera. This reduced in surface reflections even further, indeed, this set-up was so effective that (at least to the eye) it eliminated reflections completely [1].

The controller of the system was based on an Atmel chip flashed with the Arduino bootloader allowing programming in C++. The micro stepping of the linear translation axis was performed with an Allegro A4988 chip, while manual adjustment of the axis was possible with a joystick. End-stops were realized with Hall sensors. A Six-Axis (Gyro + Accelerometer) MEMS MotionTracking™device (MPU-6050) was used to track all movements of the scanner, which could be caused by the external influences; high motion amplitudes postponed the capture of images. The triggers to the camera and whether the cameras were actually triggered could be sensed through the connection of a synchronization (or flash-) cable between the devices [1].

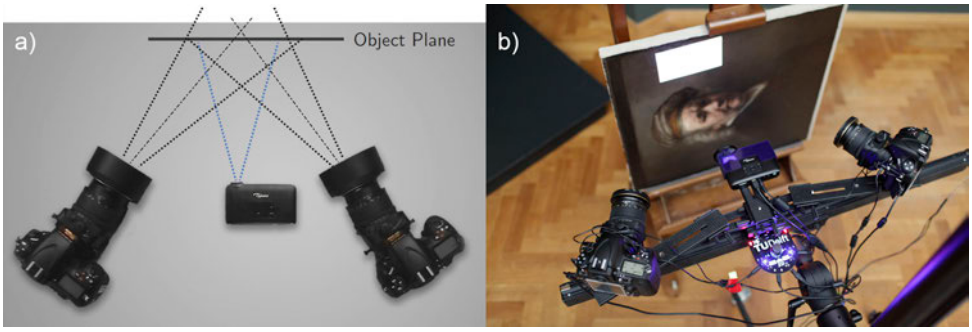

Figure 2.2: (a) Top view of scanner setup including projector and two cameras, (b) top view of the camera including linear translation axis and PCB.

Figure 2.3: Video 1: Scanning *The Jewish Bride* at the Rijksmuseum

With the above described setup the image was sampled at a resolution of 22 µm. Due to discrete sampling and the fact that the cameras were rotated towards our plane of interest around the vertical axis, the effective resolution is lower (in the latter case only the horizontal resolution (X) is lower). Using ISO guidelines for resolution measurement the in-plane sampling efficiency was determined [15]. The

in-plane effective resolution was found to be 65 µm (X) and 46 µm (Y). Expressed in dots per inch (dpi) this is respectively 390dpi and 550dpi, the first being slightly lower that the printing resolution (see next paragraph). No guideline exists yet for resolution measurement of depth (Z), however the effective resolution was found to be 9.2 µm [1]. Figure 2.4 shows a detail of the hat of Rembrandt in the *Self-portrait*; the color map in RGB and depth map in gray scale.

Table 2.1: Properties of one scanned image

	X	Y	Z
Size	17 cm	10 cm	1 cm
Sampled Resolution	22 µm	22 µm	N/A
Effective Resolution	65 µm	46 µm	9.2 µm
Accuracy	68 µm	26 µm	38 µm

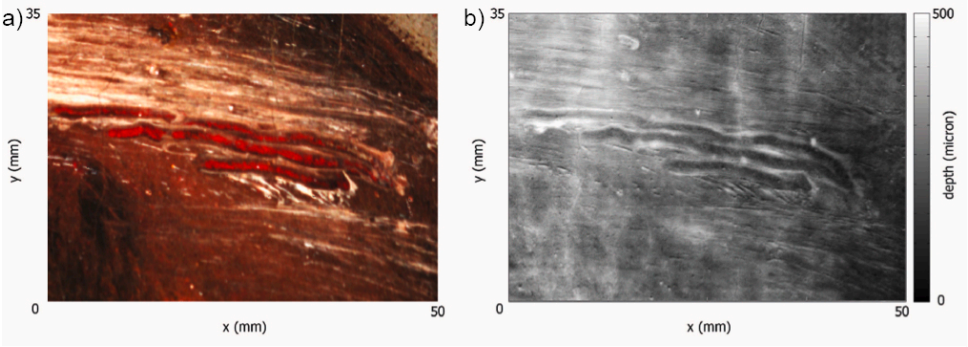

Figure 2.4: (a) Detail of Self-portrait RGB color map, (b) detail of Self-portrait depth map in gray scale

2.2.2. 3D printing

The two 2D maps (X, Y); a gray scale depth map (Z) and RGB color map formed the input for the 3D printing process [16]. The maps were used to make a physical reproduction of the data using a new developed (Océ High Resolution) 3D printing technology. The printer builds up the relief layer for layer with 5 UV-curable inks (CMYK and White). The 3D printer deposits relief layers to create the specified height (Z) for every coordinate (X,Y) in the image, with color layers on top (see Figure 2.5). The print was printed on a rigid support medium (see Figure 2.6). The resolution of the print is approximately 450 dpi (X,Y).

2.2.3. Paintings and reproductions

For the evaluation of the scanning and reproduction technology, three iconic Dutch paintings were selected and reproduced: *Self-portrait* by Rembrandt (owned by the Mauritshuis), *Flowers in a Blue Vase* by Vincent van Gogh (owned by Kröller Müller

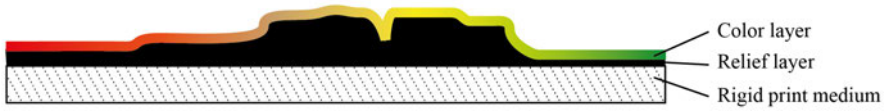

Figure 2.5: Graphical representation of the 3D print layers

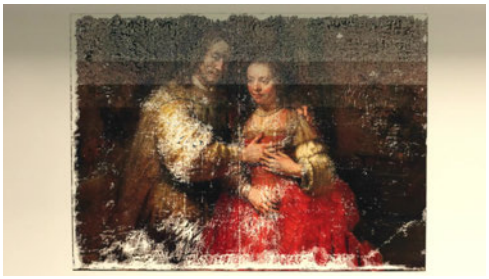

Figure 2.6: Video 2: Printing the *The Jewish Bride* on Océ High Resolution 3D printer

Museum), and *The Jewish Bride* by Rembrandt (owned by the Rijksmuseum). These paintings were selected for the fact that they all have a pronounced impasto. Figure 2.7 shows details of the reproductions.

A quite straightforward procedure was followed for this first evaluation: Besides camera color calibration (with 24-patch color checker) [1], no additional color matching with the original painting was undertaken.

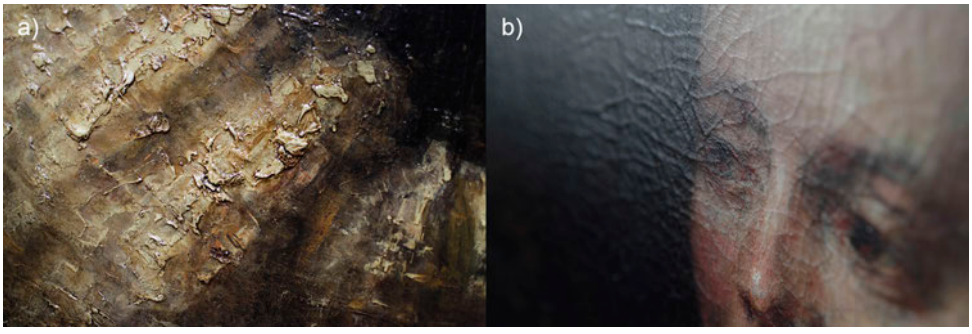

Figure 2.7: (a) Detail of impasto of *The Jewish Bride* (left), (b) detail of crackle on *The Jewish Bride* (right)

2.2.4. Evaluation of reproductions

The reproductions were evaluated with expert interviews, as we expected them to be critical and most able to spot small differences. Each evaluation encompasses a 4-step procedure in which the reproductions were evaluated:

1. Singly by the expert from a distance, meaning a viewing distance of > 75 cm
2. Singly by the expert at close range, meaning a viewing distance of <75 cm
3. In a side-by-side comparison with the original painting, where the reproduction and painting are standing/hanging or lying next to each other from a distance
4. In a side-by-side comparison with the original painting, where the reproduction and painting are standing/hanging or lying next to each other in close range (see Figure 2.8)

Figure 2.8: Evaluation of *Flowers in a Blue Vase* step 4: close range side-by-side comparison

During each step there was an semi-structured interview with the experts to collect answers to our questions. A pilot interview was carried out evaluating the *Flowers in the Blue Vase*. The interview questions were thereafter slightly revised to include relevant feedback topics, which emerged from this first interview.

The following topics were covered in the interviews: general evaluation of the reproduction; feedback on color, texture, gloss and transparency/layers; and potential applications for the technology. It should be noted that although we asked experts for feedback on gloss and transparency/layers, these aspects were not measured in paintings and for this research not actively addressed in the reproduction. In addition to this we are aware that the comparison of reproduction and painting took place in situ, which is not ideally suited for color evaluation, as set in ISO standard *Graphic technology and photography – Viewing Conditions* [17]. We had to deviate from the ISO standard for practical reasons, as museums are not keen to move their precious paintings. In total six interviews were conducted with fine art experts, working at the respective museums (see Table 2.2). The experts are employees of the before mentioned museums, in charge of these paintings. All experts

had a background in art history and/or conservation-restoration and have multiple years of experience in this field; they are trained in observation and evaluation of paintings. Most participants were excited to evaluate the technical advancements of 3D scanning and printing, although some were skeptical, especially of the scientific relevance for the field of art history and conservation-restoration.

Table 2.2: Expert interviews

Reproduction of	Number of experts	Professional background of experts
Flowers in a Blue Vase by Vincent van Gogh	1	Conservator-restorer
The Jewish Bride by Rembrandt	2 2	Heads of Fine Art Department Conservator-restorers
Self-portrait by Rembrandt	1	Head of Conservation/Restoration Department

2.2.5. Analysis of interviews

At the pilot interview, notes were taken and summarized in a report. The other five interviews were recorded and transcribed. This data was analyzed by applying the qualitative data analytic process of data coding [18]. Several complementary first cycle coding methods were used: descriptive coding, in vivo coding, evaluation coding, values coding and domain and taxonomic coding. In the second cycle coding, similar codes were clustered and reorganized following an axial coding method. A summary was sent to the experts to provide opportunity for correction.

2.3. Results

2.3.1. Feedback on reproduction evaluation and comparison

Table 2.3 gives and overview of codes that were assigned to the data that was related to the evaluation of the reproduction and the comparison of the reproduction to the respective painting. The codes are grouped into four main categories: (1) feedback on the visual appearance, (2) causes/effects of how painting techniques and methods lead to the current visual appearance of the painting, (3) comments on viewing conditions and viewing strategies, and (4) feedback regarding the tactile sensation. We will discuss each code in this chapter.

Color

When viewing the reproduction of the *Flowers in the Blue Vase* and the *Self-portrait* singly the colors were evaluated good and ok, respectively. In side-by-side comparison experts could however spot several differences. They evaluated the colors in the *The Jewish Bride* reproduction as too saturated. The Jewish Bride was "too red", and the "red nearly looks like rosacea in the faces". In all paintings experts

Table 2.3: Codes: Evaluation of reproduction and comparison to painting

Visual appearance	Color	Saturation[a] Hue[a] Brightness[a] Contrast Overall score/evaluation
	Texture	Added Effect Difference Sharpness Overall score/evaluation
	Gloss	Visual effect of gloss Overall score/evaluation
	Transparency/ layers	Visual effect of transparency/gloss Overall score/evaluation
	Sharpness & smoothness	Edge sharpness[a] Smoothness[a]
	Total effect	Pictoral depth perception 'Magic' of a painting Overall score/evaluation
Cause/effect	Painting techniques/ materials	Painting materials Painting techniques Material aging/damage/degradation
Viewing condition/strategy	Viewing light Evaluation strategy	
Other senses	Touch	

[a] These perceptual attributes are also used in image quality evaluation of 2D color images [19]

evaluated that the hue was 'off' in various colors (green, blue, red and yellow) when comparing the reproduction to the painting. The flesh tones in *Self-portrait* were evaluated as being good. Also the brightness of the colors was not evaluated as 'spot on'; the *The Jewish Bride* and *Flowers in the Blue Vase* were too dark and in the *Self-portrait* the black tones were not intense enough. Overall the reproduction of color was evaluated 'below average' in the evaluation and 'low' when compared to the original painting. The distance to the painting and reproduction had little influence on the evaluation.

Texture

The experts thought the texture was impressive. They stated the reproduction "approaches the original". However, they also observed a difference between the reproduction and the original. At close evaluation they noted that the texture lacked

"crispness" and that the edges seemed rounded, therefore remaining on a reproduction level. Overall the texture was evaluated as average to good.

Gloss

Experts perceived the gloss of the reproductions as too uniform compared to the original paintings. They stated that the gloss of paintings varies throughout the surface of a painting and also between paintings. The "uniform gloss emphasizes that it is a reproduction, not original". The gloss makes the reproduction look "plastic" and gives it a "synthetic appearance". Overall the gloss is quite a good match to a painting: not too glossy, not too matte.

Transparency/layers

It was evaluated that layering (of paint) and the transparency of layers are missing in the reproductions of the Rembrandt paintings. A "large contribution of the brown ground is coming through", making the contribution of the ground layer too "harsh" in the reproduction. Overall the transparency was evaluated as low. An expert explained that it is "essential to get depth from transparency". Translucent layers of lacquer create a pictorial depth effect oriented backward (where impasto creates a depth effect oriented towards the viewer). Layers were also said to create a "glowing effect" in the painting, which is missing in the reproduction.

Sharpness/smoothness

Experts mentioned that the contours seem sharper in the reproduction than the original. The "sfumato" transitions (one of the four canonical painting modes of the Renaissance) give the edges in the painting a softer appearance. In the reproduction the "linearity is sharper". At close range the experts perceive a graininess of the reproduction and mention seeing the pixels of the reproduction: "I immediately see those pixels". With a head magnifier this is even clearer. An expert commented: "You get thrown back".

Total effect of visual appearance

When looking at the overall composition of the painting, the experts concluded that the reproduction looses some of the depth that can be found in the painting: "Faces are quite flat actually", and "despite the 3D quality the reproduction appears flat". One commented that in *The Jewish Bride* the "hand falls apart".

It is interesting to note that several experts described the overall look of the painting as the "magic of the painting" or as being "enchanted by the original" and that "normally your eyes drown in these wet-in-wet details".

The overall evaluation of the experts was that the reproductions "approach the paintings closely", but remains "a copy that is not there yet". In contrast another expert exclaimed: "I thought this was a real painting for a minute", when someone touched the surface of the reproduction.

Cause/effect

The experts reasoned what they see in the painting in comparison to the reproduction by their knowledge of the painting. For instance: "Rembrandt used a transparent lacquer on a opaque underlayer". They also explained the colors they perceived

by the knowledge of the pigments that were used: "I know the painting is bone black", and that the layering of the painting by the knowledge that the "ground is a brown color". An expert explained that the gloss between paintings can vary because "You can have a very glossy varnish on a painting and also a matter varnish". Also for the gloss variation within a painting they had an explanation at hand ("some areas are more porous that others") and they also knew that the painting was "painted with different kind of pigments that absorb varnishes to different degrees". Furthermore, they also explained the sharpness of the texture by the technique that Rembrandt used "with a sharp tool, the back end, pffft, scratched into it [the painting]".

Experts also partially explained the visual presence of the paintings was by the aging of the materials. They generally evaluate a painting by looking for original paint, later additions but also sign of material aging: changes in gloss and color. Degradation can "vary from centimeter to centimeter", for instance chemical degradation: "surface whitening can occur due to crystal formation", but also physical degradation in the form of cracks and abrasion.

Viewing condition, viewing strategy

All experts were aware of the influence of the ambient lighting on the visual perception of a painting. Restorers use either daylight or a daylight-simulating lighting when evaluating and restoring a painting. They need to have "real light" not "pretty light". An expert explained her strategy for the evaluation of a painting as follows: first looking from a distance, with the naked eye, and then coming closer, inspecting the material and details, and continuing with a magnifying glass and microscope: "when you come closer and closer you begin to understand". In their viewing strategy they also look at a painting from several angles. Besides that, they practice "informed looking", and state to "have a certain expectation". Their knowledge of a certain artist or period helps them to evaluate a painting.

Other senses

All experts remarked that they were fascinated by the fact that they could now "touch a painting". The reproductions were considered to be "inviting" to touch.

2.3.2. Applications of 3D reproduction technology

Experts were asked what potential they saw for 3D fine art reproduction technology. Aside from the in their eyes obvious application - commercial - various other opportunities were mentioned. The technology might be used for educational programs with museums: showing (children) how paintings are build up, and being able to touch the whole surface. This might be extension of the current practice where guides carry small, repainted fragments of paintings with them. It also might play a role in making painting more accessible for the visually impaired.

Experts remarked that the technology of creating a texture map might be useful to make so called condition reports. The condition of a painting is currently visually assessed at the departure and arrival after transport. The texture map could help to objectify this and "sideline personal vision".

Experts explained how a reconstruction of the original state of a painting could play a role in art historic research. They wonder "what was the color in the past" and "which changes take place in the painting". One expert stated: "historic color is important for the experience of fine art". But maybe even more importantly the remark was made: "How will it [the color] change in the next 100 or 200 years?" The technology may provide the opportunity to make a physical reconstruction of a painting in its original state, when it was just painted. This could also include making a reconstruction of the original size as "many paintings have missing pieces". This could never be done on an original work of art, as this would be an "enormous intervention on the original painting" and the "current construction has a history and also value".

Two examples were given of how the technology could support current restoration practice. Making "six different versions" of a piece, which needs to be restored, could help "solve a restoration dilemma". And maybe the most radical suggestion was that pieces of 3D printed material might be used as restoration material. The piece of 3D printed painting could replace a piece where "the texture is not good" or is missing. The 3D printed piece could be stuck on the painting with "stable glue", and would in itself need to be a "stable material", having no interaction with painting.

2.3.3. Values, beliefs and attitudes of experts

Several values, beliefs and attitudes toward fine art and reproductions could be extracted from the interviews. Experts value the authenticity of a painting, and find it important not to make forgeries: all current restoration work should be reversible. They believe that the "magic of a painting cannot be reproduced" and that a "reproduction is mechanical". They believe humans are very well equipped to detect subtle differences. Making an indistinguishable reproduction will be very challenging indeed. Several experts expressed that they know the evaluated painting by heart, making a literal comparison superfluous. They were also not interested in evaluating the color, as they felt only the texture had added value compared to a 2D reproduction, and was therefore the only aspect that was interesting.

2.4. Discussion

Some of the perceived color differences can be explained from the limitations of the 3D scanning, 3D printing and viewing conditions. The limitations of the 3D scanning system lay in the non-neutral illuminant (RGB-LEDs) and non-consistent illumination during the scanning procedure - when working in a museum environment with a not fully controlled lighting situation. This uncontrolled lighting situation also occurs when comparing the reproduction with the painting. In all cases the spectral properties of the illuminants in situ were not known and the painting and reproduction were not illuminated in an identical way. Although, when resolving these issues, perceivable color differences might still occur as the painting and reproduction as they are not spectrally matched. Spectral imaging and reproduction of fine art would potentially solve this, which was already explored for art reproduction by

Berns *et al.* [20].

The cause of the observed differences in texture between the reproduction and the original painting has currently not been determined. This could either be a limitation of the 3D scanner or a limitation of the current print strategy; some characterization of texture printing has been undertaken [21]. Gloss, transparency and layering – not measured or reproduced in the reproduction – were also found to play a role in the visual perception of the reproduction (gloss manipulation in prints has recently been researched [22]). The way these visual attributes play a role in the perception of paintings has not been investigated presently.

Feedback on the reproductions showed that resolution requirement of the print (300dpi) - matching the resolving power of the human eye at a viewing distance of >75cm – would probably suffice for viewing at that distance. However, when experts inspected the reproduction at much closer range, a common practice when evaluating a painting, they noticed the pixels of the reproduction. It becomes apparent that the used resolution does not suffice for observation at close range. Additionally experts observed increased edge sharpness in the reproduction. This can currently not be quantified or explained, as RAW color data was used which was not digitally sharpened.

In many instances the experts used their considerable prior knowledge of the paintings, materials and techniques - used by painters in the past - to explain differences between the painting and reproduction. This aspect should be taken into account in further research into visual perception, as currently the effect on the evaluation is unknown. What part of the feedback is really visually perceived and which parts might be inferred, based on experts' extensive knowledge of the artworks? Follow-up studies using laymen may shed light on this issue. Also, the experts' attitude towards comparison hints to this: an explicit comparison of the painting and reproduction was deemed not necessary, as they know the painting by heart. However many studies have shown that human memory can be anything but a reliable source.

2.5. Conclusions

The evaluation of the three reproductions and comparison with their respective originals by experts showed that adding texture to a printed reproduction has great added value to realistically reproducing artwork. The 3D texture has the effect that experts approach the reproductions as if they are real paintings, rather than viewing them as 'just a reproduction', like a poster or canvas print. The reproductions also open up a new dimension for appreciation, touching a painting.

However, currently experts can still observe various noticeable differences between the reproduction and the painting. The colors were not exactly the same – in some cases very clearly different - and were found to be a very dominant factor in the evaluation. Some of these perceived differences could be explained from the limitations of the 3D scanning, 3D printing and viewing conditions. This can be improved by changing illumination at capture and viewing, or potentially eliminated when resorting to multi-spectral imaging and the use of more print colors.

The texture was impressive although noticeably different, even when compared

at a distance. At close examination the experts determined that the edge sharpness of the texture appeared to create the difference. The cause of this effect remains to be determined.

Other aspects – not measured or reproduced in the reproduction – were also found to play a role in the visual perception of the reproduction. In contrast to varying gloss in a painting, the uniform gloss of the reproduction is a clear hint to the experts that they are dealing with a reproduction. It gives the reproduction a synthetic and 'plastic' look. Also the overall gloss should be matched, which varies between paintings. In addition the material buildup of the reproduction seemed to be perceivable, as compared to the paintings. (Semi) transparent layering of materials creates visually perceivable depth in an artwork and 'glowing' colors, which is currently not measured and therefore not reproduced.

The sharpness and smoothness of the reproduction also showed noticeable differences for the experts. Edges of the image (not the texture) were perceived sharper, which we can currently not explain. And at close range the pixels of the 3D print become visible to the experts. Further research must determine which viewing distance would suffice for a specific application and which resolution is attainable by the 3D scanner and 3D printer.

2.5.1. Improvements and future work

The design of the 3D scanner should be adapted to improve the color reproduction performance. This can be achieved by using a neutral illuminant, as currently a three-color illuminant (i.e. the projector) is used. Additionally, external illumination should be controlled when scanning the painting, as well as the lighting situation when evaluating the reproduction (in comparison to the painting). To further increase the performance, color calibration should be done with a reference chart containing more color patches. The reproduction of the texture should also be improved. The lack of edge sharpness needs to be quantified, the cause of this effect determined and corrected for.

Further research will be conducted into the capture and reproduction of other visual properties, which were not addressed in this research: gloss measurement and gloss reproduction. Ultimately also the transparency and layers should be measured and reproduced, in order to come close to the perfect reproduction of the visual properties of paintings, and potentially also other materials.

And finally, the role of visual perception should be investigated: how are various visual characteristics perceived, and to what level of detail do visual characteristics need to be reproduced to make an indistinguishable reproduction? A comparison might be made between experts and laymen, to determine the effect of prior knowledge but potentially also effects of trained looking and evaluation.

References

[1] T. Zaman, *Development of a Topographic Imaging Device for the Near-Planer Surfaces of Paintings*, MSc thesis (Delft University of Technology, Delft, The Netherlands, 2013).

[2] T. Zaman, J. Dik, and P. Jonker, *Modern Digitization for Cultural Heritage: Simultaneous Capture of 3D Topography and Colour in Paintings of Van Gogh and Rembrandt,* AR[t] - Magazine about Augmented Reality, art and technology , 56 (2013).

[3] E. Van de Wetering, *Rembrandt: The Painter at Work* (Amsterdam University Press, Amsterdam, 1997) pp. 175;251–252.

[4] V. Van Gogh, *The Letters of Vincent van Gogh*, edited by R. de Leeuw (Penguin, London, 1996).

[5] M. Levoy, *The Digital Michelangelo Project,* Computer Graphics Forum **18** (1999), 10.1111/1467-8659.00319.

[6] F. Bernardini, H. Rushmeier, M. M. Ioana, J. Mittleman, and G. Taubin, *Building a Digital Model of Michelangelo's Florentine Pietà,* IEEE Computer Graphics and Applications **22**, 59 (2002).

[7] C. Lahanier, G. Aitken, R. Pillay, J.-A. Beraldin, F. Blais, L. Borgeat, L. Cournoyer, M. Picard, M. Rioux, J. Taylor, B. Breuckmann, P. Colantoni, and C. de Deyne, *Two-dimensional multi-spectral digitization and three-dimensional modelling of easel paintings,* in *14th Triennial Meeting the Hague, Rome: International Council of Museums*, edited by I. Verger (National Research Council Canada, 2005) pp. 1–20.

[8] F. Blais, J. Taylor, L. Cournoyer, M. Picard, L. Borgeat, G. Godin, J.-A. Beraldin, M. Rioux, and C. Lahanier, *Ultra high-resolution 3D laser color imaging of paintings: the 'Mona Lisa' by Leonardo da Vinci,* in *7th International Conference on Lasers in the Conservation of Artworks*, edited by M. Castillejo, P. Moreno, M. Oujja, R. Radvan, and J. Ruiz (National Research Council Canada, Madrid, Spain, 2007) pp. 1–8.

[9] F. Blais, J. Taylor, L. Cournoyer, M. Picard, L. Borgeat, L.-G. Dicaire, M. Rioux, J.-A. Beraldin, G. Godin, C. Lahnanier, and G. Aitken, *Ultra-High Resolution Imaging at 50 micron using a Portable XYZ-RGB Color Laser Scanner,* in *International Workshop on Recording, Modeling and Visualization of Cultural Heritage*, edited by M. Baltsavias, A. Gruen, L. van Gool, and M. Pateraki (National Research Council Canada, Ascona, Switzerland, 2005) pp. 1–16.

[10] E. Bunsch, R. Sitnik, and J. Michonski, *Art documentation quality in function of 3D scanning resolution and precision,* Computer Vision and Image Analysis of Art II **7869**, 78690D (2011).

[11] M. Karaszewski, M. Adamczyk, R. Sitnik, J. Michoński, W. Załuski, E. Bunsch, and P. P. Bolewicki, *Automated full-3D digitization system for documentation of paintings,* in *Optics for Arts, Architecture, and Archaeology IV*, Vol. 8790, edited by L. Pezzati and P. Targowski (Munich, Germany, 2013) pp. 1–11.

[12] P. Payeur and D. Desjardins, *Structured Light Stereoscopic Imaging with Dynamic Pseudo-random Patterns,* in *6th International Conference, ICIAR*, edited by M. Kamel, , and A. Campilho (Springer Berlin Heidelberg, 2009) pp. 687–696.

[13] C. A. Curcio, K. R. Sloan, R. E. Kalina, and A. E. Hendrickson, *Human photoreceptor topography.* The Journal of comparative neurology **292**, 497 (1990).

[14] Federal Agencies Digitization Initiative (FADGI) - Still Image Working Group, *Technical Guidelines for Digitizing Cultural Heritage Materials : Creation of Raster Image Master Files*, Tech. Rep. (Federal Agencies Digitization Initiative Still Image Working Group, 2010).

[15] ISO, *ISO 12233 - Photography - Electronic still-picture cameras - Resolution measurements,* (2000).

[16] J. Geraedts, E. Doubrovski, J. Verlinden, and M. Stellingwerff, *Three views on additive manufacturing: business, research and education,* in *Ninth International Symposium on Tools and Methods of Competitive Engineering (TMCE)*, edited by I. Horváth, A. Albers, M. Behrendt, and Z. Rusák (Karlsruhe, Germany, 2012).

[17] ISO, *ISO 3664:2009 - Graphic technology and photography - viewing conditions,* (2009).

[18] J. Saldana, *The coding manual for qualitative researchers* (SAGE Publications, 2009) pp. 1–223.

[19] J. Dijk, *In search of an objective measure for the perceptual quality of printed images*, Ph.D. thesis, Delft University of Technology, Delft (2004).

[20] R. S. Berns, L. A. Taplin, P. Urban, and Y. Zhao, *Spectral color reproduction of paintings,* in *Colour in Graphics, Imaging, and Vision* (Society for Imaging Science and Technology, 2008) pp. 484–488.

[21] X. Liu, L. Chen, M. V. Ortiz Segovia, J. A. Ferwerda, and J. P. Allebach, *Characterization of relief printing,* in *Electronic Imaging: Measuring, Modeling, and Reproducing Material Appearance* (2014).

[22] T. Baar, S. Samadzadegan, H. Brettel, P. Urban, and M. V. Ortiz Segovia, *Printing gloss effects in a 2.5D system,* in *Electronic Imaging: Measuring, Modeling, and Reproducing Material Appearance*, edited by M. V. Ortiz Segovia, P. Urban, and J. P. Allebach (2014).

3

Exploring spatially-varying gloss reproduction

"I don't actually remember much about my early childhood. I fantasize that I lived at classy residences all around the Netherlands, or in places that you humans now call Belgium. It seems nobody cared much about my whereabouts at the time. At least, not enough to write it down. My earliest memory dates back to the Nationale Konst Gallerij, which was originally at Huis Ten Bosch. I must have been around 130 years old. Mind you, that is pretty young for a painting: something comparable to a teenager in human terms. Although it seemed a decent enough place to hang around, I remember we moved quite a bit in the years following.

When I turned 152, I was one of the first to move into the new Mauritshuis. But they did not reserve the most glamorous spot for me at the time; I ended up being put in the attic! Can you imagine the humiliation? I heard they even lost me for a while. Must have been the time I was gathering dust in the corner, overshadowed by that huge, grumpy painting, who was my neighbour. He seemed to deal with the humiliation even worse than I did.

I did get my time to shine later in my career, travelling the world, meeting fancy-dressed humans all the time. For a large part of my working life, I lived in Brussels, at the Dutch Embassy. It was a decent enough location. But the highlight of my working life, to date, is the trip I made to the National Museum of Contemporary Art in Seoul, South Korea. Humans loved me over there. I got photographed all the time. I guess that is what it feels like to be a rock star."

— The painting

Abstract

In the field of Fine Art reproduction, 3D scanning plus 3D printing, combined with dedicated software, now allows to capture and reproduce the color and texture of oil paintings. However, for life-like reproduction of the material appearance of such paintings, the typical gloss and translucency must also be included, which is currently not the case. The aim of this paper is to elaborate on the challenges and results of capturing and reproducing oil paint gloss (next to texture and color) using a scanning and printing system. A sample was hand-made using oil paint and acrylic varnish, and its gloss was then reproduced. A gloss map of the painted sample was acquired using a high end DLSR camera and a simple acquisition protocol. Next, Océ High Resolution 3D printing technology was used to create samples with spatially varying gloss. For this, two different strategies were combined: (1) multilevel half-toning of the colors was used to reproduce matte color layers, and (2) varnish was half-toned on top in increasing coverage to recreate increasing gloss levels. This paper presents an overview of the state-of-the-art literature in gloss reproduction and perception, our process of reproduction as well as the visual evaluation of the quality of the created reproduction.

This chapter has been published as: **W.S. Elkhuizen**, B.A.J. Lenseigne, T. Baar, W. Verhofstad, E. Tempelman, J.M.P. Geraedts, J. Dik, *Reproducing oil paint gloss in print for the purpose of creating reproductions of Old Masters*, In proceedings of Electronic Imaging: Measuring, Modeling and Reproducing Material Appearance, **9398**, (2015) Note: a few small corrections and/or clarifications have been made to the original published text.

3.1. Introduction

3.1.1. Reproduction of material appearance

There are many recent developments where one or more attributes of material appearance are reproduced, either digitally or physically, e.g. realistic rendering of fabrics (color, gloss, texture) [1], multi-spectral imaging and printing (color) [2], printing gloss variation [3], and 3D printing objects with a surface texture and color [4, 5].

The development of a 3D scanner [6] in combination with the High Resolution 3D printing technology of Océ Technologies (Canon group) is among these advances. It has already led to the possibility to capture and reproduce the color and texture of historic oil paintings (by Rembrandt and Van Gogh). However, expert evaluation has established that this does not yet recreate a life-like (realistic) material appearance: the typical gloss levels and the translucency of the paints are missing and the colors and textures are not yet sufficiently accurately reproduced [7].

The aim of Fine Art appearance reproduction is to create visually indistinguishable reproductions of works of art using a limited number of materials. This does not necessarily entail using materials that are similar to the original materials (see Figure 3.1); the criterion for the material selection is that they create a similar visual appearance and that the selected materials in combination can span a wide variety of appearances, that are typically found in Fine Art; in the way that a CMYK color space can represent a wide range of colors via optical color mixing.

3.1.2. Reproduction of oil paint gloss

In the evaluation of earlier 3D Fine Art reproductions [7], experts noted that paintings exhibit varying levels of gloss across the surface (due to aging, degradation, abrasion, overpainting, material use etc.), which contrasted clearly with the uniform level of gloss of the reproductions. Therefore, in order to create a more life-like reproduction, the reproduction system needs to be able to capture, as well as print, this spatially varying gloss of the paint surface. Moreover, the intended scanning system must be able to deal with the texture of the paint surface (as was demonstrated previously, paintings are not flat), as well as continuous color variations.

The fact that we are dealing with valuable works of art and that access to these objects is limited leads to several other requirements for the (final) scanning system. This system must be non-invasive, non-contact and portable (to make scans on

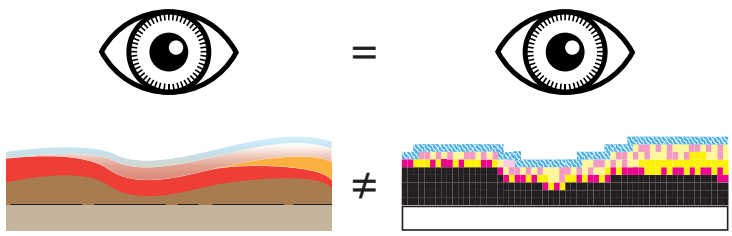

Figure 3.1: Visual appearance is similar, while material use is different (and limited for printing)

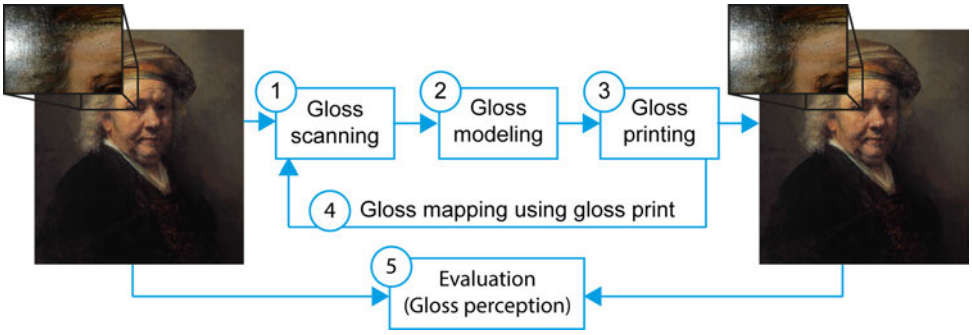

Figure 3.2: Workflow of gloss reproduction

location), and the scanning procedure (more specifically, the data acquisition) must be relatively quick: capturing a painting of 1x1m should take no more than a few hours. Furthermore, to assure exact alignment of the gloss map with the color and texture map of the 3D scanner, gloss scanning should preferably be integrated with the 3D scanner. To date, no such system is known to exist.

The following questions should be answered in relation to gloss reproduction of paintings:

- What *spatial resolution* is needed for gloss reproduction?
- Which and how many parameters should be used to describe the gloss characteristics and what is the necessary *depth resolution* of these parameters?
- Will relative gloss matching (i.e. gloss mapping) lead to a sufficiently life-like material appearance or is absolute gloss reproduction necessary?

Figure 3.2 gives an overview of the general workflow of gloss reproduction. (1) The original painting is scanned using a gloss (and color and texture) scanning system. (2) The output data is then processed and represented in one or more parameters. (3) This data can then be transferred to the printer and printed as a gloss layer either 'on top' of a 3D textured and colored print or 'as an integral part' of the print. The printed samples are used as an absolute reference for the scanning system; making it possible to (4) map the measured gloss to the printable gloss. And ultimately (5) the reproduction is evaluated (by experts) by visually comparing it to the original to provide (perceptual) feedback; this feedback is used to better understand which parameters are important for gloss reproduction and how the gloss reproduction system can be improved.

This paper elaborates on the results and challenges of capturing and reproducing oil paint gloss (in combination with color and texture reproduction) using a dedicated scanning setup and a 3D full color printing system.

3.1.3. Applications of life-like 3D reproductions

Accurate reproduction of paintings (using a digital process instead of a manual process) offers various opportunities for the field of cultural heritage. For instance, it can be used to create historical reconstructions of how the paintings looked be-

fore they experienced the effects of aging, recreate missing pieces of paintings, or support the restoration practice by providing examples of restoration variants. Of course, educational or commercial applications are also foreseen, as is making accurate databases of paintings to conserve the works in the digital domain. Apart from these applications, making reproductions of painted heritage also challenges the scientific study of perception: which aspects of material appearance really matter for making life-like reproductions? Likewise, the technology involved is challenged to reach a higher level of fidelity. Finally, it seems reasonable to assume that the knowledge can also be used for the reproduction of material appearance in other domains, such as the recreation of historic political documents or even archaeological artifacts.

3.2. Related Work

3.2.1. Gloss as an attribute of material appearance

The measurement and description of material appearance is generally subdivided into four attributes: color, texture, gloss and translucency. Currently, no model exists which fully describes a material's appearance in all four of these [8]. Therefore definitions and separate models have developed for each attribute.

The ASTM defines gloss as: "Angular selectivity of reflectance, involving surface reflected light, responsible for the degree to which reflected highlights or images of objects may be seen as superimposed on a surface" [8]. Leloup *et al.* [9] state: "physically, gloss results from the directionally selective reflectance properties of the front surface, with a preference toward the specular reflection direction". Obein *et al.* [10] describe it as: "Gloss is an attribute of visual appearance that originates from the geometrical distribution of the light reflected by the surface"; and continue: "given that gloss is a perceptual attribute, a full characterization of it will depend on both the particularities of the visual response to gloss and the underlying physics of the phenomenon". The physical phenomenon of gloss is determined by the refractive index of a material and the surface roughness.[1] The amount of incident light that reflects diffusely or specularly can be calculated using the Fresnel reflection formula [11].

3.2.2. Gloss modeling

In material appearance rendering, the reflectance of objects is modeled using a Bidirectional Reflectance Distribution Function (BRDF). The BRDF describes how light is reflected by a surface dependent characteristics of that surface, having various other external characteristics (e.g. viewing direction, illumination parameters) as input. The six-dimensional spatially varying BRDF (svBRDF) is used to describe

[1] This holds for smooth, opaque surfaces, while for rough and/or translucent surfaces the BRDF will also depend on the microscale surface geometry and possibly on subsurface scattering phenomena. Moreover, the effects of sub-surface scattering are generally ignored for simple reflectance models. Such complex material-light interactions and their perceptual effect, also in relation to fabrication, remain to be further investigated

reflection characteristics that vary across the surface.[2] In case of a textured surface, a Bidirectional Texture Function (BTF) is often employed for more realistic rendering; the main difference with the svBRDF is that the BTF also accounts for surface shadowing, shading and occlusion by taking into account the planar material position. However, BTF models have no geometric information, as they are solely based on observed texture appearance; therefore these models (e.g. based on modeling the *apparent* BRDF, linear factorization based compression or sampling) do not lead to relevant parameter(s) for gloss (see Filip and Haindl [12] for an overview and categorization of BTF models). Additionally in our case the 3D shape (and albedo) of the surface is known, and this information can be used in the elimination of shadowing and shading effects, to arrive at a gloss parameter by fitting a svBRDF model.

Montes and Ureña [13] made an overview of BRDF models. They categorize BRDF models into physically plausible and non-physical models, in which the physical plausible models obey with three properties: (1) its BRDF is non-negative, (2) it complies with the law of energy conservation i.e. reflected energy cannot exceed incoming energy, and (3) it generally is symmetrical (meaning that it complies with the Helmholtz Reciprocity Rule; some exceptions exist here). Additionally, they distinguish between empirically-, theoretically- and experimentally-based models. In the case of experimentally based BRDF models, the BRDF is measured from a physical sample (also see paragraph 2.3). This data can be used directly for rendering, or an analytical model can be fitted to the data.

Various BRDF models have been used to describe (oil) paint reflectiveness for the purpose of (real-time) rendering or remote sensing (see Table 3.1):

Westlund and Meyer [14] extended the *Beard Maxwell BRDF model*, a model originally developed to describe the reflection of painted surfaces. This model first assumes that light reflects off the outer surface based on a micro-facet representation, and secondly that light is scattered out of the surface after having first entered the sub-surface medium (i.e. volumetric reflectance). The Beard-Maxwell reflectance model utilizes the assumption that the surface-reflected light reflection retains its polarization and that sub-surface scattering causes depolarization. Measurements are made using parallel and cross-polarized illumination. Although this reflection model is assumed to also be applicable for oil paint, this has not yet been measured or fitted.

Chen *et al.* [15] captured the gloss of eight different painted samples and modeled these using the *Phong* and *Torrance-Sparrow BRDF model*. They concluded that the two models have equal performance in modeling matte surfaces, but the Torrance-Sparrow model performs better than the Phong model on glossy surfaces. Additionally they concluded that at least nine measurement angles (a subset of 42 captures they made) are needed to accurately model the reflectance of their glossy samples using the Torrance-Sparrow model.

[2] It is common in the notation of the svBRDF, to omit the wavelength (λ) as an explicit variable, assuming that the wavelength is the same for both the incoming and reflected light. This if valid, as we are not modelling iridescence, luminenscence or structural coloration. The svBRDF is commonly described for every sampled channel (e.g. RGB), and in some cases, λ is even neglected for the specular component of a svBRDF.

Snel [16] also aimed at acquiring, fitting and rendering painted samples. He used an extended version of the *Lafortune BRDF model*. The BRDF model is extended to be an svBRDF by specifying the parameters per point on the surface; also, surface normal vectors are added to account for variations in the surface orientation i.e. texture.

Sun *et al.* [17] developed a time-varying BRDF, where they model a surface reflectance that changes over time, capturing the drying of oil paint. They combined the *Oren-Nayar BRDF model* (diffuse reflection) and the *Torrance-Sparrow BRDF model* (specular reflection).

Tominaga and Tanaka [18] estimated the reflectance properties of painting using the *Cook-Torrance BRDF model*. They imaged paintings using a 6-channel multispectral imaging system and estimated the surface normal and surface-spectral reflection function from the diffuse reflection component. However, their model does not capture the spatial variation of the reflectance.

Darling and Ferwerda [19] used a surface normal map in combination with the Ward BRDF model render paintings, soft-proofs and manuscripts, which can be viewed interactively. They implemented the *Ward BRDF model*, which has a small number of parameters, to enable real-time rendering. The reflective properties of the surfaces (uniform across the surface) can be manipulated by the use or loaded from a database. The interactive viewing example of a manuscript utilizes measured (and fitted) reflectance data created by Gardner *et al.* [20]

Hasegawa *et al.* [21] also implemented the *Torrance-Sparrow BRDF model* to model the reflectance of paintings. For moderately glossy paintings, they were able to produce spatially varying gloss. However, for glossy surfaces, they averaged the specular reflectance across all highly specular areas (measurement of the specular reflection tends to be inaccurate with sparse sampling). They suggested that this might be improved by increasing the sampling density in (near-) specular directions.

3.2.3. Capturing gloss

In the paint and printing industry, gloss meters are widely used for gloss measurement [22]. A gloss meter measures light reflection in the specular direction (relative to a gloss standard), typically in 1-3 angles of incidence/reflection. Despite the ubiquity of these devices and their importance (just consider the value of paint quality for the automotive industry), many studies have found that the measurements of a glossmeter relate only poorly to how gloss is perceived by humans (e.g. [10, 23, 24]). Glossmeters that take additional measurements in the off-specular directions mitigate some of these shortcomings, but these measurements are still hard to interpret. Another disadvantage of these devices is that they integrate the gloss value over a certain area [approx. 4 mm^2], making this the maximum achievable resolution. Additionally, to be reliable glossmeters require either surface contact or measurements at close range (<4mm) and a smooth measurement surface, making them unsuitable for measuring gloss on a painting especially if the gloss measurement is to be integrated with the 3D scanning.

Table 3.1: Overview of BRDF models used for modelling (oil) paint and their characterization

	BRDF model	Physically plausible	Experimental/ Theoretical/ Empirical	Type of (physical) model
Westlund & Meyer [14]	Beard-Maxwell	Yes	Theoretical	Layered reflection model
Chen *et al.* [15]	Phong Torrance-Sparrow	No Yes	Empirical Theoretical	Cosine lobe Microfacet
Snel [16]	Lafortune	Yes	Empirical & Experim.	Cosine lobe
Sun *et al.* [17]	Oren-Nayar Torrance-Sparrow	Yes Yes	Theoretical Theoretical	Microfacet & Geometric optics Microfacet
Tominaga & Tanaka [18]	Cook-Torrance	Yes	Theoretical	Microfacet
Darling & Ferwerda [19]	Ward	No	Empirical & Experim.	Cosine lobe
Hasegawa *et al.* [21]	Torrance-Sparrow	Yes	Theoretical	Microfacet

A multitude of devices have been developed for contactless gloss measurement, whereby gloss is measured with multiple directions of incidence (illumination) and reflection (detection), called goniophotometers. To measure the reflectance in various angles, several principle solutions exist: changing the position of the capture device, changing the position of the illuminant, or changing the orientation of the sample. Devices also differ in the density of sampling and their ability to measure either part or the full hemisphere of reflections (isotropic/anisotropic reflection behavior). The advantage of dense sampling instruments is that they can make very accurate measurements of samples (e.g. [25]), but the downside is that they are very slow, and again not suited for the Fine Art application discussed here.

In the rendering of paint gloss all above-mentioned approaches (see Table 3.1) employed some form of sparse BRDF sampling. Most used a point light source and a CCD sensor; Darling and Ferwerda [19] used a linear light source. Some employed multiple light sources or cameras to speed up acquisition time and/or increase geometrical accuracy. Westlund and Meyer [14] additionally applied light polarization. Some design implementations made use of rotating the sample; these implementations were excluded from our design considerations, as this is not implementable with valuable and larger paintings.

With the improvement of computer graphics (e.g. for animation movies and rendering software) and increasing demands for digital archiving and viewing, there became a need for fast capture (and modeling) of surfaces and objects with spatially varying gloss characteristics. Several different approaches already exist:

Linear light source reflectometry [20]: this captures an object using a camera and a linear array of LEDs, which are moved across the object's surface (multiple exposures are taken; an A4 size sample was captured in 30 minutes). Additionally, this captures the surface geometry using a laser scanner, and the light transmittance of the object is measured by illuminating the object from underneath. The researchers estimated the specular and diffuse reflection of the surface, and also generated a surface normal map. The images generated this way were used by Darling and Ferwerda [19], in their dynamic viewing interface on a laptop.

Reflectance transformation imaging (RTI or *Polynomial Texture Mapping*) [26, 27]: this captures an object using one camera and multiple light sources (typically in the range of 30 LEDs) arranged in a dome-shaped configuration. The location of the light sources is extracted from the camera image using reflecting spheres. The output is an angle dependent color value and a surface normal map, which can be viewed in a dynamic viewer.

Manifold bootstrapping [28]: the material reflectance of an object is captured using a camera and a point light source in a two-step process: (1) a selected amount of characteristic points are measured with high density sampling, creating a BRDF of these points, and (2) the entire surface is then sampled with a much lower sampling rate, and the BRDFs were matched to these areas (also linear combinations of BRDFs is possible).

Pocket reflectometry [29]: an object is captured in conjunction with a self created 'gloss' reference, containing an assortment of materials with widely varying BRDFs. The svBRDF of the sample is then estimated by calculating linear combina-

tions of the reference materials.

svBRDF capture in the frequency domain [30]: in this last approach, the surface reflectance is captured using a camera and a computer monitor (as illuminant) that projects a distinct pattern onto the object. The model outputs the diffuse albedo, the specular component and a surface normal map, which can be used for rendering purposes.

All of these approaches are potentially viable for the capture of paint gloss, although a drawback of many is that they require capturing a large amount of images (>30) of a relatively small area (approximately A4 size). Combined with the already very high file sizes of the color and texture maps, this challenges the applicability already in terms of file size alone, not to mention complications in terms of requisite time.

In closing this section, we should take note that in capturing the gloss, a combination of the surface reflection and diffuse scattering of light is measured; there is no easy way to distinguish between these two components (although the Beard-Maxwell model attempts to do this via polarization splitting). Therefore, you capture the gloss as well as the color. The two parameters are effectively linked. In most above implementations the reflectance is split into a specular reflection and a diffuse scattering of light, but this is not the case for all approaches; the RTI approach only applies interpolation between the sampling angles of the total reflectance.

3.2.4. Printing gloss

Several studies exist that attempt to reproduce gloss of surfaces:

Matusik *et al.* [31] combined inks with various reflectance properties to create a print with a spatially varying BRDF. They had 12 basis inks to their disposal including several metallic inks and foils, and though layering of inks they created a total of 57 ink combinations with a unique BRDF. They made linear combination of inks to create the target BRDF and employed gamut mapping to maintain relative glossiness between different areas. Two limitations of their system are that they are only able to print 2D images (also no anisotropic effects) and that the resolution is limited by the printing system they employed. The limited resolution (only 150-200dpi) made it necessary to compare the originals and prints from at least half a meter, to avoid seeing the printer half-toning patterns.

Lan *et al.* [3] reproduced anisotropic svBRDFs using a 3D printer in combined with a glossy spray paint and a flatbed color printer. The anisotropic behavior was estimated with 5x5 pixel patches, which were individually optimized and in iteration optimized with respect to each other. The BRDF was estimated using a linear combination of input BRDFs; there were assumed to be isotropic. They first used a 3D printer to print the textured surface, which was then sprayed with a metallic spray paint, and selectively overprinted with matt white ink and colored inks. They conclude that their effective resolution was limited by the use of 5x5 pixel patches, and the accuracy of the 3D printer. Additionally the manual alignment process between the two printing systems was a drawback.

Baar *et al.* [32] varied the printing strategy to create gloss variation in print. They varied the time between different printing passes; printing in multiple passes

(this does not mean stacking of ink layers) created a matter effect, than printing everything in one pass. They conducted a psychophysical experiment using cylinders with different gloss levels, and found an average correlation of 0.8139 (Spearman's) between the perceptual gloss rank and glossmeter measurements (at 20°, 60° and 85°), using samples with varying combinations of CMYK.

The approaches of Matusik *et al.* [31] and Baar *et al.* [32] are both potentially relevant for the gloss reproduction of paintings; even a combination of approaches could be implemented, in order to maximize the BRDF 'gamut' and minimize the amount of materials needed to achieve this. We assume that anisotropic reflectance inference is of less importance for the reproduction of paintings, and that we might assume isotropic reflections of painted surfaces.

3.2.5. Gloss perception

As stated by Obein *et al.* [10], gloss appearance is a perceptual attribute. Therefore, to be able to evaluate the accuracy of a gloss reproduction system, gloss perception also needs to be taken into account. If we understand which parameters are important for gloss perception, a reproduction system[3] might be optimized for these parameters.

Hunter [33] in 1975, stated that at least six visual criteria could be used to evaluate gloss: 1) *Specular gloss*: related to the perceived shininess or brilliance of highlights; 2) *Contrast gloss (or luster)*: associated with the observed contrast between the specular highlights and the diffusely reflecting surface areas; 3) *Sheen*: describing the perceived gloss at grazing angles of otherwise matte surfaces; 4) *Absence-of-bloom gloss or haze*: related to the presence of haze or a milky appearance adjacent to reflected highlights; 5) *Distinctness-of-image (DOI) gloss*: perceived distinctness and sharpness of the observed mirror image after reflection from the surface; and 6) *Surface-uniformity gloss*: associated with the perceived surface smoothness and freedom from visible non-uniformities such as texture or orange peel.

Billmeyer and O'Donnell [34, 35] (1987) found with their experiments only one dimension to be sufficient to describe visual evaluations of painted samples. Observers scaled the apparent gloss difference between multiple sets of achromatic painted samples in relation to a reference pair. Billmeyer and O'Donnell applied a multidimensional scaling to the visual evaluation results and found only one dimension could explain the gloss variation. However, Lindstrand [36] noted that caution should be taken to generalize this conclusion and hypothesized that the one-dimensional scaling might be due to coherency of the used samples.

Ferwerda *et al.* [37] (2001) carried out research on gloss perception more recently, based on gloss difference scaling of computer-generated images (using the Ward BRDF model). They found two dimensions explaining gloss perception, and inferred *contrast gloss*, and *distinctness-of-image* to be important. However, also in this case caution should be taken in generalization of the results: as the results are based on computer generated images, which in turn are based on a simplified light reflection model, it is difficult to know how well this represents gloss in general.

[3] A reproduction system is defined to include appearance *capturing* as well as appearance *fabrication*.

Two studies found that there is a non-linear relationship between gloss scaling and glossmeter measurements [10, 23]. Ji *et al.* [23] found that gloss measured using a spectrophotometer (difference between specular-included and specular-excluded measurements) was a better fit for visual gloss scaling. They found no differences between the scaling of chromatic and achromatic samples.

Wills *et al.* [38] also investigated gloss perception using computer-generated images in a paired comparison experiment. They generated 55 images using Matusik *et al.* [39] data-driven BRDF model. Multi-dimensional scaling led to a two-dimensional embedding. These were correlated to nine gloss measurements as well as the parameters of several analytical BRDF models. *Contrast gloss* and *diffuseness* seem to best describe the two dimensions found by Wills *et al.* [38]. With regards to the BRDF models, the dimensions had the strongest correlation with parameters describing diffuse reflection (all models) and parameters describing the spread of the specular reflection lobe (or 'roughness' parameter), which exist in the Ward model, Ward-Duer and Cook-Torrance model.

Besides determining perceptual dimensions of gloss, Leloup *et al.* [9] also provide an overview of other aspects that play a role in gloss perception, which should be carefully considered in the setup of a gloss perception experiment: type and geometry of illumination; object properties (shape, roughness, color); and viewing conditions (binocular vision, motion, and viewing distance).

Fleming [40] also provides an interesting theory on how material properties like gloss are visually inferred from an image or a real-world scene. He argues there might be two approaches for determining material characteristics: categorization (by learning the boundaries of material groups we can assign a material to a group); and estimating material properties (arguing that a statistical based model is a more likely approach than the reverse optics theory); and that these approaches may be complementary to one another. This is interesting for the following reason: if we attempt to create a life-like reproduction, it might not be necessary to make an exact replication of the gloss, but a reproduced gloss within the range of the material group boundaries (including it's 'natural' variation), would be sufficient to create a life-like reproduction.

3.3. Experimental Method

3.3.1. Painted Sample

A hand-painted sample was created for the purpose of gloss scanning and reproduction. Although a newly painted sample is likely to differ in gloss from old paintings, creating and using such samples offers two advantages: (1) the color of the sample is uniform and can be controlled (therefore differences in appearance can be attributed to gloss and not to e.g. spatial color variation or color reproduction being out-of-gamut); and (2) various levels of gloss[4] can be created within one sample (using various varnishes and varnish application methods), therefore providing a wider range of gloss that can be found on paintings.

[4]Here we treat "level of gloss" as that of an opaque smooth surface, as measured by a glossmeter, taking a 1-dimensional measurement of the specular reflectance.

The sample was created by painting monochromatic bands using oil paint in thirteen colors (Talens Rembrandt artist quality oil paint) on a 30x40cm MDF panel (prepared with smooth gesso ground). Three gloss levels were created on top of every color: 1/3 of every color band was left unvarnished, 1/3 was varnished with a matte acrylic varnish (Talens Acrylic varnish Matte no. 115) and 1/3 was varnished with glossy acrylic varnish (Talens Acrylic varnish Glossy no. 114). The paint was applied as smooth as possible using a pallet knife (some texture is visible) and the varnish was applied with a brush (see Figure 3.3, left image).

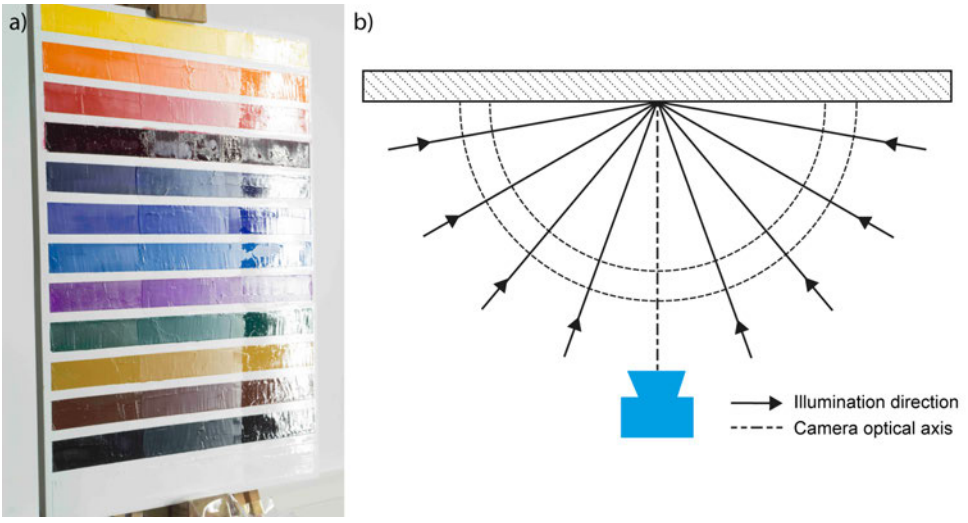

Figure 3.3: (a) Sample with three levels of gloss: left side is unvarnished; middle is matte varnish; and right side is glossy varnish, (b) Capture setup showing sample and camera orientation and illumination directions

3.3.2. Capturing gloss

In order to capture the spatially varying gloss of the sample, a setup was built consisting of a professional grade camera and a linear array of LEDs. Illumination was provided by a strip of white LEDs (length 100 cm) positioned vertically at the same height as the sample, 130 cm away from the center of it; the light source is moved around the sample (from 0 to 180 degrees, with 20 degree steps) retaining an equal distance to the center of the sample. The position of the camera was fixed, facing the sample and a 90 degrees angle, at 130cm from the sample (see Figure 3.3, right image). For each sample condition, High Dynamic Range (HDR) images are acquired using a Nikon D800E DSLR camera fitted with a Nikon PC-E Micro Nikkor 85 mm lens opened at f/4.2. Seven images are used to build the HDR data with an exposure time of 1/60s, 1/30s, 1/15s, 1/8s, ¼s ½s and 1s at ISO 100 and with a custom white balance. Images were acquired as full resolution raw data.

3.3.3. Creating a gloss map

The raw data files were converted to 8 per color bits uncompressed Tiff. During the conversion process, camera white balance and dark frame subtraction are applied to each image (dark frame images made at the end of the experiment). The camera HDR response curve was calculated using the method of Debevec and Malic [41]. The camera curve was calculated over a single test HDR sequence and the same curved was used to generate all the HDR images in the experiment. Further image processing consisted of a RGB to log-luminance conversion for each HDR image:

$$Y(x,y) = \log(0.299R(x,y) + 0.587G(x,y) + 0.114B(x,y)) \tag{3.1}$$

Gloss estimation for every pixel is based on the standard deviation of the pixel's log luminance during sampling of the BRDF.[5] Glossiness is normalized within the [0,1] range. Higher values represent more glossy areas. Figure 3.4 (left) shows the resulting gloss map and (right) shows the same gloss map, where the white borders are excluded for the purpose of printing. Note the fourth color band from above where the paint was not let to dry long enough.

3.3.4. Printing gloss samples

Printed samples were created using the Océ High Resolution 3D printing technology, with varnish printing capability. In order to match the color of the painted samples, measurements of the painted samples were made using a spectrophotometer. The painted colors are approximated using an absolute colorimetric color profile. Two different strategies were combined to create varying gloss in the print. First, to create a matte effect, the color layers were printed using a multilevel half-toning algorithm, as described by Baar *et al.* [32]; this generated the most matte effect as a base for the varnish layer. Secondly, on top of the matte colors, half-toned varnish was added in increasing coverage to create increasing gloss levels (also see [42]).

3.4. Results

Five samples were printed using the measured colors printed with the multilayer 'matte' printing mode as basis. One was printed with gloss patches with increasing gloss coverage. Figure 3.5(b) shows gloss patches with increasing varnish coverage ranging from 0 to 100% coverage (left to right). Notice the decrease in spread of the specular reflection from the left to the right of the image. Also note that patches ranging from 60% to 100% coverage (right side of the image) do not differ much in

[5] Assuming that the specular reflection can be modelled with a gaussian curve (similar to several BRDF models), and the total reflectance is equal between different gaussian curves, then with a linear increasing spread (σ) of the gaussian curve, the standard deviation on the *luminance values* shows an exponential decay. This was linearized using a log-function. Additionally, if we assume that the modelling of the reflectance can be treated as a additive model of a diffuse and a specular component (similar to for instance the Ward BRDF model), the diffuse component (assumed to be constant across the hemisphere), should not influence the standard deviation of the luminance values. Furthermore, in experiments, Ferwerda et al. [37] found that the (rated) perceived gloss had an inverse linear relation to the roughness parameter of the Ward BRDF model (spread of the specular lobe), giving some basis that this might be an appropriate approach for measuring gloss.

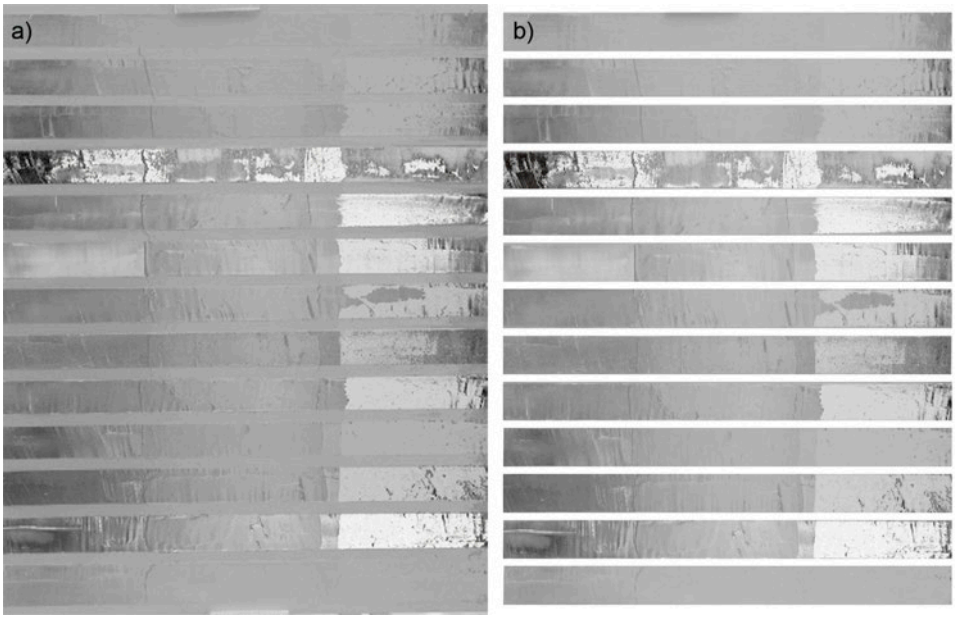

Figure 3.4: (a) gloss map of sample in gray scale, normalized within the [0,1] range, (b) gloss map of samples where gloss mapping of unpainted areas was excluded. This was used for printing.

appearance. It was found (from visual inspection) that from >60% coverage (input data) the surface is already fully covered with varnish. A second sample was printed with a continuous gloss gradient. Figure 3.5(c) shows a gloss gradient ranging from 0% to 60% varnish coverage (60% was chosen as a maximum as this already creates a full surface coverage). Also here the decrease in specular reflection spread can be observed. Another sample was created using glossmeter measurements. Figure 3.5(d) shows a printed sample with matched gloss values from glossmeter measurements. A single measurement of every patch on the painted sample was made (see Table 3.2). This was matched to gloss measurement of an earlier created print sample. Some clipping occurred at the lowest gloss levels, as the lowest printable gloss is only 20 Gloss Units (GU).[6] A fourth sample was printed using the gloss map as depicted in Figure 3.4 (right). The gloss was mapped non-linearly with a gamma correction of 3.0 (see Figure 3.5(e)). This produced the best visual match to the painted sample. The final sample combined the gloss printing with 3D printing. Figure 3.5(f) shows a printed sample with the texture of a painting and gloss patches similar to Figure 3.5(b). Here the decrease of spread in specular reflection is still noticeable. but the distinction between the different patches is much less obvious.

One aspect of reproduction which is not very clear from the images in Figure 3.5

[6]Measurements were made using an industrial glossmeter, which uses a polished, black glass plate as a standard reference; gloss is expressed in Gloss Units (GU) (scaled between 0 and 100), which provides a measurement relative to the reference [43]

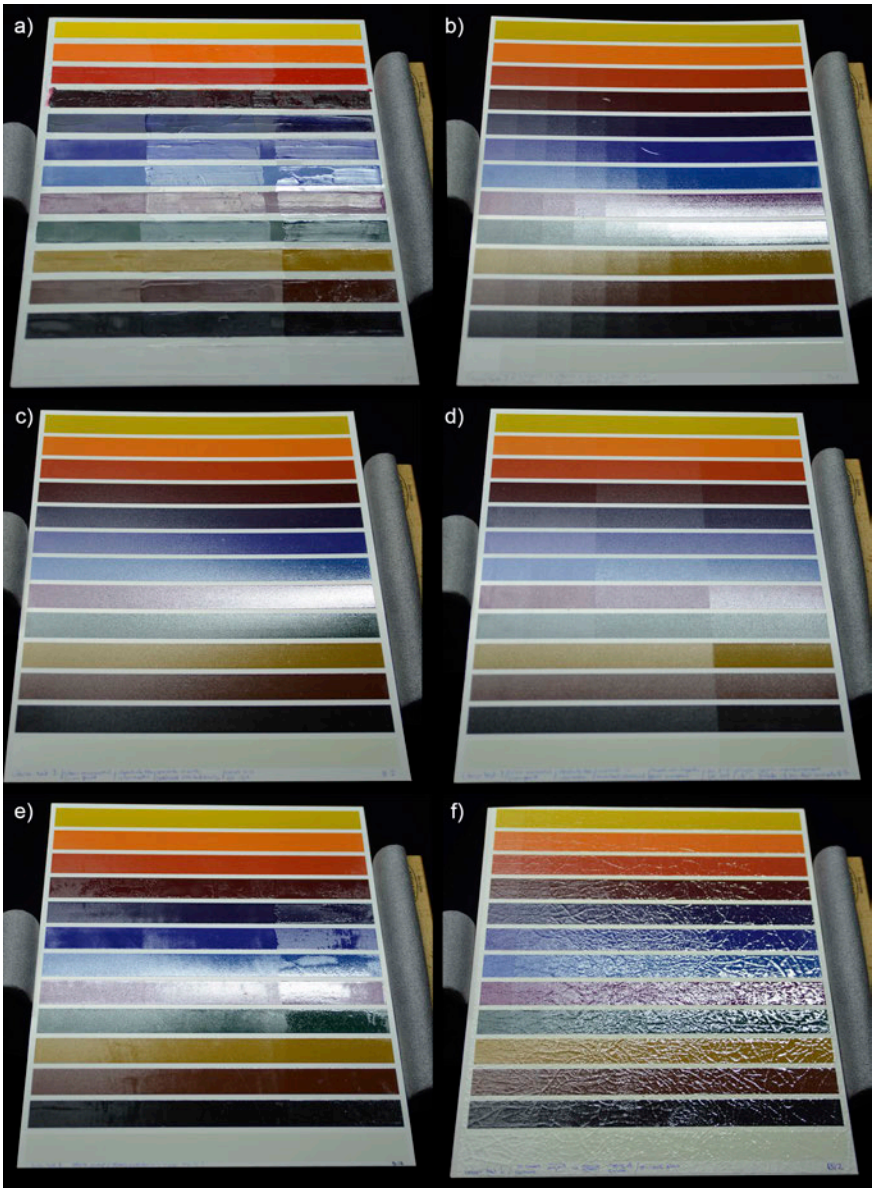

Figure 3.5: Samples illuminated under directional lighting; (a) Painted sample, (b) Printed sample with gloss patches of increasing varnish coverage (0 - 100% in 10 steps), (c) Printed sample with gloss gradient ranging from 0-60%, (d) Printed sample with matched glossmeter measurements, (e) Printed sample with gloss map with nonlinear mapping (gamma correction=3), (f) Printed gloss patches (varnish coverage 0 - 100% in 10 steps) on painting texture.

Table 3.2: Gloss measurement using glossmeter (in gloss units GU); one measurement for every color/gloss patch. The 60° gloss values were used for matching the gloss. The gray gloss values could not be reproduced with the printer, as the lowest printable gloss level is 20 Gloss Units (GU).

Color	Unvarnished (left)			Matte varnish (middle)			Glossy varnish (right)		
	20°	**60°**	85°	20°	**60°**	85°	20°	**60°**	85°
Yellow	1.9	**12.6**	10.7	2.8	**26.2**	57.3	9.7	**44.7**	52.9
Orange	1.9	**13.5**	13.8	3.1	**28.9**	52.5	19.3	**57.8**	71.3
Red	6.2	**37.7**	48.4	3.8	**33.6**	66.4	31.5	**69.1**	74.2
Dark Red	12.4	**49.6**	53.3	4.0	**32.8**	49.6	12.5	**49.7**	36.6
Dark blue	0.4	**5.6**	11.2	3.9	**37.7**	72.6	10.9	**50.2**	65.1
Med. blue	0.2	**1.2**	2.5	4.3	**38.4**	72.6	5.6	**37.5**	54.6
Light blue	0.5	**4.6**	7.1	3.7	**35.9**	68.5	11.5	**50.4**	59.6
Purple	1.4	**12.9**	17.1	2.9	**30.8**	57.4	12.9	**49.7**	52.2
Green	0.3	**3.8**	3.0	2.8	**30.2**	63.9	7.8	**40.7**	49.6
Beige	5.6	**39.1**	58.5	4.4	**38.5**	75.7	43.4	**80.7**	83.1
Brown	1.9	**18**	34.6	4.2	**36.0**	72.5	12.7	**48.8**	66.8
Black	5	**36.2**	50.7	3.5	**35.5**	73.8	25.4	**65.7**	76.6
White	6.7	**41.0**	58.3	5.3	**40.1**	70.1	46.6	**80.9**	80.6

is that a large part of the colors of the painted sample lie outside the color gamut of the printer. Especially the yellow, orange and red appear quite different in the print when compared to the painted sample.

Figure 3.6 shows some details of the painted and printed sample. Notice the very different surface structure of the paint and print at close range. Additionally. when viewing the print at close range. it can be observed that the varnish of the printer tends to coalesce (already from a coverage >20% and with coverage >60% full surface coverage is reached).

Figure 3.7 shows another detail of the painted and printed sample. which has a clear gloss variation (due to improper varnishing). The same gloss feature can also be recognized in the printed sample.

3.5. Discussion and future work

This work represents a first step towards the full reproduction of surface, color and material appearance of oil paintings. Especially, we have established a complete workflow for the acquisition and reproduction of varying gloss of oil paintings, together with the perceptual evaluation of the quality of the reproduction. A painted sample presenting varying colors in one direction and varying varnishes in the other one was used to evaluate the workflow. A simple method to build relative gloss maps using a standard DSLR camera and an uncalibrated light source is proposed and several printing techniques for varying gloss over a colored surface are evaluated. The study led to the following conclusions:

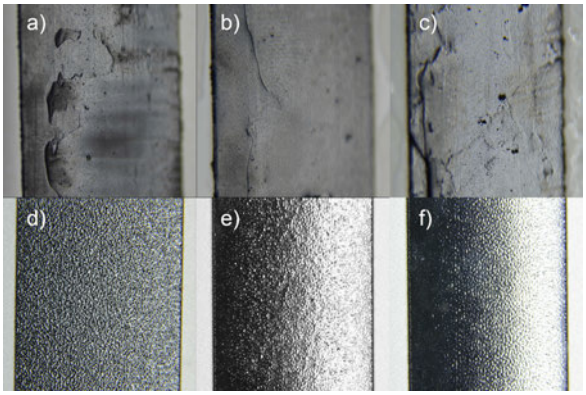

Figure 3.6: Details of painted and printed sample (black color) (a) unvarnished paint, (b) matte varnish on paint, (c) Glossy varnish on paint, (d) low gloss printed patch, (e) medium gloss printed patch, (f) high gloss printed patch

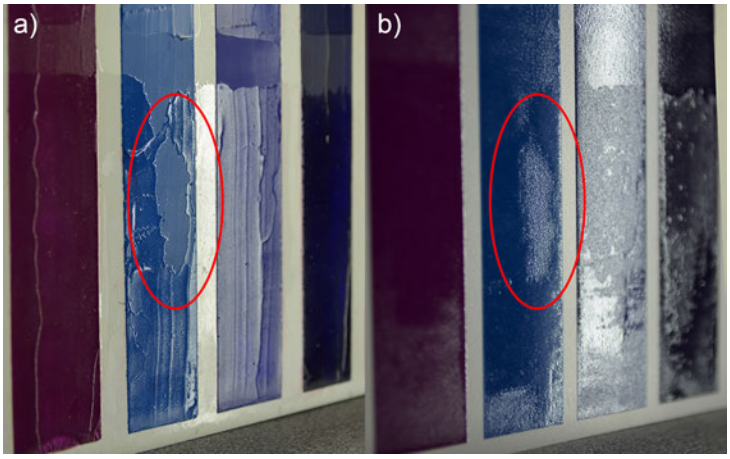

Figure 3.7: Detail of gloss variation with clear spatial features, (a) painted sample, (b) printed sample.

Material appearance such as gloss and translucency is a fundamental aspect of the perception of Fine Art masterpieces and must be taken into account for high accuracy reproduction. High-resolution color and texture maps can be built from state-of-the art technology but the acquisition of other material properties remains a challenge.

Variations of the log luminance of the surface under varying illumination are a clue toward variations in the specular characteristics of the BRDF of the surface; Such variations can be quantified using HDR imaging. High accuracy gloss maps require taking into account the texture of the sample and the variability in the direction of the incident light. Relative gloss maps are sufficient for reproduction but an accurate Fine Art reproduction would require calibrated data; Exact reproduction is only possible if both the colors and gloss range of the sample match the capabilities

of the printer (gamut and gloss range).

The printed samples show the possibility to create various distinct gloss levels, but also smooth transitions. An advantage of our printing approach is that the gloss appearance is created by superimposing a transparent layer on top of a (textured) print, making the printing of gloss (partially) independent of the color and texture. This creates the opportunity for the development of new varnishes with very specific gloss characteristics, to match oil paint gloss, and possibly the gloss of many other materials.

Evaluation of the quality of the reproduction must take place at a perceptual level and is highly dependent on the conditions of the evaluation and on the level of expertise of the subject.

Due to various limitations in our current approach (method of gloss measurement, spatial resolution of the scan, out-of-gamut colors) the research questions posed in paragraph 3.1.2, cannot be answered directly. We believe our current scanning resolution is likely too low, when for example comparing details like the one shown in Figure 3.7. The depth resolutions of our gloss scan and printing do seem adequate, i.e. the gloss scan shows subtle difference in gloss and we are able to print smooth gloss transitions. Whether relative gloss matching is able to create a life-like appearance of Fine Art remains to be determined.

For future work we would like to create samples with in-gamut colors and smooth samples (without texture), to ensure that we only evaluate differences in gloss appearances, and not differences in color or texture reproduction. Additionally we think the scanning method could be improved, to account for the texture i.e. the orientation of the surface relative to the sampling and illumination direction. Also the resolution of scanning can be increased (by capturing a smaller area at the time), to fully utilize the printing resolution (approx. 50 µm). Additionally by scanning a painted and printed sample using the same approach, we could gain more insight in the difference in reflectance characteristics, to achieve better gloss mapping. And finally, the varnish of the print system could be improved to be better attuned to half-toning (less coalescence), and better suited to print matte appearances.

References

[1] S. Zhao, W. Jakob, S. Marschner, and K. Bala, *Building volumetric appearance models of fabric using micro CT imaging,* ACM Transactions on Graphics **30** (2011), 10.1145/1964921.1964939.

[2] P. Urban, *Spectral-based Image Reproduction Workflow,* in *Jahrbuch der Druckingenieure* (2009).

[3] Y. Lan, Y. Dong, F. Pellacini, and X. Tong, *Bi-scale appearance fabrication,* ACM Transactions on Graphics **32** (2013), 10.1145/2461912.2461989.

[4] Stratasys, *Company website,* (Accessed: 2019-05-25).

[5] 3D Systems, *Company website,* (Accessed: 2019-05-25).

[6] T. Zaman, P. Jonker, B. Lenseigne, and J. Dik, *Simultaneous capture of the color and topography of paintings using fringe encoded stereo vision,* Heritage

Science **2**, 1 (2014).

[7] W. S. Elkhuizen, T. Zaman, W. Verhofstad, P. P. Jonker, J. Dik, and J. M. P. Geraedts, *Topographical scanning and reproduction of near-planar surfaces of paintings,* in *Electronic Imaging: Measuring, Modeling and Reproducing Material Appearance*, Vol. 9018, edited by M. V. Ortiz Segovia, P. Urban, and J. P. Allebach (SPIE-IST, 2014).

[8] Commission Internationale de l'Eclairage, *A framework for the measurement of visual appearance*, Tech. Rep. (International Commission on Illumination, Vienna, Austria, 2006).

[9] F. B. Leloup, G. Obein, M. R. Pointer, and P. Hanselaer, *Toward the soft metrology of surface gloss: A review,* Color Research & Application **39**, 559 (2014).

[10] G. Obein, K. Knoblauch, and F. Viénot, *Difference scaling of gloss: Nonlinearity, binocularity, and constancy,* Journal of Vision **4**, 711 (2004).

[11] Y. Dong, S. Lin, and B. Guo, *Material Appearance Modeling: A Data-Coherent Approach* (Springer Berlin Heidelberg, Berlin, Heidelberg, 2013).

[12] J. Filip and M. Haindl, *Bidirectional Texture Function Modeling: A State of the Art Survey,* in *IEEE Transactions of pattern analysis and machine intelligence*, Vol. 31 (IEEE Computer Society, Los Alamitos, CA, USA, 2009) pp. 1921–1940.

[13] R. Montes and C. Ureña, *An Overview of BRDF Models*, Tech. Rep. (University of Granada, 2012).

[14] H. B. Westlund and G. W. Meyer, *A BRDF Database Employing the Beard-Maxwell Reflection Model,* in *Graphics Interface* (2002) pp. 189–201.

[15] Y. Chen, R. S. Berns, and L. A. Taplin, *Model Evaluation for Computer Graphics Renderings of Artist Paint Surfaces,* in *15th Color Imaging Conference: Color Science and Engineering, Systems, Technologies and Applications, Color Imaging Conference* (2007) pp. 54–59.

[16] E. Snel, *Acquisition, Fitting and Rendering of Paintings*, Tech. Rep. April (Delft University of Technology, Delft, 2007).

[17] B. Sun, K. Sunkavalli, R. Ramamoorthi, P. N. Belhumeur, and S. K. Nayar, *Time-Varying BRDFs,* IEEE Transactions on Visualization and Computer Graphics **13**, 595 (2007).

[18] S. Tominaga and N. Tanaka, *Spectral image acquisition, analysis, and rendering for art paintings,* Journal of Electronic Imaging **17** (2008), 10.1117/1.3036180.

[19] B. A. Darling and J. A. Ferwerda, *The tangiBook: a tangible display system for direct interaction with virtual surfaces,* in *17th Color Imaging Conference* (IS&T, 2009) pp. 260–266.

[20] A. Gardner, C. Tchou, T. Hawkins, and P. Debevec, *Linear light source reflectometry,* ACM Transactions on Graphics **22**, 749 (2003).

[21] T. Hasegawa, N. Tsumura, T. Nakaguchi, and K. Iino, *Photometric approach*

to surface reconstruction of artist paintings, Journal of Electronic Imaging **20** (2011), 10.1117/1.3533329.

[22] ISO, *ISO 3664:2009 - Graphic technology and photography - viewing conditions,* (2009).

[23] W. Ji, M. R. Pointer, R. M. Luo, and J. Dakin, *Gloss as an aspect of the measurement of appearance,* Journal of the Optical Society of America **23**, 22 (2006).

[24] F. Leloup, *New Methods and models improving the prediction of visual gloss perception*, Ph.D. thesis, Katholieke Universiteit Leuven (2012).

[25] F. B. Leloup, S. Forment, P. Dutré, M. R. Pointer, and P. Hanselaer, *Design of an instrument for measuring the spectral bidirectional scatter distribution function.* Applied optics **47**, 5454 (2008).

[26] J. Redman and M. Mudge, *The Simultaneous Capture of Spectral and Textural Information,* in *Archiving Conference* (Society for Imaging Science and Technology, 2007).

[27] G. Earl, P. Basford, A. Bischoff, A. Bowman, C. Crowther, J. Dahl, M. Hodgson, L. Isaksen, E. Kotoula, K. Martinez, H. Pagi, and K. E. Piquette, *Reflectance Transformation Imaging Systems for Ancient Documentary Artefacts,* in *Electronic Visualisation and the Arts* (2011).

[28] Y. Dong, J. Wang, X. Tong, J. Snyder, Y. Lan, M. Ben-Ezra, and B. Guo, *Manifold bootstrapping for SVBRDF capture,* ACM Transactions on Graphics **29** (2010), 10.1145/1778765.1778835.

[29] P. Ren, J. Wang, J. Snyder, X. Tong, and B. Guo, *Pocket reflectometry,* ACM Transactions on Graphics **30** (2011), 10.1145/2010324.1964940.

[30] M. Aittala, T. Weyrich, and J. Lehtinen, *Practical SVBRDF capture in the frequency domain,* ACM Transactions on Graphics **32** (2013), 10.1145/2461912.2461978.

[31] W. Matusik, B. Ajdin, J. Gu, J. Lawrence, H. P. A. Lensch, F. Pellacini, and S. Rusinkiewicz, *Printing spatially-varying reflectance,* ACM Transactions on Graphics **28**, 1 (2009).

[32] T. Baar, S. Samadzadegan, H. Brettel, P. Urban, and M. V. Ortiz Segovia, *Printing gloss effects in a 2.5D system,* in *Electronic Imaging: Measuring, Modeling, and Reproducing Material Appearance*, edited by M. V. Ortiz Segovia, P. Urban, and J. P. Allebach (2014).

[33] R. S. Hunter, *The measurement of appearance* (John Wiley & Sons, 1975).

[34] F. X. O'Donnell and F. W. Billmeyer Jr., *Psychometric scaling of gloss,* in *Review and Evaluation of Appearance: Methods and Techniques, ASTM STP 914*, edited by J. Rennilson and W. Hale (American Society for Testing and Materials, Philadelphia, USA, 1986) pp. 14–32.

[35] F. W. Billmeyer and F. X. D. O'Donnell, *Visual gloss scaling and multidimensional scaling analysis of painted specimens,* Color Research and Application **12** (1987).

[36] M. Lindstrand, *Instrumental Gloss Characterization – In the Light of Visual Evaluation: A Review,* Journal of Imaging Science and Technology **49** (2005).

[37] J. A. Ferwerda, F. Pellacini, and D. P. Greenberg, *A psychophysically-based model of surface gloss perception,* in *Human Vision and Electronic Imaging*, Vol. 4299 (2001) pp. 291–301.

[38] J. Wills, S. Agarwal, D. Kriegman, and S. Belongie, *Toward a Perceptual Space for Gloss,* ACM Transactions on Graphics **28**, 1 (2009).

[39] W. Matusik, H. Pfister, M. Brand, and L. McMillan, *A data-driven reflectance model,* ACM Transactions on Graphics **22** (2002), 10.1145/1201775.882343.

[40] R. W. Fleming, *Visual perception of materials and their properties,* Vision research **94**, 62 (2014).

[41] P. E. Debevec and J. Malik, *Recovering high dynamic range radiance maps from photographs,* in *Proceedings of the 24th annual conference on Computer graphics and interactive techniques - SIGGRAPH '97* (ACM Press, New York, New York, USA, 1997) pp. 369–378.

[42] T. Baar, H. Brettel, and M. V. Ortiz Segovia, *Towards gloss control in fine art reproduction,* in *Electronic Imaging: Measuring, Modeling and Reproducing Material Appearance*, edited by M. V. Ortiz Segovia, P. Urban, and F. H. Imai (SPIE-IST, 2015).

[43] ISO, *ISO2813:2014 - Paints and varnishes - Determination of gloss value at 20, 60 and 85 degree,* (2014).

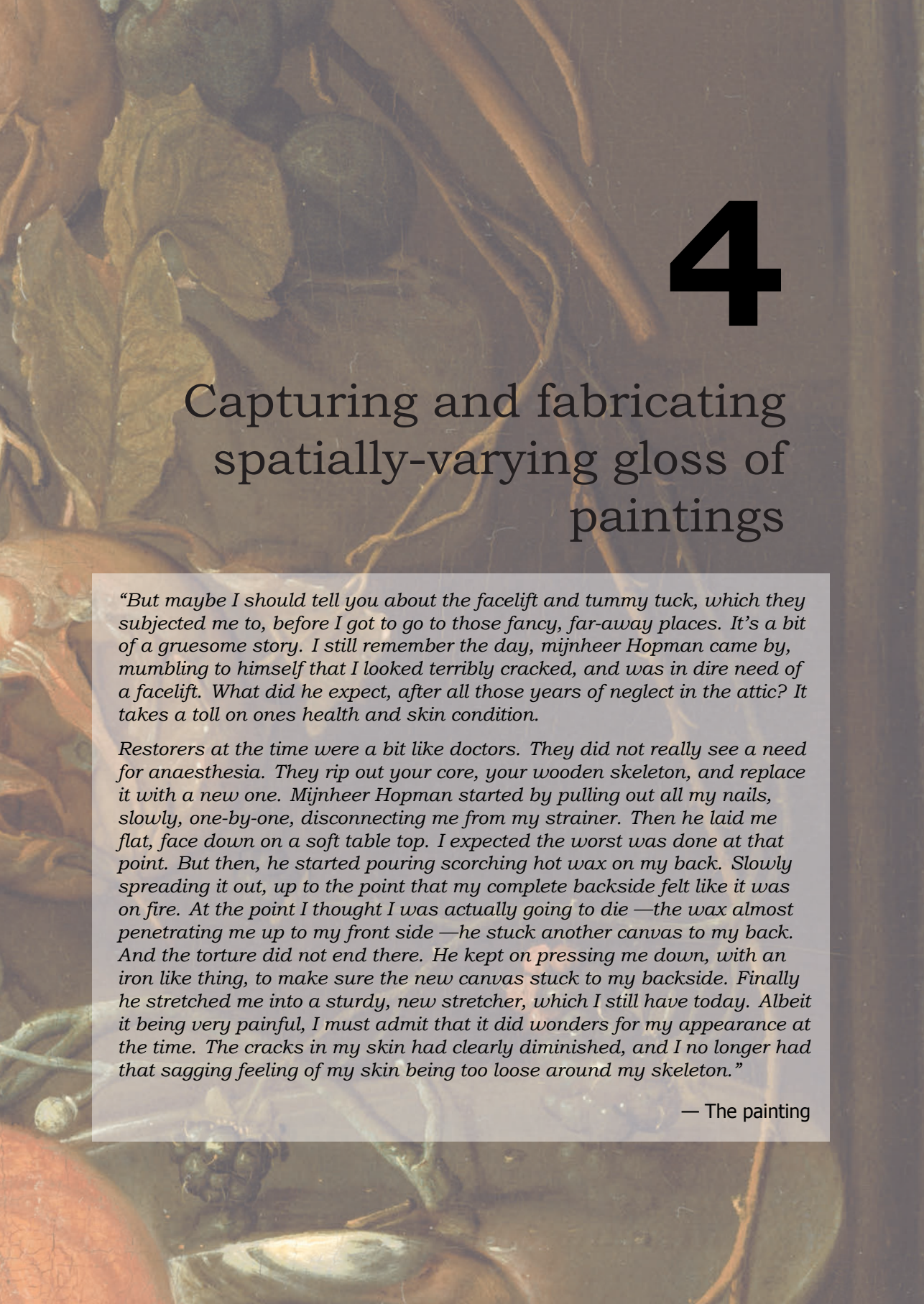

4

Capturing and fabricating spatially-varying gloss of paintings

"But maybe I should tell you about the facelift and tummy tuck, which they subjected me to, before I got to go to those fancy, far-away places. It's a bit of a gruesome story. I still remember the day, mijnheer Hopman came by, mumbling to himself that I looked terribly cracked, and was in dire need of a facelift. What did he expect, after all those years of neglect in the attic? It takes a toll on ones health and skin condition.

Restorers at the time were a bit like doctors. They did not really see a need for anaesthesia. They rip out your core, your wooden skeleton, and replace it with a new one. Mijnheer Hopman started by pulling out all my nails, slowly, one-by-one, disconnecting me from my strainer. Then he laid me flat, face down on a soft table top. I expected the worst was done at that point. But then, he started pouring scorching hot wax on my back. Slowly spreading it out, up to the point that my complete backside felt like it was on fire. At the point I thought I was actually going to die —the wax almost penetrating me up to my front side —he stuck another canvas to my back. And the torture did not end there. He kept on pressing me down, with an iron like thing, to make sure the new canvas stuck to my backside. Finally he stretched me into a sturdy, new stretcher, which I still have today. Albeit it being very painful, I must admit that it did wonders for my appearance at the time. The cracks in my skin had clearly diminished, and I no longer had that sagging feeling of my skin being too loose around my skeleton."

— The painting

Abstract

High fidelity reproductions of paintings provide new opportunities to museums in preserving and providing access to cultural heritage. This paper presents an integrated system which is able to capture and fabricate color, topography and gloss of a painting, of which gloss capturing forms the most important contribution. A 3D imaging system, utilizing stereo imaging combined with fringe projection, is extended to capture spatially-varying gloss, based on the effect of specular reflectance polarization. The gloss is measured by sampling the specular reflection around Brewster's angle, where these reflections are effectively polarized, and can be separated from the unpolarized, diffuse reflectance. Off-center gloss measurements are calibrated relative to the center measurement. Off-specular gloss measurements, following from local variation of the surface normal, are masked based on the height map and corrected. Shadowed regions, caused by the 3D relief, are treated similarly. The area of a single capture is approximately 180x90mm at a resolution of 25 µm x 25 µm. Aligned color, height, and gloss tiles are stitched together off-line, registering overlapping color regions. The resulting color, height and gloss maps are inputs for the poly-jet 3D printer. Two paintings were reproduced to verify the effectiveness and efficiency of the proposed system. One painting was scanned four times, consecutively rotated by 90 degrees, to evaluate the influence of the scanning system geometric configuration on the gloss measurement. Experimental results show that the method is sufficiently fast for practical application, i.e. to scan a whole painting within eight hours, during closing hours of a museum. The results can well be used for the purpose of physical reproduction and other applications needing first-order estimates of the appearance (e.g. conservation diagnostics and condition reports). Our method to extend appearance scanning with gloss measurements is a valuable addition in the quest for realistic reproductions, in terms of its practical applicability - number of images needed for reconstruction and speed - and its perceptual added value, when added to color and topography reproduction.

This chapter is accepted as: **W.S. Elkhuizen**, T.T.W. Essers, Y. Song, J.M.P. Geraedts, S.C. Pont, J. Dik, *Gloss, Color and Topography Scanning for Reproducing a Painting's Appearance using 3D printing*, ACM Journal on Computation and Cultural Heritage, (2019). Note: a few small corrections and/or clarifications have been made to the original published text.
A short version of this chapter has been published as: **W.S. Elkhuizen**, T.T.W. Essers, B.A.J. Lenseigne, C. Weijkamp, Y. Song, S.C. Pont, J.M.P. Geraedts, J. Dik, *Reproduction of Gloss, Color and Relief of Paintings using 3D Scanning and 3D Printing*, In proceedings of Eurographics Workshop on Graphics and Cultural Heritage, (2017).

4.1. Introduction

Developments in 3D scanning and 3D printing systems provide new opportunities to create high-fidelity physical reproductions of paintings. Facsimiles (one-to-one reproductions simulating the artifact's appearance), are already made of artifacts like manuscripts, for instance to support storytelling in exhibitions, when the original is too fragile to show. Up to recently, copies with such likeness did not exist for paintings [1]. Facsimiles of paintings, in addition to the original artwork, can play a role in museums' missions of preserving as well as providing access to cultural heritage. Possible applications of scanning and reproduction include: Multi-modal documentation of an artwork (e.g. adding to high-resolution photography, infrared, and X-ray imaging, as shown in the Bosch Research and Conservation Project [2, 3]), showing an artwork outside a museum context, showing reconstructions of the original state of an artwork (e.g. [4]), creating records of an artwork in different stages of a restoration process, or selling high-end reproductions.

All these applications require reproductions that closely resemble the original artwork's appearance. For this, various modalities need to be captured and reproduced: color, topography (three dimensional height variations of the surface), gloss, and translucency. Zaman *et al.* [5] presented a system which is able to reproduce only the color and topography of a painting's surface using 3D scanning and 3D printing technology. Using this system, three reproductions were made and compared to the original painting. It was found that the uniform gloss of the reproductions' surfaces, made these look artificial or even "plastic", which clearly distinguishes them from paintings, which exhibit spatially-varying gloss [6].

In this paper, we present an integrated system which is able to capture the color, topography and gloss of paintings for the purpose of 3D printing, of which gloss *capturing* forms our most important contribution. The main contributions of this paper are: a) a novel approach to gloss capturing using reflection polarization, and b) an integrated scanning procedure which is sufficiently fast for appearance capturing of large areas for practical application. Two oil paintings, named *Two Wrestling Figures* and *Sunflowers*, both painted *in the style of* Vincent Van Gogh, are reproduced. The painting *Two Wrestling Figures* is a reconstruction of a lost painting by Vincent Van Gogh, which was rediscovered using XRF scanning [7], and recreated, using oil paint, for a Dutch television program [8]. The *Sunflowers* painting was made by an anonymous painter.

The remainder of this paper is arranged as follows: in Section 4.2, literature on capturing and reproduction of material appearance is reviewed. Section 4.3 presents the system and and Section 4.4 the approach that is deployed to measure and fabricate color, topography and spatially-varying gloss. An experiment was conducted utilizing the proposed system and the scanning and printed results are presented in Section 4.5. The advantages and limitations of the proposed system are discussed in Section 4.6 and conclusions are drawn in Section 4.7.

4.2. Related work

This section reviews the state-of-the-art regarding the reproduction of material appearance, covering capturing as well as fabrication of material appearance. The focus of the review lies on methods targeted at capturing and/or fabricating the appearance of planar (but non-flat) surfaces like paintings, bas-reliefs, parchments, and fabrics, which exhibit spatially-varying reflectance.

4.2.1. 2D color reproduction

2D color reproduction is a mature field, where standards and guidelines exist to support the color reproduction workflow from capturing an image (e.g. for digitizing cultural heritage [9, 10]) to the conversion of this data for printing [11]. Limitations of RGB imaging and CMYK printing are known; for instance in terms of a limited printer gamut, and color mismatch in different illumination conditions (metamerism). Multi-spectral imaging systems (summarized in [12]) have been developed to capture the diffuse reflectance of paintings more accurately. Berns *et al.* [13, 14] combined multi-spectral imaging with multichannel printing to create painting reproductions, minimizing color metamerism effects. Although successful, they speculated that this improvement alone is probably too small to justify the investment in developing a multi-spectral reproduction workflow [13]. Furthermore, even if the color would be very accurately reproduced for all illumination conditions, this does not comprise the total appearance. Our approach relies on RGB imaging and CMYK (and White) printing, for replicating the diffuse color appearance.

4.2.2. 2D gloss capturing

Various approaches have been proposed to capture the angular appearance variation of painted surfaces, largely for the purpose of computer rendering [15–18]. These approaches assume a spatially uniform reflectance, represented by a Bidirectional Reflection Distribution Function (BRDF) [19], and therefore use the angular reflectance measurements of individual points across all points on the surface. However, in a previous evaluation of 3D printed reproductions [6] conservation experts remarked that the lack of *spatial variation* of gloss is one of the aspects that distinguishes the reproductions from paintings, meaning these methods do not suit our goal to reproduce the original artwork's appearance.

Angular-spatial appearance variation is often compactly represented by a Spatially-Varying Bidirectional Reflection Distribution Function (SVBRDF), describing the relation between incoming irradiance and the outgoing (reflected) radiance for every point on a surface.[1] In order to achieve a complete representation of the surface reflectance, it would be necessary to measure this relationship for every point on the surface (defined by an x,y coordinate), for every possible incoming irradiance direction (defined by two angles), and every possible outgoing radiance direction

[1] It is common in the notation of the svBRDF, to omit the wavelength (λ) as an explicit variable, assuming that the wavelength is the same for both the incoming and reflected light. This if valid, as we are not modelling iridescence, luminenscence or structural coloration. The svBRDF is commonly described for every sampled channel (e.g. RGB), and in some cases, λ is even neglected for the specular component of a svBRDF.

(also defined by two angles). As sampling of this full 6-dimensional space is not feasible for every point on a larger surface, a trade-off is made between acquisition speed and measurement accuracy. Several approaches employ sparse sampling using point light sources (e.g. [20–23]). However, high gloss surfaces are not (well) modeled in these approaches. Either the specular reflectance is not separately modeled (in polynomial fitting), or becomes noisy, leading to crosstalk between parameters. As a solution, surfaces are sorted into material groups, and the angular measurements are combined within each group, and shared across the spatial domain. Other approaches also rely on the assumption that the surface is comprised of a limited number of homogeneous materials, grouping appearance into regions, taking advantage of spatial reflectance sharing (e.g. [24, 25]). For instance, Holroyd *et al.* [26] took a clustering approach in their synchronous estimation of geometry and surface reflectance. However, as (old) painted surfaces cannot be segmented into a limited set of distinct, uniform materials - they show gradual as well as sudden changes in specular reflectance due to a mixture of materials and other factors which influence the surface state - these approaches are not suitable for our application.

To achieve a denser angular sampling of the surface reflectance, a linear light source has been employed to recover a SVBRDF [27–29]. Alternatively, an LCD screen has been used to project a series of patterns in the frequency domain [30]. Similarly Ghosh *et al.* [31] utilize an LCD projector to project spherical gradient illumination patterns and use the effect of polarization to recover anisotropic specular roughness. These approaches require a large number of images per sample region (see table 4.1) to accurately estimate the reflectance (model parameters) at each point.

In contradiction to rendering applications, printing requires a spatial resolution of at least 300 dpi (85 µm) [32]. At this spatial resolution the above mentioned methods are very time consuming in terms of data acquisition and processing (i.e. due to their angular resolution), limiting their practical use for reproducing whole paintings, which have dimensions typically in the range of 0.5 m^2 to 2 m^2. Moreover, famous paintings often need to be scanned in a limited time slot. In our approach we can suffice with only two reflectance model parameters: the color, representing the diffuse reflectance, and a gloss parameter, representing the magnitude of the specular reflectance peak. To capture these parameters, we need a negligible angular resolution.

Another approach to describe textured surfaces (exhibiting self-shadowing and shading) is the so called Bi-directional Texture Function (introduced by [33]). This approach is an image based technique, whereby the mesoscopic effects of the surface on its appearance are included into the measurement. This approach does not construct a parameterized representation of the surface, meaning that the specular and diffuse reflectance, shadowing, shading, etc. are not separately modeled for every point. For this reason and the fact that this method also requires a high sampling density (typically 200 images per scan area) to accurately capture the appearance, this approach is also not suitable for our application.

Table 4.1: High sampling density SVBRDF methods, their scanning area and the number of needed individual scans

Method	Authors	No. captures	Scan area size (est.)
Linear lightsource reflectometry	Gardner *et al.* [27]	400	20x30cm
Generalized linear lightsource reflectometry	Chen *et al.* [29]	240	20x30cm
Pocket reflectometry	Ren *et al.* [28]	900	16x17cm
SV-BRDF capturing in the frequency domain	Aittala *et al.* [30]	131	15x15cm
Second order spherical gradient illumination	Ghosh *et al.* [31]	9 x "large set"	5x15cm

4.2.3. 2D gloss fabrication

In fabricating spatially-varying gloss, several approaches have been demonstrated; Combining inks with various reflectance properties [34], combining a mono-color 3D printed micro texture with a reflective layer and a (2D) color print [35]; changing the printer parameters to influence the micro-structure of printed surfaces and thereby the gloss [36]; or half-toning a transparent ink on top of a color print [37–39]. The latter approach is the most viable approach in terms of practical applicability (limited number of inks needed), flexibility (can be manipulated independent of sub-layers) and accuracy (in terms of registration), and is therefore also applied in this paper.

4.2.4. 3D color and topography capturing

Various systems can capture the color as well as topography of paintings' surfaces; using three-color laser scanning [40, 41], combining line-laser scanning with color imaging [42], and fringe projection 3D scanning (e.g. [43–45]). A limitation of using RGB laser light for the color capturing, is that the narrow spectral bandwidth leads to poor color rendition. A downside of combining two imaging technologies is the need for image registration and potential misalignment of the color and 3D data. A limitation of the fringe projection system (with only one camera) is that the resolution is limited by the projector (which is typically much lower than a camera sensor). Although examples indicate that the resolution and accuracy of photogrammetry and other passive shape-from-x methods are sufficient for the application of computer rendering (e.g. [46]), we belief that they are less suited to capture high-resolution 3D details for the purpose of creating 3D printed replicas. In using these methods the lack of measured 3D detail can be 'masked' by texture mapping (i.e. shadows and highlights in the color texture, mask the lack of actual depth information). Moreover, 3D printing requires higher resolution data, as well as color information free from highlights and shadows. The approach in this paper utilizes the method of Zaman *et al.* [5], combining fringe projection with

stereo vision, for simultaneous, high-resolution capture of color and topography, which mitigates the above mentioned issues. To our knowledge only a few of these scanners [5, 41, 47] have been utilized for capturing input data to create physical, full-color reproductions of paintings, which include topography.

4.2.5. 3D color and topography fabrication

The above mentioned scanners have been used in conjunction with the Elevated Printing technology by Océ Technologies [48, 49] to create 3D printed reproductions of paintings. Other systems currently capable of making high-quality full color 3D prints are the (adapted) Stratasys Connex3 or J750 [50], or the custom built Multifab printing system [51]. Limitations of these systems are the limited print area (max. 490x390mm), and the translucency of the inks, leading to blurring of fine details, and the need to digitally compensate for these effects, in turn resulting in a lower effective resolution [52–55]. Other approaches to physical appearance reproduction of paintings use a hybrid fabrication technique, combining plaster casting, 2D color printing, and artisan hand painting and varnishing to create life-like reproductions [42, 56]. 3D reproductions have also been created by the Van Gogh Museum. From publicly available information it can be deduced that these reproductions are created using a hybrid technique of 2D color imaging, 3D scanning, molding and 2D color printing [57]. A limitation of this reproduction approach is the need for alignment of the color and topography in the fabrication stage. Further details on for instance scanning method, fabrication procedure, scanning and printing resolution, and ultimately the overall reproduction quality are unknown to the authors.

In conclusion, currently there is no digital reproduction workflow integrating all modalities of appearance, namely color, topography, gloss and translucency. In the following section we will present an approach to an integrated digital capture and reproduction of the appearance of paintings, which includes the color, topography and gloss variations across the surface. Note that the current setup is not yet able to capture or replicate the translucency of a painted surface (i.e. found in paintings which are built up in various translucent layers, using glazes).

4.3. Materials

4.3.1. Scanning system

The scanning system consists of two modules: the 3D scanning module, which is used to capture color and topography, and the gloss scan module, used for capturing the gloss. The modules capture the same small region of the painting, and their capturing routine runs sequentially for every scan position. Figure 4.1 shows the scanner and a setup of the experiment. The following paragraphs describe it's components.

3D scanning module

The major components for the 3D scanning module are a projector (Acer X113H) and two cameras (Nikon D800E) (see Figure 4.1), all these fitted with polarization

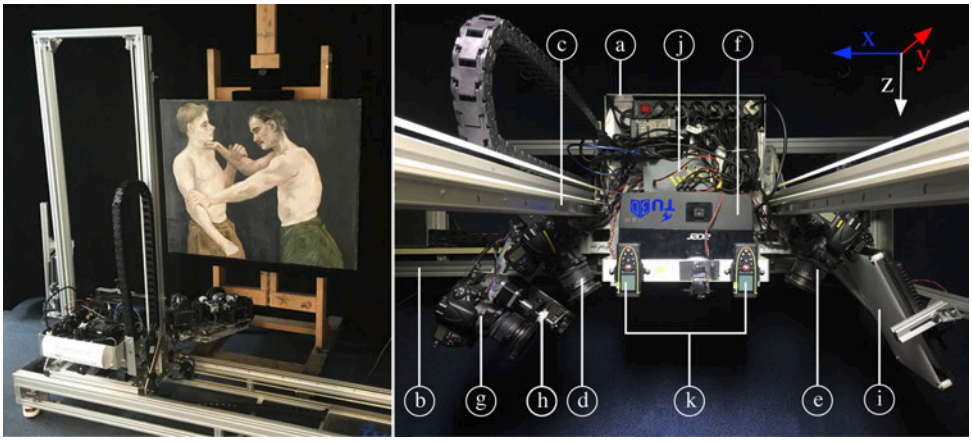

Figure 4.1: Scanning system. Left: Scanner positioned in front of painting. Right: Top view of (a) the scanning platform guided along (b) a horizontal and (c) vertical frame. 3D scanning module: (d, e) two cameras, and (f) a projector. Gloss scanning module: (g) a camera, (h) a stepper motor driving the rotation of polarization filter, and (i) LED array light source with diffuser. All components are controlled by (j) an Arduino® micro controller and the scanner is equipped with (k) two distance meters.

filters (Hoya HD) to eliminate reflections (cross-polarization). The cameras are fitted with Scheimpflug lenses (Nikkor PC-E 85 mm), to align the focal plane of the cameras with the painting surface. The cameras have a resolution of 7424 pixel by 4924 pixels, and the projector a resolution of 800 pixel by 600 pixels. Through defocusing the projector slightly, a continuous sinusoidal fringe pattern is projected, thereby not limiting the effective scanning resolution. The cameras capture an area of roughly 180 mm × 100 mm at the time, hereafter referred to as a *tile*.

The 3D scanning module has nearly the same configuration as described by Zaman *et al.* [5], but the RGB-LED pico-projector was replaced by a projector using a high-pressure mercury lamp as light source (Acer X113H). Figure 4.2 shows that the absolute irradiance is much larger for the new projector compared to the old projector (allowing an increased shutter speed, which in turn gives a better signal-to-noise ratio), and that the radiant energy of the new projector covers the full visible spectrum (390 nm to 700 nm), and thereby better approaches the spectrum of CIE standard illuminant D50 (improving color rendition) [58]. Based on conservation guidelines [59] it is estimated that the level of illumination of the projector (9.0 klx) would lead to a 'Just Noticeable Change' (JCH) on the painting (categorized as medium sensitivity, category 5) after 1 month to 3.5 months of exposure. As the exposure is limited to several minutes for any given area, it is estimated to have a minimal impact, similar to the exposure during photography, or during restoration or treatment. The scanner was safely applied, scanning two authentic Dutch, Golden Age paintings, from the collection of the Mauritshuis [60, 61].

Although the configuration of components and working principle of our system in terms of 3D topography capture is similar to commercially available structured light scanners, like the Atos Compact Scan [62], our scanner has a higher resolution

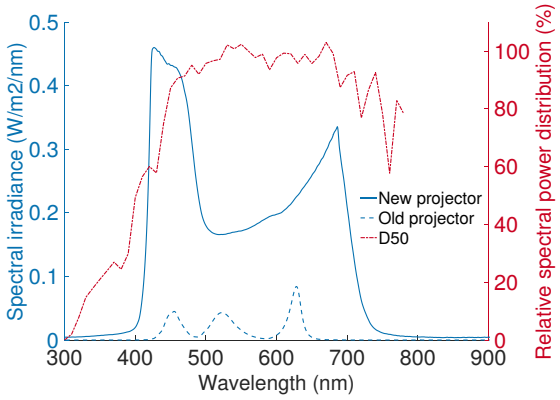

Figure 4.2: Spectral irradiance of new projector with high pressure mercury lamp illuminant (Acer X133H, solid blue line) in comparison to the old projector with RGB LED illuminant (Optoma PK301 pico-projector, dashed blue line), both with a polarization filter; and relative spectral power distribution of the CIE standard illuminant D50 (solid red line), normalized to a value of 100 at a wavelength of 560 nm [58].

(using 40Mp sensors versus 12Mp camera sensors), meaning that our system can capture a higher resolution for the same capture area.[2] An advantage of using RGB sensors in our setup is the ability to directly register the color information on the 3D data, as they are captured simultaneously. Additionally, the use of Scheimpflug lenses and polarization filters is specifically tuned for the application of scanning planar objects. The alignment of the focal plane to the object plane, means the scan can be made with a larger aperture, leading to faster exposure times. Cross-polarization makes it possible to scan the highly reflective surfaces of paintings. Ultimately, an open system makes it possible to calibrate and register images of the third camera, which is used to capture the spatially varying gloss.

Gloss scanning module

The gloss scan module consists of an LED panel (Bresser SH-900, 280 mm × 280 mm) with a diffuser (4 mm translucent Plexiglas), a camera (Nikon D800E, also with a Nikkor PC-E 85 mm lens) and stepper motor driving the rotation of a polarization filter, which is mounted on the camera lens.

System integration and image processing

Both scanning modules are mounted to a platform, which in turn is movable horizontally and vertically along the frame, for scanning paintings with maximum dimensions of 1.3x1.3m. All components are controlled via an Arduino® micro-controller. The scanner is manually positioned in front of the painting. Two distance meters are used to achieve the best possible parallel alignment between the painting and projection plane (measuring four corners of the painting) and for positioning the painting at the right distance, thereby making sure that the whole surface is in focus. Camera calibration, image processing and stitching is done using a self-developed

[2]Note: due to de-focusing the projector, it does not limit the resolution of the 3D scanner.

software based on Matlab® 2017a. A Spectralon® panel (300 mm × 300 mm) and color calibration target (X-rite Colorchecker® SG) are used for calibration of the color images.

4.3.2. Printing system

An adapted version of Océ Technologies [63] *Elevated Printing* technology [48] is used for printing. The ink-jet system utilizes UV-curable inks. A transparent ink is added to the default CMYK and White ink channels, which can be used to create spatially-varying gloss. This experimental printer has a build volume of 1.25 m × 2.5 m (xy) and 5 mm (z) height. The printing system has a planar resolution of 450 dpi (56 µm), and the smallest possible layer resolution is 2 µm.

4.4. Method

4.4.1. Calibration and scanning workflow

Figure 4.3 presents the workflow for calibration and scanning of a painting when the scanner is assembled. Firstly, all devices are set to the appropriate settings and the white balance, the color and the lens distortion of three cameras are calibrated based on multi-view geometry [64]. Images are then captured for 3D, color and gloss reconstruction regarding each tile. After scanning the color, topography and gloss images are processed off-line for each tile, and then they are stitched to form the color, topography and gloss images of the whole painting. The gloss image is mapped to the printable gloss range, and finally a 3D print is made using the color, topography and gloss map. Details on color and topography capture, gloss capturing and fabrication are presented in the following sections.

4.4.2. Color and topography capturing

The color and 3D topography of the surface are captured using a hybrid solution of fringe projection and stereo imaging (described in [5]). A 6-phase shifting sinusoidal greyscale pattern (fringe) is projected horizontally and vertically to acquire 3D information of the projected area (24 images). Fringes are unwrapped and a sparse stereo matching is employed to match the fringes of both camera images. Once the fringes are matched a lookup table is generated for both cameras, encoding both images. Finally a dense stereo matching is made, using the ray-tracing principle, taking into account the camera calibration. One additional image is captured with a uniform illumination of the projector, which is used as the color image. With the frontal illumination of the projector, shadowing is very limited and free of specular reflections (due to the cross-polarization). Also the effect of local shading (whereby the captured color is actually the product of the diffuse albedo and the dot product between the surface normal and the normalized lighting direction) is minimal, not leading to visual artifacts. In short the color image can be used as a proxy for the diffuse albedo. The color image is corrected for the non-uniform illumination of the projector (i.e. caused by lens vignetting), using the frame-filling calibration image captured of the Spectralon® panel. The current setup is able to achieve an in-plane resolution of 25 µm × 25 µm (XY), outputting an RGB color image and a height map.

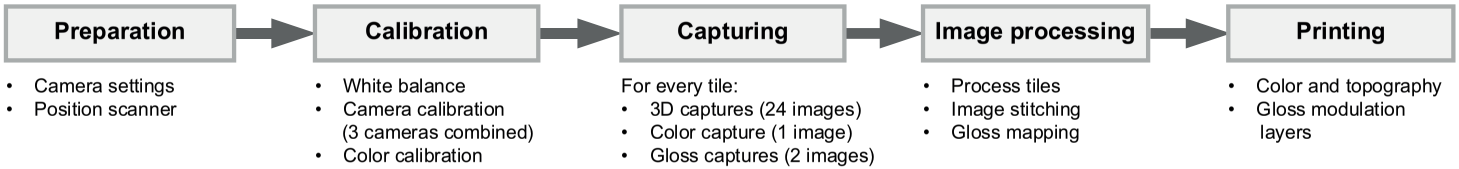

Figure 4.3: Overview of workflow for the reproduction of color, gloss and topography.

Table 4.2: Reflection coefficients R_s and R_p (see Equation (4.2)), and percentage of reflection that remains unpolarized, for minimum, average and maximum refractive index found in oil paintings, when the scanner is configured at the average Brewster's angle ($\theta = 56.3°$), at the left image boundary (A), center (B) and right image boundary (C).

	$n_2 = 1.47$			$n_2 = 1.495$ (average)			$n_2 = 1.52$		
	A	B	C	A	B	C	A	B	C
R_p coefficient	0.0037	2.08×10^{-5}	0.0047	0.0044	0	0.0042	0.0052	2.18×10^{-5}	0.0037
R_s coefficient	0.098	0.138	0.181	0.1045	0.1456	0.1899	0.111	0.153	0.199
$R_\mathrm{p}/(R_\mathrm{p}+R_\mathrm{s})$ err (%)	3.66	0.015	2.18	4.06	0	2.18	4.47	0.014	1.84

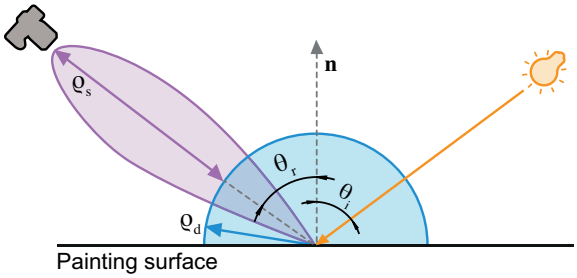

Figure 4.4: Dichromatic reflection model, where θ_i is the incidence illumination angle and θ_r the reflection angle, ρ_d and ρ_s represent the diffuse and specular reflectance components.

4

4.4.3. Gloss capturing

Following Shafer's Dichromatic Reflection Model [65], we assume that the surface reflectance can be modeled with a diffuse (or 'body') and specular (or 'interface') reflectance component, as a function of the incident angle (θ_i), reflectance angle (θ_r), the phase angle (ϕ), and the wavelength (λ):

$$\begin{aligned} L(\theta_i, \theta_r, \phi, \lambda) &= L_s(\theta_i, \theta_r, \phi, \lambda) + L_d(\theta_i, \theta_r, \phi, \lambda) \\ &= \rho_s(\theta_i, \theta_r, \phi) c_s(\lambda) + \rho_d(\theta_i, \theta_r, \phi) c_d(\lambda) \end{aligned} \tag{4.1}$$

where ρ_d represents the magnitude of the diffuse component and ρ_s of the specular component, which depends only on geometry and is independent of wavelength. Figure 4.4 shows a schematic representation of Shafer's BRDF model, showing the incident illumination angle θ_i, the reflection angle θ_r (at the specular peak), and the reflectance components ρ_d and ρ_s. The magnitude of the specular component (ρ_s) is extracted across the surface, varying in relative intensity due to micro-scale roughness scattering (low intensity for a rough surface and high for a glossy surface), as the input parameter for the gloss printing.

Brewster's angle reflectance polarization

In the proposed approach the reflectance is sampled at the mirror reflection angle ($\theta_i = \theta_r$) .[3] We assume that the magnitude of the specular reflectance is influenced by the scattering effect due to the surface roughness (the refractive index is similar across the surface, and the illuminance and Fresnel effects are normalized). In perception experiments it was found the roughness parameter is a good predictor of the perceived glossiness [66, 67]. Here we assume that the specular peak reflectance of a point is dominant over the contribution of the spread of the specular lobe of neighboring points.

The proposed approach also assumes that most of the painted surface is sufficiently flat that the measurement is close enough to the specular peak (or locally corrected for using the height map, see Section 4.4.3) for reproducing the spatially-varying gloss characteristics of a painting's surface.

[3] see paragraph *Surface normal and shadow correction* on the corrections applied to mitigate the effects of non-planarity of a painting's surface

Extracting the specular reflectance component is achieved by utilizing the polarization of reflections. The intensity and polarization of reflections, can be calculated using the Fresnel equations [68]:

$$R_{\mathrm{s}}(\theta) = \left(\frac{n_1 \cos\theta_{\mathrm{i}} - n_2 \cos\theta_{\mathrm{t}}}{n_1 \cos\theta_{\mathrm{i}} + n_2 \cos\theta_{\mathrm{t}}}\right)^2 \quad \text{and} \quad R_{\mathrm{p}}(\theta) = \left(\frac{n_1 \cos\theta_{\mathrm{t}} - n_2 \cos\theta_{\mathrm{i}}}{n_1 \cos\theta_{\mathrm{t}} + n_2 \cos\theta_{\mathrm{i}}}\right)^2 \tag{4.2}$$

where reflection coefficients R_{s} and R_{p} correspond to the perpendicular (Senkrecht, in German) and parallel directions to the surface. n_1 and n_2 are the refractive indexes of air and the material being scanned. θ_{i} and θ_{t} are the incident and transmission angles, whereby the latter can be substituted using Snell's law and trigonometric identities [68]:

$$\frac{n_2}{n_1} = \frac{sin(\theta_{\mathrm{i}})}{sin(\theta_{\mathrm{t}})} \quad \Rightarrow \quad \cos(\theta_{\mathrm{t}}) = \sqrt{1 - \left(\frac{n_1}{n_2}\sin(\theta_{\mathrm{i}})\right)^2} \tag{4.3}$$

Hereof, the incident angle where the reflection is fully polarized ($R_{\mathrm{p}} = 0$), called Brewster's angle, can be calculated as follows [68]:

$$\theta_{\mathrm{B}} = \arctan(\frac{n_2}{n_1}) \tag{4.4}$$

Oil paints and varnishes that are typically used in oil paintings have a refractive index in the range of 1.47 to 1.52 [69], yielding a Brewster's angle between $55.8°$ and $56.7°$. The averaged refractive index ($n_2 = 1.495$), which gives a Brewster's angle (θ) of $56.3°$, is adopted in the setup of the system and data processing (for estimations of errors due to refractive index variation see Table 4.2). The relationships between reflection coefficients (R_{s} and R_{p}) and the incident angle are plotted in Figure 4.5 (for $n_2 = 1.495$). As reflection coefficient R_{p} goes to zero at Brewster's angle, the light is effectively polarized at (and for the most part around) this angle. This effect ($R_p \approx 0$) can be used to discriminate the specular reflectance from the diffuse reflectance.

Area capture of specular reflectance using polarization

In the setup of the scan modules (see Figure 4.6), a diffuse light source which is a flat panel illuminates the surface of the painting ($k = 450$mm). The camera captures the illuminated area. Given point B in the painting, which is the center of the scan area, the angle θ between the plane normal ($\vec{n}$) and the perpendicular direction of the light source (k) is set as Brewster's angle ($\theta = 56.3°$). The angle between the plane normal ($\vec{n}$) and the optical axis of the camera (m) is set as Brewster's angle as well. The width of a single gloss capture is approximately 180 mm on the painting (distance between point A and C), corresponding to the field-of-view of the 3D scan module. The distances are estimated based on the camera calibration and measurements using a laser distance meter.

Given our assumption that the specular peak reflection is dominant over the spread of the specular lobe, we simplify the reflection model that any point (J)

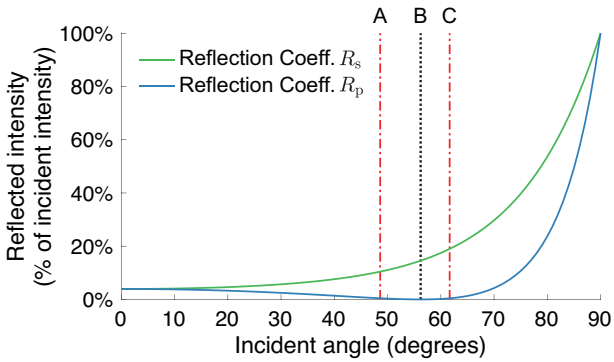

Figure 4.5: Reflection coefficients R_s and R_p are plotted for the average refractive index ($n_2 = 1.495$) for every incident angle. The plots show the point of maximum polarization at Brewster's angle (black dotted line), and the mirror reflection angles at the edge of the scan region at point A and C (red dashed lines, see Figure 4.6)

has a corresponding mirror reflection angle (θ_j), at distance (k_j) to the lamp and distance (m_j) to the camera. Note that the light source is sufficiently large to include the mirror angle for every surface point within a capture region. In Figure 4.5 the region between the red-dashed lines indicates the mirror angle range (and their corresponding coefficient ranges) that are present in a single capture. To extract the specular reflectance, two images are captured, one image containing specular reflections (I_1) and one image where the specular reflections are filtered by rotating the polarization filter in front of the camera lens by $90°$ (I_2). The images are converted from RGB to HSL color space, where the lightness channel (L) is used for further image processing, safely neglecting the wavelength dependency of the specular reflectance. Here we assume the paint behaves as a dielectric material, and therefore does not alter the spectral properties of the reflections [70]. The difference between these two images is calculated:

$$I_g = I_1(\rho_d + \rho_s) - I_2(\rho_d + \rho_s) \tag{4.5}$$

As the diffuse reflectance is unpolarized, the contribution of the diffuse reflectance will be identical in both images ($I_1(\rho_d) = I_2(\rho_d)$) and from the Fresnel equations follows that the specular component in the second image goes to zero ($I_2(\rho_s) \approx 0$). Therefore I_g is the gloss map ($I_g = I_1(\rho_s)$), giving the relative magnitude in specular gloss across the surface.[4]

Gloss calibration

If we consider the surface to act like a mirror (either highly reflecting or scattering) due to the angular configuration, the distance between the lamp and camera is not constant over the surface (i.e. $(k' + m) \neq (k'_j + m_j)$, see Figure 4.6). Additionally,

[4]Note that due to the polarisation effects at Brewster's angle, the contribution of illumination arriving at any given point (J) from any other direction than the mirror reflection angle, will also be negligible, as these will have equal contribution in image (I_1) and (I_2) as they will not be (completely) polarized.

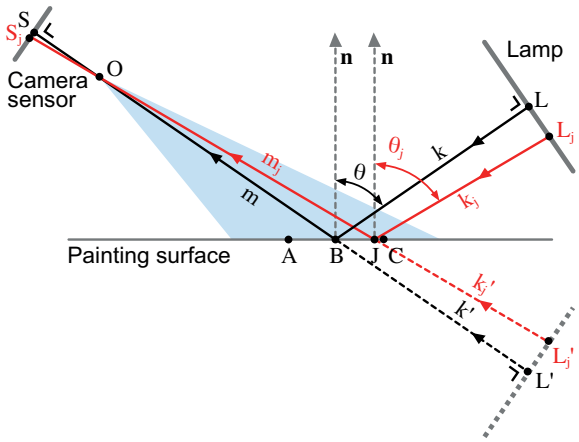

Figure 4.6: Schematic top view of gloss scanning module, consisting of a lamp (right) and camera (left) both rotated by Brewster's angle (θ) w.r.t. the surface normal ($\vec{n}$). Point B denotes the scan area center, and point A and C the 3D scan area boundaries, and blue shaded region represents the gloss camera field-of-view. Any point (J) on the surface has a mirror reflection angle (θ_j) with distances k_j to the lamp and m_j to the camera optical center O (k_j' is the distance from the surface to the Lamp's mirror image).

as the mirror reflection angle varies across the surface, the reflected intensity also varies, following from the Fresnel equations (see R_s in Figure 4.5). The gloss map is rescaled relative to the center of the image, taking both into account. Although it seems easy to correct the irradiance variation using the image of a Spectralon® panel illuminated by the LED panel as a reference object, such a image cannot capture the correct irradiance variation. It would give the illumination sum from the whole LED panel for any surface point, rather than just the illumination arriving from the mirror reflection angle. For this reason a model based correction better represents the irradiance variation, applicable for the specular reflectance component.

First, the measured gloss map (I_g) is scaled relative to the center of the image (at B) to correct for the variation in irradiance arriving at the sensor from the lamp, reflected by any point (J), applying the inverse-square law [68]:

$$\frac{E(Sj)}{E(S)} = \frac{(k+m)^2}{(k_j+m_j)^2} \quad \text{thus,} \quad E(Sj) = E(S)\frac{(k+m)^2}{(k_j+m_j)^2} \tag{4.6}$$

where $E(S)$ and $E(Sj)$ are the irradiance at points S and S_j on the sensor, corresponding to point L and L_j on the lamp, reflected at point B and J, respectively.

Secondly, the intensity is scaled for the radiance specularly reflected at every point, relative to the center of the scan, by using the difference between reflection coefficients as scaling factors:

$$E(S_j) = E(S)\frac{R_s(\theta) - R_p(\theta)}{R_s(\theta_j) - R_p(\theta_j)} \tag{4.7}$$

where $E(S)$ and $E(S_B)$ is the irradiance measured at point S and S_j on the sensor, corresponding to the reflection at point B and J, respectively. R_s and R_p are reflection coefficients as a function of the incident angle (see Equation (4.2) and Figure 4.5). This describes the relationship in reflected intensity, assuming equal irradiance and equal scattering.

As the measured irradiance is proportional to the intensity as well as the reflection coefficient ratio, the above formulas can be translated to scaling factors:

$$I_{g,cor}(J) = e * f * I_g(J) \quad \text{where} \quad e = \frac{(k+m)^2}{(k_j+m_j)^2}, \quad f = \frac{R_s(\theta) - R_p(\theta)}{R_s(\theta_j) - R_p(\theta_j)} \tag{4.8}$$

where $I_{g,cor}(J)$ in the corrected gloss intensity of point J, and e and f are scaling factors relating to the varying irradiance and reflection coefficient ratios. The output of the gloss scanning is a gray-scale gloss map, scaled between the minimum and maximum measured gloss intensity. Based on the camera calibration matrix, using multi-view geometry[64], the gloss image is mapped to the height map.

Table 4.2 shows the reflection coefficients R_s and R_p at the mirror reflection angles of points A, B and C, for the minimum, average and maximum refractive index, found in oil paintings. For the average refractive index ($n_2 = 1.495$), 4.1% and 2.2% of the reflected light remains unpolarized at the boundaries of the image ($I_2(\rho_s) \neq 0$ in equation (4.5)). The theoretical maximum measurement error is 4.5% (found at point A), when a painted surface with a higher refractive index ($n = 1.52$) is imaged at the chosen configuration. In the calculation of the scaling factors in equation (4.7), the error introduced by variation of refractive index is less than 1%. Both errors are neglected in our approach.

Surface normal and shadow correction

Due to the 3D structure of the painting, the surface normal varies locally, and therefore some parts of the painting are not captured at the (Brewster's) mirror angle. Utilizing the height map, the local surface normal is determined, and regions which exceed an experimentally determined threshold are masked, as illustrated by the green, crossed pixels in Figure 4.7a. The normal mask threshold was experimentally determined at $\theta_h > 10°$, where we saw a sharp transition in gloss intensity, in regions where we expect a continuous glossiness. Additionally, the incident angle of light combined with 3D structure, causes shadows and shaded regions. An additional shadow mask is created, also utilizing the height map (illustrated by the green, crossed pixels in Figure 4.7b). The surface normal and shadow mask are combined and in the data processing, gloss information in the masked regions is discarded and filled using the local maximum value. For every pixel, the local maximum value is determined, sampling the closest pixels (in a radius of 40 pixels). These values are used to fill the pixels which fall within the mask. Here we assume some local continuity in gloss, and that the local maximum is produced by the region which is measured at the mirror angle (the local surface normal coincides with the global normal). Alternatively, more sophisticated interpolation algorithms (for instance a Poisson infilling strategy [71]) might also be applied here, to minimize visual artifacts.

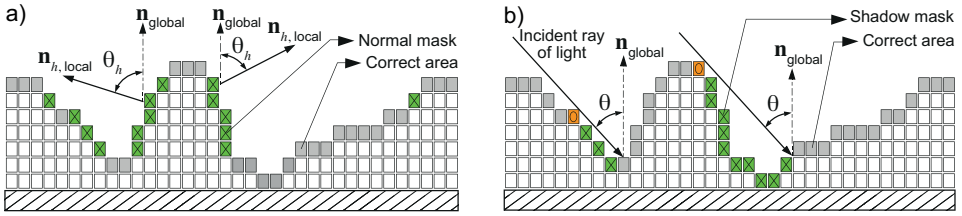

Figure 4.7: (a) Surface normal mask (left), showing the angle (θ_h) between the local ($\vec{n}_{h,\mathrm{local}}$) and global surface normal ($\vec{n}_{\mathrm{global}}$) and the pixels (green, crossed) belonging to the mask, which exceed an experimentally determined threshold; (b) Shadow mask (right), showing Brewster's angle (θ) between incident ray of light and the global surface normal ($\vec{n}$), the critical edge pixel (orange, oval) and the pixels belonging to the mask (green, crossed).

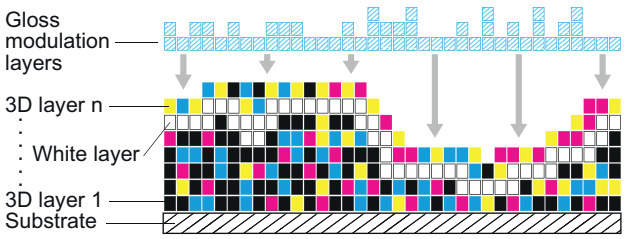

Figure 4.8: Cross section diagram of 3D print showing the stratigraphy of the substrate, topography/color layers with intermediate white layer, and gloss layers.

4.4.4. Tile stitching

Images are stitched using a self-developed algorithm. First, based on the assumption that a painting is generally a planar surface, a best-fit plane is found for the center tile. Then the 3D topography data of each tile is fitted to this plane individually and the transformation matrix of each tile is documented. As the 3D topography, color and gloss are aligned for each tile, color images and gloss images of this tile can be transformed to fit this plane by the same transformation matrix. Then, adjacent tiles are matched using a cost function which features the RGB color as well as 3D information. The images are first matched and stitched in rows, after which the rows are stitched to form the complete image. The height data is aligned using the mean height of the overlapping regions, and a (residual) slope difference is removed. The data is then merged, blending the low frequency variations, whilst superimposing the high frequency variations of one of both images, leading to satisfactory stitching with minimal visual artifacts. More sophisticated merging, for instance using minimal deformation strategies, might further improve stitching.

4.4.5. Appearance fabrication

To fabricate the appearance, three input files are used: a color image, a height map (resembling the 3D topography) and the gloss map. Through the use of Océ Technologies custom 3D slicer software, the color image and height map are combined to form a stack of bitmaps. The color of every position (X-Y) is printed in the

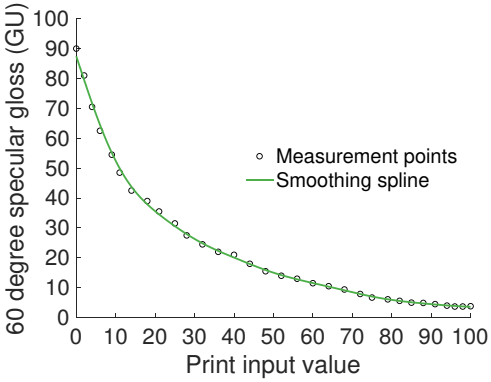

Figure 4.9: Relationship between print input values and 60° specular gloss in gloss units (GU), measured using a glossmeter.

layer corresponding to the height specified for that position (Z). Consequently, the voxels below that point are set to print in white ink, to form a boundary between the bulk of the print (printed with all color channels) and the outer color layer, as the color printing is based on subtractive color mixing on a white substrate (which is this case is the white ink). Thus, the color and topography are printed integrally using cyan, magenta, yellow, black and white ink (see Figure 4.8).

Spatially-varying gloss is created with six consecutive layers of transparent ink, printed on top of the 3D color layers (see Figure 4.8). The first layer is a high gloss layer; the ink is applied in a full coverage and left to flow across the surface before it is cured, hereby creating the highest printable gloss level. This high gloss layer across the whole surface ensures the creation of a smooth gloss gradient, from high gloss to matte. In the following layers an input gloss gradient is dithered, so that the matte part receives the most ink coverage. Each of these 6 layers are cured directly after printing, creating a rougher surface finish. Sample gloss patches were printed (given a printer input value between 0-100), and measured with a glossmeter (Byk Micro-tri-glossmeter) to determine their glossiness. The relationship between the printer input values (0-100% gloss) and 60° specular gloss, is depicted in Figure 4.9. As this relationship is non-linear, the gloss map is multiplied by the inverse of the fitted function, as to create a linear gloss mapping to the glossmeter values:

$$P = f(G_{60})^{-1} * I_{\mathrm{g,cor}} \tag{4.9}$$

where, P is the print value, $f(G_{60})$ is the function that described the relationship between print values and 60° specular (G_{60}) gloss, and $I_{\mathrm{g,cor}}$ is the corrected glossmap. The gloss map, scaled between the minimum and maximum measured value, is mapped to the full printable gloss scale.

4.5. Results

4.5.1. Scan results

Two paintings, *Two Wrestling Figures* and *Sunflowers*, both in the style of Vincent van Gogh, were used as a case study for the proposed reproduction workflow. *Two Wrestling Figures* (99 cm × 79 cm) was captured in 140 tiles and the *Sunflowers* (30 cm × 40 cm) in 42 tiles, both with an overlap of approximately 30% between tiles to enable stitching. Per tile, 24 images are captured for the 3D reconstruction (12 by each 3D camera), 2 images for color (1 by each 3D camera, also used for the sparse stereo matching), and 2 consecutive images for the gloss reconstruction by the gloss camera. In total 3780 images of 40 Mpixel were captured for one scan of the *Two Wrestling Figures*, and 1134 for the *Sunflowers*, of which 7.4% (280 and 84 images, respectively) are needed for the gloss reconstruction.

With our current implementation, capturing a single tile (including movement to the next position) takes on average 7 min 50 s, meaning that the *Sunflowers* can be captured in 4 h 18 min and the *Two Wrestling Figures* in 18 h 16 min. The images are processed off-line, where reconstructing the 3D image and gloss combined takes approximately 12 minutes per tile. Finally, the tiles are stitched to create the complete image, taking approximately four hours in the case of the *Sunflowers* painting.

Details of the scans are shown in Figure 4.10. Figure 4.10(a) shows the RGB color images. The heightmaps, with a maximum height variation of 1.1 mm are shown in Figure 4.10(b). The uncorrected glossmap, the shadow and normal mask mask on the glossmap (depicted in green), and the corrected gloss map are shown in Figure 4.10(c-f)). For the *Sunflowers* painting, the normal mask covers 13.3% of the total surface and the shadow mask 0.4%, where 0.35% of the surface is masked by both. For the *Two Wrestling Figures*, these percentages are 30.1% and 22.6%, where 9.6% of the surface is masked in both. We found that even for these paintings (with relatively pronounced topography), there is still enough unmasked area to fill in the masked regions.

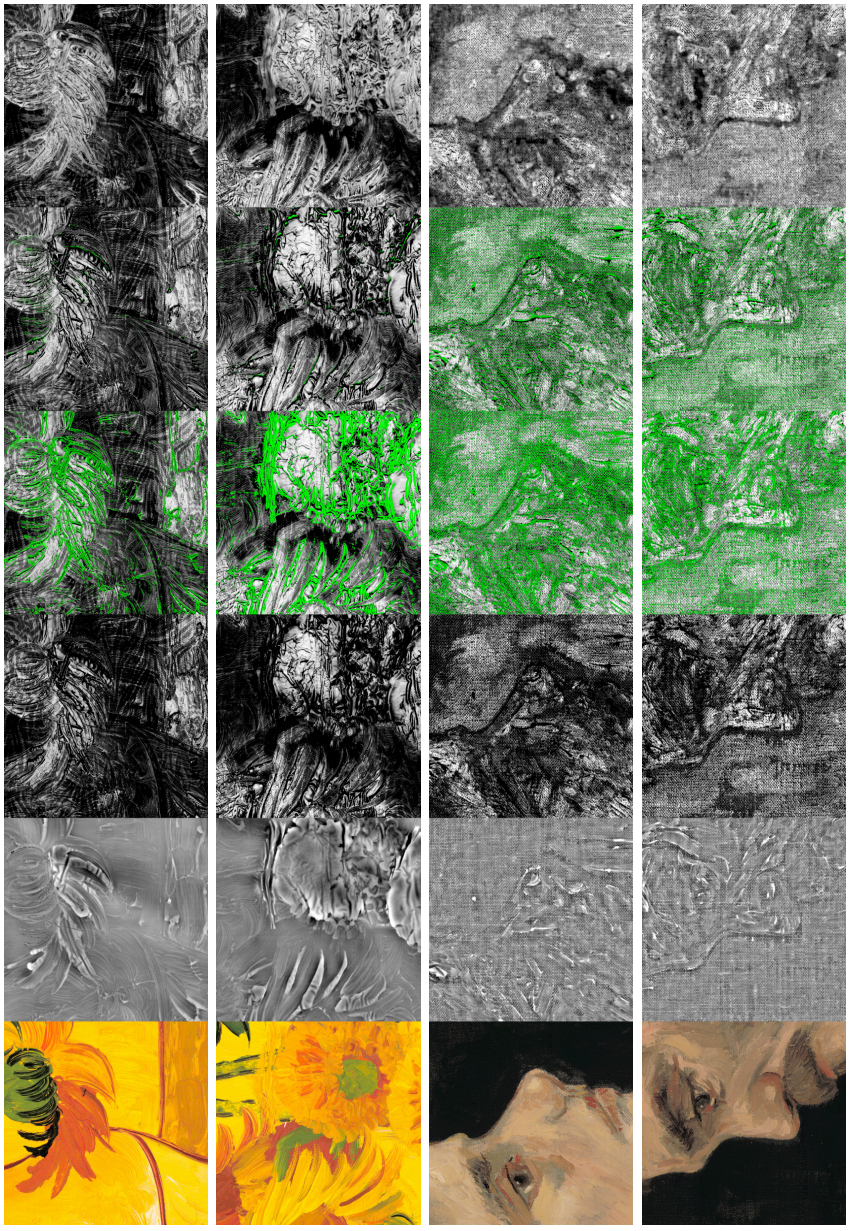

(a) Color image (b) Heightmap (c) Glossmap uncorrected (d) Normal mask on glossmap (e) Shadow mask on glossmap (f) Glossmap corrected

Figure 4.10: Scan results, details of *Sunflowers* (top two rows) and *Two Wrestling Figures* (bottom two rows)

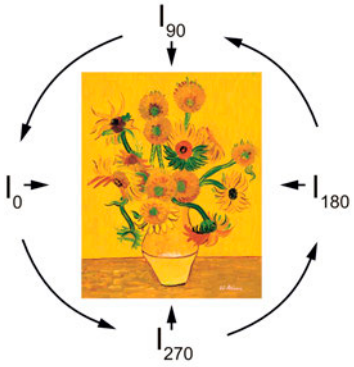

Figure 4.11: Illumination directions for the four scans, I_0, I_{90}, I_{180} and I_{270}. Note that in practice the painting is rotated 90° counterclockwise for every scan

Table 4.3: The table shows the means (μ) and standard deviations (σ) of the differences between the illuminations directions (I_0 to I_270) for a sample region (see Figure 4.12(a)). The data is scaled between the minimum and maximum measured gloss values (over all images)

Histogram	μ	σ
$I_{90} - I_0$	-0.05%	10.92%
$I_{180} - I_0$	-0.22%	11.69%
$I_{270} - I_0$	-0.21%	11.61%
$I_{90} - I_{180}$	0.16%	12.14%
$I_{270} - I_{180}$	-0.01%	11.13%
$I_{270} - I_{90}$	-0.17%	11.81%

To evaluate the effect of the scanning geometry on the measurement, the *Sunflowers* painting was scanned four times, every time rotating the painting by 90 degrees. Figure 4.11 depicts the effective illumination direction for every scan, labeling the subsequent scans I_0 (upright position of the painting), I_{90}, I_{180} and I_{270}. Note that in reality the painting was rotated relative to the scanner. A sample region of every scan was overlaid, based on local feature matching. The gloss values of the four scans are scaled between the minimum and maximum measured gloss values over all scans. A detail of the four scans and their reciprocal differences are depicted in Figure 4.12, showing a detail of scan I_0 in Figure 4.12(a), and subsequently the absolute differences between I_0 and the other scanning orientations in Figures 4.12(b-d). (e) shows the absolute difference of I_{90} and I_0 (as depicted in (b)), with a semi-transparent, red overlay of the combined mask of scan I_{90} and I_0. (f) shows two boxplots of the absolute differences (for $|I_{90} - I_0|$), of the masked and non-masked regions (as shown in (e)). The average differences are respectively 7.0% ($\pm 6.2\%$) and 7.8% ($\pm 8.1\%$) (similar for fig.4.12(c-d)). Figures 4.12(e-f) show, that although the masked areas are close to the regions with the largest errors, the infill of the masked regions themselves are not responsible for the largest error. Figure 4.12(g) shows the histogram of the differences (for $|I_{90} - I_0|$, between -40 and 40%) with a fitted Laplace distribution, and Table 4.3 shows the means and standard deviations of the distributions as depicted in Fig. 4.12(b-d). The differences are expressed as percentages of the maximum possible difference, meaning that for instance 100% difference would indicate that I_0 had a normalized gloss value 0 (completely matte) and I_{90} a normalized gloss value of 100 (high gloss). Note that differences can also occur due to the discrete sampling (at pixel resolution), and the fact that the alignment was not solved on a sub-pixel level, meaning that if you have a high-frequency gloss pattern, you might find differences which are not necessarily the effect of the scanning geometry. Seeing that the differences closely follow a Laplace distribution, we believe that our calibration and off-center corrections are not introducing any systematic error between the images.

(e) $|I_{90} - I_0|$ with combined mask of I_{90} and I_0 (red)

(f) Abs. Glosslevel differences of masked and non-masked areas of $(I_{90} - I_0)$

(g) Glosslevel differences of $(I_{90} - I_0)$

Figure 4.12: Effect of scanning orientation on gloss measurement showing (a) a sample region of the gloss scan I_0, (b-d) the absolute differences between gloss levels for the scan orientations (see Fig. 4.11), displayed between 0 and 40%, (e) the absolute difference map of $(I_{90} - I_0)$, with a red, semi-transparent overlay of the combined masks from image I_{90} and I_0 (see Fig. 4.10(d-e)), (f) the boxplots of the absolute differences for the masked and unmasked areas (of $|I_{90} - I_0|$, as in (e)), (g) shows the histogram of differences (of $I_{90} - I_0$), plotted between -40% and 40%, as a percentage of the maximum possible difference. All data is scaled between the minimum and maximum measured gloss values (over all images).

4.5.2. Print results

Printing the reproductions takes 1/2 hour for the *Sunflowers* painting and 3 hours for the *Two Wrestling Figures* painting. Figure 4.13 shows the *Sunflower* painting and 3D printed reproduction, photographed under an identical mirror illumination and viewing angle. Figure 4.13(a) depicts the painting, 4.13(b) the print without gloss layers added (showing the default, uniform gloss appearance of Océ's Elevated Printing process), and 4.13(c) showing the print with spatially-varying gloss. In the top row of the figure, the reflections are removed using a polarization filter, to better visualize the diffuse color appearance; the bottom row shows the images with the specular reflections included, which is most like their appearance to the human eye, when viewing them at this angle. These results show that the scan data can successfully be used to reproduce the spatially-varying gloss of the painting's surface, although it is apparent that the most matte regions on the painting (Fig. 4.13(a)), appear more matte than the most matte regions in the reproduction (Fig.4.13(b)). This is most clear in the yellow background, where the reproduction appears glossier than the painting, as the printer is unable to match the matteness level of the painting.

Figure 4.14 shows a detail of the *Two westling figures* prints, where Figure 4.14(a) shows the diffuse color appearance (polarized), Figure 4.14(b) shows no gloss layers printed, Figure 4.14(c) shows the first high gloss layer printed, and 4.14(d) shows the print when all gloss layers are added. The top part is printed *without* elevation and the bottom part *with* elevation, to emphasize the contribution of the printed gloss variation on the appearance at this viewing angle.

Figure 4.15 shows a printed detail of the *Sunflowers* where 4.15(a) shows the diffuse color appearance (polarized), 4.15(b) the same area captured when the painting is rotated by 90° ($I_9 0$), 4.15(c) when rotated by 180°($I_1 80$), and 4.15(d) when rotated by 270 ° ($I_2 70$). Results show visually very similar spatially-varying gloss characteristics, thereby suggesting that the scan orientation is of limited influence on the reproduced gloss.

Figure 4.13: Comparison between (a) the painting, (b) a print without gloss modulation layers (which are used to create spatially-varying gloss) and (c) a print with gloss modulation layers, captured under identical mirror angle illumination conditions, without reflections using a polarization filter (top), and including specular reflections (bottom). Note that (b) the print without gloss modulation layers is semi-glossy, which is the intrinsic glossiness of the printed color layers, which exhibits the 'plastic' appearance that participants referred to in previous comparisons to paintings [6].

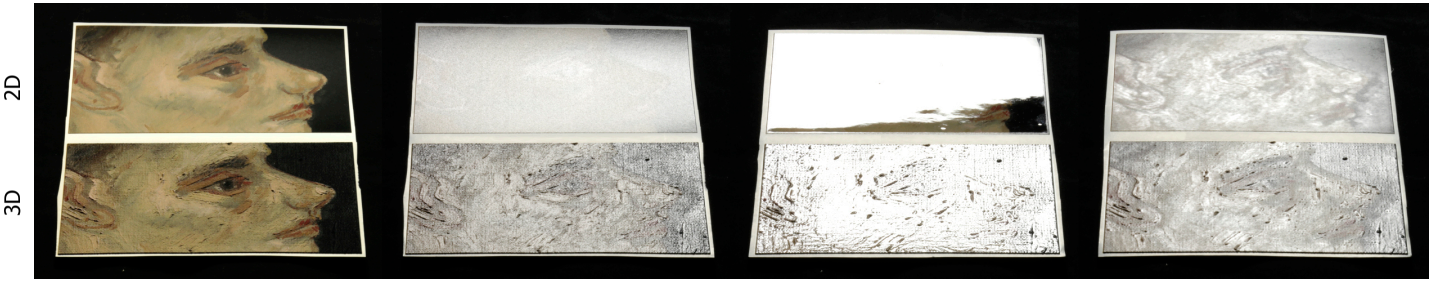

(a) No reflections (b) No gloss modulation layers (c) First gloss modulation layer (d) All gloss modulation layers

Figure 4.14: Printed details of *Two Wrestling Figures*, (a) the diffuse color appearance (polarized), (b) the same detail printed without gloss layers, (c) printed with first (high) gloss layer and (d) printed with all gloss layers. The top row has no topography (2D), the bottom row shows the print including topography (3D), both having the same gloss layers. Note that the print without gloss layers is semi-glossy (b), which is the intrinsic glossiness of the color layers.

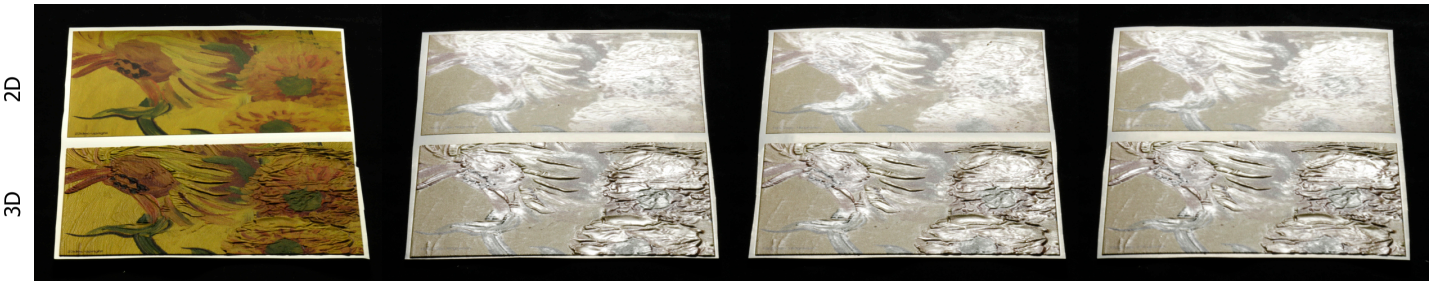

(a) No reflections (b) Glossmap I_{90} (c) Glossmap I_{180} (d) Glossmap I_{270}

Figure 4.15: Printed details of *Sunflowers*, (a) the diffuse color appearance (polarized), (b) the same detail of glossmap I_{90}, (c) glossmap I_{180}, and (d) glossmap I_{270}. The top row has no topography (2D), the bottom row shows the print including topography (3D), both having the same gloss modulation layers.

4.6. Discussion

The proposed system demonstrates that it is possible to capture spatially-varying gloss of a painting's surface with sufficient accuracy for the purpose of 3D printing. Visual inspection indicates that the approach is able to authentically reproduce the color, topography and spatially-varying gloss of a painting. The approach seems effective in trading angular measurement accuracy (present in many BRDF capturing approaches for rendering purposes) for speed and spatial resolution, making it suitable for 3D printed appearance reproduction.[5] Additionally, we are able to print a range of gloss levels with one transparent material - in analogy to CMYK(W) printing, which creates a wide range of colors with only 5 materials - making it a suitable starting point for further full appearance (re)production workflows.

4.6.1. Scanning paintings and (other) heavily textured surfaces

The current setup is configured for materials with a refractive index typical for (varnished) oil paintings. Therefore the scanner will need to be reconfigured if a surface with a very different refractive index needs to be scanned. Moreover, a rough estimate of the refractive index is needed, and therefore some knowledge of the surface material, in order to configure the scanner.

A limitation of the current approach is the need for off-center normalization of the scan measurements, whereby the further the measurement is away from the exact Brewster's angle at center of the image, the more correction is needed. In other words, there is a trade-off between speed (larger scan area) and accuracy of the measurement. Another limitation is that with heavily textured surfaces, a large portion of the gloss map is masked and has to be filled by interpolation, leading to less accurate results. This approach will therefore work best on surfaces which are relatively flat, which is generally the case for pre-modern panel and canvas paintings. We would like to argue that paintings with moderate height variations (like the ones shown in this paper) are also reproducible. However, paintings were the paint encloses empty space between the paint and the canvas (creating 'overhangs' in 3D printing terminology) cannot be reproduced by the proposed 3D scanning approach, nor the 3D printing system, due to the method of plane projection, and the lack of a removable support material.

4.6.2. Influence of scanning geometry on gloss measurements

The results also show that there is a consistency between the scan results from the four rotation angles (I_0 - I_{270}), meaning the influence of the scanning geometry on the measurement is limited. Here we should note that some of the differences found (as presented in Figure 4.12) might be explained by image misalignment and

[5] This approach also overcomes several disadvantages of the gloss capturing method presented in Chapter 3, i.e. needing less images to capture the spatially-varying gloss, and the ability to capture the mirror reflection angle (necessary for highly reflecting surfaces), whilst the effects of area capture of gloss (i.e. influence of area illumination and interactions between neighboring pixels) appear to have a limited effect. We have now also provided an implementation at a higher resolution, useful to capture the high-frequency gloss variations, which can be observed.

the discrete sampling of high-frequency gloss variation.

Figure 4.12(e) shows that largest errors are not found directly at the masked regions, indicating that the masking and infill itself is not causing the largest error. However, the areas with the largest errors are found in the vicinity of the masked areas. From theory it can be expected that the largest errors in gloss measurement will occur in *high* gloss regions, where the surface normal varies (due to height variations). This is due to the increased concentration of the specular reflection and around the mirror reflection angle for high gloss surfaces, whereby only a small deviation in surface normal, causes a large difference in measurement. In our sample area (Fig. 4.12(a), coincidently the high gloss regions are also the regions with larger height variation in our sample. We can therefore not directly disentangle this effect based on scan of these paintings, which are in essence under defined. No significant difference was found in the shape of the histogram if we compare a high gloss area to a low gloss area, within our sample.

4.6.3. Other interactions between gloss, color, and topography scanning and fabrication

Although the gloss map seem to depict the spatial variation and intensity of gloss, proportionally to the visual sensation, it remains to be investigated if the gloss measurement is completely independent of the diffuse color. Additionally, it remains to be investigated what the effect is in terms of scanning as well as fabrication of the gloss on the height. Currently it is unknown what the effect of (semi)-transparent varnish layers is on the height measurement. Likewise, the effect of the printed gloss layers has an effect of the surface topography of the print. The extent of this remains to be investigated, as this is currently not corrected for.

4.6.4. Scanning speed and capturing larger paintings

Whereas we argue that the current scanning and image processing times (as mentioned in Section 4.5.1) are reasonable for the purposes of conducting a case study, the authors would like to emphasize that the current implementation was not optimized for scanning and processing speed. If the capturing procedure was to be optimized for speed, the exposure time of the images, and overhead time for movement and storing data are of main importance. Assuming a (realistic) exposure time of 2 seconds per image (and overhead of 2 seconds), it would be possible to capture $1\,m^2$ within 1 hour. Capturing larger areas would require either creating a larger frame (which can be done up to a certain extent), or repositioning the frame. The capturing method (carried out by the equipment on the scanner platform) would remain the same. The printable area is currently limited to $1.25\,m \times 2.5\,m$, but prints might also be tiled to create larger areas. The printable area is not easily extended.

4.6.5. Gloss mapping and perceptual evaluation

In terms of fabrication, the measured gloss values are mapped to the full range of printable gloss levels. Scanning printed reference samples, may discover better relations between the measured gloss values and the printable gloss levels. In the (likely) case that the printable range of gloss is not sufficient, a strategy should

be developed for gloss mapping - in analogy to gamut mapping of color - through psychophysical experiments.

Additionally, further quantitative and qualitative evaluation of the reproductions should be conducted to validate the scanning and printing results, now that the printed results are at a level suitable for perceptual testing. Finally, we would like to argue that, when viewing Figure 4.14 and 4.15, we can conclude that reproducing spatially-varying gloss provides added perceptual value, only when it is reproduced in conjunction with other material appearance attributes, like color and topography. Reproducing the spatially-varying gloss and color, without the topography, does not bring the appearance closer to the original than visa versa.

4.7. Conclusions

In this paper, we present a painting appearance reproduction system with a focus on capturing gloss appearance. The spatially-varying gloss of a painting is measured by sampling the specular reflection close to Brewster's angle. A mathematical model is developed to normalize off-center deviations of the gloss measurements. Deviations in the local surface normal, as well as shadows are masked by the height map and filled with relevant gloss information. Experiment results indicate that the proposed system is able to simultaneously reproduce the color, the 3D topography and especially the gloss information of a painting. Figure 4.13 shows how the simultaneous reproduction of color, topography and gloss variations results in a visually convincing 3D print. Figure 4.15 shows that the effects of the scanning orientation are limited with respect printed results.

Limitations of the system are also identified regarding the off-center normalization, local deviations in surface normals and shadowing, possible color dependency, and relations between gloss measurements and printable gloss levels, which highlight the future work of the authors.

References

[1] H. Brigstocke, *The Oxford Companion to Western Art* (Oxford University Press, 2001).

[2] R. G. Erdmann, *Bosch project web page,* (2016), (Accessed: 2017-12-11).

[3] M. Ilsink, J. Koldeweij, R. Spronk, L. Hoogstede, R. G. Erdmann, R. K. Gotink, H. Nap, and D. Veldhuizen, *Hieronymus Bosch, Painter and Draughtsman, Catalogue Raisonné* (Mercatorfonds, Brussels, 2016).

[4] W. S. Elkhuizen, B. A. Lenseigne, C. Weijkamp, S. C. Pont, J. M. Geraedts, and J. Dik, *A 3D printed reconstructing of a painting's original size - Showing the original size of Saul and David by Rembrandt,* in *Visual Science of Art Conference* (Barcelona, Spain, 2016) p. 1.

[5] T. Zaman, P. Jonker, B. Lenseigne, and J. Dik, *Simultaneous capture of the color and topography of paintings using fringe encoded stereo vision,* Heritage Science **2**, 1 (2014).

[6] W. S. Elkhuizen, T. Zaman, W. Verhofstad, P. P. Jonker, J. Dik, and J. M. P.

Geraedts, *Topographical scanning and reproduction of near-planar surfaces of paintings,* in *Electronic Imaging: Measuring, Modeling and Reproducing Material Appearance*, Vol. 9018, edited by M. V. Ortiz Segovia, P. Urban, and J. P. Allebach (SPIE-IST, 2014).

[7] M. Alfeld, G. Snickt, F. Vanmeert, K. Janssens, J. Dik, K. Appel, L. van der Loeff, M. Chavannes, T. Meedendorp, and E. Hendriks, *Scanning XRF investigation of a Flower Still Life and its underlying composition from the collection of the Kröller Müller Museum,* Applied Physics A **111**, 165 (2013).

[8] M. Pos, *Het Geheim van de Meester - Vincent van Gogh, De Worstelaar,* (2017).

[9] Federal Agencies Digitization Initiative (FADGI) - Still Image Working Group, *Technical Guidelines for Digitizing Cultural Heritage Materials : Creation of Raster Image Master Files*, Tech. Rep. (Federal Agencies Digitization Initiative Still Image Working Group, 2010).

[10] H. V. Dormolen, *Metamorfoze Preservation Imaging Guidelines*, Tech. Rep. (National Library of the Netherlands (Koninklijke Bibliotheek), The Hague, The Netherlands, 2012).

[11] ISO, *ISO/PAS 15339 - Graphic technology - Printing from digital data across multiple technologies,* (2015).

[12] C. Fischer and I. Kakoulli, *Multispectral and hyperspectral imaging technologies in conservation: current research and potential applications,* Studies in Conservation **51**, 3 (2006).

[13] R. S. Berns, F. H. Imai, P. D. Burns, and D.-Y. Tzeng, *Multi-spectral-based color reproduction research at the Munsell Color Science Laboratory,* in *Electronic Imaging: Processing, Printing, and Publishing in Color*, Vol. 3409 (Zurich, Switzerland, 1998) pp. 1–12.

[14] R. S. Berns, L. A. Taplin, P. Urban, and Y. Zhao, *Spectral color reproduction of paintings,* in *Colour in Graphics, Imaging, and Vision* (Society for Imaging Science and Technology, 2008) pp. 484–488.

[15] H. B. Westlund and G. W. Meyer, *A BRDF Database Employing the Beard-Maxwell Reflection Model,* in *Graphics Interface* (2002) pp. 189–201.

[16] Y. Chen, R. S. Berns, and L. A. Taplin, *Model Evaluation for Computer Graphics Renderings of Artist Paint Surfaces,* in *15th Color Imaging Conference: Color Science and Engineering, Systems, Technologies and Applications, Color Imaging Conference* (2007) pp. 54–59.

[17] S. Tominaga and N. Tanaka, *Spectral image acquisition, analysis, and rendering for art paintings,* Journal of Electronic Imaging **17** (2008), 10.1117/1.3036180.

[18] T. Chen, L. A. Taplin, and R. S. Berns, *Artist Material Database BRDF Fitting*, Tech. Rep. (Rochester Institute of Technology, College of Science, Center for Imaging Science,Munsell Color Science Laboratory, Rochester, USA, 2011).

[19] F. Nicodemus, J. Richmond, J. Hsia, I. Ginsberg, and T. Limperis, *Geometrical*

Considerations and Nomenclature for Reflectance, Tech. Rep. (Washington, D.C., 1977).

[20] J. Padfield, D. Saunders, and T. Malzbender, *Polynomial Texture Mapping : a New Tool for Examining the Surface of Paintings,* in *ICOM Committee for Conservation, 14th Triennial Meeting*, Vol. 1 (2005) pp. 504–510.

[21] J. Redman and M. Mudge, *The Simultaneous Capture of Spectral and Textural Information,* in *Archiving Conference* (Society for Imaging Science and Technology, 2007).

[22] T. Hasegawa, N. Tsumura, T. Nakaguchi, and K. Iino, *Photometric approach to surface reconstruction of artist paintings,* Journal of Electronic Imaging **20** (2011), 10.1117/1.3533329.

[23] J. A. Paterson, D. Claus, and A. W. Fitzgibbon, *BRDF and geometry capture from extended inhomogeneous samples using flash photography,* Computer Graphics Forum **24**, 383 (2005).

[24] J. Wang, S. Zhao, X. Tong, J. Snyder, and B. Guo, *Modeling anisotropic surface reflectance with example-based microfacet synthesis,* ACM Transactions on Graphics **27**, 1 (2008).

[25] Y. Dong, J. Wang, X. Tong, J. Snyder, Y. Lan, M. Ben-Ezra, and B. Guo, *Manifold bootstrapping for SVBRDF capture,* ACM Transactions on Graphics **29** (2010), 10.1145/1778765.1778835.

[26] M. Holroyd, J. Lawrence, and T. Zickler, *A coaxial optical scanner for synchronous acquisition of 3D geometry and surface reflectance,* ACM Transactions on Graphics **29** (2010), 10.1145/1833351.1778836.

[27] A. Gardner, C. Tchou, T. Hawkins, and P. Debevec, *Linear light source reflectometry,* ACM Transactions on Graphics **22**, 749 (2003).

[28] P. Ren, J. Wang, J. Snyder, X. Tong, and B. Guo, *Pocket reflectometry,* ACM Transactions on Graphics **30** (2011), 10.1145/2010324.1964940.

[29] G. Chen, Y. Dong, P. Peers, J. Zhang, and X. Tong, *Reflectance scanning: Estimating Shading Frame and BRDF with Generalized Linear Light Sources,* ACM Transactions on Graphics **33** (2014), 10.1145/2601097.2601180.

[30] M. Aittala, T. Weyrich, and J. Lehtinen, *Practical SVBRDF capture in the frequency domain,* ACM Transactions on Graphics **32** (2013), 10.1145/2461912.2461978.

[31] A. Ghosh, T. Chen, P. Peers, C. a. Wilson, and P. Debevec, *Estimating Specular Roughness and Anisotropy from Second Order Spherical Gradient Illumination,* Computer Graphics Forum **28**, 1161 (2009).

[32] Fogra Research Insitute for Media Technologies, *ProcessStandard Digital Handbook*, Tech. Rep. (Aschheim (Munich), Germany, 2018).

[33] K. J. Dana, B. van Ginneken, S. K. Nayar, and J. J. Koenderink, *Reflectance and Texture of Real-World Surfaces,* ACM Transactions on Graphics **18**, 1 (1999).

[34] W. Matusik, B. Ajdin, J. Gu, J. Lawrence, H. P. A. Lensch, F. Pellacini, and

S. Rusinkiewicz, *Printing spatially-varying reflectance,* ACM Transactions on Graphics **28**, 1 (2009).

[35] Y. Lan, Y. Dong, F. Pellacini, and X. Tong, *Bi-scale appearance fabrication,* ACM Transactions on Graphics **32** (2013), 10.1145/2461912.2461989.

[36] T. Baar, S. Samadzadegan, H. Brettel, P. Urban, and M. V. Ortiz Segovia, *Printing gloss effects in a 2.5D system,* in *Electronic Imaging: Measuring, Modeling, and Reproducing Material Appearance*, edited by M. V. Ortiz Segovia, P. Urban, and J. P. Allebach (2014).

[37] T. Baar, H. Brettel, and M. V. Ortiz Segovia, *Towards gloss control in fine art reproduction,* in *Electronic Imaging: Measuring, Modeling and Reproducing Material Appearance*, edited by M. V. Ortiz Segovia, P. Urban, and F. H. Imai (SPIE-IST, 2015).

[38] S. Samadzadegan, T. Baar, P. Urban, M. V. Ortiz Segovia, and J. Blahová, *Controlling colour-printed gloss by varnish-halftones,* in *Electronic Imaging*, Vol. 9398, edited by M. V. Ortiz Segovia, P. Urban, and F. H. Imai (2015).

[39] W. S. Elkhuizen, B. A. J. Lenseigne, T. Baar, W. Verhofstad, E. Tempelman, J. M. P. Geraedts, and J. Dik, *Reproducing oil paint gloss in print for the purpose of creating reproductions of Old Masters,* in *Electronic Imaging: Measuring, Modeling and Reproducing Material Appearance*, Vol. 31, edited by M. V. Ortiz Segovia, P. Urban, and F. H. Imai (2015).

[40] F. Blais, J. Taylor, L. Cournoyer, M. Picard, L. Borgeat, G. Godin, J.-A. Beraldin, M. Rioux, and C. Lahanier, *Ultra high-resolution 3D laser color imaging of paintings: the 'Mona Lisa' by Leonardo da Vinci,* in *7th International Conference on Lasers in the Conservation of Artworks*, edited by M. Castillejo, P. Moreno, M. Oujja, R. Radvan, and J. Ruiz (National Research Council Canada, Madrid, Spain, 2007) pp. 1–8.

[41] Arius 3D, *Laser-based optical scanning systems for three-dimensional digitization of art,* (2017), (Accessed: 2019-05-25).

[42] Factum Arte, *Lucida: Discovering an artwork through its surface*, Tech. Rep. (Factum Foundation, Madrid, Spain, 2016).

[43] D. Akça, A. Grün, B. Breuckmann, and C. Lahanier, *High Definition 3D-Scanning of Arts Objects and Paintings,* in *Optical 3-D Measurement Techniques VIII*, Vol. II, edited by A. Gruen and H. Kahmen (Zurich, Switzerland, 2007) pp. 50–58.

[44] B. Breuckmann, *3-Dimensional Digital Fingerprint of Paintings,* in *19th European Signal Processing Conference* (IEEE, Barcelona, Spain, 2011) pp. 1249–1253.

[45] M. Karaszewski, M. Adamczyk, R. Sitnik, J. Michoński, W. Załuski, E. Bunsch, and P. P. Bolewicki, *Automated full-3D digitization system for documentation of paintings,* in *Optics for Arts, Architecture, and Archaeology IV*, Vol. 8790, edited by L. Pezzati and P. Targowski (Munich, Germany, 2013) pp. 1–11.

[46] Cultural Heritage Imaging, *Photogrammetry,* (Accessed: 2019-05-25).

[47] W. S. Elkhuizen, T. T. W. Essers, B. Lenseigne, C. Weijkamp, Y. Song, S. C. Pont, J. M. P. Geraedts, and J. Dik, *Reproduction of Gloss, Color and Relief of Paintings using 3D Scanning and 3D Printing,* Eurographics workshop on Graphics and Cultural Heritage , 1 (2017).

[48] Océ Technologies BV - a Canon Company, *Project Eiger Elevated printing,* (), (Accessed: 2019-05-25).

[49] Verus Art, *Verus Art textured reproductions,* (2017), (Accessed: 2019-05-25).

[50] Stratasys, *Company website,* (Accessed: 2019-05-25).

[51] P. Sitthi-Amorn, J. E. Ramos, Y. Wangy, J. Kwan, J. Lan, W. Wang, and W. Matusik, *MultiFab: A Machine Vision Assisted Platform for Multi-material 3D Printing,* ACM Transactions on Graphics **34** (2015), 10.1145/2766962.

[52] A. Brunton, C. Ates Arikan, and P. Urban, *Pushing the Limits of 3D Color Printing,* ACM Transactions on Graphics **35**, 1 (2015).

[53] V. Babaei, K. Vidimče, M. Foshey, A. Kaspar, P. Didyk, and W. Matusik, *Color contoning for 3D printing,* ACM Transactions on Graphics **36**, 1 (2017).

[54] O. Elek, D. Sumin, R. Zhang, T. Weyrich, K. Myszkowski, B. Bickel, A. Wilkie, and J. Křivánek, *Scattering-aware Texture Reproduction for 3D Printing,* ACM Transactions on Graphics **36** (2017), 10.1145/3130800.3130890.

[55] W. S. Elkhuizen, Z. E. Doubrosvki, N. Van Apeldoorn, T. T. Essers, and J. M. Geraedts, *Digital manufacturing of fine art reproductions for appearance: current state and looking ahead,* in *International Conference on Innovation in Art Research and Technology* (Parma, Italy, 2018).

[56] D. Zalewski, *The factory of fakes - how a workshop uses digital technology to craft perfect copies of threatened art,* The New Yorker , 66 (2016).

[57] Van Gogh Museum, *Van Gogh Museum Edition Collection,* (Accessed: 2017-10-13).

[58] ISO, *ISO 11664-2 Colorimetry - Part 2: CIE standard illuminants,* (2007).

[59] S. Michalski, *Agent of Deterioration: Light, Ultraviolet and Infrared*, Tech. Rep. (Canadian Conservation Institute, Ottowa, 2016).

[60] W. S. Elkhuizen, T. T. W. Essers, Y. Song, S. C. Pont, J. M. P. Geraedts, and J. Dik, *Gloss Calibration and Gloss Gamut Mapping for Material Appearance Reproduction of Paintings,* in *Eurographics Workshop on Graphics and Cultural Heritage* (2018).

[61] Mauritshuis, *The Girl in the Spotlight - Scientific Examination of the 'Girl with a Pearl Earring' (c.1665) by Johannes Vermeer,* (2018), (Accessed: 2019-01-23).

[62] GOM, *Atos Compact Scan,* (2018), (Accessed: 2018-09-27).

[63] Océ Technologies BV - a Canon Company, *Company website,* (), (Accessed: 2019-05-25).

[64] J.-Y. Bouguet, *Camera Calibration Toolbox for Matlab,* (2013).

[65] S. A. Shafer, *Using Color to Separate Reflection Components*, Tech. Rep. (Uni-

versity of Rochester, Rochester, New York, 1984).

[66] J. A. Ferwerda, F. Pellacini, and D. P. Greenberg, *A psychophysically-based model of surface gloss perception,* in *Human Vision and Electronic Imaging*, Vol. 4299 (2001) pp. 291–301.

[67] R. W. Fleming, R. O. Dror, and E. H. Adelson, *Real-world illumination and the perception of surface reflectance properties.* Journal of vision **3**, 347 (2003).

[68] E. Hecht, *Optics*, 4th ed. (Addison-Wesley, San Francisco, 2002).

[69] E. R. de la Rie, J. K. Delaney, K. M. Morales, C. a. Maines, and L.-P. Sung, *Modification of Surface Roughness by Various Varnishes and Effect on Light Reflection,* Studies in Conservation **55**, 134 (2010).

[70] G. J. Klinker, S. A. Shafer, and T. Kanade, *Using a Color Reflection Model to Separate Highlights from Object Color,* in *Prox. ICCV* (IEEE, 1987) pp. 145–150.

[71] P. Pérez, M. Gangnet, and A. Blake, *Poisson image editing,* in *ACM SIGGRAPH* (ACM Press, New York, New York, USA, 2003) pp. 313–318.

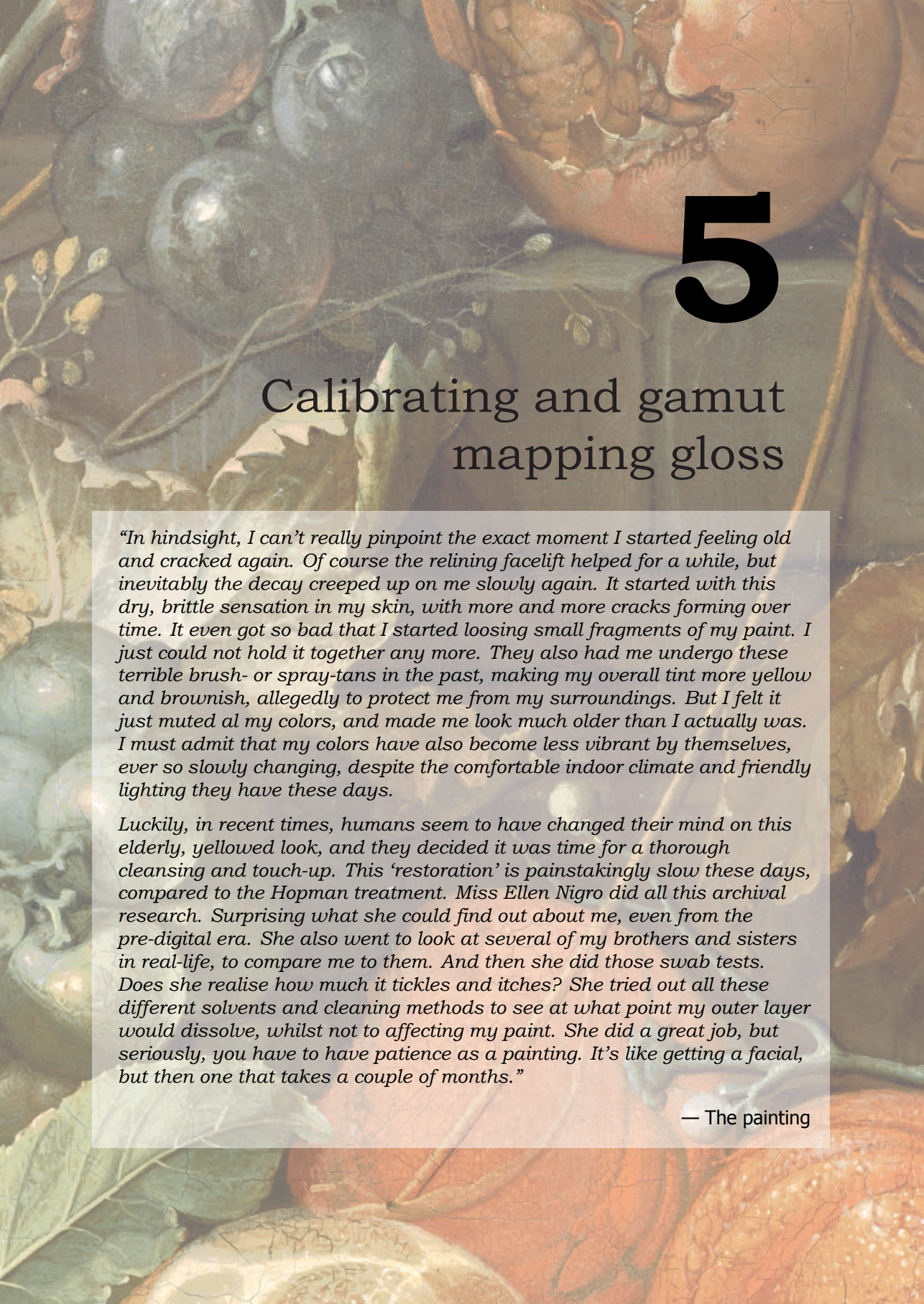

5

Calibrating and gamut mapping gloss

"In hindsight, I can't really pinpoint the exact moment I started feeling old and cracked again. Of course the relining facelift helped for a while, but inevitably the decay creeped up on me slowly again. It started with this dry, brittle sensation in my skin, with more and more cracks forming over time. It even got so bad that I started loosing small fragments of my paint. I just could not hold it together any more. They also had me undergo these terrible brush- or spray-tans in the past, making my overall tint more yellow and brownish, allegedly to protect me from my surroundings. But I felt it just muted al my colors, and made me look much older than I actually was. I must admit that my colors have also become less vibrant by themselves, ever so slowly changing, despite the comfortable indoor climate and friendly lighting they have these days.

Luckily, in recent times, humans seem to have changed their mind on this elderly, yellowed look, and they decided it was time for a thorough cleansing and touch-up. This 'restoration' is painstakingly slow these days, compared to the Hopman treatment. Miss Ellen Nigro did all this archival research. Surprising what she could find out about me, even from the pre-digital era. She also went to look at several of my brothers and sisters in real-life, to compare me to them. And then she did those swab tests. Does she realise how much it tickles and itches? She tried out all these different solvents and cleaning methods to see at what point my outer layer would dissolve, whilst not to affecting my paint. She did a great job, but seriously, you have to have patience as a painting. It's like getting a facial, but then one that takes a couple of months."

— The painting

Abstract

Being able to link captured material characteristics and fabricable material appearance attributes is important for creating life-like reproductions. In this paper we propose a method for gloss calibration, and an approach for gloss gamut mapping, as part of an integrated approach for color, topography and gloss reproduction. For gloss calibration, gloss calibration targets were printed in the primary printing colors (CMYK and White), with uniform gloss in equal distant gloss levels. These targets were scanned using the proposed gloss scanner. To create the gloss gamut map, a monotonic curve was fitted to the mean gloss scan values at different gloss levels. Analysis of fitted curves indicated that the gloss mapping is independent of the diffuse colors. As a case study, the painting 'Fruit Still Life' by Cornelis de Heem was scanned, and the measured gloss was mapped to printable gloss levels using the relation described by the fitted curve. The printed result shows good correspondence to the painting's appearance, with clearly distinguishable gloss features for the in-gamut glass values.

This chapter was published as: **W.S. Elkhuizen**, T.T.W. Essers, Y. Song, S.C. Pont, J.M.P. Geraedts, J. Dik, *Gloss Calibration and Gloss Gamut Mapping for Material Appearance Reproduction of Painting*, In proceedings of Eurographics Workshop on Graphics and Cultural Heritage, (2018).

5.1. Introduction

The appearance of a painting is determined by various characteristics of the surface of the painting. A poster showing the depiction presented in a painting will not easily be mistaken for the original painting. One of the reasons for this is that a poster is a flat color print and lacks the subtle height variations of a painting's surface as well as variations in gloss and translucency of the paint layers [1]. If these aspects can be captured and replicated, a more life-like reproduction might be created. Reproducing the appearance of objects and materials is not new. Artifacts have been (partly) copied since ancient times. In most cases, artifacts and material appearance reproductions are either handmade by highly skilled craftsmen or mass-produced, where a limited set of appearances is fabricated. Advances in computer graphics have made it possible to accurately capture and digitally render material appearance. Meanwhile, the development of multi-material 3D printing in the past decades also made it possible to reproduce the captured information physically. For this, a connection needs to be made between the captured information and the fabrication of appearance. However, extensive literature study did not reveal any methods for gloss calibration and gamut mapping (independent of diffuse color mapping). Building on previous research [2], this paper presents a method for calibrating the captured information for gloss reproduction.

5.2. Related work

(2D) color reproduction is already largely standardized using color calibration targets, and procedures where input and output devices can be connected through a device independent 'Profile Connection Space' [3]. In most cases where a printing system has a more limited color space than the imaging device, gamut mapping needs to be applied where, according to a rendering intent, the input colors are mapped to the range of possible printable colors [4]. However, a (standardized) calibration and gamut mapping approach for gloss does not exist (yet). Glossmeters are often used instruments in the printing industry, to take spot measurements of specular reflection gloss of a surface [5]. Glossmeters use a polished, black glass plate as a standard reference, and gloss is expressed in Gloss Units (GU), which provide a relative measurement to the reference [5]. Although these can be used to verify gloss uniformity, their applications in capturing spatially varying gloss are limited due to the data capturing speed and the need for surface contact. Various methods have been developed to capture spatially-varying reflectance for globally flat surfaces (e.g. [6–9]). Most have been developed for the purpose of computer rendering. Therefore the gloss levels and the printable color spectrum are not associated. Several approaches have been proposed for the fabrication of spatially-varying reflectance. Matusik et al. [10] fabricated isotropic material appearances (2D printing) using a linear combination of multiple printer inks. A distance metric, based on rendered spheres of the BRDFs, was used to map the target BRDFs (input) to the print BRDFs. Lan *et al.* [11] were able to fabricate anisotropic BRDFs by combining a 3D printed micro-structure, with a (2D) color printing on top. They measured their printer BRDFs using linear light source reflectometry [7]. Isotropic

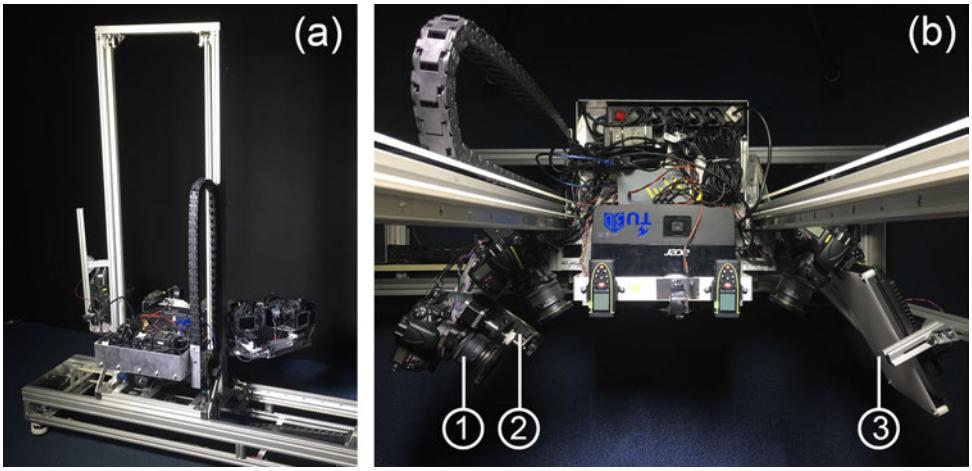

Figure 5.1: Scanning system showing (a) the frame with the platform holding the two scanning modules and (b) a top view of the platform where the gloss scanning module consists of (1) a camera, with (2) a rotating polarization filter and (3) the LED array with a diffuser.

ink BRDFs and the height field were then iteratively optimized, taking shadowing and shading effects into account. Baar *et al.* [12] and Samadzadegan *et al.* [13] also suggested different approaches to fabricating spatially-varying gloss, although not in conjunction with gloss gamut mapping.

5.3. Scanning and fabrication

The scanning system comprises of a frame with two scanning modules, the 3D scanning module (described in [1]) and the gloss scanning module (described in [2]) (see Figure 5.1). These two modules are able to capture color, topography and gloss variations of a globally-flat surface. Components used for gloss scanning are: a camera with a rotating polarization filter, and an LED array with a diffuser, mounted at opposing mirror angles (see Figure 5.1(b)). The gloss scanning module captures spatially-varying gloss by imaging the surface under Brewster's angle, which is defined by the refraction index of the material. The difference between a capture with reflections (parallel polarization) and without reflections (cross-polarization) provides a measure for the gloss variation. The measurement is corrected for illumination non-uniformity, off-center specular measurements and shadowing, which is caused by local surface normal variations. An adapted version of Océ Technologies "Elevated Printing" technology [14] is used for the fabrication of the material appearances which utilizes UV-curable inks. First, the 3D full color relief is printed with CMYK and White (CMYKW). Then, a transparent ink is used to create spatially-varying gloss through different amount of half-toned varnish layers at each position of the 3D full color relief [2].

5.4. Gloss calibration

For the purpose of gloss calibration, flat targets in the primary printer colors (CMYKW) were fabricated with increasing levels of uniform gloss. The targets were printed using the Elevated Printing Technology. Six equal-distant levels were created (11 for Cyan), based on 60° gloss measurements of a set of test patches using a BYK micro-tri-glossmeter [15]. Figure 5.2 shows four of the 35 targets. The input and output gloss values (measured with the glossmeter), are plotted in Figure 5.3. The figure shows the average (left axis) and standard deviation (right axis) of the gloss values (60° gloss, in GU) of 5 measurements across the surface, per color. As the deviation of printed gloss values is small regarding the input values as well as the standard deviation (< 1.9), the targets will be treated as uniform and equal-distant for all colors. All gloss calibration targets were scanned and an area of 7250x3000 pixels (approx. 18x7.5cm) was cropped from all scans, approximating the full width and 4/5 of the scan height of a single capture (excluding a region with the target reference information). A 1-term exponential, monotonic function ($f(x) = ae^{bx} + c$) was fitted to means of the scanned gloss values in the cropped areas (to all colors individually and combined). The exponential function, provided the best prediction of the variance, with the lowest residuals (also see results in Section 5.6). The fitted function (averaging all colors) was used to gamut map the gloss values of a painting scan to the printable glosslevels.

A one-to-one gloss gamut mapping strategy was applied for in-gamut glosslevels, while clipping gloss values to the minimum and maximum value measured on the calibration cards (analogous to a *colorimetric* rendering intent in color printing). With this approach the in-gamut gloss contrast was preserved, while details were

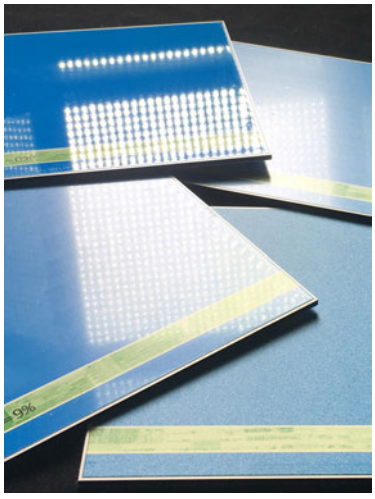

Figure 5.2: Gloss calibration targets (cyan). Note the varying sharpness of the reflections.

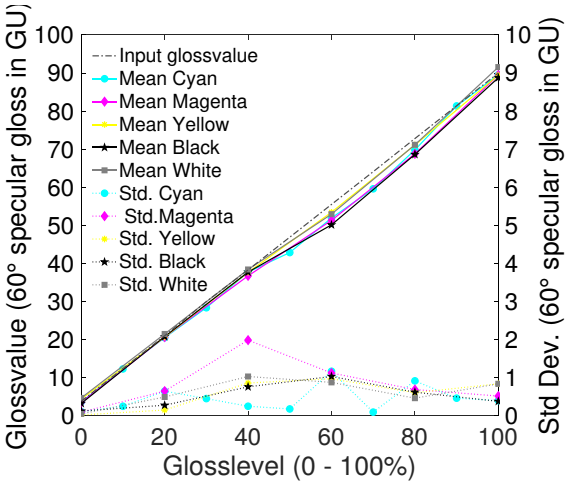

Figure 5.3: 60° specular gloss (in GU) of calibration targets, showing the mean (left axis) and standard deviation (right axis) of 5 points across the surface, per color.

lost for out-of-gamut gloss. This approach was chosen over an overall rescaling of the gloss gamut (analogous to a *perceptual* rendering intent), to be able to evaluate the ability to match the gloss in an absolute sense and reproduce local gloss contrast (for in-gamut gloss).

Figure 5.4: Painting with partially removed varnish in front of the scanner.

5.5. Case Study

Our reproduction approach (incl. gloss gamut mapping) is applied to a painting named *Fruit Still Life* by Cornelis de Heem (c.1670), which is in the collection of the Maurithuis, The Netherlands. The painting was undergoing restoration, where the varnish was already partially removed, providing two distinct regions: One glossy, varnished region, and a matte, unvarnished region, the latter showing some subtle gloss variations (see Figure 5.4 and 5.9). Although not esthetically appealing, the high and low gloss regions provided a good test case for mapping gloss levels of the painting.

5.6. Results

Figure 5.5 shows the means and standard deviations of the cyan gloss targets for 11 equal distant gloss levels, as well as the fitted exponential function. The noise on the gloss measurement might be explained by that the printing resolution (450dpi $\approx$ 56µm) is lower than scanning resolution ($\pm$25µm), whereby the individual 'dots of ink' influence the gloss measurement. The noise is highest for matte targets, which have more dots placed side-by-side, versus more smooth high gloss print.

In figure 5.6 the means of all colors are plotted at 6 equal-distant gloss levels, with their respective fitted curves. Figure 5.7 shows the surface plot of cyan gloss targets for 0%, 20%, 60% and 100% gloss. The highest gloss levels show some non-random variation across the surface (cloudy appearance, similar for all colors), which might be created by the lamp diffuser (shown in Figure 5.1, the diffusion might be non-uniform).

The histogram of the gloss values measured on the painting, is plotted in Figure 5.8. A distinct division is visible between the part where varnish is removed (highest peak) and the part that still has varnish (lower peak). It also shows the range of the printable gloss (blue), and the values clipped to the minimal and max-

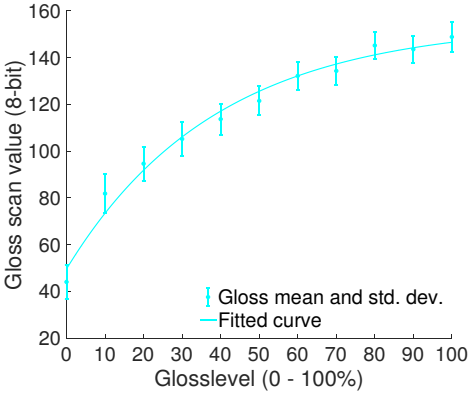

Figure 5.5: Mean and std. dev. of sample area (7250x3000 pixels, approximating a single capture tile) for glosslevels 0-100% on cyan calibration targets (11 equal-distant steps), with fitted curve.

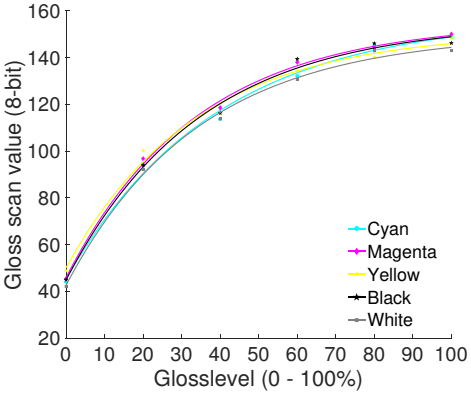

Figure 5.6: Mean of sample area (7250x3000 pixels, approximating a single capture tile) for glosslevels 0-100% on all calibration targets (six equal-distant steps, limiting printing cost and scanning time), with fitted curves per color.

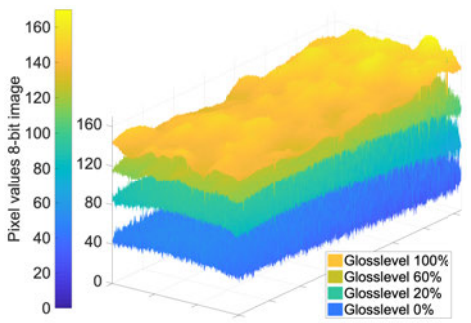

Figure 5.7: Gloss scan surface plots of 0%, 20%, 60% and 100% gloss (8-bit pixel value), of cyan calibration targets, sampling every tenth pixel.

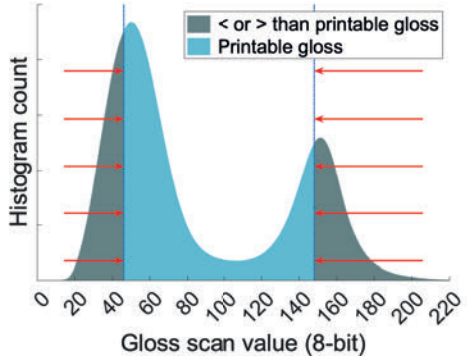

Figure 5.8: Gloss scan values histogram of painting, showing values in- and outside the printable gloss range, which are clipped (arrows) to printable gloss range.

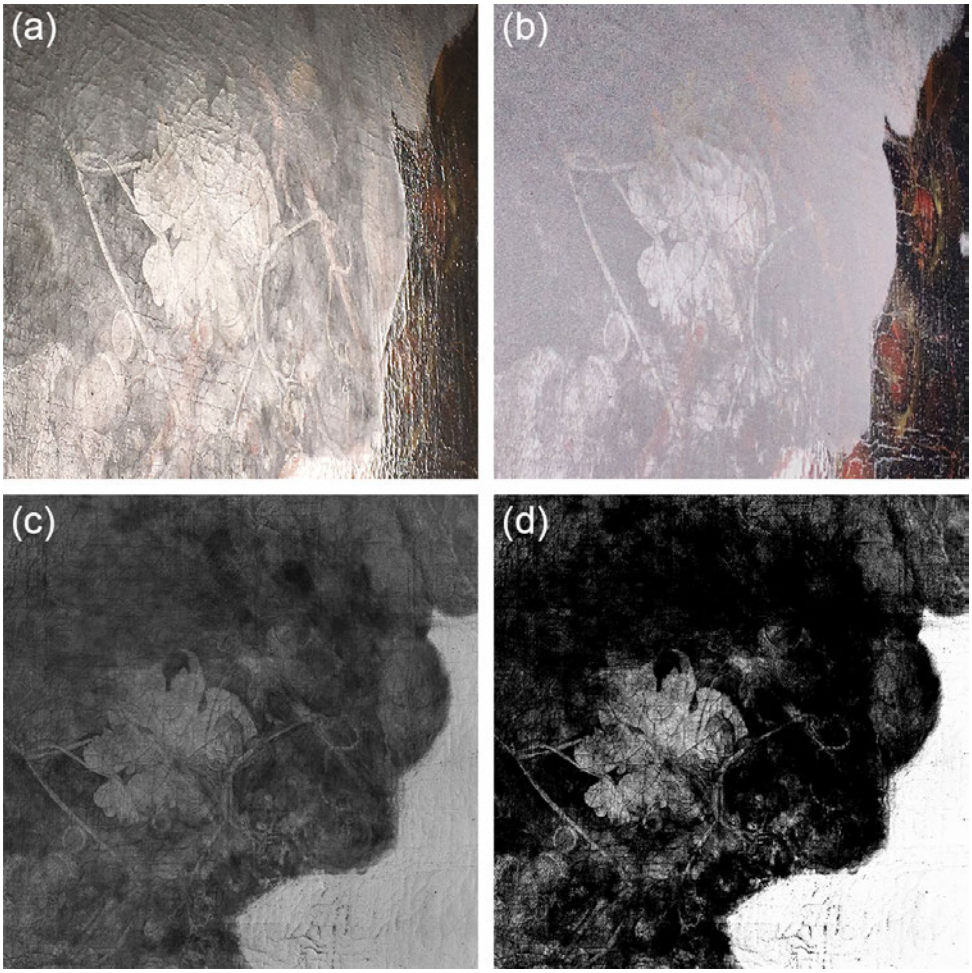

Figure 5.9: Detail of reproduced painting, which was undergoing restoration, with varnish layer(s) still present in bottom right corner, showing (a) the painting, (b) the 3D printed result including color, relief and gloss variations (c) gloss scanning result, and (d) gloss values mapped to printable gloss. Figure (a) and (b) are photographed under similar illumination and viewing angles to show the reflection of the surface.

imum printed gloss (dark green).

Figure 5.9(a) depicts a detail of the painting, (b) a detail of the 3D reproduction including color, relief and gloss variations, (c) the gloss scanning result, (d) the gloss scanning result mapped to printable gloss levels. Figure 5.9(a) and (b) were photographed under an angle, to be able to visualize the reflections on the surfaces. Clipping of gloss values to the minimal and maximum printable gloss did not seem to lead to obvious banding (a clear boundary at clipping edge) in (b) the printed result or (d) the gloss map.

5.7. Discussion and conclusion

The measurement of the calibration targets shows that gloss levels can be distinguished across the surface. However, the gloss measurements showed some systematic variations, which were similar across all colors. Part of the systematic variation seems to be caused by the non-uniformness of the LED diffuser, which causes 'cloudy' patterns. This pattern is more obvious in measuring the high gloss target than the lower targets, as the high gloss targets basically acts as a mirror and the lower gloss target diffuses lights. High frequency noise appears in all measurements, and might be explained by the printing resolution being lower than the scanning resolution, whereby individual print dots may influence the measurements. Furthermore, the planarity of the gloss measurement remains to be investigated. In this paper, only one gloss gamut mapping strategy has been implemented. The downside of the absolute mapping approach is that out-of-gamut details are lost and there is a potential for banding (a clear boundary at clip edge), although this was not obvious in the case study. More research is needed to determine perceptually relevant gloss mapping strategies to, for instance, using the work of Ferwerda *et al.* [16] or Obein *et al.* [17] on perceptually uniform gloss scaling, as a starting point. Moreover, the current approach implements a direct link between the gloss input device (scanner) and gloss output device (printer). Color gamut mapping links profiles through a device independent 'profile connection space'. The advantage of this is that the calibration can be done for the scanning and printing device separately, which makes it possible link any input device to any output device. An equivalent for gloss gamut mapping, has yet to be determined.

In this paper an approach is presented for the gloss calibration and gamut mapping, by using printed gloss targets to associate printable gloss (output) to scan data (input). Results indicate that the gloss measurement approach is independent of the diffuse color. The mean gloss values were plotted and an exponential function was fitted to the data. The painting *Fruit Still Life* by C. de Heem was scanned, exhibiting high and low gloss regions, due to partial varnish removal. The scanned gloss was mapped to the printable gloss using the function fitted to gloss calibration data and clipping to the minimum and maximum printable glosslevel (analogous to a colorimetric rendering intent). The mapped and printed result shows that the approach is able to reproduce the gloss details in the in-gamut range and does not show obvious banding effects, due to clipping. Limitations of the gloss calibration approach are also identified in terms of gloss measurement uniformity, gloss mapping strategy and gloss printing, which highlight the future work of the authors.

References

[1] W. S. Elkhuizen, T. Zaman, W. Verhofstad, P. P. Jonker, J. Dik, and J. M. P. Geraedts, *Topographical scanning and reproduction of near-planar surfaces of paintings,* in *Electronic Imaging: Measuring, Modeling and Reproducing Material Appearance*, Vol. 9018, edited by M. V. Ortiz Segovia, P. Urban, and J. P. Allebach (SPIE-IST, 2014).

[2] W. S. Elkhuizen, T. T. W. Essers, B. Lenseigne, C. Weijkamp, Y. Song, S. C.

Pont, J. M. P. Geraedts, and J. Dik, *Reproduction of Gloss, Color and Relief of Paintings using 3D Scanning and 3D Printing,* Eurographics workshop on Graphics and Cultural Heritage , 1 (2017).

[3] International Color Consortium, *ICC.1:2010 - Image technology colour management - Architecture, profile format, and data structure*, Tech. Rep. (International Color Consortium, 2010).

[4] R. S. Berns, *Principles of Color Technology*, 3rd ed. (John Wiley & Sons, New York, New York, USA, 2000).

[5] ISO, *ISO2813:2014 - Paints and varnishes - Determination of gloss value at 20, 60 and 85 degree,* (2014).

[6] J. Padfield, D. Saunders, and T. Malzbender, *Polynomial Texture Mapping : a New Tool for Examining the Surface of Paintings,* in *ICOM Committee for Conservation, 14th Triennial Meeting*, Vol. 1 (2005) pp. 504–510.

[7] A. Gardner, C. Tchou, T. Hawkins, and P. Debevec, *Linear light source reflectometry,* ACM Transactions on Graphics **22**, 749 (2003).

[8] P. Ren, J. Wang, J. Snyder, X. Tong, and B. Guo, *Pocket reflectometry,* ACM Transactions on Graphics **30** (2011), 10.1145/2010324.1964940.

[9] M. Aittala, T. Weyrich, and J. Lehtinen, *Practical SVBRDF capture in the frequency domain,* ACM Transactions on Graphics **32** (2013), 10.1145/2461912.2461978.

[10] W. Matusik, B. Ajdin, J. Gu, J. Lawrence, H. P. A. Lensch, F. Pellacini, and S. Rusinkiewicz, *Printing spatially-varying reflectance,* ACM Transactions on Graphics **28**, 1 (2009).

[11] Y. Lan, Y. Dong, F. Pellacini, and X. Tong, *Bi-scale appearance fabrication,* ACM Transactions on Graphics **32** (2013), 10.1145/2461912.2461989.

[12] T. Baar, S. Samadzadegan, H. Brettel, P. Urban, and M. V. Ortiz Segovia, *Printing gloss effects in a 2.5D system,* in *Electronic Imaging: Measuring, Modeling, and Reproducing Material Appearance*, edited by M. V. Ortiz Segovia, P. Urban, and J. P. Allebach (2014).

[13] S. Samadzadegan, T. Baar, P. Urban, M. V. Ortiz Segovia, and J. Blahová, *Controlling colour-printed gloss by varnish-halftones,* in *Electronic Imaging*, Vol. 9398, edited by M. V. Ortiz Segovia, P. Urban, and F. H. Imai (2015).

[14] Océ Technologies BV - a Canon Company, *Project Eiger Elevated printing,* (Accessed: 2019-05-25).

[15] BYK Additives and Instruments, *Gloss Meters,* (Accessed: 2019-05-25).

[16] J. A. Ferwerda, F. Pellacini, and D. P. Greenberg, *A psychophysically-based model of surface gloss perception,* in *Human Vision and Electronic Imaging*, Vol. 4299 (2001) pp. 291–301.

[17] G. Obein, K. Knoblauch, and F. Viénot, *Difference scaling of gloss: Nonlinearity, binocularity, and constancy,* Journal of Vision **4**, 711 (2004).

6

Comparing three 3D scanning techniques for paintings

"Midway through this facelift, literally halfway through removing those ugly, yellow layers, they decided to do a photo shoot of me. Even a special kind of photoshoot. The researchers that carried it out, said they would be able to capture all my intricate details; the color of my skin, the shape of my skin, and even the variation in glossiness of my skin. I bet those images would look weird, with half my skin being matte and half being glossy from the varnish removal. I doubt those images are very flattering. But still, I do feel grateful that they picked me over any of the other paintings. It's not often I get to undergo these special procedures. I still feel privileged.

The scanning itself was a bit of a weird experience, my complete surface meticulously recorded, in small areas, one after the other. Those lights they have on the scanner, kept turning on and off. Did those researchers not realise how annoying that is, and that I need my beauty sleep during the day? And the amount of pictures they made! Those cameras just kept on clicking. I don't think I have ever been photographed that much in my entire life."

— The painting

Abstract

A 17th-century canvas painting is usually comprised of varnish and (translucent) paint layers on a substrate. A viewer's perception of a work of art can be affected by changes in and damages to these layers. Crack formation in the multi-layered stratigraphy of the painting is visible in the surface topology. Furthermore, the impact of mechanical abrasion, (photo)chemical processes (such as soap formation) and treatments can affect the topography of the surface and thereby its appearance. New technological advancements in non-invasive imaging allow for the documentation and visualization of a painting's 3D shape across larger segments or even the complete surface. In this manuscript we compare three 3D scanning techniques, which have been used to capture the surface topology of 'Girl with a Pearl Earring' by Johannes Vermeer (c. 1665): a painting in the collection of the Mauritshuis, The Hague. These three techniques are: Multi-scale optical coherence tomography, 3D scanning based on fringe-encoded stereo imaging (at two resolutions), and 3D digital microscopy. Additionally scans were made of a reference target and compared to 3D data obtained with White-light confocal profilometry. The 3D data sets were aligned using a scale-invariant template matching algorithm, and compared on their ability to visualize topographical details of interest. Also the merits and limitations for the individual imaging techniques are discussed in-depth. We find that the 3D microscopy and the multi-scale optical coherence tomography offer the highest measurement accuracy and precision which is maximally three times more accurate than the 3D scanning based on fringe-encoded stereo imaging. However, the small field-of-view of these techniques, makes these techniques relatively slow, and thereby less viable solutions for capturing larger (areas of) paintings. For 'Girl with a Pearl Earring' we find that the 3D data provides an unparalleled insight into the surface features of this painting, specifically related to 'moating' around impasto, the effects of paint consolidation in earlier restoration campaigns and aging, through visualisation of the crack pattern. Furthermore, the data sets provide a starting point for future documentation and monitoring of the surface topology changes over time. These scans were carried out as part of the research project 'The Girl in the Spotlight'.

This chapter is provisionally accepted as: **W.S. Elkhuizen**, T.W.J. Callewaert, E. Leonhardt, Y. Song, S.C. Pont, J.M.P. Geraedts, and J. Dik, *Comparison of three 3D scanning techniques for paintings, as applied to Vermeer's 'Girl with a Pearl Earring'*, Heritage Science.

6.1. Introduction

6.1.1. The three-dimensional landscape of paintings

Paintings are generally considered in terms of their (2D) depiction, but the physical artwork also has a third dimension. The substrate is rarely completely flat, and subsequent paint and varnish layers also influence the surface topography. This effect can be intentional – using the paint to create a 3D effect – or the consequence of drying, hardening, or degradation. Artists, including Vermeer, deliberately created 3D textural effects on the surface. For instance, they used *impasto* to create additional reflections for highlights, or used 3D effects to emphasize the textural appearance of the material they were depicting. Alternatively, three-dimensional brushstrokes can be the consequence of a fast-paced, expressive painting style.

The topography of a painting can change under the influence of internal and external factors. Natural aging and (photo)chemical changes (e.g. the formation of metal soaps [1]) that occur within the different layers can result in the formation of cracks, protrusions and/or changes in gloss. The layers respond to environmental influences: for example, an increase or decrease in temperature or relative humidity can cause the support to expand or contract, resulting in cracking or deformations. Conservation treatments can also cause changes in topography. Linings, especially wax-resin linings that employ heat and pressure, can flatten the paint. Efforts to locally soften and flatten raised cracks using heat and/or pressure can also cause irreversible changes to the 3D surface structure. Mechanical damages during handling, transport or by accident can result in cracked, tenting, or flaking paint. A painting conservator is compelled to document and address these issues, but until recently, possibilities to record these changes, also over the long term, have been limited.

6.1.2. Painting documentation

During technical examination(s), it has become general practice to use a wide range of imaging techniques to visualize and document the condition and chemical composition of a painting. Imaging techniques like infrared imaging, visible light photography, X-radiography, ultraviolet (UV) imaging, macro X-ray fluorescence imaging, and hyperspectral imaging all provide information about different modalities of a painting, capturing the spatial variations across its surface ([2, 3]). Topographical variations of the surface — but also gloss and layer stratigraphy — are currently not (well) documented.

Photographs in raking light conditions — commonly made during technical examination(s) — reveal undulations in the surface and visualize features like cracks (see for example Figure 6.1(a)). Although this technique emphasizes the effect of surface topography on its appearance, it is not an exact measurement of the topography. Moreover, the exact lighting conditions and light direction used to create the raking light photography are often not (well) documented, making it difficult to recreate the exact conditions. Another drawback of raking light photography is that the topographical variations can be difficult to interpret in dark regions of a painting. Examination of the paint surface under a 3D digital microscope can reveal

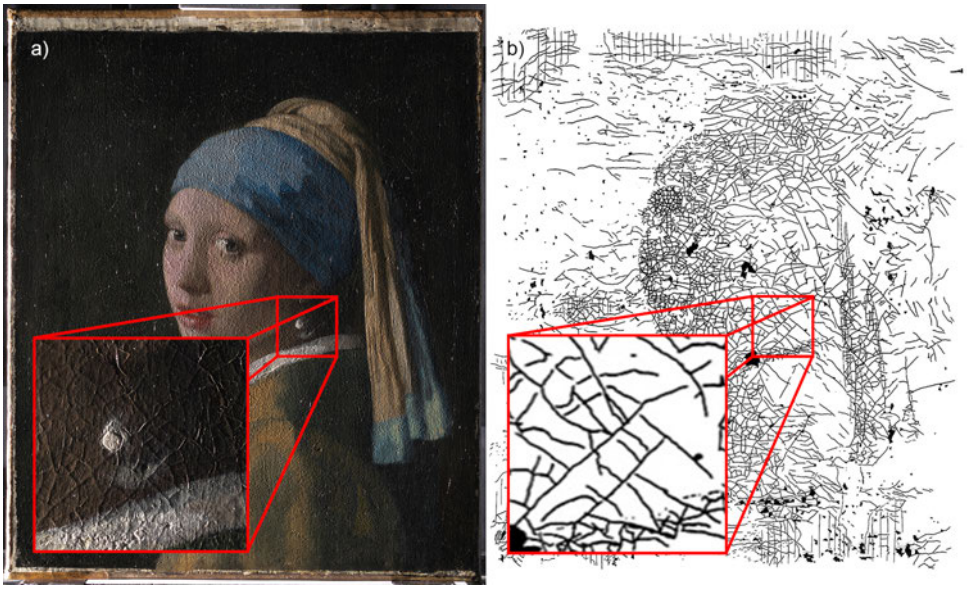

Figure 6.1: Existing documentation visualizing the surface topography of 'Girl with a Pearl Earring' (a) Raking light photography is traditionally used to emphasize the topographical variations of the surface, visualizing cracks and other unevenness of the surface (Courtesy of René Gerritsen Art and Research Photography). (b) The crack pattern of the painting was documented by manually tracing the cracks onto a transparent polyester film, placed on the painting (Courtesy of Jørgen Wadum [4]). The red inserts show an enlargement of the area around the pearl earring.

topographical differences at a microscopic level. However, due to technical and time limitations, documenting the surface topography of a complete painting at this level of detail is not yet a common practice.

In order to evaluate the long-term stability of a painting, it is important to understand and document its 3D topography. A scan of an artwork created before and after a conservation treatment (or of a reconstruction made using historically appropriate materials) can reveal the visual effect of such treatments. These treatments could involve methods that are still practiced (like locally flattening lifting paint with heat), and those (like wax-resin lining) that are seldom used by conservators nowadays. 3D scans made at periodic intervals have the potential to monitor long-term changes that occur in an artwork: for instance, changes that might occur if there is a rapid change in temperature or relative humidity, or as a result of frequent handling or transport. Depending on the frequency of monitoring, this could provide information about the speed and conditions in which these changes can occur.

6.1.3. Reproductions of paintings

Making painted copies of artworks has been practiced since ancient times: from studio assistants copying examples by the workshop master, to the academic tradition of copying as part of formal art education. The advent of photography made it possible to reproduce paintings in print (e.g. in books, posters or postcards). Digital photography has further expanded the possibilities for presenting visual reproductions of artworks to a wider public. Although these techniques are able to produce visually similar appearances, they do not capture the multitude of attributes that determine its appearance, including the surface topography.

Reproductions or facsimiles — which include (one or several) appearance attributes — can offer a wide range of opportunities for interacting with a work of art. Since touching actual artworks is strictly forbidden in most museum settings, 3D prints are a promising way to engage the museum public in the tactile nature of artworks. The use of 3D prints for reproducing works of art is gaining interest, both for the museum visitor, and for scientific and conservation purposes. For example, the 2015 Mauritshuis exhibition *Rembrandt? The Case of Saul and David* displayed a life-size 3D printed reproduction made by Delft University of Technology and Océ Technologies ([5, 6]). Its purpose was to show the original format of Rembrandt's *Saul and David* (ca. 1651-54 and c. 1655-58), which had undergone significant physical changes during its history. Reproduction might also serve a purpose in providing wider access to an artwork that has become too fragile for transport or loan (e.g. [7].)

6.1.4. Case study: 'Girl with a Pearl Earring' by Johannes Vermeer

From archival documentation and research it is known that Johannes Vermeer's *Girl with a Pearl Earring* (c. 1665), from the collection of the Mauritshuis, has undergone various conservation and restoration treatments in its lifetime. Some treatments, along with the degradation effects that can be expected of a seventeenth-century painting, have affected its surface topography [8]. It is at least certain that the painting had larger height variations in its painted surface when it left Johannes Vermeer's studio. He applied small details, like the highlight on the Girl's earring and dots on her clothing, with more *impasto* than the surrounding paint. The painting's topography has been affected by the climatic conditions in which it was stored and displayed in the past, and its conservation history. In 1882, the Antwerp restorer Van der Haeghen lined the canvas support with a starch-based paste. As part of a 1915 or 1922 treatment, restorer De Wild 'regenerated' the varnish by subjecting it to alcohol vapors and copaiba balsam. These treatments, and/or a consolidation treatment with an aqueous adhesive (date unkown), may have caused the starch-based lining to shrink. Although the paint already had some adhesion issues prior to the 1882 lining, the shrinkage may have caused more flaking and cupping of the paint. In 1960, another restorer Traas relined the painting using a wax-resin adhesive, applying heat and pressure. This wax-resin lining flattened some *impasto* details that Vermeer had applied more thickly than the surrounding paint, but ensured that the painting has remained structurally stable.

The conservation history was documented as part of the 1994 restoration campaign, conducted as part of the project *Vermeer Illuminated* [4]. During this restoration, the crack pattern was traced onto a transparent polyester film that was carefully placed on the surface of the painting (see Figure 6.1(b)). This was a way of documenting the surface condition, in addition to raking light photographs. The 2018 technical examination as part of the project *The Girl in the Spotlight* provided a new opportunity to examine Vermeer's *Girl with a Pearl Earring* using traditional examination methods as well as state-of-the-art scientific techniques. High-resolution digital photographs were made of the painting in different lighting conditions, including raking light (see Figure 6.1 (a)). Another important part of this examination was the 3D documentation of the painting's surface using the following means: Multi-scale optical coherence tomography, 3D scanning based on fringe-encoded stereo imaging at two resolutions, and 3D digital microscopy.

In this paper we compare these three imaging technologies as applied to (segments of) the painting *Girl with a Pearl Earring*. Based on the measurement results and measurements of a reference target, we present a comparison of these techniques and their respective implementations. Technological merits and limitations are discussed of each technique, regarding: resolution, flexibility, scalability, scanning range, robustness, and ability to scan (multiple) modalities. The paper has the following structure: first we present the related work regarding studies on craquelure, 3D imaging of paintings, and earlier work on the measurement of paint layer stratigraphy. In the method/experimental section the four scanning systems are described in detail, as well as their calibration and data processing procedures. Next, the results are presented: 3D data of three areas on the painting, and additionally the measurement results of the reference target. Based on these results, we discuss the (potential) use(s) of 3D scanning data in a cultural heritage context with a specific focus on their application for technical documentation and conservation. We then evaluate and compare the capabilities of the scanning techniques and their implementations. Finally, we propose directions for (potential) applications and future work to map entire paintings at high resolution.

6.2. Related Work

Various modalities of paintings can be captured, like color, topography, gloss, transparency/translucency or its layered stratigraphy. This overview focuses primarily on the state-of-the-art regarding the study, documentation and measurement of topographical features, and techniques that measure the stratigraphy of layers in a painting, as topographical information can also be extracted from the latter. We review how crack patterns — or craquelure — have been studied in the past. Literature concerning conservation or restoration treatments of cracks in paintings lies outside the scope of this review. Furthermore, we discuss 3D imaging systems that have been used to measure the three-dimensional surface of paintings. Although we specify the additional modalities that these 3D scanning techniques can capture (like color and gloss), we do not discuss the measurement of these modalities separately. Finally, literature is discussed on the measurement of layer stratigraphy of paintings.

6.2.1. Studying craquelure in paintings

The effect of craquelure on a painting's appearance has long been recognized by scientists and conservators, but surprisingly little focused study has been devoted to its causes and visual effects (as described in [9]). Research by Bucklow [10] has described and classified the types of cracks commonly found on paintings, as well as exploring the pictorial effect of crack patterns and their influence on visual perception [11]. Building on this work, El-Youssef [12] developed a method to classify paintings into four distinct geographical regions (within Europe), based on digitally extracted features of their craquelure. The aim was to link craquelure patterns to the use of different painting materials and techniques as they were practiced in distinctly separated European regions, potentially supporting questions of attributions and authenticity. Schirripa Spagnolo [13] applied automated crack detection for the purpose of digitally removing them, to be able to approximate the original appearance of the artwork.

A limitation for all of these approaches is that they only consider craquelure as a two-dimensional pictorial feature, and not its three-dimensional shape. In fact, topographical data might even be able to inform these type of algorithms, providing an additional modality for more accurate crack detection using 3D data in addition to color information. It might also be used to extend these types of algorithms, by also considering the 3D effects of craquelure: these could (in principle) also be virtually 'restored', providing even more accurate insight into a painting's original appearance.

6.2.2. 3D imaging of paintings

Various approaches for capturing (and reproducing) the fine topographical details of painted surfaces have been demonstrated. They can be classified into three categories, based on their imaging method: using 3D laser triangulation, structured light 3D scanning, and focus variation microscopy. Blais et al. captured the topography of paintings by Renoir [14] and the *Mona Lisa* by Leonardo Da Vinci [15], using a 'white' laser spot (composed of a red, green and blue laser source), and the principle of optical triangulation. Their system is able to reach a lateral resolution of 50 µm and a depth uncertainty (on flat surfaces) of 10 µm. With this approach they simultaneously capture color and shape information of the surface. This scanning principle was later commercialized and this captured data is currently used to print full-color 3D reproductions [16], sampling their scan data at a resolution of 100 µm. To create 3D reproductions with faithful color rendition, an additional (2D) reference photograph is made, whereby the 3D shape information, 3D scanner color data, and 2D color image are combined to create 3D print files [17]. Factum Arte have also developed a laser-based painting scanner [18]. Through alignment with color photographs, the scans are used as input to a hybrid fabrication technique to make a wide range of facsimiles of for instance frescos, (panel) paintings, and manuscripts [19]. Also the Van Gogh Museum has created (limited edition) 3D reproductions of several of their paintings. Information on their website suggests that they used a combination of 2D color imaging, 3D laser scanning, molding and 2D color printing [20]. However, no detailed description or specifications can be found

about their 3D scanning method. Structured light 3D scanning, using a projector combined with either one or two cameras has also been proposed to measure the topography of painted surfaces (e.g. [21–26]). With the continued development of more light-sensitive sensors, and an increasing amount of pixels, these efforts — as applied to paintings — have gradually increased in lateral resolution, from 60 µm to 7 µm. The latter approaches [24–26] use a de-focused projection pattern, whereby the sampling resolution only depends on the camera resolution, rather than the (lower) projector resolution. A third used approach to 3D imaging of a painting's surface is focus variation microscopy. This has been demonstrated for instance to analyse punchmarks — a decorative technique creating patterned indentations on a painting surface — on medieval panel paintings [27]. Another investigation focused on evaluating the 3D microscope's usefulness in supporting cleaning dirt from painting surfaces [28]. Both studies have only used this technique to capture small areas, rather than 3D imaging larger regions or a complete painting.

Besides capturing micro-scale features, studies have been conducted to measure and monitor global shape variations of paintings. For example the work by Del Sette *et al.* [29] focused on monitoring short-term changes occurring due to restoration/conservation interventions (i.e. response to tensioning tests). In this study, reference markers were mounted on or in front of the artefact to be able to align the measurements. Palma *et al.* [30] compared changes in panel shape between two independently acquired 3D scans, made in 2002 and 2015. Using non-rigid transformation to align the two meshes, they were able to distinguish low-frequency deformations of the panel and from the structural changes made in restoration campaigns. Based on their findings they were able to inform the restoration procedure, which aimed to reduce stress in — and prevent further deformation of — the panel. Although these techniques are used in relation to painting conservation treatments, their resolution does not allow for capturing the fine surface details, like craquelure. An overview of the above-mentioned 3D scanning approaches and more details about the specs of these systems can be found in Table 6.1 (see end).

6.2.3. Stratigraphy measurement of painting layers

While there are various approaches directly aimed at measuring the surface topography of paintings, there is another imaging technique that also harnesses this topographical information, namely optical coherence tomography (OCT). OCT is based on generating an image from the interference between a reference beam and the light reflected at the interface(s) of (semi-) transparent layers [31, 32]. Although conventionally OCT is used to image the stratigraphy (layering) of semi-transparent layers, the uppermost boundary also represents the topography of the surface. Its application for imaging the stratigraphy of cultural heritage artifacts was demonstrated by various studies (e.g. [33–37]). To reach sufficient lateral and axial resolution for these applications, the OCT field-of-view is limited to a scanning area of approximately 15 mm × 15 mm. By combining a high resolution spectral domain OCT (SD-OCT) setup — a specific sub-type of OCT using a broadband light source (see [37]) — with automated scanning stages, it is possible to scan much larger areas (as demonstrated in this paper, reaching a scan area of 0.04 m^2).

6.3. Methods/Experimental

Three imaging techniques suitable for the measurement of a painting's topography were used in this study of *Girl with a Pearl Earring*: Multi-scale optical coherence tomography (MS-OCT), 3D scanning using fringe-encoded stereo imaging at two resolutions (hereafter denoted as High-Res and Std-Res 3D scan) and focus variation microscopy (3D Microscopy). White light confocal profilometry (WLCP) was used as a reference instrument, for comparing the height (z) measurements of the other devices on a reference target. Although this technique itself is also suitable and safe for application on a painting, no measurements were made on the case study painting, due to time constraints. More details per device can be found in the following sub-sections. The capabilities of these scanning systems for multi-modal scanning (i.e. simultaneous capture of color, gloss etc.), are summarized in Table 6.2 (see end of Chapter), and the (potential) advantages, for instance in data interpretation, can be found in the discussion section of this paper.

6.3.1. Multi-Scale Optical Coherence Tomography

The technical examination was performed with a spectral-domain OCT system (Thorlabs Ganymede-II-HR), mounted on xyz scanning stages. The system is operated with a self-developed program in the LabVIEW software [38]. The OCT system has a source spectrum centered at 900 nm, spanning a bandwidth of 195 nm. The specified axial bandwidth-limited resolution is 3.0 µm (in air). The OCT system is operated with a telecentric imaging lens (Thorlabs LSM04-BB) that has a maximal field of view of 14.1 mm × 14.1 mm, of which a window of 5 mm × 5 mm is used for scanning. The computer (Dell precision workstation T1700) had a 16 GB RAM memory, an Intel Xeon E3-1271v3 processor and an added internal 1 TB Solid State Drive (SSD) for data storage during measurements. More information about the system specifications and raw OCT data processing can be found in [37]. The schematic depiction of our spectral-domain OCT setup is shown in Figure 6.2(a).

For large area scanning the OCT scan probe is mounted on a 3-axis stage consisting of two 20 mm(x and y-axis) scan range stages (Standa 8MT50-series) and a 100 mm (z-axis) scan range stage (Standa 8MT50-series) mounted in an x-y-z configuration. The maximum dimension of the scanned surface (limited by the scanning stages) is 200 mm × 200 mm. The OCT probe head is mounted to the setup with the aid of a customized mount, which has 2 degrees of freedom for tilt around the x axis and y axis, enabling imaging of a surface under a small angle. This is necessary to reduce the amount of over-saturation on the detector, caused by surface specular reflections reflecting back into the lens, which are then for the most part avoided. The OCT probe head and scan system is shown in Figure 6.2(b), and Figure 6.2(c) shows the instrument set up in front of the painting. An overview of the specifications can found in Table 6.2 (see end of Chapter).

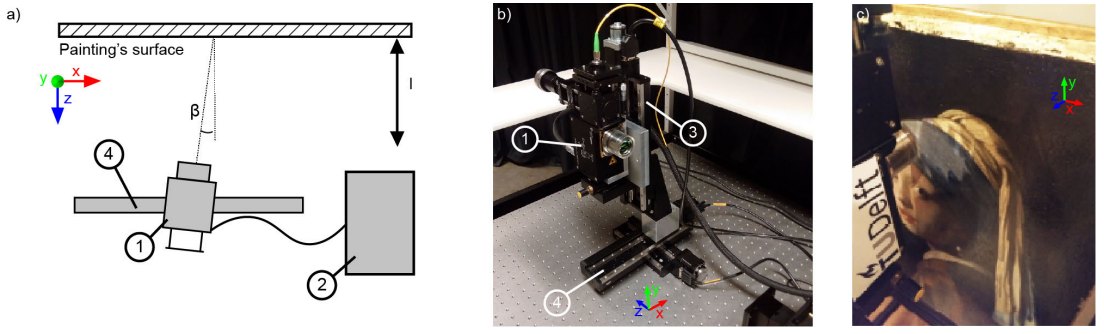

Figure 6.2: Multi-scale optical coherence tomography (MS-OCT) scanning setup, (a) simplified schematic layout of the multi-scale spectral domain OCT system (top view), (b) annotated picture of the MS-OCT setup in lab conditions, (c) MS-OCT probe in front of *Girl with a Pearl Earring* during scanning of the painting. In all images (1) is the OCT probe, (2) the spectrometer, (3) the vertical stage and (4) the horizontal stage, β the imaging angle and l the working distance to the painting.

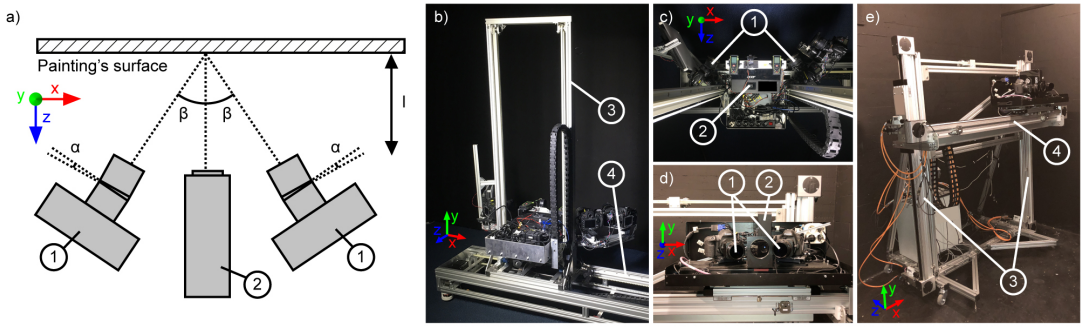

Figure 6.3: Two 3D scanning setups based on fringe-encoded stereo imaging, (a) simplified schematic layout of both 3D imaging modules (top view), (b-c) standard resolution scanner (Std-Res 3D scan, at a lateral sampling resolution of 25 µm × 25 µm) also featuring gloss scanning, where (c) is a close-up of the imaging components (top view), (d-e) high-resolution 3D scanner (High-Res 3D Scan, at a lateral sampling resolution of 7 µm × 7 µm), whereby (d) is a close-up of the imaging components (front view). In all images (1) denotes the cameras, (2) the projector, (3) the vertical stage(s) and (4) the horizontal stage, β the imaging angle, α the tilt angle of the lenses and l the working distance to the painting.

Calibration and data processing

The MS-OCT setup is positioned in front of the artwork and then carefully aligned. First, by means of an build-in video camera, the desired scanned area is correctly aligned, in the range of the scanning stages. Secondly, the focal plane of the OCT sample arm optics is set to 0.4 mm below the zero delay position (this to reduce auto-correlation artifacts in the measured spectra). Then sample regions in the scanning area are captured, to ensure that there is no height variation larger than 1.89 mm (depth-of-field), within the dimensions of a single tile. In this step also the distance between setup and object is double-checked, so that it can never be so small as to lead to a collision. Lastly, the probe is positioned at the initial scanning location and the artwork is brought in focus manually. Then, the LabVIEW scanning software is activated, which fully automatically scans the artwork and keeps it in focus. MS-OCT tile stitching is performed based on segmented surface data in volume scans. This image stitching algorithm is not dependent on tile overlap (due to high precision translation stages), but image segmentation artifacts can in rare cases results in stitching errors.

6.3.2. 3D scanning based on fringe-encoded stereo imaging

Two 3D scanning systems, both based on fringe-encoded stereo vision, were used to scan the complete painting. The imaging systems both consisted of an xy-frame able to move the imaging module in a parallel plane to the surface of a painting, in a horizontal and vertical motion. Figure 6.3(a) depicts the schematic layout for both imaging modules. The imaging modules consisted of two cameras positioned on either side of a projector, all fitted with polarization filters. This cross-polarized setup removes unwanted reflections like highlights in the images. The cameras were positioned at an angle relative to the surface normal (β in Figure 6.3(a)). Camera lenses utilizing the Scheimpflug principle (also known as tilt-shift lenses), were used to align the focal plane to the painting surface, rotated by angle α (see Figure 6.3(a)). The first system (described in [25], based on the original design by [24]), sampled at a lateral resolution (xy) of 25 µm, hereafter denoted as *Std-Res 3D Scan*. This system also featured a gloss scanning module, of which the details are out-of-scope for this paper. Two cameras (Nikon D800E) were positioned at an imaging angle of $40°$, fitted with tilt-shift lenses (Nikkor PC-E 85 mm). The projector (Acer X113H) had an illumination intensity of 2800 lm. The imaging module measured a scan area of approximately 170 mm × 100 mm, set at a tile overlap of 41% in x- and 30% in y-direction. The system has an automated scanning range of 1.3 m × 1.3 m and an approximate working distance of 440 mm from the surface. The depth-of-field of the system was approximately 8.5 mm. Based on the geometric layout of the system — imaging angle β and lateral imaging resolution — the theoretical lower boundary of the axial resolution (Z) is 27.5 µm. The second system, hereafter denoted as *High-Res 3D Scan* (described in [26]) sampled at a lateral resolution of 7 µm. Two cameras (Canon 5DS-R) were positioned at an imaging angle of $21.5°$, fitted with tilt-shift lenses (Canon TS-E 90 mm). Two 25 mm lens extenders were used (Canon EF 25 mm) in this setup to extend the focal length to 105 mm, allowing focusing at closer range, and thereby higher resolution imaging.

The projector (AXAA M6) had an illumination intensity of 1200 lm. The High-Res 3D scan system measured scan areas of approximately 60 mm × 40 mm with a tile overlap of 20% in x- and 25% in y-direction. This system has a scan range of 1 m × 1 m and a working distance of 175 mm. The depth-of-field of the system was approximately 1.0 mm. Based on the geometric layout of the system — imaging angle β and lateral imaging resolution — the theoretical lower boundary of the axial resolution (z) is 17.5 µm. Figure 6.3 (b-c) depicts the std-res 3D scan system and (d-e) the high-res 3D scan system, both showing the camera configurations and the vertical and horizontal actuators. An overview of the specifications of both scanners can be found in Table 6.2 (see end of Chapter).

Calibration and data processing

For both 3D scanning systems, the lens distortion of cameras was calibrated following a multi-view geometry calibration procedure, using a checkerboard pattern [39]. The white balance and illumination non-uniformity were calibrated using a 300 mm × 300 mm Spectralon® panel.

The color and 3D topography of the surface were captured using a hybrid solution of fringe projection and stereo imaging. To measure the topography, a 6-phase shifting sinusoidal grey-scale pattern (fringe) was projected horizontally and vertically on the painting's surface, capturing in total 24 images for a single scan area. One additional image is captured with uniform illumination from the projector, which is used as the color image. This imaging module is then moved to the next position and the procedure is repeated. Offline, fringe unwrapping is applied and a sparse stereo matching is carried out to match the fringes of both camera images. A look-up table is generated for both cameras, encoding both images. Taking into account the camera calibration, a dense stereo matching is performed, using the principle of ray-tracing. The RGB values of the uniformly illuminated image were then mapped onto the xyz datapoints. Next, a plane was fitted through the datapoints and the data was sampled in a regular xy-grid at respectively 25 µm or 7 µm intervals, which approximates the reconstructed resolution. If a single pixel contained more than one value (due to our non-parallel configuration this can occur), the average of the values is taken. Missing values were interpolated based on surrounding pixels. A more detailed description of the image processing can be found in [24, 25]. The output of these systems is an aligned color and height map.

6.3.3. 3D digital microscopy

The painting was examined using a 3D digital microscope (Hirox RH-2000), which uses the principle of focus stacking for 3D imaging. A custom bridge stand was built for the project to accommodate the size of the painting, with a 500 mm × 500 mm automatic motorized xy-stage, combined with the existing automated z-axis of the microscope. In this configuration the painting was placed horizontally on a table and the microscope moved on a motorized stand above it (see Figure 6.4). A lens (Hirox MXB-5000REZ) at a magnification of 140x was used. The lens was mounted on a motorized z-axis block (Hirox FB-E) with 85 mm manual movement and 30 mm motorized movement. The surface was illuminated with the microscope LED light-

ing, with directional light (raking light) at 100% intensity, combined with 10% light intensity of the ring light (dark field). The rationale for this configuration is that the directional lighting is able to penetrate the transparent varnish layer, but also creates underexposed areas (shadows created by topographical features). Although a dark field illumination reduces the overall contrast in the image, it is able to create the necessary contrast in the shadowed regions, needed for the 3D imaging. The tile size (field of view) (xy) was 2.1 mm × 1.31 mm, giving a lateral resolution of 1.1 µm. The overlap between tiles was set at 30%. The z-axis focus-stack range (bottom-to-top) was set to 450 µm, making sure that the height variation of the complete scan area was captured within this range. The working distance of the microscope at this magnification is 10 mm. The Hirox RH-2000 proprietary software was used to control the microscope. For this project, a new software function was developed to eliminate the pixel size limitations of traditional online 3D stitching, allowing unlimited area imaging via offline stitching. An overview of the specifications can found in Table 6.2 (see end of Chapter).

Calibration and data processing

Prior to starting the scanning, the alignment of the axis and the planarity of movement relative to the platform (and painting) was checked using Hirox-supplied reference targets. A Hirox calibration grey card was used to set the white-balance of the microscope. The xy-scale was calibrated using the Hirox-supplied, certified glass scale.

The Hirox software was also used for programming the automatic acquisition of the individual tiles. The microscope created a series of images in the z-direction capturing each focus layer individually, between the predefined top and bottom set point. These are then combining into one single all-in-focus image (multi-focus or extended depth-of-field). The microscope then moves to the next position and the multi-focus capturing procedure is automatically started again. The result for each tile is a TDR file (Hirox 3D file format) which includes a all-in-focus color image (JPG) as well as altitude in the z-axis for each pixel. The raw data — the individual focus images — was not saved due to size limitations. Hirox e-Tiling [40] software was used to stitch offline the individual 3D tiles (providing identical functionality to the online stitching of the microscope), resulting in large 3D-stitched files.

Figure 6.4: Digital 3D microscopy setup, (a) Simplified schematic layout of 3D microscope, (b) Annotated picture of the 3D microscope setup in lab conditions, (c) 3D microscope during imaging *Girl with a Pearl Earring*. In all images (1) denotes the Hirox microscope lens MXB-5000REZ mounted on the motorized z-axis focus block, (2) the LED lighting provided through optical fiber(s), (3) the motorized x-axis which moves the microscope, (4) the motorized y-axis used to move the painting platform, and l the working distance to the painting.

6.3.4. Pre-processing and alignment of data sets

The height data was measured by the researchers and stored in an array that is sampled in microns (rather than pixels). This enables interchangeable dataset comparison. Consequently the data was processed by the alignment algorithm, making use of the (open-source) implementations of SciPy [41] (scientific computational libraries) and OpenCV [42] for Python. The data comparison flowchart is shown in Figure 6.5. First, missing data is replaced by a linear interpolation result of the respective height map (Figure 6.5(a)). Secondly, the data is de-trended in order to minimize mismatching due to angled scanning, orientation of the painting during measurements and bending of the painting (which is a non-rigid object). After these initial preparation steps, a region-of-interest (ROI) is selected in which every imaging method has data and contains structures which show clear topology variations. Consequently, the height arrays are aligned with a scale invariant template matching algorithm. The sizes of the individual height arrays do not have to match with respect to the x/y pixel dimensions (scale invariance), but the aspect ratio of the surface map must geometrically be correct. This scale invariance is a requirement, since a given area will be sampled with different resolutions by every method. We find the resampled matched template (Figure 6.5(d) by computing the cross-correlation coefficient and locate its maximum value, so that the overlapping areas are positioned on top of each other. The aspect ratio (AR) with the highest cross-correlation coefficient is deemed the best match by the system and will become the overlapping area that is visualized. Finally, we apply again a detrending step (Figure 6.5(e)), in order to remove some local height variations in the datasets. For visualization purposes we align the mean height value of the datasets.

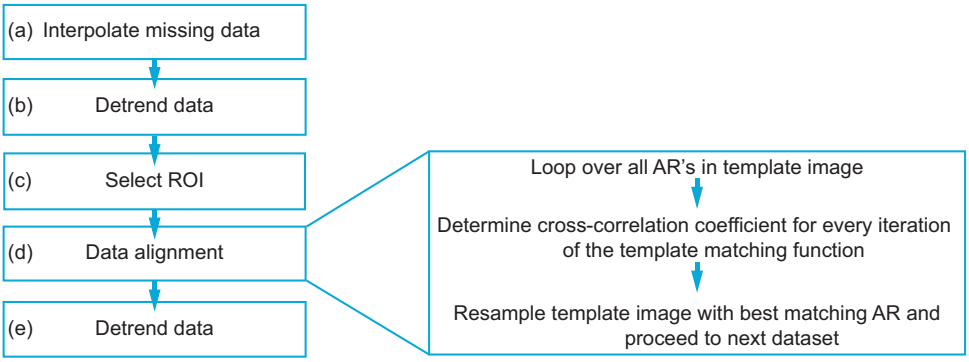

Figure 6.5: Flowchart of data processing algorithm for painting data alignment

6.3.5. Reference target measurement comparison

In order to compare each imaging technique's ability to faithfully reproduce the height profiles of the objects, we compared the measurement results of a reference target (Rubert&Co, sample no. 513E [43]). The reference target was a electro-formed nickel specimen, with a hard protective top layer of nickel-boron. This was one of the few measurement samples that could be found with features in the mm range, rather than the much more common µm range, commonly used for a variety of (contact) roughness measurements. The sample has four milled grooves, with expected (i.e. not certified, and found to be only a rough estimates of the feature sizes) milled depths of 1000 µm, 500 µm, 200 µm, and 30 µm, and widths of 3 mm, 2 mm, 2 mm, and 0.5 mm (see Figure 6.8(a)).

As the target was not certified, we did *not* compare our measurements to the provided dimensions, but rather compare them to measurements made using white light confocal profilometry (WLCP), using the Hirox Nano Point Scanner (NPS). The JYFEL NP3 measurement unit was mounted on and connected to the Hirox RH-2000 system, in a similar fashion as the 3D microscopy setup. The NP3 has a depth (z) measurement range of 1400 µm (depth-of-field), and a working distance of 12 mm. It can measure a maximum slope angle on a mirror sample of $25°$, and has a lateral resolution (x) of 2.6 µm. As the height accuracy is declared at 150 nm, it suitable as a gold standard for the other measurements, which are in the micron range. The output of this system is multiple profile measurements, across the grooves, resulting in a 3D surface.

The sample was scanned completely or in parts by the different measurement instruments (depending on the tile size), and local height variations were compared for the four grooves. The rectangles in Figure 6.8(b) show the sampling locations of the comparison areas. In fact, we compare 2D areas for every technique. For the NPS scanner there are only ten adjacent line-scans present, but this is offset by the high lateral sampling and low standard deviations found for these measurements. The data of the reference target was pre-processed and aligned in a similar fashion as the painting data.

6.4. Results

The following section provides an overview of the scan results obtained from *Girl with a Pearl Earring* by Johannes Vermeer and the reference target.

6.4.1. Painting scan results

Using the MS-OCT, the painting was scanned in four sessions overnight, each time scanning an area of 200 mm × 200 mm. The total scanned area, consisting of 4 sets of 41x41 tiles, resulting in a total scanned area of 350 mm × 400 mm (excluding overlaps).

The Std-Res 3D scanner imaged the painting overnight in the completely dark environment, and was able to capture the complete painting in a little over 2.5 hours (4x8 tiles, with an overlap of 41% in x and 30% in y). The High-Res 3D scanner captured the complete painting in 8 by 15 tiles, with an overlap of 20% in the

x-direction, and 25% in y, with a total capturing time of approximately 4.5 hours. This was carried out during open hours of the museum, *with* environmental lighting (also see Discussion section, explaining potential issues related to this). Note that the scan time did not scale linearly with the resolution between these scanners. This is due to limitations in data transfer and various differences between the two systems, including extent of scan speed optimization and capturing of gloss as additional modality (for the Std-Red 3D scan).

Due to time restrictions the 3D digital microscope scanned only ten regions of interest (ROI) on the painting at a high enough magnification to be relevant for 3D data comparison (i.e. the complete painting was also captured at 35x magnification, but the depth-of-field is then too large to yield any useful 3D data, for the scale of the details relevant for this painting). The other scanned areas are roughly similar in size to regions (b) and (c) in Figure 6.6, which are compared in this paper. A microscope magnification of 140x was used to capture the tiles that make up these regions. For instance the *Left Eye* region was scanned in 16x23 tiles (with 30% overlap), and took roughly 0.5 hours to scan. Details on the scan time and data size for every imaging system be found in Table 6.3 (see end of Chapter).

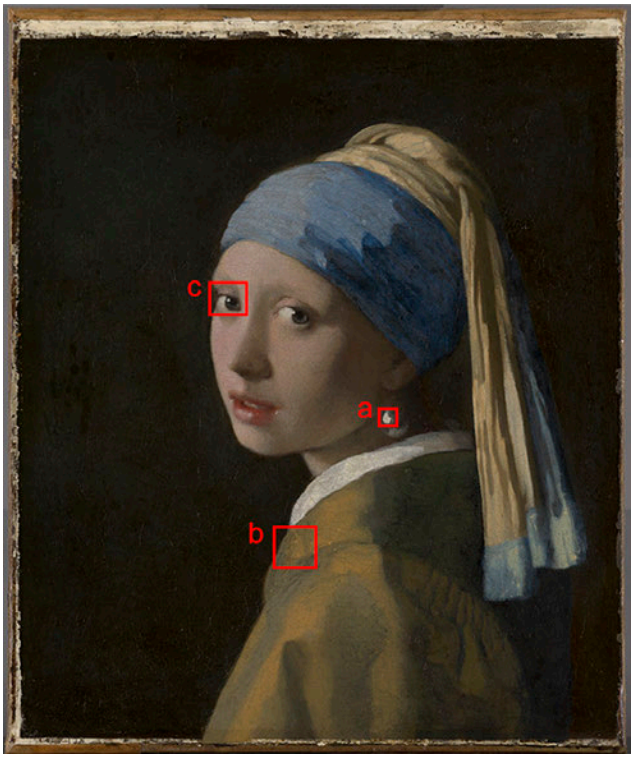

Figure 6.6: Locations on the painting of the three regions of interest compared a) the *Pearl Highlight* b) a section at the front of the *Jacket*, and c) the *Left Eye*. Detailed images of these regions are depicted in Figure 6.7.

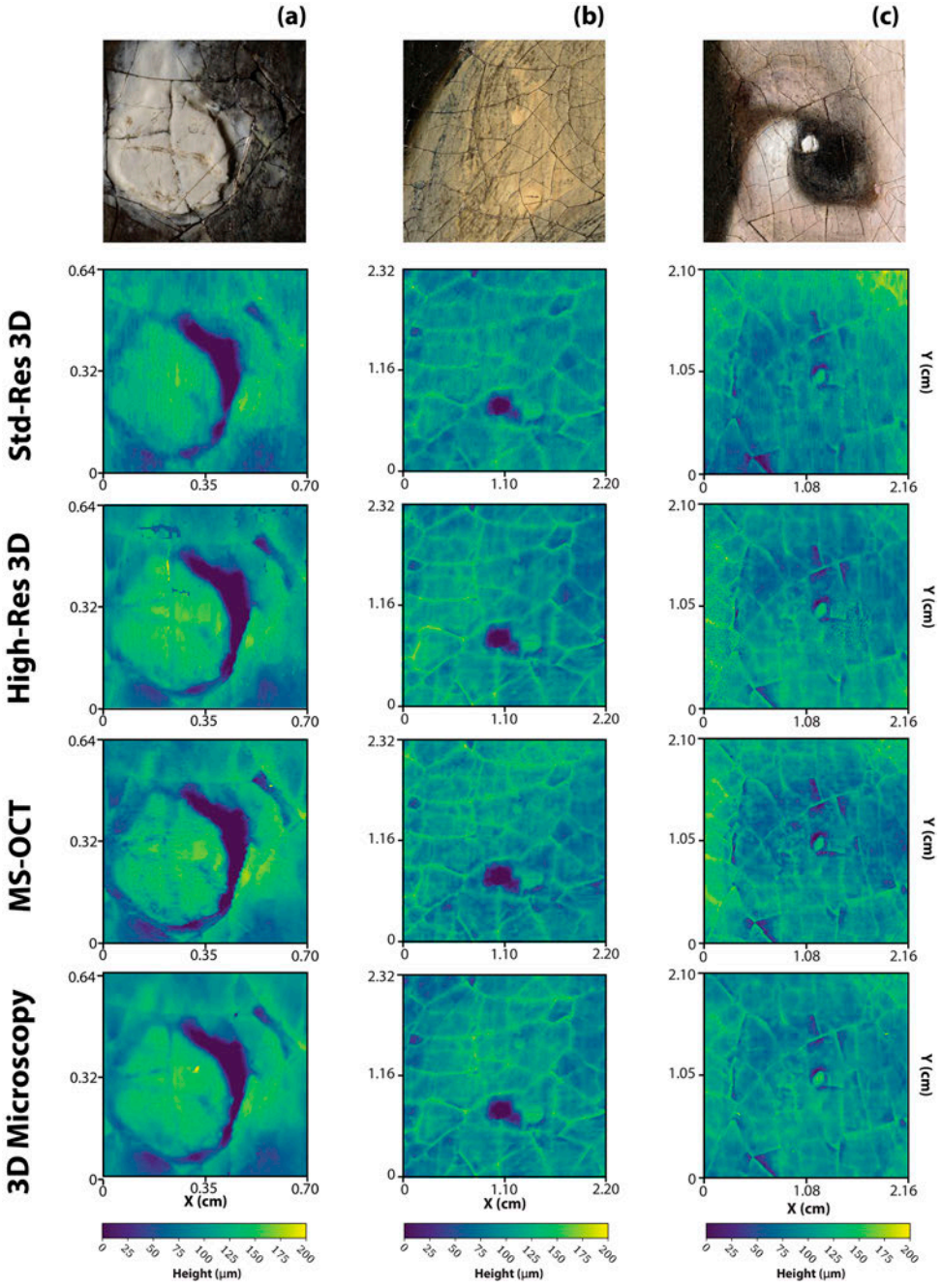

Figure 6.7: De-trended and aligned heightmaps of three regions of interest created by four scanning systems (a) *Pearl Highlight*, (b) *Jacket*, and (c) *Left Eye*. The color images are the stitched images using the 3D microscopy color data.

We compare the results of the four imaging systems by studying three of the regions scanned by the 3D microscope (here we have data of the four scanning systems). The location of the comparison areas are shown in Figure 6.6. The results per scanner of these three regions are depicted in Figure 6.7, where the top row shows the stitched color image obtained by the 3D microscope, and the following rows plots of the 3D data, of the respective imaging devices. Figure 6.7(a) shows a small detail, the *Pearl Highlight*, of 7.0 mm × 6.4 mm, (b) a part of the yellow/green *Jacket* measuring 22.0 mm × 23.2 mm, and (c) the *Left Eye* measuring 21.6 mm × 21.0 mm. All height maps are plotted on a scale between 0 and 200 µm. As mentioned in the method section, all height data is de-trended, and the means (z) are aligned. All height maps depicted in Figure 6.7 show relevant topographical details like (flattened) *impasto* (though more difficult to distinguish in (b)), and (b-c) also clearly show the craquelure pattern of their particular regions (these are larger areas than (a)). Figure 6.7(b) also shows an indentation, multiple of which can be found across the surface of the painting.

Reference target scan results

The reference target (depicted in Figure 6.8), was scanned by all four imaging system. Generally, we found that all techniques are capable of measuring the grooves in the sample (albeit the 3D scanning systems needs an non-cross-polarized setting to capture the projected fringes on this metallic artifact, also see discussion sub-section *Scanning a (metallic) reference target*). We compared the local height differences relative to the Nano Point Scanner (NPS) measurements, for the four grooves using the regions demarcated by the bounding boxes in Figure 6.8(b)). For these regions, the standard deviation is calculated, and the mean height differences between the respective region pairs. We found that the top surface of the reference target was not completely flat (also in the NPS measurement). Therefore, we fitted a curve through the NPS measurements, and corrected all the other measurements for this curvature (see Figure 6.8(b)). Table 6.4 (see end of Chapter) provides an overview of the (corrected) measurements results for every scanning system.

The (corrected) mean height differences for every groove, relative to the NPS measurements, are plotted in Figure 6.9. In this figure the dotted lines denotes the theoretical z-resolution of the scanning systems. Note that there is no theoretical z-resolution available for the 3D microscopy. We found the smallest relative errors (absolute) for the 3D microscopy (between 0 µm and 3 µm) and MS-OCT (between 0 µm and 6 µm), compared to the High-Res 3D scan (between 0 µm and 11 µm) and Std-Res 3D scan (between 8 µm and 24 µm), and that all errors except one fall within the resolution boundaries. A mean absolute error of 6 µm was found for the MS-OCT, at the 500 µm groove, which lies outside the resolution boundaries of the MS-OCT. As expected, we found that the NPS measurements have the smallest standard deviation (σ) (between 0.05 µm and 0.42 µm), which were in all cases (close to or larger than) a magnitude scale different to the other measurements. For the 3D microscopy the σ lies between 3.1 µm and 6.3 µm, for the MS-OCT between 1.4 µm and 7.4 µm, for the High-Res 3D scan between 7.2 µm and 12.9 µm, and the Std-Res 3D scan between 9.2 µm and 15.0 µm.

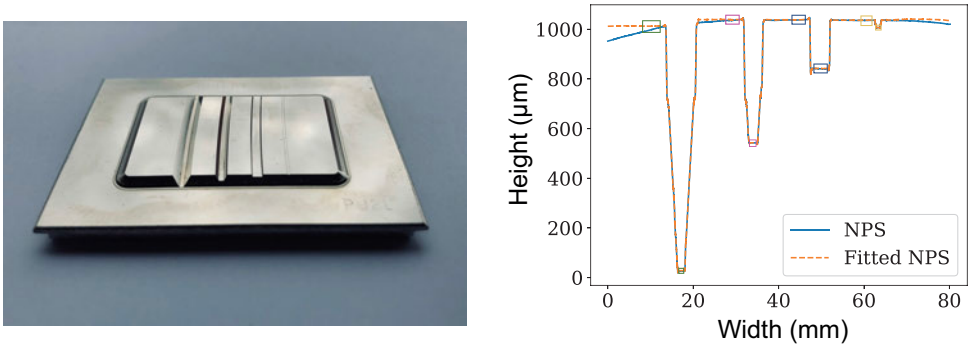

Figure 6.8: Reference target with four grooves of varying depth and width, (a) photograph depicting the (uncalibrated) reference target no. 513E, produced by Rubert & Co [43], expected groove depths (from left to right) are 1000, 500, 200 and 30 µm, (b) Hirox Nano Point Scanner (NPS) cross-section plot of the reference target. Blue line is the experimental NPS data. Orange dotted line is the fitted data, without non-affine artifacts. The boxes and their respective colors indicate the sampling locations for the results described in Table 6.4 (see end of Chapter).

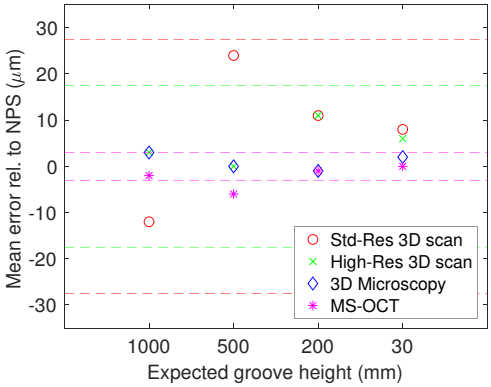

Figure 6.9: Measurement results of reference target with four grooves, mean error relative to the Hirox Nano Point Scanner (*NPS*) measurements (in µm), measured locally between top and bottom surface for every groove (see Figure 6.8), from the deepest (left) to shallowest (right) groove. Dotted lines show the theoretical scanning resolution (in x) of the imaging devices (corresponding colors).

6.5. Discussion

In the following section the scan results are discussed based on the data collected from the case study and the reference target. First, we reflect on the measurement results obtained of the painting (specifically for the three regions-of-interest), and the results obtained from the reference target. Next, we interpret 3D data obtained from Vermeer's *Girl with a Pearl Earring*, and discuss the (potential) applications of such data in the cultural heritage domain. Then, we highlight several difficulties with the (*in-situ*) scanning of paintings, the chosen reference target, and issues related to (3D) data processing (of very large data sets). Finally, we summarize the various merits and limitations of the scanning system in two stages: firstly the

ones that are inherent to the measurement techniques, secondly the ones related the (current) scanning system implementations, that were used in this case study.

6.5.1. Comparison of measurement results

When we compare the scan results of the case study (illustrated in Figure 6.7), we find that all three scanning techniques are capable of measuring a painting's topography, capturing details at the level of individual cracks. The data sets of the three imaging techniques show broad similarity in spatial layout (xy) and height values (z). However, when we zoom into the finest level of detail we see that these are not captured by the Std-Res 3D scan, missing for instance the fine craquelure details on the *Pearl Highlight* (see Figure 6.7(a)). Another difference that can be noticed between the painting scan results is the subtle variations in the global shape for the small ROI plotted in Figure 6.7 (e.g. relatively lighter or darker features between the maps), despite the de-trending. Potential reasons for these differences, and the subsequent difficulties with comparing the height data (e.g. due to non-rigid nature of a canvas painting, scanning orientation, and stitching) are discussed in the following sub-sections: 6.5.3 and 6.5.5.

The measurements of the reference target show reasonable small error, as compared to the highly accurate NPS measurements, and acceptable standard deviations for the features we try to capture. The results are in line with the expected measurement uncertainty of the different measurement devices. We find that the 3D microscopy and MS-OCT have the highest accuracy and precision, compared to the 3D scanning systems based on fringe-encoded stereo imaging. We believe that the larger error of MS-OCT at the 500 µm groove, lying outside the measurement uncertainty boundary of this device, might be attributed to a data processing, segmentation error (see sub-section 6.5.5). Furthermore, particular difficulties with scanning this (metallic) reference target are discussed in sub-section 6.5.4.

6.5.2. Applications of 3D scan data of paintings

Pintus et al. [44] provide an overview of 3D scanning techniques applied to cultural heritage, and categorize them based on scanning scale, the number of objects scanned (and compared), and the application. Following their framework our scanning efforts might be categorized as follows: our study focuses on scanning at the micro scale — capturing the smallest feature level of its surface —, scanning only a single artifact, and application might currently be categorized as "perceptual enhancement". We exemplify how the current data can be used for this application by taking a close look at the 3D data captured of *Girl with a Pearl Earring*.

Perceptual enhancement of 'Girl with a Pearl Earring'

The scanning techniques described in this case study have the potential to help a conservator evaluate the topography, condition, authenticity and conservation history of an object. They provide a documentation of the topography of *Girl with a Pearl Earring* at one specific moment in time. This data already provides information about Vermeer's technique, and the condition of the painting.

For example, the three ROI compared as part of this case study — the *Pearl*

Highlight, *Jacket* and *Left Eye* (see Figure 6.7) — contain small details that Vermeer painted more thickly than the surrounding paint (i.e. *impasto*). Visualising their height and topography in 3D reveals how much paint Vermeer loaded onto his brush, and the rheological properties of the materials he used. The height of the details in the painting's current state can be measured, but this may not give an accurate impression of their height when Vermeer applied them. Changes over the course of time, and previous treatment interventions have certainly affected the painting's topography, especially for the highest impasto. During a 1960 restoration treatment, the support was wax-resin lined [45]. Nowadays there are alternatives to such lining treatments, but at that time, this intervention was deemed necessary to address structural problems and flaking paint. The 1960 lining was almost certainly done with the painting face-down, under high heat and pressure. As a consequence, the impasto was flattened. The top of the white *Pearl Highlight* but also in the white highlight in the *Left Eye* — which presumably would have been rounded or slightly pointed when Vermeer painted it — is now planar and almost level with the surrounding paint (see Figure 6.7(a) and (c)). Directly around the impasto is a 'moat', for the *Pearl Highlight* approximately 200 µm deep (as measured using all three techniques), which formed when the paint surrounding the highlight was displaced as the impasto was flattened. This suggests that Vermeer's original impasto would have matched or exceeded the current depth of the moat to be able to make such an impression. It appears that lining had less of an effect on the impasto with lower topography — for example, in the *Jacket* — as there is no perceptible moating (see Figure 6.7(b)). This data is useful for understanding Vermeer's painting technique, but also to assess the consequences of wax-resin lining.

During restoration treatments in 1915 and 1922, Derix de Wild regenerated blanched varnish layer(s), presumably using the so-called 'Pettenkofer' process, which can incorporate copaiba balsam. This material can help to soften flaking, brittle paint during treatment, but also has the potential to cause long-term changes in the paint [46]. Previous research confirmed that some cracks in the Girl's forehead contain copaiba balsam [45]. The data captured by the three scanning techniques reveal how the topography of the treated area has been affected. This can be seen for instance in Figure 6.10(e), using a color map for visual enhancement. The affected area of the forehead is deeper than the surrounding paint. We can also see in these visualizations that the cracks in the forehead appear to have soft, rounded edges, and the cracks appear wider than the sharp-edged cracks throughout most of the painting. These scanning techniques could therefore potentially be used to discover other regions that might have been treated using the Pettenkofer method. It should be mentioned that determining the exact shape (roundness/sharpness of cracks) is limited by the scanning resolution and measurement occlusions imposed by the scanning systems.

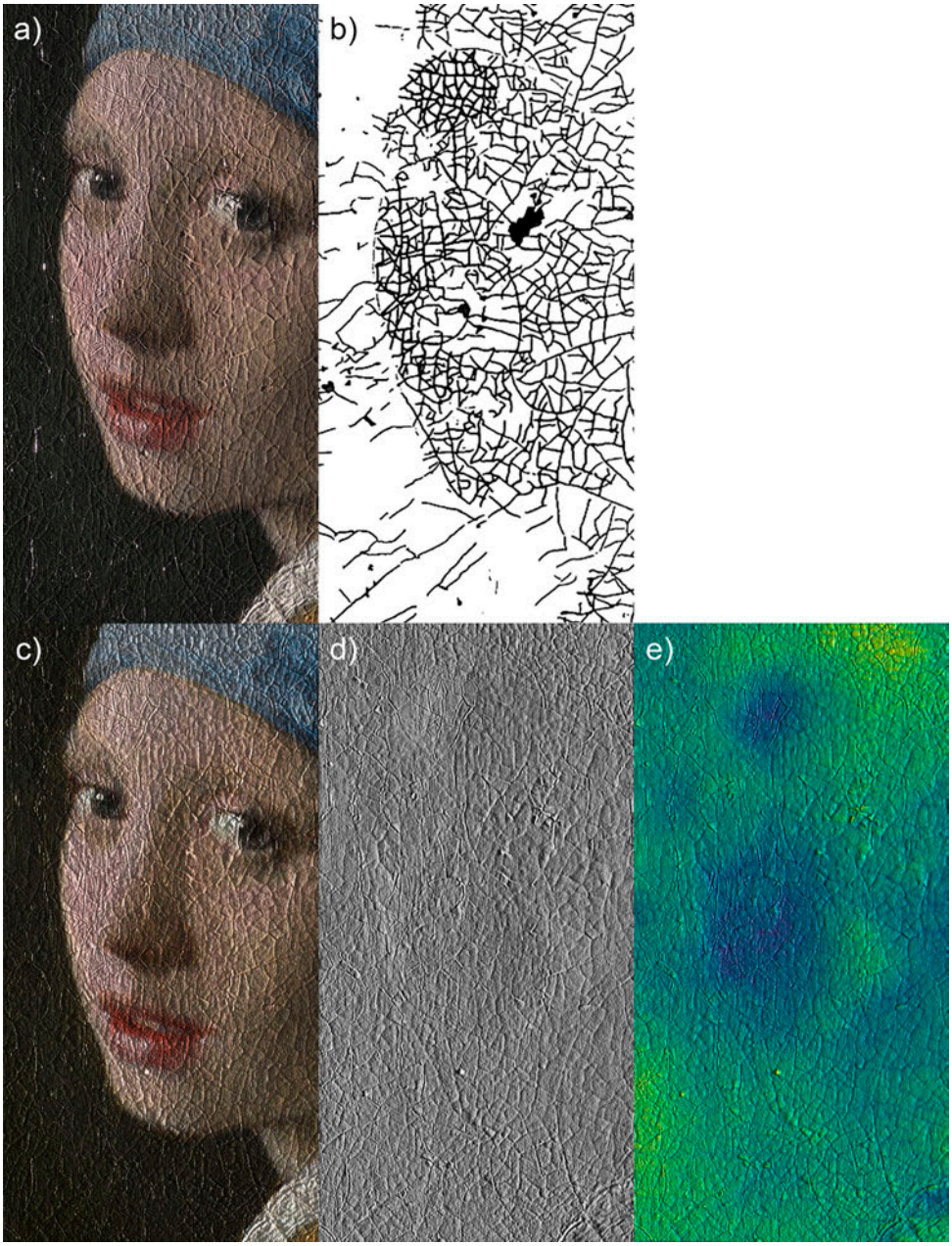

Figure 6.10: Original documentation and renderings, visualizing surface height variations of *Girl with a Pearl Earring*. Top row shows the original documentation, part of (a) of raking light photograph (see Figure 6.1(a)), and (b) crack tracing image (see Figure 6.1(b)). Bottom row rendering of 3D data from Std-Res 3D scan (c) using color and topography data, (d) rendered as a matte, white surface, and (e) rendered using a color map, to enhance the height variations. Note that for the renderings the height variations are exaggerated relative to the lateral scale, to increase their visibility.

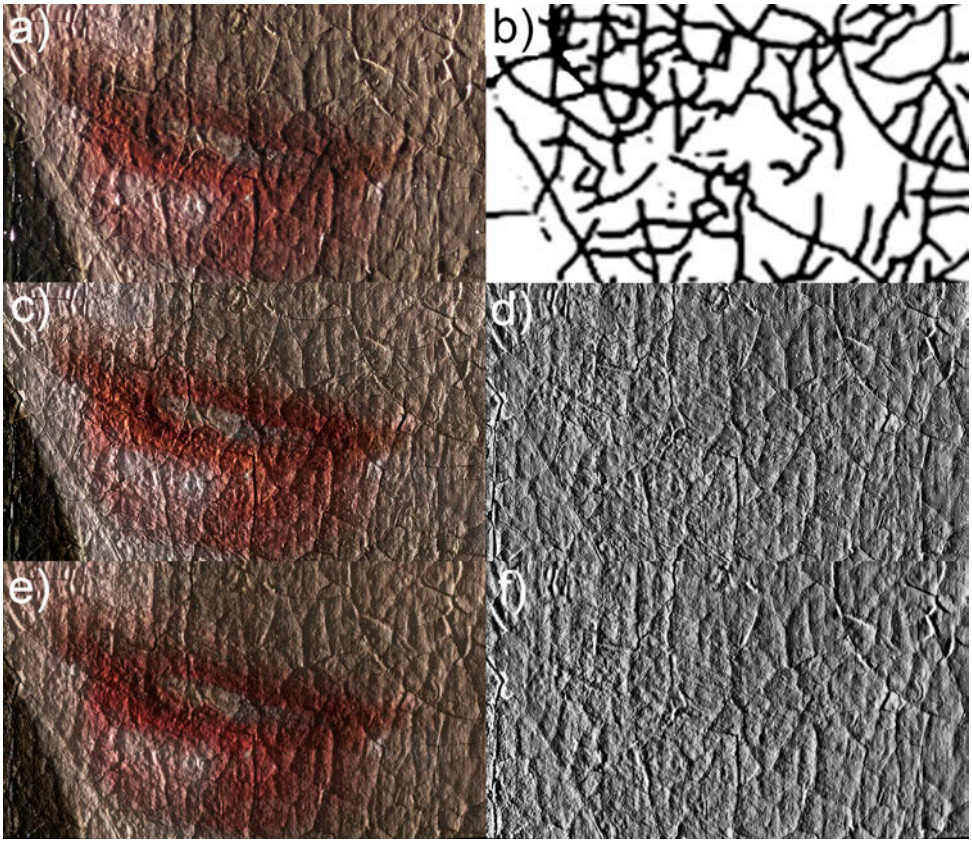

Figure 6.11: Details of original documentation and renderings, visualizing surface height variations of *Girl with a Pearl Earring*. Top row shows the original documentation, detail of (a) of raking light photograph (see Figure 6.1(a)), and (b) crack tracing image (see Figure 6.1(b)). Middle row: rendering of 3D data from 3D Microscope scan (c) using color and topography data, and (d) rendered as a matte, white surface. Bottom row: rendering of 3D data from High-Res 3D scan (e) using color and topography data, and (f) rendered as a matte, white surface. Note that for the renderings the height variations are exaggerated relative to the lateral scale, to increase their visibility.

Visualizations that can be created using 3D data are an improvement on the ways that conservators have traditionally been able to document and view craquelure. Figure 6.10(b) show the cracks that were visible with the naked eye in 1994, which the conservator traced onto a transparent polyester film. In the dark background, the dark cracks were likely more difficult to see, which gives the impression that the cracking might be less pronounced or severe in the background than in the face. In comparison, Figure 6.10(d-e) show that the relative amount of measured cracking is much more similar when comparing the face to the background. Although raking light photographs (segments shown in Figure 6.10(a) and Figure 6.11(a)) are still useful for visualising the topography, it can be difficult to interpret because the color of the paint can affect the visibility of the craquelure. With 3D scanning, the topography can be rendered as an image without the color information, only

showing the height variations (see for comparison Figure 6.10(d-e) and detailed views in 6.11(c-f)). Virtual relighting of the topography — rendering it as a matte, white surface — allows a conservator to see the topography more clearly than on a color image. It could be used to recognize vulnerable areas — e.g. where the paint is lifting, flaking or tenting — and these areas could be earmarked to be checked regularly. Also, the scanning techniques have the potential to identify blind cleavage: areas of delamination between layers beneath the surface. Blind cleavage can cause topographical changes at the surface that are difficult to perceive with the naked eye. Although it would be ideal to scan the painting at regular intervals to monitor changes any changes to the topography of the painting, simply recognising the vulnerable areas is vital for ensuring the long-term stability of the artwork.

Other (future) applications of painting 3D scan data

If we take inspiration from the categorization presented by Pintus et al. [44], we might also envision other applications for this type of 3D scanning data. In terms of applications, the 3D data might also be used for monitoring and restoration. The painting could be re-examined using one of these techniques in the future, potentially identifying topographical changes that occur of time. Similarly, 3D scanning might also be used to document and support restoration of a painting — capturing and comparing an area before and after treatment. Also the possibility of extending the application to conducting a one-to-many study might be considered. For instance studying the craquelure/brushstroke patterns of paintings by the same painter, or coming from the same region/period (e.g. supporting studies like [12]), or one that have undergone a similar treatment — like the example of the 'Pettenkofer' process. Furthermore, the 3D scan data (combined with color information) might be used for 3D printing reproductions, which could be instructive to conservators and museum visitors — used in educational and/or exhibition contexts.

6.5.3. Scanning paintings and in-situ scanning conditions

Aligning and focusing scanning systems

One of the difficulties with scanning paintings at such high resolutions is the lack of *a-priori* knowledge of the surface. This is relevant on the scale of the complete painting (i.e. warping) and at a smaller scale (i.e. impasto). For the artifact to be scanned accurately, it has to be captured within in the focused range (i.e. large enough depth-of-field). The MS-OCT system currently features an auto-focusing functionality with a range of 100 mm, assuring alignment for every tile; however, due to the imaging angle, the total height difference within a single tile cannot exceed 1.87 mm. With the High-Res 3D scan the depth-of-field is approximately 1.0 mm. A careful alignment is therefore needed to assure the complete painting is in focus during scanning. Automated axial alignment might be needed to overcome larger height variations in paintings with more extensive warping (i.e. by adding an additional axial axis). Also, if a painting has large local height variation (exceeding this approx. 1.0 mm), it might be necessary to make a lower resolution scan first to determine the maximum height variation. Based on this the maximum resolution can be chosen, assuring the total height variation is captured within every single tile.

For the 3D microscopy the focal range need to be set for the complete scanning area, assuring every point lies within this focal range. This is also important for the total scanning time. Setting the boundaries too wide leads to an unnecessary increase of the scanning time, while setting the boundaries too narrow runs the risk of *not* capturing certain areas as they remain out of focus. Also here automated axial alignment could help to efficiently scan paintings with large height variations across the surface (e.g. in the case of extensive warping). This might be achieved by pre-scanning (for instance using the NPS profilometry measurements at regular y-step intervals), or online with real-time distance measurement and adjustment.

Scanning (non-rigid) paintings

One additional difficulty with scanning and comparing data, specifically for canvas paintings, is the fact that they are painted on a flexible substrate. Actions like unframing, handling, and clamping a canvas painting onto an easel — all necessary steps for a technical examination campaign — influence the overall shape of a painting's canvas. In this case study, due to limitations imposed by the project, the painting was also moved between the different scans, inevitably leading to variations in global canvas shape. Additionally, the painting's orientation differed between the scans, which most certainly will also have had an effect on its shape. This means that there were differences in how gravitational forces and forces of the (easel) fixture, influenced the global shape of the painting. For example, it is very likely that the central part of the painting will sag more in the horizontal orientation (of the 3D microscopy setup) compared to the vertical orientations (of the other three scans). These differences might be avoided in a more controlled experiment (i.e. by not moving the painting between scans, *and* having a 3D microscopy system capable of vertically-oriented painting scanning). However, a similar situation will arise when two data sets are compared over time (i.e. for monitoring purposes). For these reasons, we will have to deal with these variations to be able to make a meaningful comparison between the data sets. In both situations — between these different scanning techniques and over time scan comparisons — care should be taken with accounting for the global shape. If this global shape removal is done too rigorously, valuable information might be lost about the painting's shape (comparison or changes). On the other hand, if the removal is not rigorous enough, comparison might not lead to any valuable insights.

Limitations of in-situ scanning

Other in-situ conditions in which *Girl with a Pearl Earring* was scanned also potentially influence the scanning results. For instance, vibrations were not measured during the scans and only to a limited extent controlled for. The High-Res 3D scanner and 3D microscope were used during opening hours with museum visitors present in the same room as the technical examination, offering multiple potential sources of vibrations affecting the scanner and/or painting. For the case of the 3D microscope system we expect that this will have had a limited influence, as the system (including painting) was placed on a low-vibration table and features active vibration compensation for the focus stacking. The MS-OCT and Std-Res 3D

scans were both captured during the night, limiting the vibrations induced by the environment.

The fact that visitors were able to view the examination also introduced another potential source of measurement error, namely external illumination. Specifically for the High-Res 3D scan the external lighting (reflecting off the surface) potentially influenced the height measurement, and might explain some measurement artifacts (i.e. measurement artifact of a repeating fringe pattern showing up in some tiles).

6.5.4. Scanning a (metallic) reference target

A metallic reference target has the advantage that it is a rigid artifact, and therefore ensures (when handled with appropriate care) that all imaging techniques are imaging the same structure. As a downside this reference target has some properties that do not (typically) occur in paintings. Consequently, we find that some imaging artifacts are introduced in the reference target measurement data, that are rare or non-existent in the painting scan data. The reflections caused by the metal surface frequently oversaturate the MS-OCT spectrometer and this results in measurement errors. In case of scanning a (larger) metal object (automatically), the oversaturation effect might also hamper the auto-focus algorithm. A consequence of its metallic surface is, that the target does not reflect light diffusely. For this reason, the reference target cannot be scanned by the 3D scanning systems (based on fringe encoded stereo imaging) with the default cross-polarized configuration. As we resorted to a non-cross-polarized setup, this led to more noise in the height data (stereo mis-matching features, due to specular reflections). Furthermore, with the High-Res 3D scan we experienced what looked like thin-film interference patterns, leading for further stereo mis-matching. We assume that this can be attributed to the (thin) protective coating on the reference target. Furthermore, the measured results are only indicative of the depth determination within a single tile of the measurement technique (specifically for the 3D microscopy and MS-OCT, as they cannot capture within one tile). Stitching errors will have additional negative influence when comparing larger areas (also see sub-section 6.5.5).

6.5.5. Effects of data processing on 3D data (comparison)

Various steps in the data processing can influence the scan results, related to the data processing algorithms used to generate every individual tile, but also in the alignment and stitching of data.

Layer segmentation in MS-OCT

The image processing algorithm of the MS-OCT includes a layer segmentation step [37]. If this segmentation fails (layers cannot be clearly distinguished), it will introduce height map artifacts. Typically, if this effect occurs it leads to local artifacts, that can be classified as outlier data. However, if this occurs along the boundary of a tile, this could lead to a stitching artifact, that propagates over multiple tiles in the height map.

Alignment and stitching (of very large datasets)

The alignment between data sets was performed using only the 3D data, aligned at the pixel level, applying only rigid transformations. A consequence of such an alignment approach is that, if the data has lateral distortions (e.g. caused by calibration errors or imaging system imperfections), the features of the height maps will not align perfectly. Whether such systematic errors occur remains to be investigated. It then also remains to be investigated if a sub-pixel, non-rigid alignment can be achieved, to improve comparison results (e.g. following the 2D alignment approach applied to other types of multi-modal painting scan data in the Bosch Research Project [47]). Additionally, as the painting was measured at different resolutions — and therefore needs re-sampling — sampling errors can also influence the comparison between height data. Furthermore, as all systems offer more than one imaging modality — such as color information — these might also be included in the alignment algorithm, potentially leading to more robust alignment results. However, care should be taken with this, as it will almost certainly lead to a different result, which then leads to the issue of determining which result is better: all are merely based on optimization. For instance, in the case of using color data, robustness of the algorithm to illumination differences — leading to differences in shadowing and shading — needs to be assured.

On the scale of the ROI, selected from our case study painting, only MS-OCT and 3D microscopy are made up of merged tiles. For the stitched data sets, which was either based on xy-axis displacement (MS-OCT, no blending), or done by the Hirox e-tiling software (3D Microscopy, method unknown) no obvious tiling artifacts were observed. It remains to be determined, which strategy is the most suitable for tile stitching and/or blending, especially in the case when data in the overlapping regions are not in agreement with each other.

With the stitching of (very) large datasets, we also run into the issue of error propagation, in the lateral (xy) as well as axial (z) direction. If tiles a stitched in a sequential manner, small errors in misalignment (xyz) can lead to much larger errors across the complete surface. Currently no topographical scans were made at the scale of the complete painting, or intermediate resolutions, which might be used for a global-to-local optimization step in alignment, (potentially) minimizing the influence of local errors and the potential for error propagation. We envision that an approach like the one used in the Bosch Research Project ([47]), might be extended for topographical data, also dealing with the height (z) data.

Furthermore, we encountered issues with stitching the High-Res 3D data set, as our current approach to stitching (as is used in for instance [25]), is limited by its memory requirements for such large data sets. Also the Hirox e-tiling software did not allow stitching the larger ROI at full resolution.

Given the currently unsolved challenges with the non-rigid nature of canvas paintings (also encountered in the case study data sets), and the various challenges related to alignment and stitching (i.e. sub-pixel, non-rigid alignment, (multi) modal alignment considerations, dealing with stitching and blending of overlapping regions, error propagation, memory issues), we deem large-scale painting data height comparison to be beyond the scope of this paper.

6.5.6. Merits and limitations of the scanning techniques

In the following, we discuss the merits and limitations that are intrinsic to the different scanning techniques.

Lateral and axial resolution differences

Each of the techniques and their implementation have quite different lateral (xy) and axial (z) resolutions, where the relationship between these resolutions and level of flexibility in choosing a resolution are also different. For the MS-OCT system the anisotropic lateral resolution is 8.53 µm × 67.56 µm/pixel and the axial sampling resolution is 3.0 µm. These resolutions are limited by system optics for the lateral resolution and by the broadband source for the axial resolution and are consequently decoupled. The technique therefore does offer the capability to measure at different lateral resolutions. For the 3D scanning the lateral and spatial resolution of the system is more flexible (in this case the High-Res 3D scan has a lateral resolution of 7 µm and an axial resolution of 17.5 µm, and the Std-Res 3D scan respectively 23.1 µm and 27.5 µm). The axial resolution (z) is determined by the imaging angle (β in Figure 6.3) and the lateral resolution (xy) (determined by the imaging distance and camera/lens combination). The axial resolution can be increased by either imaging at a higher magnification, or by increasing the imaging angle. However, with increasing magnification, the total depth-of-field will become smaller. This should, however, remain large enough to capture the full height variation of the surface within a single tile. The imaging angle is limited by the maximum tilt angle of the lenses. In short, the 3D scanning technique offers quite some flexibility in term of resolution, but is limited by the minimal needed depth-of-field, camera and lens parameters. For the 3D microscopy the ability to calculate the topography is dependent on a very small depth-of-field of all images in the focal stack. An axial resolution suitable of capturing details of a painting like *Girl with a Pearl Earring* by Vermeer, can therefore only be created at relatively high magnifications (in the range of 140x, as was chosen in the case study). This means that reaching a reasonable axial resolution also results in small scanning tiles (2.1 mm × 1.31 mm here). In general, 3D digital microscopy does have flexibility in choosing magnifications (which can be easily achieved by interchanging the microscope objective), but this should be matched to the axial scale of interest (i.e. size of 3D features that is intended to be captured).

Scalability

The scalability of the different techniques is in part governed by the limitations in resolutions and the (related) tile size (for relative scale between the imaging systems see Figure 6.12). Given that the microscope tiles are only 2.1 mm × 1.31 mm it becomes very time consuming and data intensive to scan complete paintings. Even for a relatively small painting like *Girl with a Pearl Earring*, a scan at a lateral resolution of 1.1 µm, would lead to an image of roughly 355×10^3 by 404×10^3 pixels (a 144 gigapixel image). Based on the settings as used in the case study this would take roughly 200 hours to scan the complete painting. Dealing with the sheer size of data at such resolutions (also in terms of alignment and stitching) also remains challenging to this day. Both the MS-OCT and 3D scan systems can acquire

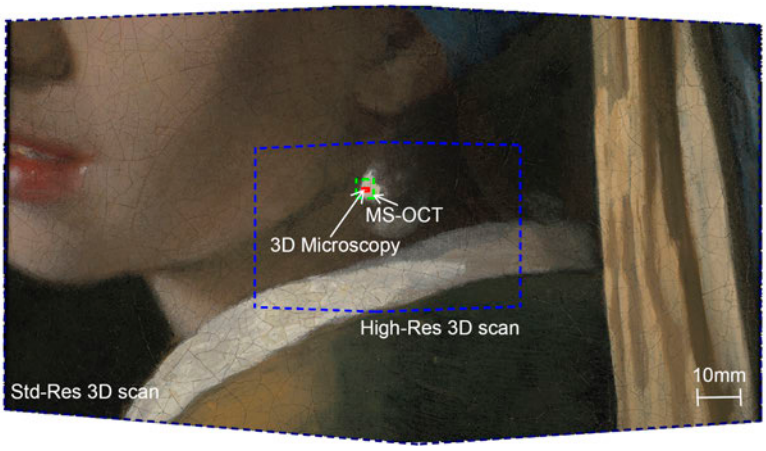

Figure 6.12: Relative scale of scan tiles, where the largest tiles are the *Std-Res 3D scan*, followed by *High-Res 3D scan*, then the *MS-OCT*, and the *3D microscopy* generating the smallest tiles. Note that the tiles of both 3D scanning systems are not rectangular. This is due to the camera mounting angle (β), relative to the painting plane. The images are captured from opposing angles, whereby the topography can only be reconstructed for those regions, that can be seen by both cameras, in turn leading to this resulting shape for every tile.

the data at a faster rate (mainly related to the relative tile size), where the MS-OCT system took four nights and the High-Res 3D scan system only several hours to scan the complete surface. Here we should note that these are not commercial systems, and optimization might still lead to even faster acquisition.

Measurement occlusions and specular reflections

All techniques have limitations in the terms of measurement occlusions. Firstly, none of the methods are (currently) able to capture 'overhangs' or undercuts on a surface, meaning they cannot imaging underneath flaking or cupping paint, or capture the underside of overhanging impasto (not typically present in Golden Age paintings). Although OCT would be able to detect these layer transitions, currently the segmentation for this is not incorporated in the data processing. It could however be made visible in a virtual cross-section using this data. Also the current method of data representation — as a 2D image — does not allow for representing these types of 3D structures. Furthermore, there are some limitations imposed by the imaging and illumination angles. Both the MS-OCT and the 3D scan systems image the surface under an angle (indicated by imaging angle β in Figure 6.2(a) and 6.3(a)), whereby deep cracks or the sides of highly sloped areas (i.e. of an impasto) might be occluded from view, and therefore not measured. In the case of the 3D scan systems this might be alleviated by adding additional cameras, providing additional imaging angles. In the 3D microscopy occlusions can occur in the areas where the shading or shadows are too dark (i.e. under-exposure), created by the raking light illumination. This can be (partially) alleviated by additional low intensity ring lighting. However, both the raking light illumination and the ring light-

ing can cause light to reflect directly into the lens, leading to over-exposure. For these pixels the 3D microscope will not be able to reconstruct the 3D topography, leading to missing data. Careful positioning of the raking light and a low-level ring lighting minimize this effect.

Measuring dark regions

As all imaging techniques rely on optics, they all have difficulty scanning areas where (almost) all light is absorbed, and therefore the spectral reflectance is low (i.e. dark/black areas). In scanning very dark areas, the 3D scan systems have scanning artifacts, showing more sporadic and noisy data. Although not specifically the case in this painting, another limitation of the 3D scanning algorithm is that it relies on (some) salient features to reconstruct the topography. If scanning tiles completely lack any features (completely uniform in color), the algorithm can fail to reconstruct the 3D shape.

Scanning additional modalities

All three techniques offer the possibility to provide other modalities in addition to scanning the topography. The MS-OCT — as is actually its main application — is capable of mapping the stratigraphy of the (semi-)transparent paint layers, providing information about varnish- and glaze-layer thickness as well as the 3D topographies of these layers. The 3D scanners and 3D microscopy both offer color information in addition to topography, which for both techniques are one-to-one intrinsically aligned data sets. MS-OCT, however, does not provide such color information. The lack of this information can be overcome by mapping the topographical (and stratigraphy) data to a color image, allowing enhanced data interpretation and ease of localization on the artwork. Furthermore, the Std-Res 3D scan system is capable of measuring additional modalities of a painting's appearance, namely measuring the spatially-varying gloss of the surface [25]. This has the potential to offer an even richer documentation of the appearance and a painting's state.

6.5.7. Merits and limitations of the scanning implementations

In addition to merits and limitations imposed by the scanning techniques themselves, the design implementations of the different scanning systems used in this case study also have their specific merits and limitations. These aspects are not fundamental to the techniques but rather a consequence of design choices made for the scanning systems and/or maturity of the systems, which includes the image processing pipeline.

Automated scanning range

Although all systems are portable (allowing *in-situ* scanning), their automated scanning range differs substantially. Where the MS-OCT has an automated range of 200 mm × 200 mm, the 3D microscope has a range of 500 mm × 500 mm, and the 3D scan systems have a range of (more than) 1 m × 1 m. These differences are not directly technically limited, as all imaging techniques might be fitted on larger

movement axes. Of all of the techniques, the 3D microscope would be most demanding in terms of step size accuracy (sub-millimeter accuracy in xy), whereas for the MS-OCT and 3D scan systems a lateral stepping in the millimeter range would suffice (if relying on other tile alignment strategies in the case of MS-OCT). An additional limitation of the current 3D microscope configuration is that the size of the painting to be scanned is limited by the dimensions of the surrounding frame (as this frame was especially developed for the *Girl in the Spotlight* project, it was limited to 500 mm × 500 mm). This could be alleviated by mounting the microscope on a vertical frame (currently under development by Hirox with similar automated range). This would also limit the amount of dust particles and fibres that settle on the painting during scanning, which are currently visible in the 3D microscopy data. The 3D microscope does currently offer the advantage of online processing of the individual tiles (and normally also online stitching, which was omitted for time reasons in this case study). The advantage of this approach is that real-time data image quality analysis might be carried out, and intervene in the case of errors (e.g. the surface moves outside the set focal range). For the MS-OCT and 3D scan systems, alignment now has to be very carefully calibrated beforehand, and the correctness and completeness of the scan can only be verified after is has been captured.

Ease-of-use

As the Hirox 3D digital microscope is a commercial system, it can be operated by a trained operator, where as the other systems are still research prototypes, requiring specialist operation for optimal functionality.

6.6. Conclusions

Based on the case study presented in this paper — 3D scanning *Girl with a Pearl Earring* by Johannes Vermeer — we conclude that all techniques are capable of capturing the spatially-varying topographical features of such a painting at a relevant scale (i.e. capable of visualizing individual cracks). However, detailed investigation of the scan results show that resolution of the Std-Res 3D scan is not sufficient to capture the finer cracks, which are of interest (see for instance Figure 6.7(a)). Measurements of a reference target, also show that these techniques have sufficient accuracy and precision to measure these fine details, although possibly not enough for capturing the finest details with the Std-Res 3D scan.

Moreover, the results show the capabilities of all four systems to combine high-resolution capture of the surface topography, with a large planer scale, surpassing existing painting scanner capabilities. Where previous laser- and structured light-based systems had a spatial resolutions between 40 µm and 100 µm, earlier work using focus variation based systems was limited to a scanning an individual tile, in the range of mm^2.

Given the level of detail (for instance shown in Figure 6.7), we argue that for the description of topography, the 3D data provides much more detail and richer information than conventional documentation techniques, and which could not be reached with existing 3D scanning systems. This moves the analysis of the topog-

raphy from a subjective and — in the case of a tracing image — binary visualization of the craquelure, to an objective measurement of these fine details. We believe this to be true for all 3D scanning techniques shown in this paper.

We show how such (objective) 3D data of a painting can be interpreted and used (e.g. for conservation purposes) based on case study data, exemplified by three ROI and rendered visualizations of a larger region and detail of the painting's surface.

6.6.1. Interpretation of case study 3D data and its (future) application(s)

Specifically for the case of the *Girl with a Pearl Earring* the 3D data provides new insights into the condition of the painting. Contrary to earlier documentation of the crack pattern (as in Figure 6.1(b)), results indicate that the extent of the craquelure is similar across the facial and background regions (see Figure 6.10(b)). Also effects like 'moating' surrounding impasto, flaking and consolidation of paint, can be visualized with the 3D data. This type of data can support conservators in evaluating the condition of the painting, and determining the need for any interventions.

In terms of application we believe that all techniques are suitable for visualizing height variations typically found on a (17^{th} century) painting. Such data can, for instance, be used to extract the crack pattern of the surface and thereby potentially support monitoring the increase of cracks over time. Automated crack pattern recognition, extraction and comparison remain to be investigated.

Currently there are no measurements of height variations of painting surfaces over time on this scale and at this level of accuracy (i.e. global shape variations on panel paintings was investigated by Palma et al. [30]). It is therefore difficult to determine if the 3D scanning techniques offer the accuracy and precision needed to monitor subtle height variations occurring on paintings over time.

All techniques capture one or more modalities of a painting: topography, color, gloss and/or stratigraphy. They provide possibilities to document the appearance of an artwork in a more complete way, complementing the many imaging techniques that are already applied during a technical examination. Documenting the painting's appearance and condition is important, as the artwork itself will inevitably degrade further in the centuries to come, unfortunately probably even up to the point of total disintegration, no matter the conservation efforts. 3D data might be used to create 3D (printed) reproductions, and could also serve as a starting point for (digital) reconstructions, showing past (and future) states of an artwork (i.e. removing or extrapolating craquelure effects).

6.6.2. Comparison of resolution, accuracy and precision

Based on the measurements of the reference target, we conclude, as expected, that Multi-scale optical coherence tomography (MS-OCT) and 3D microscopy offer the highest accuracy and precision, as compared to the 3D scanning systems (based on fringe-encoded stereo imaging). We find that the standard deviations on the measurements of the reference target all lie within the range that would be expected based on their respective measurement uncertainty, ranging between 2.5 µm and

6.4 µm for the 3D microscopy to maximum 16.0 µm for the Std-Res 3D scan. However, it remains to be investigated if the accuracy of these systems is sufficient for monitoring paintings over time, as currently no data exists on the magnitudes of topographical changes occurring in paintings, including those kept under museum conditions. It should also be noted that the metal material (and coating) of the reference target used for this comparison is not ideal for any of these 3D scanning techniques. Therefore, measurements on less reflective, dielectric materials (such as paint or plastic) are potentially more accurate, than the results presented for the reference target.

Although the MS-OCT and 3D Microscopy offer higher measurement accuracy and precision (in the height measurement), the single measurement areas (tiles) of these systems are very small. This affects the scanning speed and thereby limits their suitability to scan complete paintings, even at the size of *Girl with a Pearl Earring* (39 cm × 44.5 cm). Also the stitching of these tiles to create larger topographical maps potentially increases the measurement error. Another limitation of the MS-OCT is that it has a relatively low lateral sampling resolution 8.53 µm × 67.56 µm/pixel. However, this is independent of the axial resolution (z) and not fundamental to the technique, and could therefore potentially be increased. For the 3D Microscopy the tile size cannot be increased, without sacrificing the axial resolution. However, acquisition speed, image processing algorithms and general computing power continue to improve, offering potential of significantly faster scanning in the future. In the case of 3D scanning systems based on fringe-encoded stereo imaging, the lateral and axial resolutions are linked, and the technique offers flexibility in selecting a relevant sampling resolution; however, further increasing the axial resolution (z) has as a consequence limiting the depth-of-field, thereby limiting the maximum height variation which can be captured within one scan tile. In other words, only paintings with very high local planarity (i.e. very limited to no impasto) can be scanned at even higher resolutions.

6.7. Future work

The development of approaches to deal with high-resolution 3D scanning data of non-rigid artiacts like paintings, is considered a crucial next step to enable (over time) data comparison of paintings. Further investigation into alignment and stitching strategies capable of large-scale, non-rigid (sub-pixel) alignment in xy and z are also considered a pre-condition for meaningful comparison of painting data sets, such as collected in this case study. Also the use of multi-modal scan data should be given further consideration, to potentially improve data alignment. We believe a multi-scale scanning approach (extending, for instance the approach used in the Bosch Research Project [47]), could potentially be suitable for topography data alignment.

The applicability of 3D scanning systems for scanning complete paintings, such as discussed in this paper, might be further improved by increasing the scanning speed and automated scanning range. A vertical scanning orientation for 3D microscopy would also increase its flexibility, enabling the scanning of larger paintings (currently under development). Furthermore, the implementation of an auto-focus

or auto-alignment functionality of the focal plane for the 3D microscopy and 3D scanning systems will be needed to ensure accurate measurement of larger (and potentially more warped) paintings. As 3D scanning appears to be the most promising in terms of scan speed to capture complete paintings, we suggest further investigation into increasing the scanning accuracy, precision and robustness, by for instance improving the imaging strategy in combination with further improving the data processing algorithms.

The use of 3D scanning data in conservation/restoration (e.g. scnad before and after treatment) remains to be investigated. Investigations into the measurement of samples (i.e. reconstructions of paintings) exposed to accelerated aging might provide more insight into the accuracy and precision needed to monitor paintings over time. In addition to this, comparison of current 3D measurements of a painting kept under conservation conditions, will have to take place (in the future) to verify such findings for real-world cases.

References

[1] J. Hermans, G. Osmond, A. Van Loon, P. Iedema, R. Chapman, J. Drennan, K. Jack, R. Rasch, G. Morgan, Z. Zhang, M. Monteiro, and K. Keune, *Electron microscopy imaging of zinc soaps nucleation in oil paint,* Microscopy and Microanalysis **24**, 318 (2018).

[2] J. van Asperen de Boer, *An introduction to the scientific examination of paintings,* Nederlands Kunsthistorisch Jaarboek (NKJ) / Netherlands Yearbook for History of Art **26**, 1 (1975).

[3] S. Legrand, F. Vanmeert, G. Van der Snickt, M. Alfeld, W. De Nolf, J. Dik, and K. Janssens, *Examination of historical paintings by state-of-the-art hyperspectral imaging methods: from scanning infra-red spectroscopy to computed X-ray laminography,* Heritage Science **2**, 1 (2014).

[4] J. Wadum, *The Girl with a Pearl Earring - Restoration history,* in *Vermeer illuminated: A report on the restoration of the View of Delft and The Girl with a Pearl Earring by Johannes Vermeer* (VK Publishing/Inmerc, 1995) Chap. 3.1, pp. 18–21.

[5] W. S. Elkhuizen, B. A. Lenseigne, C. Weijkamp, S. C. Pont, J. M. Geraedts, and J. Dik, *A 3D printed reconstructing of a painting's original size - Showing the original size of Saul and David by Rembrandt,* in *Visual Science of Art Conference* (Barcelona, Spain, 2016) p. 1.

[6] Mauritshuis, *Rembrandt? The case Saul and David,* (2015), (Accessed: 2019-05-15).

[7] Van Gogh Museum, *Zonnebloemen blijven voortaan thuis,* (2019), (Accessed: 2019-02-17).

[8] A. Van Loon, *Color changes and chemical reactivity in seventeenth-century oil paintings*, Phd thesis, University of Amsterdam (2008).

[9] S. Bucklow, *The classification of craquelure patterns,* in *The conservation of easel paintings - Principles and Practice*, edited by J. H. Stoner and R. A.

Rushfield (Routledge, Abingdon, UK, 2012) 1st ed., Chap. 16.

[10] S. Bucklow, *The description and classification of craquelure,* Studies in Conservation **44**, 233 (1999).

[11] S. Bucklow, *Cracks and the perception of paintings,* (Accessed: 2019-05-15).

[12] M. El-Youssef, S. Bucklow, and R. Maev, *The development of a diagnostic method for geographical and condition-based analysis of artworks using craquelure pattern recognition techniques,* Insight - Non-Destructive Testing and Condition Monitoring **56**, 124 (2014).

[13] G. Schirripa Spagnolo, *Virtual restoration: detection and removal of craquelure in digitized image of old paintings,* in *Optics for Arts, Architecture, and Archaeology III* (SPIE Optical, Munich, Germany, 2011) pp. 1–9.

[14] F. Blais, J. Taylor, L. Cournoyer, M. Picard, L. Borgeat, L.-G. Dicaire, M. Rioux, J.-A. Beraldin, G. Godin, C. Lahnanier, and G. Aitken, *Ultra-High Resolution Imaging at 50 micron using a Portable XYZ-RGB Color Laser Scanner,* in *International Workshop on Recording, Modeling and Visualization of Cultural Heritage*, edited by M. Baltsavias, A. Gruen, L. van Gool, and M. Pateraki (National Research Council Canada, Ascona, Switzerland, 2005) pp. 1–16.

[15] F. Blais, J. Taylor, L. Cournoyer, M. Picard, L. Borgeat, G. Godin, J.-A. Beraldin, M. Rioux, and C. Lahanier, *Ultra high-resolution 3D laser color imaging of paintings: the 'Mona Lisa' by Leonardo da Vinci,* in *7th International Conference on Lasers in the Conservation of Artworks*, edited by M. Castillejo, P. Moreno, M. Oujja, R. Radvan, and J. Ruiz (National Research Council Canada, Madrid, Spain, 2007) pp. 1–8.

[16] Verus Art, *Verus Art textured reproductions,* (2017), (Accessed: 2019-05-25).

[17] M. K. Jackson and L. MacDonald, *Color Management in 3D Fine-Art Painting Reproduction,* in *Color and Imaging Conference* (Society for Imaging Science and Technology, Vancouver, Canada, 2018) pp. 396–401.

[18] Factum Arte, *Lucida: Discovering an artwork through its surface*, Tech. Rep. (Factum Foundation, Madrid, Spain, 2016).

[19] D. Zalewski, *The factory of fakes - how a workshop uses digital technology to craft perfect copies of threatened art,* The New Yorker , 66 (2016).

[20] Van Gogh Museum, *Van Gogh museum - Relievo collection,* (Accessed: 2017-10-13).

[21] D. Akça, A. Grün, B. Breuckmann, and C. Lahanier, *High Definition 3D-Scanning of Arts Objects and Paintings,* in *Optical 3-D Measurement Techniques VIII*, Vol. II, edited by A. Gruen and H. Kahmen (Zurich, Switzerland, 2007) pp. 50–58.

[22] M. Karaszewski, M. Adamczyk, R. Sitnik, J. Michoński, W. Załuski, E. Bunsch, and P. P. Bolewicki, *Automated full-3D digitization system for documentation of paintings,* in *Optics for Arts, Architecture, and Archaeology IV*, Vol. 8790, edited by L. Pezzati and P. Targowski (Munich, Germany, 2013) pp. 1–11.

[23] B. Breuckmann, *3-Dimensional Digital Fingerprint of Paintings,* in *19th Euro-*

pean Signal Processing Conference (IEEE, Barcelona, Spain, 2011) pp. 1249–1253.

[24] T. Zaman, P. Jonker, B. Lenseigne, and J. Dik, *Simultaneous capture of the color and topography of paintings using fringe encoded stereo vision,* Heritage Science **2**, 1 (2014).

[25] W. Elkhuizen, T. Essers, Y. Song, J. Geraedts, S. Pont, and J. Dik., *Gloss, Color and Topography Scanning for Reproducing a Painting's Appearance using 3D printing,* Journal of Computing and Cultural Heritage , 1 (2019).

[26] M. van Hengstum, T. Essers, W. Elkhuizen, D. Dodou, Y. Song, J. Geraedts, and J. Dik, *Development of a high resolution topography and color scanner to capture crack patterns of paintings,* in *Eurographics workshop on graphics and cultural heritage*, edited by R. Sablatnig and M. Wimmer (The Eurographics Association, Vienna, Austria, 2018) pp. 1–10.

[27] I. Cacciari, P. Nieri, and S. Siano, *3D Digital Microscopy for Characterizing Punchworks on Medieval Panel Paintings,* Journal on Computing and Cultural Heritage **7**, 1 (2014).

[28] K. J. Van den Berg, M. Daudin, I. Joosten, B. Wei, R. Morrison, and A. Burnstock, *A comparison of light microscopy techniques with scanning electron microscopy for imaging the surface of cleaning of paintings,* in *9th International Conference on NDT of Art* (Jerusalem, Israel, 2008) pp. 25–30.

[29] F. Del Sette, F. Patané, S. Rossi, M. Torre, and P. Cappa, *Automated displacement measurements on historical canvases,* Heritage Science **5**, 1 (2017).

[30] G. Palma, P. Pingi, E. Siotto, R. Bellucci, G. Guidi, and R. Scopigno, *Deformation analysis of Leornado da Vinci's "Adorazione dei Magi" through temporal unrelated 3D digitization,* Journal of Cultural Heritage , 1 (2019).

[31] C. S. Cheung, M. Spring, and H. Liang, *Ultra-high resolution Fourier domain optical coherence tomography for old master paintings,* Optics Express **23**, 1 (2015).

[32] M. Wojtkowski, *High-speed optical coherence tomography: basics and applications,* Applied Optics **49**, 1 (2010).

[33] P. Targowski, B. Rouba, M. Wojtkowski, and A. Kowalczyk, *The Application of optical coherence tomography to non-destructive examination of museum objects,* Studies in Conservation **49**, 107 (2004).

[34] H. Liang, R. Cucu, G. M. Dobre, D. A. Jackson, J. Pedro, C. Pannell, D. Saunders, and A. G. Podoleanu, *Application of OCT to examination of easel paintings,* Second European Workshop on Optical Fibre Sensors **5502**, 378 (2004).

[35] M. L. Yang, C. W. Lu, I. J. Hsu, and C. C. Yang, *The use of Optical Coherence Tomography for monitoring the subsurface morphologies of archaic jades,* Archaeometry **46**, 171 (2004).

[36] P. Targowski and M. Iwanicka, *Optical Coherence Tomography: its role in the non-invasive structural examination and conservation of cultural heritage objects—a review,* Applied Physics A **106**, 265 (2012).

[37] T. Callewaert, J. Dik, and J. Kalkman, *Segmentation of thin corrugated layers in high-resolution OCT images,* Optics Express **25**, 1 (2017).

[38] National Instruments, *LabVIEW,* .

[39] J.-Y. Bouguet, *Camera Calibration Toolbox for Matlab,* (2013).

[40] Mitani Cooperation Visual System, *e-tiling software,* (Accessed: 2019-07-03).

[41] *SciPy for Python,* .

[42] *OpenCV,* .

[43] Rubert & Co Ltd, *Precision reference specimens,* (2019), (Accessed: 2019-05-02).

[44] R. Pintus, K. Pal, Y. Yang, T. Weyrich, E. Gobbetti, and H. Rushmeier, *A Survey of Geometric Analysis in Cultural Heritage,* Computer Graphics Forum **35**, 4 (2016).

[45] K. Groen, I. Van der Werf, K. Van der Berg, and J. Boon, *Scientific Examination of Vermeer's 'Girl with a Pearl Earring',* in *Vermeer studies*, edited by I. Gaskell and M. Jonker (National Gallery of Art, 1998) pp. 169–183.

[46] S. Schmitt, *Examination of paintings treated by Pettenkofer's process,* Studies in Conservation **35**, 81 (2014).

[47] L. Hoogstede, R. Spronk, R. G. Erdmann, R. K. Gotink, M. Ilsink, J. Kolderweij, H. Nap, and D. Veldhuizen, *Image Processing for the Bosch Research and Conservation Project,* in *Hieronymus Bosch: Painter and Draughtsman - Technical Studies* (Mercatorfonds, 2016) Chap. II, pp. 30–51.

[48] T. Zaman, *Development of a Topographic Imaging Device for the Near-Planer Surfaces of Paintings*, MSc thesis (Delft University of Technology, Delft, The Netherlands, 2013).

Table 6.1: Characteristics of scanning systems used to capture painting topography, including: The scanning technique, modalities captured by the 3D scanners, resolution, scanner field-of-view (or scan tile), orientation of the painting, size of the automated scanning range, the flexibility to scan large areas (yes or no), scanning speed, and a short description of the scan setup. The flexibility in range (Flex. range) is judged negatively, if the frame limits the size of the painting to be scanned, or in the case of using a cartesian frame, which is deemed difficult to extend or move.

	Scanning technique	Scan modalities		Resolution (xy)	Accuracy (z)	Field of view (scan tile)	Orient.	Autom. range	Flex. range	Scan speed	Scan setup
		Top.	Color								
Laser Triangulation											
Blais et al. [14, 15]	RGB laser spot triangulation	x	x	60 µm	10 µm	N/A	v	40 mm × 120 mm	y	≈23 h/m^2	Tripod, manual positioning
Verus Art [16, 17]	RGB laser spot triangulation	x	x	100 µm	?	N/A	v	≈1 m × 1 m[1]	n(?)	?	Automated xy-frame (?)
Factum Arte [18, 19]	Laser line triangulation	x		100 µm	25 µm	N/A	v	480 mm × 480 mm	y	4 h/m^2	Partial xy-automation, manual positioning on larger frame
Del Sette et al. [29]	Laser spot triangulation	x		50 µm(x), 20 mm(y)	20 µm	N/A	v	300 mm × 300 mm	y	0.8 h/m^2	Partial xy-automation, manual positioning on larger frame
Van Gogh Museum [20]	Laser triangulation	x		?	?	?	?	?	?	?	?

Continued on next page

[1] Estimated based on video footage of scanner

Table 6.1 – continued from previous page

	Scanning technique	Scan modalities		Resolution (xy)	Accuracy (z)	Field of view (scan tile)	Orient.	Autom. range	Flex. range	Scan speed	Scan setup
		Top.	Color								
Structured light projection											
Akca et al. [21]	Structured light projection	x	x	60 µm	15 µm	60 mm × 80 mm	v	Not automated	y	?	Tripod, manual positioning
Breuckmann [23]	Structured light projection	x	x	40 µm	5 µm	≈100 mm × 125 mm	v	Not automated	y	≈5 h/m^2	Tripod, manual positioning
Karaszewski et al. [22]	Structured light projection	x	x	≈60 µm[2]	N/A	50 mm × 50 mm	v	≈2 m × 2 m	n	≈270 h/m^2[3]	xy-automation, manual z-alignment
Zaman et al. [24, 48][4]	Structured light projection	x	x	50 µm	38 µm	≈170 mm × 100 mm	v	1 m (x)	y	5 h/m^2	Linear automation (x) on tripod, manual positioning per row
Palma et al. [30]	Structured light projection	x		500 µm	?	1100 mm × 900 mm	v	Not automated	y	?	Tripod, manual positioning

Continued on next page

[2]Estimated based on projector resolution and specified field-of-view
[3]Reported time includes data processing
[4]This system can be regarded as the predecessor of the High-Res and Std-Res 3D scan systems used in this case study

Table 6.1 – continued from previous page

	Scanning technique	Scan modalities		Resolution (xy)	Accuracy (z)	Field of view (scan tile)	Orient. range	Autom.	Flex. range	Scan speed	Scan setup
		Top.	Color								
Focus variation microscopy											
Van den Berg et al. [28]	Focus variation microscopy	x	x	≈1 µm	2.5 µm[5]	≈1 mm × 2 mm	h	None used	n	?	Microscope stage, small samples
Cacciari et al. [27]	Focus variation microscopy	x	x	≈60 µm	unknown	≈1 mm × 1.3 mm	h	Not automated	n	N/A	xy-frame, manual re-positioning(?)

[5] Although advertised at this level of accuracy the authors mention that this is probably not realistic based on their findings

Table 6.2: Specifications of 3D scanning systems used in this case study, including: system design, scan modalities, system components, computational hardware used, resolution, scan area, settings used, and the configuration of the setup. The latter specifies the orientation of the painting during scanning, the imaging distance l, which is the closest point of the system to the painting's surface, and the imaging angle β, describing the angle between the painting's surface normal and the optical axis of the imaging components.

	MD-OCT	Std-Res 3D scan	High-Res 3D scan	3D Microscopy	White Light Confocal Profilometry
System model	Custom	Custom, 2nd gen.	Custom design, 3rd gen.	Hirox RH-2000	Hirox Nano Point Scanner
Scan modalities(s)					
Topography	x	x	x	x	x
Color		x	x	x	
Stratigraphy	x				
Gloss		x			
Imaging component(s)	1	2	2	1	1
Camera model	N/A	Nikon D800E	Canon 5DS-R	Hirox	JYFEL
Lens model	Thorlabs LSM04-BB	Nikkor PC-E 85mm	Canon TS-E 90mm	MXB-5000REZ at 140x	NP3
Lens extension tube(s)	N/A	N/A	Canon EF25 II	N/A	N/A
Filter(s)	N/A	3 Hoya HD polarizers	3 Canon polarizers	N/A	N/A
Illumination component(s)	1	1	1	2	1
Type	SLD	Projector	Projector	Fiber optics LED	Fiber optics LED
Model/type	N/A	Acer X113H	AXAA M6	Hirox	JYFEL
Illumination intensity	N/A	2800 lm	1200 lm	Raking Light at 100% & Dark Field at 10%	100%
Computational hardware					
Computer	Dell T1700	ASUSTeK	ASUSTeK	Apple iMac	Apple iMac
Processor	Intel Xeon E3-1271v3	Intel Core i7	Intel Core i7	Intel Core i5	Intel Core i5
RAM Memory	16 GB	128 Gb	128 Gb	32 GB	32 GB
Memory	1 TB SSD	500 Gb SSD	500 Gb SSD	1TB SSD	1TB SSD

Continued on next page

Table 6.2 – continued from previous page

	MD-OCT	Std-Res 3D scan	High-Res 3D scan	3D Microscopy	White Light Confocal Profilometry
Scan sampling resolution					
Lateral resolution (xy)	8.5 µm × 67.6 µm	25 µm	7 µm	1.1 µm	2.6 µm
Depth resolution (z)	3.0 µm	27.5 µm	17.5 µm	N/A	<0.150 µm[6]
Scan area					
Tile size (xy)	5 mm × 5 mm	170 mm × 100 mm	60 mm × 40 mm	2.1 mm × 1.31 mm	N/A
Depth-of-field	1.87 mm	≈8.5 mm	≈1 mm	0.05 mm	1.40 mm
Automated range (xy)	0.2 m × 0.2 m	1.3 m × 1.3 m	1.0 m × 1.0 m	0.5 m × 0.5 m	0.5 m × 0.5 m
Settings					
ISO	N/A	100	100	Gain 0 dB	N/A
Aperture	N/A	1/16	1/16	Full open	N/A
Shutter speed	N/A	0.5 s	3.2 s	1/250s	N/A
Other parameters	N/A	N/A	N/A	Edge=9, Sat.=2, Color=2	N/A
Images per tile	1024	26	26	≈50 for 450 µm top-bottom range	N/A
Tile overlap	N/A	41%(x), 30%(y)	20%(x), 25%(y)	30%	N/A
Configuration					
Painting orientation	vertical	vertical	vertical	horizontal	horizontal
Imaging distance (l)	≃42 mm	440 mm	175 mm	10 mm	12 mm
Imaging angle (β)	≈5.0°	40°	21.5°	0°	0°

[6] Stated depth accuracy by manufacturer

Table 6.3: Scan results of four 3D imaging systems for *Girl with a Pearl Earring* by Johannes Vermeer

	MS-OCT	Std-Res 3D Scan	High-Res 3D Scan	3D Microscopy
Data size (per tile)[7]				
Raw data	525Mb	2.0Gb	1.6Gb	N/A[8]
Processed data	525Mb	15.0Gb[9]	11.4Gb[9]	4Mb
Data size equivalent (per m^2)[10]				
Raw data	210 Gb	111 Gb	666 Gb	N/A[8]
Processed data	210 Gb	882 Gb[9]	4.75 Tb[9]	1.45 Tb
Imaging time				
Capture time (per tile)	20s	5m00s	2m14s	3s
Processing time (per tile)	50s[11] (offline)	6m20s (offline)	8m45s (offline)	2.6s (online)

[7]Note that the tile sizes are very different between systems
[8]The individual images which constitute a focus stack are not saved, due to storage limitations
[9]This is the total data size per tile, including raw and processed image files (i.e. conversion of camera RAW format to TIFF)
[10]This excludes any overlap between tiles
[11]This includes the time needed for de-trending and stitching the tiles, which was integrated in the processing of the individual tiles

Table 6.4: Comparison of reference target measurements (sample no. 513E by Rubert & Co [43], as depicted in Figure 6.8). The Nano Point Scanner (NPS) measurements are taken as the gold standard. The grooves are labeled from the deepest (1) to most shallow (4) groove, where (t) denotes the measurement at the sample's top surface and (b) the measurement at bottom of the groove. For every measurement region, N denotes the number of measurements, σ the standard deviation of those measurements, Δ the height difference between the top and bottom (mean difference), and Err. the error with respect to the NPS measurement. Except N all the results are specified in µm. The errors (relative to the NPS measurements) are plotted is Figure 6.9.

Groove	Exp. depth	NPS				MS-OCT				Std-Res 3D scan				High-Res 3D scan				3D microscopy			
	Δ (µm)	N	σ (µm)	Δ (µm)	Err. (µm)	N	σ (µm)	Δ (µm)	Err. (µm)	N	σ (µm)	Δ (µm)	Err. (µm)	N	σ (µm)	Δ (µm)	Err. (µm)	N	σ (µm)	Δ (µm)	Err. (µm)
1 (t)	1000	1220	0.22	984	N/A	250	7.4	982	-2	22.5k	15.0	972	-12	7000	12.9	987	3	340k	3.5	987	3
1 (b)		20	0.05			250	6.2			150	9.2			2250	8.6			240k	3.1		
2 (t)	500	1050	0.42	496	N/A	400	5.8	490	-6	10.5k	10.2	520	24	7750	12.2	496	0	348k	2.5	496	0
2 (b)		10	0.12			300	1.6			2400	17.7			1000	7.2			228k	3.8		
3 (t)	200	910	0.21	195	N/A	990	4.5	194	-1	12k	10.3	206	11	2250	8.6	206	11	560k	3.2	194	-1
3 (b)		200	0.08			550	1.4			7500	9.3			7000	8.3			456k	3.4		
4 (t)	30	1100	0.21	29	N/A	600	3.0	29	0	4500	10.8	37	8	6250	10.1	35	6	125k	6.3	31	2
4 (b)		10	0.05			400	4.1			750	10.4			1050	10.3			155k	5.2		

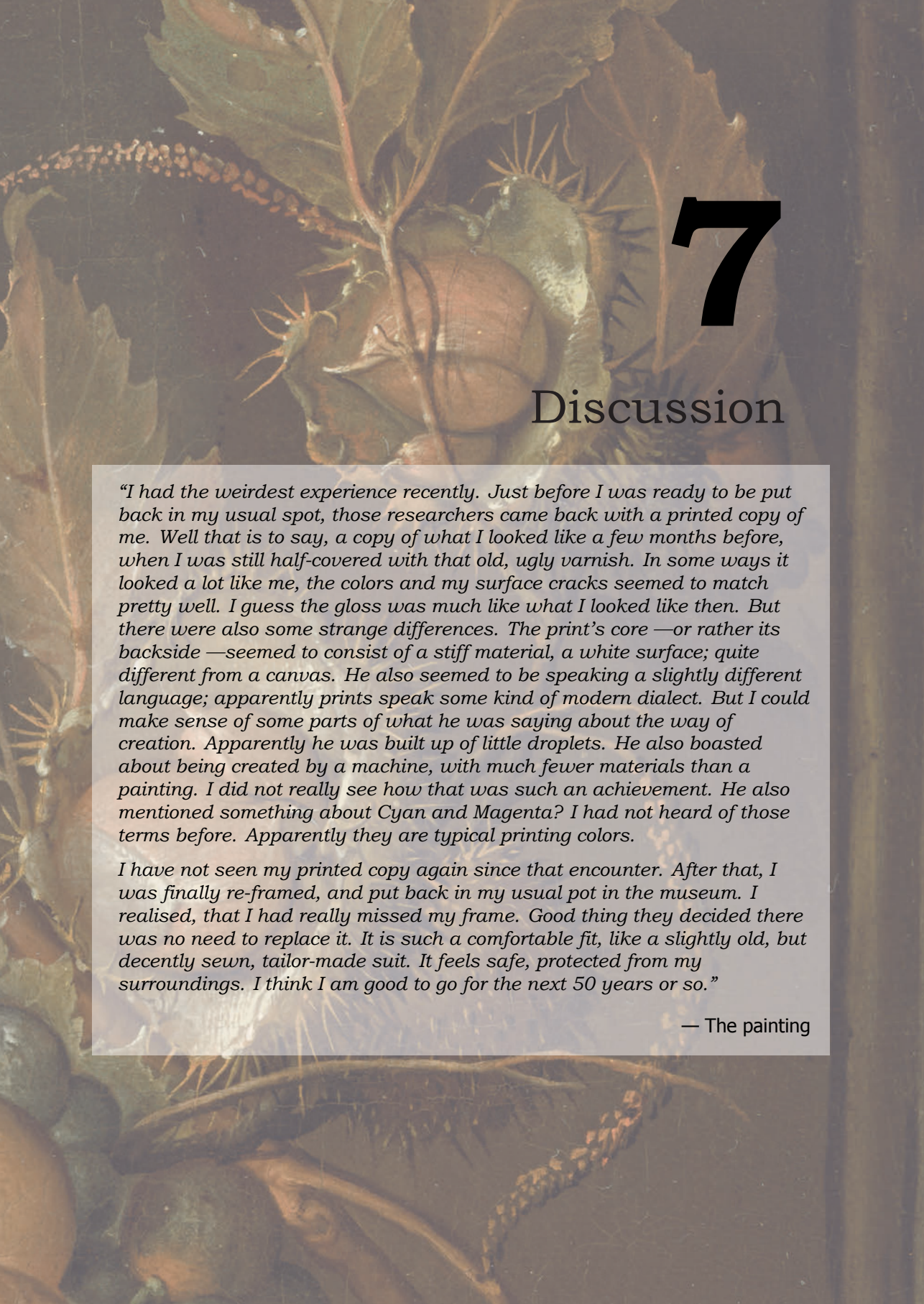

7

Discussion

"I had the weirdest experience recently. Just before I was ready to be put back in my usual spot, those researchers came back with a printed copy of me. Well that is to say, a copy of what I looked like a few months before, when I was still half-covered with that old, ugly varnish. In some ways it looked a lot like me, the colors and my surface cracks seemed to match pretty well. I guess the gloss was much like what I looked like then. But there were also some strange differences. The print's core —or rather its backside —seemed to consist of a stiff material, a white surface; quite different from a canvas. He also seemed to be speaking a slightly different language; apparently prints speak some kind of modern dialect. But I could make sense of some parts of what he was saying about the way of creation. Apparently he was built up of little droplets. He also boasted about being created by a machine, with much fewer materials than a painting. I did not really see how that was such an achievement. He also mentioned something about Cyan and Magenta? I had not heard of those terms before. Apparently they are typical printing colors.

I have not seen my printed copy again since that encounter. After that, I was finally re-framed, and put back in my usual pot in the museum. I realised, that I had really missed my frame. Good thing they decided there was no need to replace it. It is such a comfortable fit, like a slightly old, but decently sewn, tailor-made suit. It feels safe, protected from my surroundings. I think I am good to go for the next 50 years or so."

— The painting

7.1. 3D scanning and digital fabrication in the cultural heritage domain

In this thesis we focused on 3D scanning and digital fabrication to create reproductions of paintings. With these rapid developments in 3D scanning and digital fabrication technology, the (potential) applications of these technologies in relation to cultural heritage (CH) domain is fast expanding.

As was recognized in the course of this PhD thesis, 3D scanning of paintings might have more applications than solely to create reproductions. The use of 3D scanning in the CH domain was recently reviewed by Pintus *et al.* [1], and clustered based on three types of classifications: the geometric scale on which the scanning focuses — micro, meso and macro scale —, the number of artifacts scanned and compared within an analysis — single, one-to-many, and many-to-many —, and the application — perceptual enhancement, restoration and preservation, monitoring, interpretation, and collection analysis —. We argue that our contribution mainly falls in the application class of *perceptual enhancement*, although we envision that 3D data of paintings can also contribute to other applications like restoration and preservation, and monitoring. An overview of (potential) applications is provided in Section 7.1.1.

Scopigno *et al.* [2] recently reviewed the use of digital fabrication techniques (including subtractive and additive techniques), and their (potential) applications, for the CH domain. In their survey, digital fabrication techniques are qualitatively evaluated on various aspects. One aspect that is particularly relevant for this thesis is "*material adequacy*". They state that the response to a reproduction can be very different depending on the *look and feel* created by a fabrication technique, going on to say that CH "practitioners consider the material, colour and texture as very important aspects of a reproduction"[2]. This, we believe, is in line with our findings (see Chapter 2). In their discussion they mention the need for better color reproduction (improving on binder-jetting 3D printing technology), higher geometrical precision (introduced by layer stacking, for instance in Fused Deposition Modeling (FDM)), and the inclusion of *surface reflection properties*. We would argue the 3D printing technique employed in our case studies, overcomes many of these limitations, on color and geometric precision, relative to the techniques that they review. Furthermore, work presented in this thesis provides major contributions on the topic of surface reflection properties, as we have specifically focused on spatially-varying gloss reproduction.

Scopigno *et al.* [2] recognize a wide range of applications for digital fabrication techniques in the CH domain, having an impact in various CH sub-disciplines like restoration, education, creativity and dissemination. We find that the work conducted in this thesis, and a variety of related and similar projects, show the potential of painting reproductions for a large number of the mentioned applications. Moreover, some project carried out, related to this PhD project, additionally show the potential of the used digital fabrication technique — full-color material jetting — in relation to CH. Examples of (potential) applications are provided in Section 7.1.2.

7.1.1. 3D scan data of paintings and its applications

Besides using scanning capabilities to create printed reproductions, the scan data might also serve other purposes. The color, relief and gloss data might for instance be used to create (interactive) visualizations of a painting's surface. This could potentially support restorers in understanding (the extent of) degradation of a painted surface, or in visualizing their restoration efforts. Such renderings might also prove interesting to museum visitors, allowing them to zoom in on intricate details of the painting, for instance by interactively rendering the material properties to match the viewing angle and local illumination (e.g. like Darling and Ferwerda [3]).

The suitability of the scanning technology for applications as mentioned above, was explored in the case study scanning *Girl with a Pearl Earring* by Johannes Vermeer, in the context of *The Girl in the Spotlight* research project [4]. We show that the 3D data can be used to visualize the crack patterns of a painting, and can thereby support the interpretation of its condition and conservation history (as discussed in Chapter 6). Figure 7.1, gives an impression of how the data might be visualized. We provide an example of using data from the *Girl with a Pearl Earring* by Johannes Vermeer, where Figure 7.1(a) combines color and topography data, (b) the topographical data rendered as a white, diffuse surface to enhance visibility of topography (in dark areas), and (c) the topography rendered as color map, to emphasize topographical features.

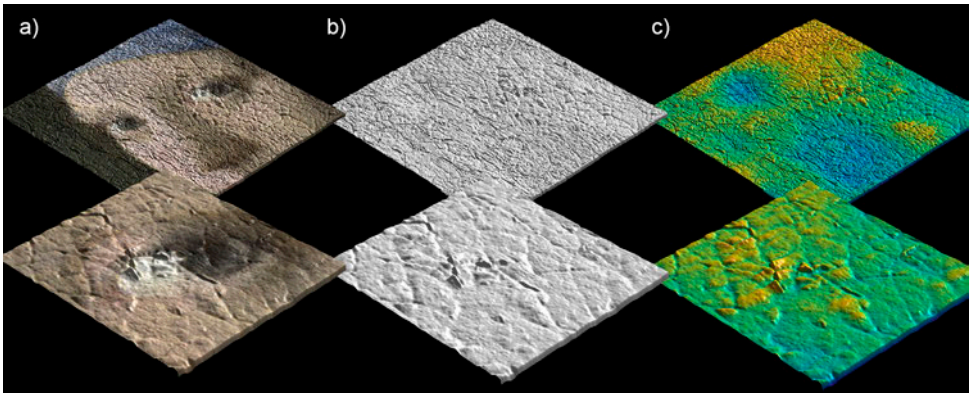

Figure 7.1: Visualizations of *Girl with a Pearl Earring* by Johannes Vermeer, showing the same area and a detail (a) rendered with color and topography, (b) topography as a white, matte surface, and (c) topography with a color map. Note that the height data is exaggerated for increased 'readability'.

Going forward, multi-modal appearance scanning (including color, topography, gloss, and translucency) might also be used as a more extensive documentation of the artwork's appearance than the current photographs that are taken. Furthermore, as the original painting continues to degrade — as is inevitable with all artifacts — the data might remain as a future reference for its appearance at this moment in time. Repeated scans over time, might even be able to support the monitoring of artworks, documenting changes in their structure and appearance. This might be specifically relevant when for instance transporting an artwork, thereby determining the impact of transport on its physical state.

7.1.2. Painting reproductions and their applications

Reproductions created in the context of this research project, but also similar painting facsimiles, have already been used for a variety of applications. First, we provide examples how such reproductions, but also the printing technology, were and are used in the CH domain. Furthermore, we describe several envisioned (future) applications for painting reproductions, which in part were suggested by CH professionals (see Chapter 2).

In the course of this PhD project reproductions have been on show in various locations — inside and outside a museum — providing new ways of interacting with an artwork, which would not be possible with the original (e.g. at Lowlands, a Dutch music and culture festival [5]). At these occasions, visitors were allowed to *touch* the reproductions, which was much appreciated by them, and found to be an interesting additional opportunity for new interactions. An exposition prototype was developed based on a reproduction of *Flowers in a Blue Vase* by Vincent van Gogh, which was illuminated with dynamic, touch-sensitive lighting, synchronized to an audio description, providing additional interaction opportunities [6, 7]. Other possibilities for using painting reproductions — and more widely the printing technology — were explored. For instance, building interactive prototypes to encourage children's playful interactions with an artwork [8], and making paintings accessible for visually impaired [9]. Moreover, a reproduction of the *Girl with a Pearl Earring* by Johannes Vermeer, was on show during the two-week technical examination of the painting in 2018, as a temporary replacement for the original [10, 11].

A reconstruction was made of the original size of the painting *Saul and David* by Rembrandt van Rijn, which was exhibited during a temporary exhibition at the Mauritshuis [12] alongside the original artwork, visualizing the drastic changes the painting had undergone in past conservation treatments. Also, a reconstruction was attempted of the original appearance of *Flowers in a Blue Vase* by Vincent Van Gogh, based on scientific research into the degradation of cadmium yellow paint in that painting [13], which has led to drastic color changes over time. For both reconstructions it is likely impossible but certainly undesirable to show these types of changes — caused by human interventions or (photo)chemical degradation processes — using only the original artwork. This would mean, for example, that you would have to again cut up and reassemble the painting (in the case of the Rembrandt), or scrape off a top layer of original paint (in the case of the Van Gogh). Such drastic actions are irreversible in nature, and are deemed unethical in the current day conservation practice [14]. Alternatively, showing these differences on a screen, ignores all materiality of a painting and the visual effects created by this — specifically what makes a painting look like a painting and be appreciated as a painting.

Furthermore, various examples exist where *similar* reproductions [15–17] — featuring color and relief — are sold as high-end art reproductions. Verus Art [16] also advertises the possibility for (youth) educational programs using their reproductions. This is also envisioned by museum experts that were interviewed in this project (as discussed in Chapter 2). They suggested that life-like reproductions might be used to support educational programs of museums, or even support the

restoration practice, whereby multiple solutions to a restoration can be visualized using this technique, combined with digital restoration.

And finally, the most radical, and possibly controversial, application would be that reproductions play a role substituting paintings, for instance in cases that the original painting is not on view for a long period of time due to restoration, or cannot be shown elsewhere, as it has become too fragile to transport.

7.2. Immaterial aspects to creating life-like reproductions

As 3D printed reproductions are created with increased visual similarity to the original painting, it inevitably raises questions on the immaterial aspects of making such reproductions. Although these questions may seem specific to these digitally created reproductions, making visually similar reproductions is of course not new. Historically, making (hand-made) copies of artworks was actually common, serving various purposes i.e. to disseminate works of art, to replace disintegrating or destroyed artworks, or for (apprentice) craftsmen to train in the mastery of creation.

How such reproductions are viewed and appreciated varies greatly over time, but also depends on the cultural context [18]. Specifically, with the development and uptake of mechanical reproduction processes in the beginning of the 20th century (i.e. photography and film), issues were raised on the role of authenticity and its importance for art appreciation. It was for instance argued by Walter Benjamin [19] that mechanical reproductions lead to a decay of the 'aura' of the original, as they lack any connection to a physical and historical past.

Should we then discard painting reproductions as mere copies, that do not do the original justice? But what would be the alternative? We would (further) damage the original artwork beyond repair? Or what if great masses of people are not longer able to enjoy these great works of art, which are a testament of human civilization and artistic achievement?

Based on the case studies carried out for this thesis (and other related cases), we would argue that reproductions of paintings have their own merit and purpose, potentially complementing the function and aesthetics of the original painting, much like other facsimiles or replicas serve such purpose. We believe reproductions can be a part of the solution to CH conservation and dissemination. Moreover, we believe that these modern, digital reproductions can take on a similar role as their historic (hand-made) counterparts, e.g. in disseminating art, recreating (lost) art and training — in this case scientists — about the intricate skills of making certain appearances.

In the end, whether and how reproductions are appreciated, also depends a great deal on the context, application and the way that they are implemented. Moreover, the appreciation of the original artwork likely also lies in the appreciation of the artist's mastery of skill, which one could argue is lost in a digital reproduction. On the other hand, we might argue that our appreciation of this mastery might even further increase, as we painstakingly try to unravel these complex appearances, in an attempt to replicate them.

In any case, it is important, — even enforced by the International Council of Museums [14] — when showing reproductions in a museum context, that this is communicated to the viewer i.e. the fact that they are looking at a reproduction, rather than the original artwork. The use of reproductions clearly does not have the intention to deceive the viewer, but rather provide them with an experience that cannot (realistically) be achieved otherwise.

Of course, if and how reproductions or reconstructions (of paintings) are implemented, remains for a large part up to museums and/or owners of the artworks. One of the reasons for this is that access to the original artwork is necessary to create such reproductions. We would however, advocate that museums and other CH institutes take an active role in exploring these new possibilities. We believe that the opportunities these new technologies offer, cannot solely be theoretically explored, and should not, for the fear of change, simply be ignored. In actively participating in such explorations, museums and CH institutes have the opportunity to help define and shape the way these new digital technologies are used.

Furthermore, a solely technological perspective on these immaterial aspects of creating and using reproductions will not be sufficient. We believe these issues ask for a wider reflection from multiple perspectives i.e. from museology, art history, restoration and conservation, and art education. Preliminary work, to frame digitally fabricated painting reproductions, from an art historic, conservation and museological perspective, was already conducted by Tissen [20].

Figure 7.2: Photographs of (a) the painting *Girl with a Pearl Earring* by Johannes Vermeer (Courtesy of Mauritshuis/photographer René Gerritsen-Kunst en Onderzoeksfotografie), (b) a reproduction featuring color and topography, and (c) a reproduction featuring color, topography and spatially-varying gloss, taken in similar studio lighting conditions, camera settings, and identically processed. Note that differences in color appearance between the painting and reproduction can occur, as they were photographed under a lamp with unknown spectral properties instead of D50 illumination (reference illuminant for color printing)).

7.2.1. Distinguishing a digitally fabricated reproduction from a painting

Whether a reproduction is directly recognized as such, depends a great deal on factors like the context, level of expertise of the viewer, but also the viewing distance, illumination and viewing conditions. For instance, consider viewing a reproduction at a music festival, compared to viewing the same reproduction (in an elaborately decorated frame), on the wall in a museum. This might trigger a different expectation on its originality. Furthermore, a conservation expert is more likely (upon close inspection) to notice that the surface of a reproduction does not look exactly like paint, based on their extensive experience with looking at and judging paint and paintings. The influence of context and expertise, on the recognition of a reproduction, were not specifically researched in the context of this thesis. In the following, we will go into discussing the appearance similarity and differences between painting and reproduction, at different scales.

Figure 7.3: Photographs of (a) the painting *Fruit Still Life* by Cornelis de Heem (Courtesy of Mauritshuis/photographer Ellen Nigro), (b) a reproduction featuring color, topography and spatially-varying gloss, taken during restoration, in similar studio lighting conditions, camera settings, and identically processed. Note that the scan was made some time after the photograph was taken, where in the mean time more varnish removal took place, specifically in the central area above the grapes. Also note that differences in color appearance between the painting and reproduction can occur, as they were photographed under a lamp with unknown spectral properties instead of D50 illumination (reference illuminant for color printing).

At a regular viewing distance — which we would consider to be the macro scale —, a painting and a reproduction might look remarkably similar. Figure 7.2(a) shows the painting *Girl with a Pearl Earring* by Johannes Vermeer, 7.2(b) our reproduction printed with color and topography, but without gloss layers, and 7.2(c) our reproduction printed with color, topography *and* spatially-varying gloss. We argue that Figure 7.2(a) and 7.2(c) look remarkably similar photographed in this studio lighting configuration. Figure 7.3 shows a comparison between (a) the painting *Fruit Still Life* by Cornelis de Heem, and (b) its reproduction, during restoration, midway through varnish removal. Notice that the top left half, where the varnish was already removed, appears more matte in both painting and reproduction.

Due to the specific nature of these digital reproductions — using a limited set of six inks and a different fabrication technique — they are clearly distinguishable from a painting, when examined at *close range* i.e. several centimeters from the surface. A viewer can, with the naked eye or with the help of a small magnification, already detect that they are looking at a digital fabricated reproduction, rather than a painted surface. The nature of the surface up-close appears quite different from a painted surface, where the juxtaposition of small dots of ink in the primary printing colors can be observed, rather that a solid paint color. This effect is shown in Figure 7.4 with micro photographs taken of (a) the painting, and (b) the same spot in its reproduction. The top images are captured at 0.8x and bottom images at 5x magnification. In (b) the primary printing colors Cyan, Magenta, Yellow, Black and White can be distinguished. This also means, that due to the fundamental difference in material use and fabrication, a digitally fabricated reproduction can be easily recognizable as such, even with further improvement of the technology.

Furthermore, also cross-sections of the painting (taken during the conserva-

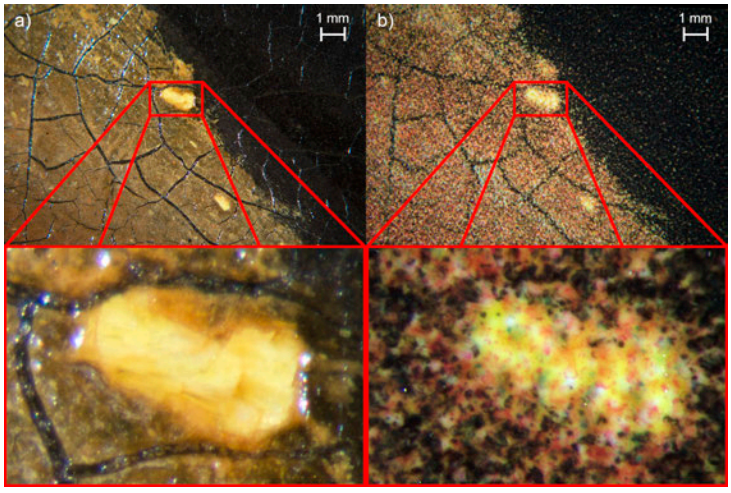

Figure 7.4: Micro photographs of a detail of (a) the painting *Fruit Still Life* by Cornelis de Heem (Courtesy of Mauritshuis/photographer Ellen Nigro), and (b) the same area on the reproduction, where the top images have a magnification of 0.8x and the bottom images 5x magnification.

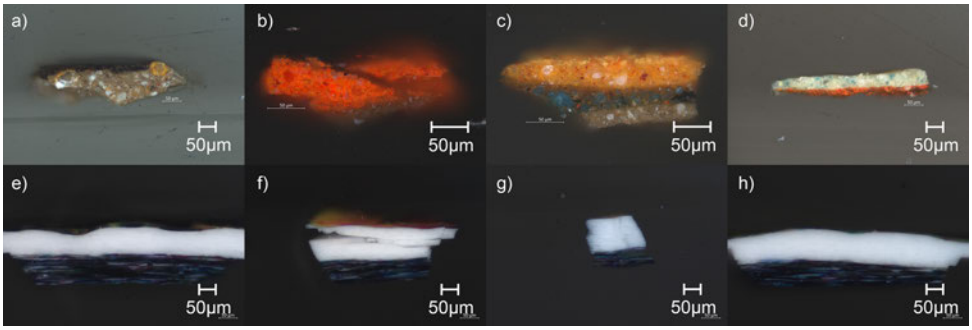

Figure 7.5: Cross sections of (a-d) painting *Fruit Still Life* by Cornelis de Heem (Courtesy of Mauritshuis/photographer Ellen Nigro), and (e-h) reproduction (Courtesy of Mauritshuis/photographer Fahed Ibrahim).

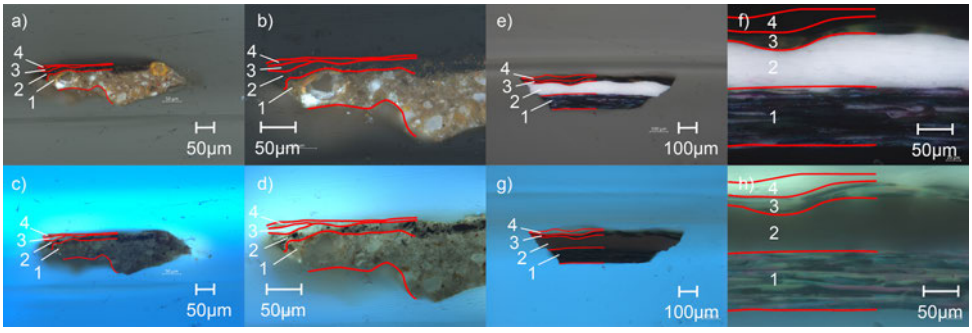

Figure 7.6: Cross sections of (a-d) painting *Fruit Still Life* by Cornelis de Heem (Courtesy of Mauritshuis/photographer Ellen Nigro), and (e-h) reproduction, under visible light (top) and UV illumination (bottom) (Courtesy of Mauritshuis/photographer Fahed Ibrahim).

tion treatment), and our reproduction, show that the buildup of the reproduction is indeed very different from painting, as was originally schematically depicted Figure 1.7. Figure 7.5 (a-d) show cross-sections at for different locations in the painting, showing very different layer buildup at every location. Contrary to this, Figure 7.5 (e-h), taken at roughly the same locations as the print, show very similar buildup at every location. For one set of cross-sections the difference in layer buildup is detailed in Figure 7.6 shown in (top) visible light and (bottom) UV light. Figure 7.6 (a-d) show the painting's stratigraphy, made up of (1) ground layer, (2) paint layer and (3-4) (pigmented) varnish layers. Figure 7.6 (e-h) show the reproduction's stratigraphy made up of (1) the topography layers, to create the height variation in the surface, built up with voxels in all printing colors (CMYKW), (2) several white intermediate layers (W), (3) color layer(s) (CMYKW), and (4) varnish layer(s) (T). Also note here that, contrary to the painting, the individual pigment particles in the inks cannot be distinguished. Therefore, we conclude that also at this microscopic level, the painting and digitally fabricated reproduction are very different, and will continue to be, as a consequence of their respective fabrication method.

7.3. Applications outside cultural heritage domain

Besides the range of applications that painting reproductions (might) serve (described in Section 7.1), we should also consider a wider application of knowledge generated and technical capabilities explored in this thesis.

7.3.1. Applications as research probes

When taking a closer look at literature on visual perception (summary in Chapter 1), it becomes clear that many of the (recent) insights in material perception are based on research using computer rendered stimuli, of which a surprising large amount is based on systematic variations of green, rendered 'blobs' and green, bumpy surfaces. Those stimuli are on different levels simplifications of real-world appearances around us. For one, the world we see around us is for the most part not made up of green blobs and surfaces. Furthermore, the fact that these surfaces are rendered (in an artificial environment), means that they have undergone a necessary simplification, through the modeling of their appearance. Though (very) advanced, these computer rendering tools still make use of models approximating material properties, light and their interactions. An alternative, as for instance practiced by Zhang *et al.* [21], is to make hand-crafted research probes. The variation within the physical artifacts created, is then limited by available materials (e.g. a limited range of matte, satin-gloss, and high gloss paints). This limitation can be overcome by using a technique called optical mixing, creating 'virtual' materials by digitally mixing various discrete appearances (e.g. [21], [22]). Such an approach, however does ask for very careful alignment, cannot be created for every material (e.g. with different refractive indexes), limits handling and manipulation of the artifacts, and represents challenges in representing spatially-varying appearance (from a fabrication perspective). 3D Printing technology, such as material jetting, with its ability to vary material compositions on a voxel-by-voxel scale, is capable of spatial (or volumetric) variations in topography, color, gloss and translucency. Such 3D printed research probes could then be used to study material perception. Despite the mentioned limitations, this might also be combined with the optical mixing technique, whereby only a limited set of appearances is fabricated, and all intermediate appearances are created through optical mixing (which was to some extent shown by Miyashita *et al.* [22], to create more complex shapes).

Two existing examples of studies using 3D printed probes, were conducted by Baar *et al.* [23], who studied the interaction between gloss and topography using 3D printed samples and Vu *et al.* [24], who studied translucency perception using 3D printed samples. Other advantages of using 'real' (3D) objects, is the ability for physical manipulation (i.e. moving/rotating the sample, whereby changing the viewing angle), and ability to have a real-world viewing conditions like binocular vision. We envision that 3D printing technology might be more extensively employed for this purpose in the future. However, an aspect that should be taken into account, is the ability to manipulate various properties in a truly independent manner (i.e. manipulating topography and gloss separately, also see Section 7.4).

7.3.2. Applications in product design

Material appearance and appearance reproduction plays an important role in many (if not all) of the products surrounding us. Products are generally meticulously designed to have a specific appearance, in an effort to appeal to consumers, and is therefore a relevant subject of research at the Faculty of Industrial Design Engineering.

Many examples exist, historic and modern, of imitating material appearances, ranging form imitating gold, marble, and precious stones, to modern day examples like chrome-look plastic, laminate floors, and imitation leather. In all of these examples the aim was or is to create luxurious appearances with more affordable means. In many of these cases, it was also considered worthwhile to copy these natural occurring, complex, and intricately detailed appearances. Here, capturing appearance (color, topography, gloss and translucency), and digital manufacturing, are the logical next step to widen the range of appearances which can be reproduced. A range of such applications might already be explored based on the current workflow, geared at reproducing (roughly) planar surfaces.

One particular product category where the importance of appearance is particularly obvious, are prostheses. Think of for instance matching and realistic looking teeth, eyes, (facial) prostheses, and prosthetic limbs. In all these cases, also translucency plays a crucial role in the matching of appearance. Although is was postulated by Mori [25] in the 1970s that we should probably stay away from very realistic appearance reproduction in the design of (robots and) prosthetic hands, to avoid creating eerie sensations, recent research seems to suggest that such an *uncanny valley* does not exist for prosthetic hands [26–28]. Therefore, knowledge of appearance capture and fabrication can be usefully extended to such product design domains. For this, of course, the capabilities should be extended to 3D object capturing and fabrication.

Here, we might also envision using digitally fabricated appearances, possibly in combination with optical mixing (i.e. as in [22]), as a material visualisation, communication and selection tool.

Furthermore, the knowledge and skill gained in the reproduction of appearance is also one of the necessary ingredients to a more deliberate and informed approach to material appearance synthesis.

7.4. Limitations

The following paragraphs describe limitations, regarding the case studies carried out, the reproduction workflow, and the techniques applied in the context of this thesis.

7.4.1. Case studies and generalisation of results

The case studies carried out in the context of this PhD thesis, were limited to the appearance reproduction of (varnished) oil paintings. This therefore makes it difficult to generalize the results to other (painting) materials and appearances. Whether the current approach is suitable to reproduce appearances of other (painting) ma-

terials remains to be investigated. Furthermore, although the paintings reproduced in the case studies show a variety of appearances, they by no means cover all appearances that can be created with oil paint (on a substrate). It remains to be investigated what the limits are in terms of appearance capturing and reproductions, specifically for topography and gloss. For instance: At what point does the topographical variation become too much, that is become impossible to reliably capture gloss with the current approach? It is however clear, that 'overhangs' — or undercuts — cannot be scanned or represented with the current approach, meaning we cannot image underneath flaking or 'cupping' paint, or capture the underside of an overhanging impasto.

7.4.2. Appearance reproduction workflow

The current appearance reproduction workflow is limited to capturing and reproduction of (roughly) planar surfaces, and thereby not suitable for capturing and reproduction of 3D objects. Specifically, the approach used for gloss reproduction (capture and fabrication) will have to be altered to enable similar replication for three-dimensional objects. For example, the ability to fabricate a high gloss surface, currently relies on adding a single layer of transparent ink, across the complete surface. For a three-dimensional surface, this will not be possible on curved or vertical surfaces, as these are created in multiple layers, and therefore cannot (all at once) be reached at a later point in the print process.

Additionally, the current gloss reproduction workflow relies on directly linking the scanner output to the printer input. The gloss calibration is carried out by scanning printed samples (see Chapter 5). In the case of color reproduction, workflows are defined based on device independent color connection spaces (using ICC-profiles [29]). An equivalent for gloss, a *gloss connection space*, or more generally formulated, *total appearance connection space* does not yet exist, although recently Urban *et al.* [30] proposed an approach for including a device-independent, nearly perceptually-uniform translucency parameter to existing (3D) color reproduction workflows.

The current gloss calibration approach, relies on scanning printed reference targets (with different uniform gloss levels). A limitation of this approach (especially when further increasing the spatial resolution) is that the printing resolution lies very close to the scanning resolution. This means that the scanner is able to capture at the resolution of the individual ink droplets. At this level the macroscopic scattering effect of the surface is lost, whereby the spatially-varying gloss variations (differences in the magnitude of specular reflection), are no longer be captured, and the gloss measurement breaks down into measuring individual highlights on every single droplet, leading to a noisy gloss measurement across the surface. Gloss reference calibration targets, creating gloss variation through roughness variations at a smaller scale, might offer a solution to this issue. This remains to be investigated.

Currently, the installation and calibration of the 3D scanning are rather lengthy procedures, requiring accurate (manual) setting and alignment. Sensor measurements and feedback loops in the system (e.g. auto-focusing, automated planar orientation, and real-time data processing and analysis) could greatly increase the

speed and efficiency of making 3D scans. One other practical issue of the current reproduction workflow, is the vast amounts of data that are generated and need to be processed to be able to create an image of a complete painting. New, more efficient approaches to (processing and) stitching need to be developed and implemented, in order to be able to stitch large data sets, especially for the high-resolution 3D scanning data sets (as discussed in Chapter 6).

7.4.3. Appearance capturing

Based on the case studies presented in this thesis, we conclude that the appearance capturing system that was developed is able to capture color, topography and gloss variations of a surface, is suitable as input for an appearance reproduction workflow. However, there are several limitations to capturing the various appearance modalities.

The capturing of all appearance modalities is limited to (roughly) planar artifacts. In the current implementations, the automated scanning range is limited to approximately 1 m × 1 m, although this can relatively easily be adapted.

Focusing on scanning the individual modalities, the color reproduction is limited to a colormetric color matching workflow (i.e. captured in RGB). As a multi-spectral workflow was not available for the used 3D printing system, multi-spectral appearance capturing was deemed futile at this point in time. Moreover, multi-spectral imaging, would substantially increase scanning time (increasing for every addition channel measured) as well as further increasing the demands for data processing and storage (also see Section 7.4.2). With the development of multi-spectral printing capabilities, the current scanning system does have the flexibility to be adapted, following for instance the approach of Berns *et al.* [31] or Shi *et al.* [32], by interchanging the cameras (and possibly illuminant) of the system. In our case studies we found the influence of local shading (introduced by the topography of the surface) on the color measurement to be limited, whereby we directly took the measured RGB value at every point as a proxy for the diffuse albedo. Correcting for local shading however, might further improve the color reproduction.

Case studies have shown the flexibility of the 3D scanning technique to measure the topography of paintings at different resolutions (see Chapter 6). However, with the increase in resolution, the depth-of-field is reduced, thereby limiting the height variations which can be captured in one tile. Moreover, global non-planarity (i.e. warped paintings) might require active planar alignment, to ensure the surface remains in focus throughout the whole scan. Limitations of the 3D scanning are also imposed by the imaging angle, whereby deep cracks or the sides of highly sloped areas (i.e. of an impasto) might be occluded from view (for one of the cameras), and therefore not measured. Based on our case study scans, we find that the topography scanning is largely independent of color, and encountered no issues with capturing highly reflecting surfaces. However, as with all optical systems, scanning surfaces that have limited to no reflectance (i.e. dark/black), was found to be challenging. Moreover, the 3D scanning approach is limited to di-electric materials (i.e. which have diffuse reflectance), due to the cross-polarized setup.

As was described in Chapter 4, the gloss scanning is influenced by the topogra-

phy of the surface. To circumvent this issue, an approach was suggested to correct gloss measurements of parts, where the local normal deviates from the global plane normal (beyond a certain threshold). However, a data-driven approach, using (reference) angular gloss measurements, might be able to reach better estimates for the local surface reflectance. In the calibration of gloss scanning, presented in Chapter 5, we found that the gloss measurement was to a large extent independent of the color measurement, when measuring printed reference targets. We believe this is also the case for scanning of painted surfaces. However, validating this was found to be quite complicated, due to difficulties creating very smooth *(oil) painted* surfaces with a uniform gloss levels. Furthermore, the gloss scanning approach preferably requires some knowledge of the refractive index of the material, as this determines the gloss imaging angle (i.e. Brewster's angle). Alternatively, this could be experimentally determined, by searching for the imaging angle where the (polarized) specular reflections are completely eliminated with a polarization filter in front of the camera lens (see gloss scanning approach in Chapter 4). The gloss scanning approach also relies on the assumption that the refractive index is (very similar or) identical across the complete surface.

Furthermore, as was defined in the scope of this project, the current appearance reproduction workflow does not capture translucency.

7.4.4. Appearance fabrication

The 3D printing system, used in the context of this thesis, is the Océ Technologies High-Resolution 3D Printing system [33]. The printing materials and material processing workflow is currently limited to Cyan, Magenta, Yellow, Black, White and Transparent (CMYKWT) ink. The amount of materials that can be printed at any time is limited by the hardware, i.e. by the number of ink channels available. To our knowledge, no 3D printing system exists which has more ink channels. However, the MultiFab 3D printing system (developed at MIT, described by Sitthi-Amorn *et al.* [34]), can be used to print up to 11 different colored materials, although they do need 3 print passes to achieve this (using 5 independent ink channels) [32]. This is however, an inefficient approach to print a large number of layers — needed for 3D printing — as material switching is needed between the print passes. In general, extending the range of printable materials (e.g. for a multi-spectral reproduction workflow, or potentially translucency reproduction) can prove to be challenging and time consuming (to reach stable printing behaviour), as many additional requirements need to be taken into account related to print-ability of an ink: like viscosity, printing behaviour, curing properties, and stability of pigments in the ink. Whether, for instance, varying translucency printing can be achieved with the existing (or a new, limited set of) six materials (i.e. as in Urban *et al.* [30], Brunton *et al.* [35]), or an extension of the ink range (and therefore adaption of the printer hardware) is needed, remains to be determined. Furthermore, to our knowledge 3D printing systems currently do *not* offer the ability to print special optical effects like fluorescence, pearlescence or sparkle as part of a full-color 3D printing workflow. Additionally, the Océ Technologies 3D printing system, currently also lacks a (removable) support material, making it impossible to print undercuts.

The Océ Technologies high-resolution 3D printing system currently offers a unique planar range of 1.2 m × 2.4 m, and the possibility for printing up to 5 mm in height (commercially available settings). This build volume defines a maximum size of a one-piece reproduction, though the possibility of tiling several panels together to create even larger reproductions, has been explored by Océ Technologies. Alternatively, other existing (full-color) 3D printing systems offer quite different build volumes, with much smaller planar range (volumes in the range of 400 mm × 300 mm × 400 mm), which does offer the possibility to print truly three-dimensional objects (also featuring support materials).

With the fabrication of the spatially-varying gloss, we found that the adding of several layer of transparent ink on top of the (full-color) topographical layers, significantly influenced the details of the topographical features i.e. it had the effect of slightly smoothing the surface. It remains to be investigated, if this effect can be reduced or compensated for in the printing workflow, or to what extent such adaptions are needed to create perceptually convincing reproductions.

7.4.5. Appearance perception

Within the context of this PhD project, the investigation into the perception of (spatially-varying) gloss (as an integral part of appearance reproduction) was limited. A systematic investigation into color, gloss and topography perception and their interactions remains to be further investigated, in the context of complex, real-world material appearance reproduction cases. Logically, also the translation of such knowledge into design possibilities and requirements for an appearance reproduction workflow, also remains to be investigated. As with color metamers, it is well possible that other perceptual interactions can be used to make more convincing reproductions, leading to perceptual enhancement, which could in turn support the readability, understanding and/or potentially the appreciation of the artwork.

7.5. Reflecting on research in and designing for the cultural heritage domain

The following section reflects on the specific nature of studying paintings and working in the cultural heritage (CH) domain. Furthermore, a reflection is given on the societal relevance of 3D scanning and (digitally fabricated) reproductions within the CH domain.

7.5.1. Paintings as the ultimate case studies

Although we are surrounded by objects, that all have their particular appearance, that might to be interesting to study, paintings prove to be unique and challenging artifacts to study, on multiple levels. One aspect is the complexity of the artifact itself. Paintings exhibit a wide range of appearances, with complex layered buildup, and spatial variation in color, topography, gloss and translucency. For this reason they are deemed the ultimate case study, to capture and replicate this complexity. This is therefore also one of the reasons paintings were studied in this thesis. On another level, painting are also interesting to study, in the way that paint lends

itself so well (when applied by highly skilled painters), for realistically *depicting* the physical world around us. In the latter sense, painting also form very relevant study objects, for instance for the purpose of studying material perception, but also light perception (e.g. [36–39]). Such studies provide us with very relevant insights on (material) perception, and could potentially even provide input for appearance reproduction of the artifacts themselves.

7.5.2. Designing for the cultural heritage context

From a technical perspective, *researching in* the CH domain, specifically in the interaction with CH artifacts, generally also requires *designing for* this context. The following describes several key insights to take into account when designing systems interacting with artifacts, for the CH domain.

Designing for the CH context has proven to be a challenging endeavour. Having very valuable and unique artifacts as your object of interest, demands many careful considerations in the design process. Dealing with priceless paintings leaves no margin for error.

Designers in this context should be aware that any handling and irradiation inevitably carries risk and has impact on an artwork (like paintings). For instance, careful consideration should be made, if and to what extent exposure to electromagnetic radiation (including visible light) is acceptable. Any superfluous radiation to an artwork should be avoided, as this can contribute to more and faster degradation. Such considerations are of course always taken in deliberation with, and in the end, up to the (team of) conservators and museum specialists. Nevertheless, a designer should be aware of minimizing the impact and (potential) risk of using their equipment on an artwork.

Another consideration which also plays an important role in the design process is the limitations that are imposed on the total available scanning time. Especially for very important collection pieces, museums want to limit the time they are not on show, sometimes even to the point, that the whole (scanning) procedure has to take place during closing hours of the museum. Effort should therefore be put into optimizing the scanning speed. This might however, come at a cost, for instance, of having to eliminate real-time data processing, which has an advantage that the scanning process can be monitored. For the same reason, it is worth optimizing a system's portability and time needed for installation and calibration.

Moreover, in our experience, the domain of restoration and conservation remains a rather conservative field. For instance, we found that conservators are actually more likely to prefer manual manipulation of a machine (or artifact), rather than relying on automated movement (especially for close range scanning). Only after careful consideration, positioning, checking, and visual confirmation might the automated movement of a machine be started. This requires designers to think about, how such (manual) confirmations can be shown and built in into their designs, or if automation is deemed suitable at all.

One other difficulty with designing for CH context, is the limited *a priori* knowledge on the exact shape of artifacts. Assuming, for instance, that a painting is planar and static is a gross simplification, that will potentially lead to issues when

scanning a painting at very high resolution. One other issue is the difficulty of predicting the exact response of a painting to environmental influences, especially when it is unframed (less fixated and protected). For instance, it is unknown to what extent a painting changes shape, due to environmental influences (even in an air-conditioned location), during a day, but also over longer periods of time. Even relatively small variations (on the mm scale) can become relevant when you scan a painting at the µm scale. Real-time measurement and automated re-positioning might provide an outcome here, but then, the inherent safety will have to be guaranteed (see previous comment).

If we consider appearance reproduction in a broader context, we should realise that collections are generally made up of a vast variety of artifacts. This makes it impossible, to offer a one-size-fits all solution to replicating all of them. With an (even wider) range of materials and appearances, careful consideration should be given to for instance the scanning scale and variety of artifacts that can be scanned, or if, in some cases, a customized solution is justified.

Given the complexity of the CH context, we believe designing for it, asks for a truly multi-disciplinary approach. Technical disciplines should work in close collaboration with CH professionals, but also the role of designers should not be overlooked. In our experience, the translation of the context, the protocols and practices of CH professionals (as the envisioned users of the technology) are too often overlooked. This is where designers can play an crucial role, as is their profession, to match user requirements (including all contextual information), technological capabilities, (and potentially business aspects) into a suitable design solution.

7.5.3. Societal relevance

The added value of capturing and reproduction of paintings' appearances, where these paintings are (historic) manifestations of culture, ultimately lies in the preservation of this heritage for current but also future generations. These new technologies can support the way CH can be accessed (in time and place), made accessible to a wider public, and (potentially) also scholars. And even though paintings are kept under the (what we now know to be) best possible conditions, they will inevitably continue to degrade. Capturing (and replicating) them, can at least preserve the appearance of their current state, to be enjoyed and appreciated for the stories they tell, be it in a slightly different form, by future generations. Ultimately, new technology should also lead to more inclusion, providing access to our CH for new and different groups in society (e.g. providing solutions for people with impairments or disabilities).

We might also see the capturing and replication of CH in light of various events and societal debates related to CH. Firstly, let's consider the case of catastrophic loss. Examples, for instance of the destruction of art (or even complete CH sites) in war time (like the destruction of the Assyrian city of Niniveh by ISIS [40, 41]), or due to a fire (like the Notre Dame in Paris ([42, 43]). These unexpected events show the limitations of the data that is currently collected, and the difficulties this poses for the attempts to recreate this CH. Also, as mentioned before, capturing and reproductions might also play a role, considering the inevitable (slow) degra-

dation of CH, leading for instance to the decision not to loan fragile pieces of art (like recently announced by the Van Gogh Museum [44]). Another topic, that has recently gained international attention is the matter of colonial art in western museums [45]. Although reproductions cannot solve the issue to have the original artifact in two locations at once, it would be useful to explore how reproductions can be a part of the solution to this dilemma, for instance in the role they might be able to play in exhibitions.

References

[1] R. Pintus, K. Pal, Y. Yang, T. Weyrich, E. Gobbetti, and H. Rushmeier, *A Survey of Geometric Analysis in Cultural Heritage,* Computer Graphics Forum **35**, 4 (2016).

[2] R. Scopigno, P. Cignoni, N. Pietroni, M. Callieri, and M. Dellepiane, *Digital Fabrication Techniques for Cultural Heritage: A Survey,* Computer Graphics Forum **36**, 6 (2017).

[3] B. A. Darling and J. A. Ferwerda, *The tangiBook: a tangible display system for direct interaction with virtual surfaces,* in *17th Color Imaging Conference* (IS&T, 2009) pp. 260–266.

[4] Mauritshuis, *The Girl in the Spotlight - Scientific Examination of the 'Girl with a Pearl Earring' (c.1665) by Johannes Vermeer,* (2018), (Accessed: 2019-01-23).

[5] W. Elkhuizen, M. Baay, S. C. Pont, and J. M. Geraedts, *Lowlands Science - exposition of 3D printed reproductions,* (2015).

[6] M. Baay, *SmartFrame: Design of an exposition setup for 3D-printed fine-art replicas*, MSc thesis (Delft University of Technology, Delft, The Netherlands, 2016).

[7] W. Elkhuizen, M. Baay, B. Peeters, S. C. Pont, and J. M. Geraedts, *Dutch Design Week: 4TU Mind the Step Exhibition - exposition of SmartFrame,* (2016).

[8] J. Stuijt, *A new Art Experience: The design of an exhibit for Science Centre Delft*, MSc thesis (Delft University of Technology, Delft, The Netherlands, 2018).

[9] H. De Bliek, *Making art accessible to visually impaired museum visitors*, MSc thesis (Delft University of Technology, Delft, The Netherlands, 2019).

[10] Mauritshuis, *New research into Vermeer's Girl with a Pearl Earring,* (2018), (Accessed: 2019-06-03).

[11] AD, *Publiek mag meegenieten van onderzoek naar Meisje met de Parel,* (2018).

[12] Mauritshuis, *Rembrandt? The case Saul and David,* (2015), (Accessed: 2019-05-15).

[13] G. Van der Snickt, K. Janssens, J. Dik, W. De Nolf, F. Vanmeert, J. Jaroszewicz, M. Cotte, G. Falkenberg, and L. Van der Loeff, *Combined use of Synchrotron Radiation Based Micro-X-ray Fluorescence, Micro-X-ray Diffraction, Micro-X-ray*

Absorption Near-Edge, and Micro-Fourier Transform Infrared Spectroscopies for Revealing an Alternative Degradation Pathway of the Pigment Cadmium Ye, Analytical chemistry **84**, 10221 (2012).

[14] International Council of Museums, *ICOM code of ethics for museums*, Tech. Rep. (2017).

[15] Van Gogh Museum, *Van Gogh Museum Edition Collection,* (Accessed: 2017-10-13).

[16] Verus Art, *Verus Art textured reproductions,* (2017), (Accessed: 2019-05-25).

[17] Mauritshuis, *Museum shop,* (Accessed: 2019-04-15).

[18] N. Ex, *Zo goed als oud: de achterkant van restaureren* (De Boekerij BV, Amsterdam, The Netherlands, 1993).

[19] W. Benjamin, *The Work of Art in the Age of Mechanical Reproduction (original essay from 1936),* in *Illuminations*, edited by H. Arendt (Schocken Books, New York, USA, 1969) pp. 217–252.

[20] L. N. Tissen, *Indistinguishable likeness - 3D replication as a conservation strategy and the moral and ethical discussion on our perception of art,* (2018).

[21] F. Zhang, H. de Ridder, P. Barla, and S. Pont, *A systematic approach to testing and predicting light-material interactions,* Journal of Vision **19**, 1 (2019).

[22] L. Miyashita, K. Ishihara, Y. Watanabe, and M. Ishikawa, *ZoeMatrope: A System for Physical Material Design,* ACM Transactions on Graphics **35**, 1 (2016).

[23] T. Baar, S. Samadzadegan, P. Urban, and M. V. Ortiz Segovia, *Interrelation between gloss and texture perception of 2.5D-printed surfaces,* in *Electronic Imaging: Measuring, Modeling, and Reproducing Material Appearance* (Society for Imaging Science and Technology, 2016) pp. 1–6.

[24] B. M. Vu, P. Urban, T. M. Tanksale, and S. Nakauchi, *Visual perception of 3D printed translucent objects,* in *24th Color and Imaging Conference* (Society for Imaging Science and Technology, 2016) pp. 94–99.

[25] M. Mori, *Translation of: 'The Uncanny Valley' (1970) (in Japanese),* (2012), (Accessed: 2019-06-03).

[26] S. Sansoni, A. Wodehouse, A. McFadyen, and A. Buis, *The aesthetic appeal of prosthetic limbs and the uncanny valley: The role of personal characteristics in attraction,* International Journal of Design **9**, 67 (2015).

[27] E. Poliakoff, N. Beach, R. Best, T. Howard, and E. Gowen, *Can looking at a hand make your skin crawl? Peering into the uncanny valley for hands,* Perception **42**, 998 (2013).

[28] E. Poliakoff, S. O'Kane, O. Carefoot, P. Kyberd, and E. Gowen, *Investigating the uncanny valley for prosthetic hands,* Prosthetics and Orthotics International **42**, 21 (2018).

[29] International Color Consortium, *Standards that refer to ICC profiles,* (Accessed: 2019-05-25).

[30] P. Urban, T. Madan Tanksale, A. Brunton, B. M. Vu, and S. Nakauchi, *Redefin-*

ing A in RGBA: Towards a Standard for Graphical 3D Printing, ACM Transactions on Graphics **38**, 1 (2019), arXiv:arXiv:1204.6216v2 .

[31] R. S. Berns, L. A. Taplin, P. Urban, and Y. Zhao, *Spectral color reproduction of paintings,* in *Colour in Graphics, Imaging, and Vision* (Society for Imaging Science and Technology, 2008) pp. 484–488.

[32] L. Shi, V. Babaei, C. Kim, M. Foshey, Y. Hu, P. Sitthi-Amorn, S. Rusinkiewicz, and W. Matusik, *Deep Multispectral Painting Reproduction via Multi-Layer , Custom-Ink Printing,* ACM Transactions on Graphics **37**, 1 (2018).

[33] Océ Technologies BV - a Canon Company, *Project Eiger Elevated printing,* (Accessed: 2019-05-25).

[34] P. Sitthi-Amorn, J. E. Ramos, Y. Wangy, J. Kwan, J. Lan, W. Wang, and W. Matusik, *MultiFab: A Machine Vision Assisted Platform for Multi-material 3D Printing,* ACM Transactions on Graphics **34** (2015), 10.1145/2766962.

[35] A. Brunton, C. A. Arikan, T. M. Tanksale, and P. Urban, *3D printing spatially varying color and translucency,* ACM Transactions on Graphics **37**, 1 (2018).

[36] B. Sayim and P. Cavanagh, *The art of transparency,* i-Perception **2**, 679 (2011).

[37] T. Kartashova, H. de Ridder, S. F. te Pas, M. Schoemaker, and S. C. Pont, *The visual light field in paintings of Museum Prinsenhof: comparing settings in empty space and on objects,* Human Vision and Electronic Imaging XX **9394**, 1 (2015).

[38] F. Di Cicco, M. W. A. Wijntjes, and S. C. Pont, *Understanding gloss perception through the lens of art: Combining perception, image analysis, and painting recipes of 17th century painted grapes,* Journal of Vision **19**, 1 (2019).

[39] M. Van Zuijlen, P. Upchurch, S. Pont, and M. Wijntjes, *Material property space analysis for depicted materials,* in *Vision Science Society* (2019) p. 251.

[40] K. Romey, *Exclusive Photos Show Destruction of Nineveh Gates by ISIS,* (2016), (Accessed: 2019-06-09).

[41] N. van Apeldoorn, *3D Reconstruction of Niniveh: A casestudy on the Bas-reliefs of the Southwest Palace of Sennacherib with monocular images*, Msc thesis, Delft University of Technology (2017).

[42] BBC News, *Notre-Dame: Massive fire ravages Paris cathedral,* (2019).

[43] S. Murray and A. Tallon, *Paris, Cathédrale Notre-Dame,* (2015), (Accessed: 2019-06-09).

[44] Van Gogh Museum, *Zonnebloemen blijven voortaan thuis,* (2019), (Accessed: 2019-02-17).

[45] The Economist, *The clamour to return artefacts taken by colonialists - Former colonies want their cultural treasures back,* (2019).

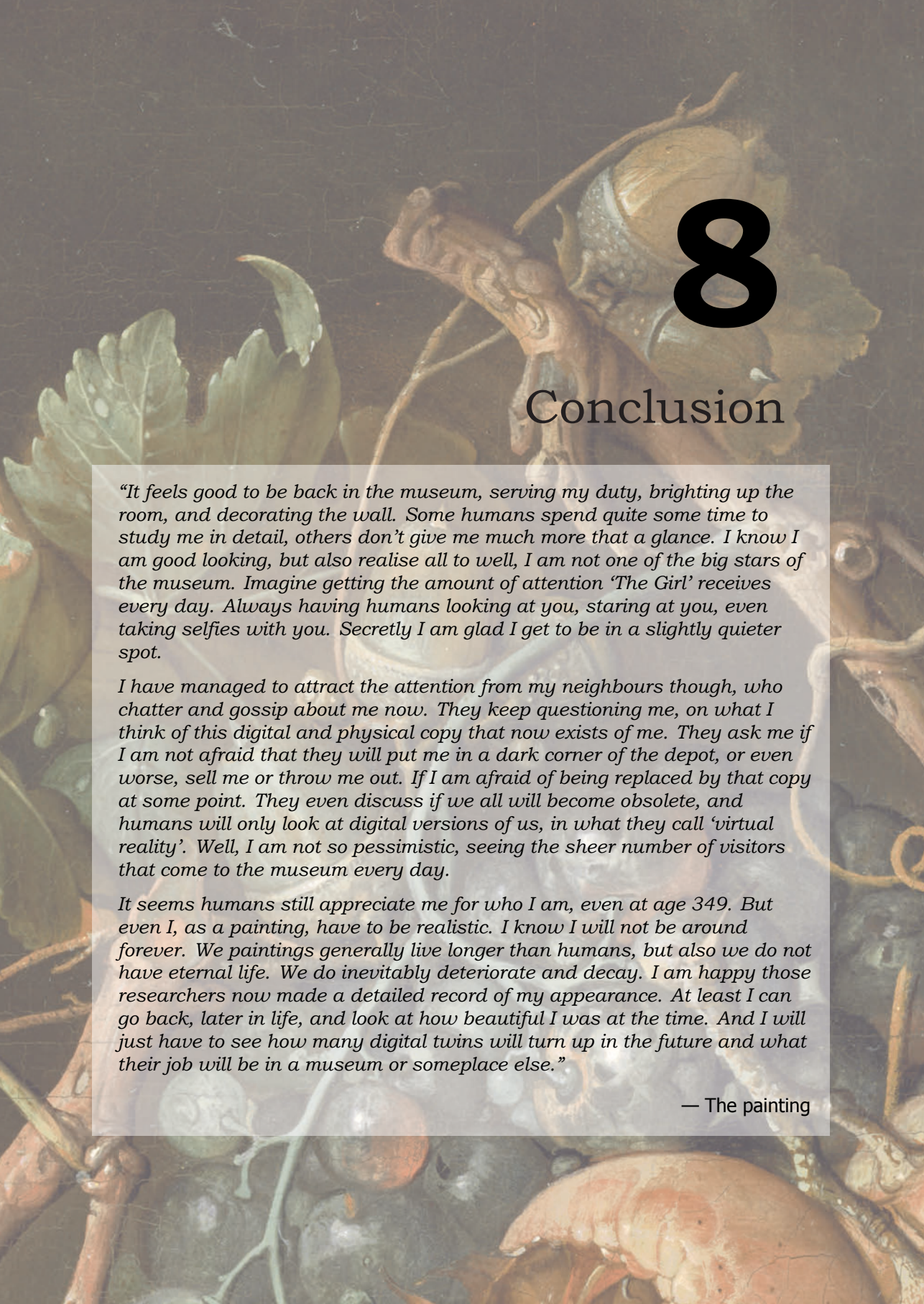

8

Conclusion

"It feels good to be back in the museum, serving my duty, brighting up the room, and decorating the wall. Some humans spend quite some time to study me in detail, others don't give me much more that a glance. I know I am good looking, but also realise all to well, I am not one of the big stars of the museum. Imagine getting the amount of attention 'The Girl' receives every day. Always having humans looking at you, staring at you, even taking selfies with you. Secretly I am glad I get to be in a slightly quieter spot.

I have managed to attract the attention from my neighbours though, who chatter and gossip about me now. They keep questioning me, on what I think of this digital and physical copy that now exists of me. They ask me if I am not afraid that they will put me in a dark corner of the depot, or even worse, sell me or throw me out. If I am afraid of being replaced by that copy at some point. They even discuss if we all will become obsolete, and humans will only look at digital versions of us, in what they call 'virtual reality'. Well, I am not so pessimistic, seeing the sheer number of visitors that come to the museum every day.

It seems humans still appreciate me for who I am, even at age 349. But even I, as a painting, have to be realistic. I know I will not be around forever. We paintings generally live longer than humans, but also we do not have eternal life. We do inevitably deteriorate and decay. I am happy those researchers now made a detailed record of my appearance. At least I can go back, later in life, and look at how beautiful I was at the time. And I will just have to see how many digital twins will turn up in the future and what their job will be in a museum or someplace else."

— The painting

8.1. Reflecting on the research aim

We conclude that we can successfully reproduce color, topography and spatially-varying gloss of paintings, in an integrated way. This can be achieved by combining 3D scanning — based on fringe-encoded stereo imaging — with gloss scanning — based on reflection polarization. Experimental results show that the method is sufficiently fast for practical application, i.e. to scan a painting (the size of 1 m × 1 m) within eight hours, during closing hours of a museum. Furthermore, we conclude that the results can well be used for the purpose of creating physical reproductions. Results show that our proposed method to extend appearance scanning with gloss measurements is a valuable addition in the quest for more realistic reproductions, in terms of its practical applicability — number of images needed for reconstruction and speed — and its perceptual added value, when added to color and topography reproduction. For fabrication we propose a minimal set of *just* six printing materials, consisting of Cyan, Magenta, Yellow, Black, White and Transparent ink.

Furthermore, we conclude that 3D scanning data of paintings — captured using fringe encoded stereo imaging — has good correspondence to other more accurate and precise 3D imaging techniques like 3D digital microscopy — based on focus variation — and Multi-Scale Optical Coherence Tomography (MS-OCT). Moreover, our 3D scanning technique was found to be more suitable for scanning larger areas — i.e. complete paintings — in terms of tile size, capturing speed and flexibility in resolution. We show that topographical data of a painting (of all of the above techniques) can be used to visualize height variations of a painting's surface, much more accurately, than existing photography or manual tracing techniques. These visualizations can support conservators in evaluating the state of the painting, and determining the need for any interventions.

The reproductions and 3D data sets created within the context of this PhD project, but also the custom-built scanning systems, serve as demonstrators, and are in effect accumulations of the knowledge generated in the project.

8.2. Answering the research questions

Based on the (literature) research, we conclude that a great number of factors govern the appearance of a painting and 3D printed reproduction (RQ 1). First, the physical characteristics of both artifacts play a role (i.e. the shape of the surface, refractive index of the materials, surface roughness, selective spectral absorbance, layered structure). Also the illumination (i.e. the spectrum, intensity, geometric configuration), determines the appearance, when viewing the painting and reproduction, but also in the process of scanning the painting. Furthermore, the characteristics of the imaging system (i.e. camera settings, camera response curve, geometric configuration) influence the measurements and thereby the resulting appearance of reproduction. Similarly, the characteristics of the printing system (i.e. inks, printing resolution, printing strategy) affect the appearance of the reproduction. Of course, the human visual system also plays a vital role in the perception of appearance (i.e. color vision, binocular vision, temporal effects, movement).

In the initial comparison between three reproductions — featuring only color and relief — and their respective original, experts observed differences in various attributes of appearance: the color, relief, gloss *and* translucency (see Chapter 2), which suggests a focus on a wide range of factors to study to minimize material appearance (RQ 2). Based on the evaluation and literature research, improvements were made to the scanner design and calibration procedure to improve the existing color and topography reproduction (as described in Chapter 4). As any further significant improvement in color reproduction is largely limited by technical barriers (for instance the printing system lacking a multi-spectral workflow), this focus was no further pursued. Furthermore, we believe that this is not the most significant appearance difference to be solved between paintings and (2D) reproductions. A choice was made to integrate gloss reproduction, driven by literature research, and a technical exploration (see Chapter 3). The possibilities for translucency reproduction were also technically limited - in measurement and fabrication.

In the approach proposed for reproducing spatially-varying gloss (see Chapter 4), various parameters are important, some of which can be measured and/or manipulated (RQ 3). First, the degree of topographical variation of the surface is important. Surfaces which are heavily textured are less suitable for scanning using this method, as larger off-specular regions will have to be masked and interpolated, making the measurement less accurate. Also the refractive index of the painting materials needs to be known, as this determines the angle of maximum reflection polarization, in turn determining the illumination and imaging angle of the scanning system. Illuminant characteristics (i.e. spatial uniformity, intensity, diffuseness) influence the measurement, and should be optimized to create the highest possible spatial uniformity. Many printing system parameters might be manipulated to influence the spatially varying gloss. For fabrication, we manipulated parameters related to the printing strategy like the layering of inks, half-toning and (time before) curing.

Although we attempt to study the different appearance attributes in isolation, we find that in reality all attributes interact with each other, technically — in terms of capturing and fabrication — as well as perceptually (RQ 4). In capturing, many of these interactions are already known, and experienced also by art photographers (as for example shown in Figure 1.5). The measurement of color is influenced by the surface topography, for instance in shaded and shadowed regions. In our proposed design we do manage to (largely) eliminate the influence of the surface reflectance on the color measurement, by using a cross-polarized setup. Also gloss and color measurement can interact, through the inter-reflection between different surfaces (e.g. in valleys or indentations in the surface). In measuring the topography, areas can be occluded for view and therefore not reconstruction in 3D, due to the camera configuration, also inhibiting color measurement at those points. Our approach to measuring spatially-varying gloss, shows interactions between the gloss and topography, through influencing the surface normal in relation to the scanning direction, and through shading and shadowing. Also in fabrication interactions between appearance attributes occur: adding the digital varnish, has a smoothing effect on the topography, thereby influencing the appearance of the relief. In short, the mea-

surement and fabrication of a specific attributes in a real life case, is influenced by other appearance attributes. On top of this, there are perceptual interactions. Currently such mechanisms are still largely unknown. For this reason, we conclude that the safest approach for appearance reproduction for now is probably to start from a point of achieving a physical similarity per attribute, and from that study the interactions.

All three 3D imaging techniques, compared in Chapter 6, show the capability to capture the fine topographical features of a painting's surface, showing good visual correspondence between the data sets (RQ 5). We show that the used scanning resolutions are suitable for visualizing the topographical details that are of interest to a conservator, to evaluate the state of a painting, and determine the course of action for conservation or (potential) treatment. We find that one of the difficulties for all scanning systems, is dealing with the lack of *a priori* knowledge of the painting. Little is known about for instance the maximum height variation within the surface of a painting, nor the changes that occur in topography due to changes in environmental conditions, even within the time period of making one scan. Another limitation of the case study was that the painting was moved between scans. Which, as it was painted on a canvas - a flexible substrate - most certainly changed in global shape between the scans, adding another source of variance to the data, that needs to be accounted for. This would of course also be the case when repeat measurements are taken of the same painting over time. It remains to be investigated if the used scanning resolutions are also suitable for the purpose of monitoring the state of a painting (over time), as such high-resolution data sets have not been captured before, which might be used for comparison. Likely, using 3D scanning to monitor more controlled experiments — i.e. using accelerated aging techniques on reference samples — can also provide more insight into this matter.

8.3. Thoughts on future work

A great number of opportunities are still open, to further increase capabilities of appearance reproduction, in conjunction with an increased understanding of appearance perception. Compared to color reproduction, topography and gloss reproduction can still be regarded as being in its infancy, in terms of capabilities for reproduction and understanding of its perception. Increasing our understanding of topography and gloss perception, also in complex, real-world cases, could help to determine the most appropriate approach to their reproduction. Possibly this increased understanding might also lead to appearance 'metamers', where a desired appearance can be created through altering/enhancement of another attributes.

Existing limitations in fabrication of spatially-varying gloss, as well as gloss gamut mapping, should also be further explored. As we know from material appearance research but also for instance from the field of computer graphics, translucency can be vital to appearance of an artifact. Incorporating translucency capturing and fabrication would therefore greatly expand the capabilities of appearance reproduction.

For the broad application, and inter-operability between scanning and fabrication systems, it is crucial to develop a device-independent *total appearance connection*

space, as an extension of current color connection spaces.

The case studies in this thesis were limited to the reproduction of oil paintings on canvas. To be able to generalize the findings of this thesis, other paintings and/or artifacts made from different materials will need to be replicated and evaluated.

Furthermore, the application of appearance data, as well as physical reproductions can be explored further, specifically in the context of cultural heritage (CH) documentation, monitoring and restoration. Also possibilities for creating reconstructions - of original color, total appearance, or reconstructing missing (pieces of) paintings - should be further explored, also employing new methods from the domains of for instance artificial intelligence, and data science.

We would urge that the application of appearance data, and physical reproductions should be explored and evaluated in a broad multi-disciplinary context, also involving CH sub-disciplines, like museology, art history, restoration and conservation and art education. Only then, can we come to meaningful innovations, and consensus on their usefulness and suitability within the CH domain.

The expansion to appearance reproduction to truly three-dimensional artifacts remains a challenging direction for future research. This is also deemed relevant outside the CH domain, such as the medical domain, for instance applying appearance reproduction to prostheses.

And finally, we also envision that various appearance reproduction efforts could be accumulated into a practical framework for appearance reproduction, providing guidance to choosing a suitable capturing and fabrication technique, capable to (best) match a range of appearance-related and other requirements (e.g. structural, size, or functional related). This framework should be developed in conjunction with a theoretical underpinning on appearance perception, applicable to appearance capturing and fabrication, supporting the efforts of appearance reproduction and perceptual enhancement.

Acknowledgements

First and foremost I would like to thank my husband Mark, for providing me with the necessary support to be able to achieve my goals. You are the best in providing the mental support I need, tempering my (sometimes unrealistic) ambitions, providing the necessary distraction, and of course providing the necessary tech support in desperate times. Also I would like thank my son Siem, for being a happy and cheerful addition to my life. I love you both with all my heart. Both of you help me to put everything in perspective.

Next, I would like to thank my parents, for providing me with all the love and support I needed, to make it to this point; early on, in (financially) supporting me throughout my studies, and in recent years with regular babysitting of Siem. Also, thanks to my parents and sister for all the fruitful discussions we had about my work, and motivating talks to keep me going. Similarly, I would also like to thank Ton and Lia, for the support in recent years, and seeing their enjoyment in babysitting Siem regularly. Furthermore, I would like to also thank the rest of my family(-in-law), for showing interest in my work, and being supportive. Same goes for my friends, with a special dedication to my former rowing teams 'EJD 2005 - Living on the Edge' and 'Pure Evil', and my fellow board members of 'B61', and 'jaarclub Aito'. I am glad to count you as my friends, for all the fun we have, as well as the serious conversations on work, life and the (lack of) balance between them ;).

I would like to thank my promotors and supervisors. First of all, Jo, for providing me with this exiting and challenging topic for my PhD project. I have truly enjoyed working with you on my research project. I am happy to this day, to have made the career switch that I did, which came along, in my view, mostly by coincidence. You have helped me to find a new passion: building and tinkering with prototypes, exploring new and exciting technologies. You are the best type of professor, striking a perfect balance between dedication, support, and leadership, enabling me (and others) to thrive and achieve the best we can possibly do. And Joris, thanks for facilitating that I could work on the coolest and most famous of paintings. Thank you for all the discussions that we had, providing insight in the world of museums and conservation, as well as supporting me in finding a (new) work-life balance. I am also particularly thankful to Sylvia, for you have played a crucial role in my research project. Although you only joined as a supervisor to my project mid-way, I feel you played a pivotal role for the content and on a personal level. You have helped me by providing critical and in-depth feedback on my work, making sure that I get the maximum out of it. I have appreciated the weekly meetings of the π-lab, providing an insight into the work of other researchers and PhDs. This has contributed greatly to my understanding of conducting academic research and writing. But foremost, you were a great support on a personal level, and (still are) an inspiration and role model to me. I would also like to say thanks to Wolf. You were a tremendous help figuring out all the image processing details for the

gloss scanning, and the high-resolution scanning at the Mauritshuis. I love our collaboration dynamic; how, from chaotic discussions, and differences in insight and viewpoint, we always manage to make it work in the end. Furthermore, I would like to thank Erik Tempelman, Boris Lenseigne, and Tim Zaman, for their support in the early phases of my research project.

I would also like to express my gratitude to research partners, who have been instrumental to the success of my research project. I would like to thank Océ Technologies B.V. (a Canon Company) for sponsoring this research project. Specifically, I would like to thank Clemens Weijkamp, Wim Verhofstad, Aswin Draad and others from Océ Technologies B.V. in Venlo, and Jun Hirabayashi from Canon Japan, for their support with printing, and fruitful discussions on the printing technology, 3D and gloss scanning. Furthermore, I would like to thank Teun Baar, Maria Ortiz Segovia and others (previously with Océ Print Logic Technologies S.A.), for their support in the early stages of my research, with 3D and gloss printing.

Additionally, I would like to express my gratitude to the Mauritshuis, the Rijksmuseum and Kröller-Müller Museum, for the opportunities they provided to me, to scan invaluable pieces of their collection. In particular, I would like to thank Abbie, Carol, Sabrina, Boy, Petria, and students and interns, among whom were Ellen Nigro, Fahed Ibrahim and Laurens van Giersbergen (currently or in the past affiliated with the Mauritshuis), for their support with the execution of my 3D scanning case studies at the Mauritshuis. Furthermore, I would like to thank other collaborators in the *Girl in the Spotlight* Research Project, especially Emilien Leonhardt and Tom Callewaert. I am also grateful to the team of 'Het Geheim van de Meester' for providing the painting *Two Wrestling Figures* in the style of Vincent van Gogh, which was used as one of the case studies.

I would also like to thank all my colleagues and lab-co-inhabitants over the years (who I know will be reading this section to check if I mentioned them, so I hope I did not overlook anybody by accident), who make it so much fun to work at TU Delft: Zjenja, Argun, Jouke, Tim, Rado, Doloris, Doris, Mariet, Tao, Yusheng, Jun, Helen, Guoxin, Chengkai, Farzam, Linda, Elvis, Adrie, Martin, Joris, Mascha, Bram and Herman. Except Rob, he has not been any fun or help. If any, he has had a negative contribution (just kidding ;), I also love working with *Rob*ots). And of course a special, extra heartfelt thank you to Tessa, who has been the best support in my research project, from being my graduation student to colleague. You are the best is keeping me organised and on track with my research. I had fun on all our (3D scan) expeditions, and our night-at-the-museum. Also thanks for the great time, the researchers and PhDs of the π-lab: Sylvia, Huib, Maarten, Jess, Fan, Tatiana, Ling, Francesca, Christina, Lisa and Mitchell. And thanks to my recently-found partners-in-crime Bahar and Sander, who are a joy to collaborate with, in redeveloping the Minor Advanced Prototyping. And finally, I would like to thank the graduation students that I had the pleasure to work with: Tessa, Michiel, Hester, Marco, Xiaoying and student assistant Bart. You have all helped me to explore the boundaries of my research topic, providing new insights on the topic.

About the author

Willemijn Sietske ELKHUIZEN

08-05-1984 Born in Den Helder, The Netherlands.

Education

2013–2019 PhD in Industrial Design Engineering
Delft University of Technology, The Netherlands
Thesis: This is not a painting - Scanning and printing a painting's appearance
Promotors: Prof. dr. ir. J.M.P. Geraedts
Prof. dr. J. Dik
Prof. dr. S.C. Pont

2007–2010 Master of Science in Strategic Product Design
Delft University of Technology, The Netherlands

2003–2007 Bachelor of Science in Industrial Design Engineering
Delft University of Technology, The Netherlands

1997–2003 Gymnasium
Jan Arentsz, Alkmaar, The Netherlands

Professional Experience

2017–2019 Teacher/Researcher
Delft University of Technology, The Netherlands

2011–2013 Researcher & Project leader
Océ Technologies B.V., The Netherlands

Patent

2014 A cartridge for holding ink pellets
Patent date: September 17, 2014
Issuer and number: US WO2015040091A1

(Scientific) output

List of publications

Journal Publications (Peer reviewed)

[Provisionally accepted] **W.S. Elkhuizen**, T.W.J. Callewaert, E. Leonhardt, A. Vandivere, Y. Song, S.C. Pont, J.M.P. Geraedts, J. Dik, *Comparison of three 3D imaging techniques for paintings, as applied to 'Girl with a Pearl Earring' by Johannes Vermeer*, Heritage Science.

T. Hou, **W.S. Elkhuizen**, C.C.L. Wang, J. Jiang, J.M.P. Geraedts, Y. Song, *Design of 3D Wireless Power Transfer System Based on 3D Printed Electronics*, IEEE Access, **7**, (2019).

[Accepted] **W.S. Elkhuizen**, T.T.W. Essers, Y. Song, J.M.P. Geraedts, S.C. Pont, J. Dik, *Gloss, Color and Topography Scanning for Reproducing a Painting's Appearance using 3D printing*, Journal of Computation and Cultural Heritage, (2019).

T. Kuipers, **W.S. Elkhuizen**, J. Verlinden, E.L. Doubrovski, *Hatching for 3D prints: Line-based halftoning for dual extrusion fused deposition modeling*, Computers & Graphics, **74**, (2018).

Conference Proceedings (Peer reviewed)

Y. Yang, **W.S. Elkhuizen**, T. Hou, T.T.W. Essers, and Y. Song, *Optimal camera configuration for 3D scanning of human hand*, In proceedings of ASME International Design Engineering Technical Conferences & Computers and Information in Engineering Conference (IDETC/CIE), (2019).

T. Hou, Y. Yang, **W.S. Elkhuizen**, J.M.P. Geraedts, and Y. Song, *Optimizing the printing of conductive traces in 3D printed electronics*, In proceedings of ASME 2019 International Design Engineering Technical Conferences & Computers and Information in Engineering Conference (IDETC/CIE), (2019).

W.S. Elkhuizen, T.T.W. Essers, Y. Song, S.C. Pont, J.M.P. Geraedts, J. Dik, *Gloss Calibration and Gloss Gamut Mapping for Material Appearance Reproduction of Paintings*, In proceedings of Eurographics Workshop on Graphics and Cultural Heritage, (2018).

M.J.W. van Hengstum, T.T.W. Essers, **W.S. Elkhuizen**, D. Dodou, Y. Song, J.M.P. Geraedts, J. Dik, *Development of a high resolution topography and color scanner to capture crack patterns of paintings*, In Proceedings of Eurographics Workshop on Graphics and Cultural Heritage, (2018).

T. Hou, Y. Song, **W.S. Elkhuizen**, J. Jiang, J.M.P. Geraedts, *3D wireless power transfer based on 3D printed electronics*, In proceedings of IEEE International Conference on Automation Science and Engineering, (2018).

W.S. Elkhuizen, T.T.W. Essers, B.A.J. Lenseigne, C. Weijkamp, Y. Song, S.C. Pont, J.M.P. Geraedts, J. Dik, *Reproduction of Gloss, Color and Relief of Paintings using 3D Scanning and 3D Printing*, In proceedings of Eurographics Workshop on Graphics and Cultural Heritage, (2017).

W.S. Elkhuizen, B.A.J. Lenseigne, T. Baar, W. Verhofstad, E. Tempelman, J.M.P. Geraedts, J. Dik, *Reproducing oil paint gloss in print for the purpose of creating reproductions of Old Masters*, In proceedings of Electronic Imaging: Measuring, Modeling and Reproducing Material Appearance, **9398**, (2015)

W.S. Elkhuizen, T. Zaman, W. Verhofstad, P.P. Jonker, J. Dik, J.M.P. Geraedts, *Topographical scanning and reproduction of near-planar surfaces of paintings*, In proceedings of Electronic Imaging: Measuring, Modeling and Reproducing Material Appearance, **9018**, (2014).

Posters

W.S. Elkhuizen, E.L. Doubrovski, N. van Apeldoorn, T.T.W. Essers, J.M.P. Geraedts, *Digital Manufacturing of Fine Art Reproductions for Appearance*, Poster at International Conference on Innovation in Art Research and Technology, (2018).

W.S. Elkhuizen, B.A.J. Lenseigne, C. Weijkamp, S.C. Pont, J.M.P. Geraedts, J. Dik, *A 3D printed reconstructing of a painting's original size - Showing the original size of Saul and David by Rembrandt*, Poster at Visual Science of Art Conference, (2016).

W.S. Elkhuizen, B.A.J. Lenseigne, C. Weijkamp, S.C. Pont, J.M.P. Geraedts, J. Dik, *Making 3D Fine Art reproductions shine: Capturing and printing spatially varying gloss of a painting*, Poster at Symposium on Computational Fabrication, (2016).

Other (scientific) output

Conference presentations

2019 Technart Conference (invited)
Brugge, Belgium
Title: The Girl in the Spotlight: A technical re-examination of Vermeer's 'Girl with a Pearl Earring'
Speakers: A. Vandivere PhD (Mauritshuis)
W.S. Elkhuizen MSc

2014 International Conference on Additive Manufacturing & 3D Printing
Nottingham, United Kingdom
Title: Old Masters and New Sounds: 3D Printing Cultural Heritage
Speakers: W.S. Elkhuizen MSc
E.L. Doubrovski MSc (TU Delft)

Research prototypes

The reproductions created within the context of this PhD project, but also the custom built scanning system, serve as demonstrators, and are in effect accumulations of the knowledge generated in the project:

- (Re)design of scanning system for integrated capture of color, topography and gloss of a painting
- Digitally fabricated reproductions featuring color, topography and gloss of:
  - *Girl with a Pearl Earring* by Johannes Vermeer (c. 1665), in the collection of the Mauritshuis, The Hague
  - *Fruit Still Life* by Cornelis de Heem (c. 1670), in the collection of the Mauritshuis, The Hague
  - *Two Wrestling Figures*, by Charlotte Caspers (2017) painted for the Dutch Television program *Het Geheim van de Meester*. It is a painted reconstruction of a work by Vincent van Gogh
  - *Sunflowers*, signed as W. Adam (c. 2015), a painting in the style of Vincent van Gogh, purchased by the author
- 3D reproduction, featuring color and topography, showing a reconstruction of the original size of painting *Saul and David* by Rembrandt van Rijn, (c. 1651 - 1654 and c. 1655 - 1658), in the collection of the Mauritshuis, The Hague

Media exposure and research dissimination

2019 Interview with *BNR Techniektour* (Dutch radio program)
Episode: De techniek achter restauratie

2017 3D reproduction featured in *Het Geheim van de Meester* (Dutch television program)
Episode: Vincent van Gogh - Stilleven met akkerbloemen en rozen

2016 Lecture with *Universiteit van Nederland* (Dutch online platform)
Title: How do you make the perfect copy of a Rembrandt using modern technology?

2016 Interview with *Eenvandaag* (Dutch daily news program)
Item: The art of reproduction: China's Van Goghs

2016 Design prototype shown at *Mind the Step* (4TU exhibition)
Dutch Design Week, Eindhoven
Title: SmartFrame: Interactive exposition setup for 3D printed reproductions

2015 3D printed reconstruction shown in temporary museum exhibition
Mauritshuis, The Hague
Title: Rembrandt? The case Saul and David

2015 Interview & 3D printed reproductions shown at *Lowlands* (Dutch music and arts festival)
Item: Touching a Rembrandt

2014 Interview with *Arte FuturMag* (French/German television program)
Episode: September 13, 2014